Population structure of *Magnaporthe oryzae* from different geographic regions and interaction transcriptomes with rice genotypes at high temperature

Dissertation

to obtain the Ph.D. degree

in the International Ph.D. Program for Agricultural Sciences in Goettingen (IPAG)

at the Faculty of Agricultural Sciences,

Georg-August-University Göttingen, Germany

Geoffrey Onaga

Born in Ngora, Uganda

Göttingen, May 2014

D7

1. Name of referee: Prof. Dr. Andreas von Tiedemann

2. Name of co-referee: Prof. Dr. Kerstin Wydra

Date of disputation: 9th of July 2014

Contents

Contents

Contents

Contents

Chapter 1: Introduction

It is currently assumed that climate change could lead to global warming. Factors associated with climate change are considered to include an increase in average temperatures and alteration of wind, rainfall regimes, humidity and carbondioxide concentrations (Bokszczanin and Fragkostefanakis, 2013). The effects of altering these climatic factors on the pathogen cycles, epidemiology and plant host resistance remains less clear. Although several authors have attempted to summarize the evidence in systematic reviews, overlapping evaluations are often presented, with several reports indicating that climate change could probably cause variation even in individual pathosystems, with positive, negative and neutral interactions predicted to occur (Pangga et al., 2011; Juroszek and von Tiedemann, 2012). With respect to temperature, there is evidence that elevated temperature effects on pathosystems may vary not only at the host genotypic level but also at the resistance (R) gene -pathogen interaction level (Gousseau et al., 1985; Lain, 2007; Webb et al., 2010; Jorgensen, 2012). Such variation indicates that plants have some parallels in their defense response to pathogens.

Rice is a major host of *Magnaporthe oryzae*, the most destructive pathogen of rice worldwide (Xue et al., 2012). The rice-*M. oryzae* pathosystem is well-studied at both the phenotypic and genomic level. The scientific advancement in both organisms makes them suitable for understanding the mechanisms underlying plant pathogen interaction at high temperature. The genomes of both organisms have also been sequenced, which enables genomic studies of their interaction (IRGSP, 2005; Dean et al., 2005). The sequenced genome of rice is represented by two rice varieties, Nipponbare from Japan and 93-11 from China, belonging to two major Asian cultivated rice subspecies, *Oryza sativa* L. *japonica* and *indica*, respectively. The sequenced genome of *M. oryzae* is represented by a rice-infecting, fully fertile strain 70-15 (Mat1-1), which was obtained by numerous back crosses to the wild isolate Guy 11 (Leung et al., 1988; Dean et al., 2005).

The primary breeding tool for rice blast management is to introduce resistance (R) genes into elite rice cultivars. The hallmark of R gene resistance is hypersensitive response, characterized by necrotic lesions resulting from localized host cell death at the site of infection. The hypersensitive response is connected to the induction of hydrogen peroxide, salicylic acid and jasmonic acid. These molecules are well known signaling compounds which play a role in the induction of PR genes, cell wall phenolics, phytoalexins and callose deposition. However, R gene mediated resistance has been shown to break down within 2-3

years after varietal release. This has been associated with mutations or functional loss of the corresponding *Avr* genes, and selection of novel virulence factors in a pathogen that could evade detection (Wu et al., 2015).

Effectiveness of R genes has been shown to vary with the genetic backgrounds (Palloix et al., 2009). For instance, in rice the background of *japonica* ecotypes have been shown to be more resistant to *Xoo* strains as compared to the *indica* background (Cao et al., 2007). Similar findings have been reported in Arabidopsis, in which the function of an allele of the Arabidopsis *R* gene *RPS2* was found to be influenced by the genetic background (Banerjee et al., 2001). This suggests that substantial differences in the genomic regions controlling disease resistance between the two ecotypes exist, and could be interesting experimental situation to study.

Notwithstanding these differences in resistance patterns, little is known about how the two rice subspecies interact with *M. oryzae* at elevated temperature. Although a risk analysis of rice blast epidemics and plant growth associated with climate change previously suggested increased blast severity in the cool sub-tropical zones of Asia (Luo et al., 1998), this study did not consider the differences associated with *O. japonica* and *O. indica* rice subspecies in response to pathogens. Thus, to date, we know little about the infection of rice by *M. oryzae* at elevated temperatures, as influenced by *O. japonica* and *O. indica* genetics. Besides this, it is not known whether the phenotypic differences associated with the host response to *M. oryzae* infection at high temperature are due to R genes or the genetic background in which the R gene is introgressed. Because *M. oryzae* infects rice by regulating protein secretion, which enables the pathogen to either avoid recognition by the plant resistance proteins or to turn off plant defense (Giraldo et al., 2013), it is expected that elevated temperature may also affect *M. oryzae* pathogenicity. However, the direction of high temperature effect on pathogenicity is not well understood.

The recent developments in high-throughput RNA-Seq, including Solexa/Illumina and ABI/SOLiD, has enhanced the value of transcriptomics and offers effective means for gene expression profiling and discovery of novel transcripts (Garber et al., 2011). These technologies provide a new opportunity for understanding the molecular basis of virulence in pathogens as well as understanding key host defense responses at the same time. Recently, RNA-Seq was used to understand the *in planta* transcriptome changes in *M. oryzae* at 24 h

after infection and during appressorium development (Kawahara et al., 2012; Soanes et al., 2012). These studies provided insights into molecular processes regulated by *M. oryzae* during infection, and were helpful in understanding the early events associated with *M. oryzae* infection. The same authors analyzed the reaction of rice host plant to *M. oryzae* at the transcriptome level and found several plant genes and pathways affected by *M. oryzae* infection. Notwithstanding the identified transcriptional changes associated with rice host plant-*M. Oryzae* interaction reported before, the use of RNA-seq to understand the changes in gene expression, as influence by the genetic backgound, high temperature and *M. oryzae* infection remains unclear.

On the other hand, understanding host-pathogen interaction is greatly dependent on the knowledge of the diversity of the pathogen at the field level (Banniza et al., 1999). Hundreds of pathotypes have been reported in various *M. oryzae* rice infecting populations, which cause widespread epidemics (Urashima, 2001). It is expected that the recent warming trend of about 0.5°C in East Africa (Hepworth and Goulden, 2008) may have caused emergence of virulent *M. oryzae* strains, leading to episodes of blast epidemics, including the blast outbreak observed in the farmers' fields in Kenya in 2009 (Kihoro et al., 2009). Because no prior genetic diversity studies have been conducted on *M. oryzae* in East Africa, deciphering the current status of *M. oryzae* population structure will provide a basis for future studies on climatic factors influencing this pathogen's biology.

Our goal for this research therefore was to better understand the effect of high temperature on phenotypic and transcriptional changes in the rice-*M. oryzae* interaction, and explore the pathogen population structure in less studied areas of East Africa compared to populations of typical rice blast regions in West Africa and the Philippines.

The first objective of this work was to determine transcriptome profiles and biochemical changes that relate to temperature induced phenotypic defense alterations in the rice-*M. oryzae* interaction using *O. japonica* and *O. indica* genetic backgrounds commonly used for the development of rice NILs. We used RNA-seq to test whether increase in temperature from 28°C to 35°C has an influence on the interaction of *M. oryzae* with Li-Jiang-Xin-Tuan-He-Gu (LT; *Oryza japonica*) and Co39 (CO; *Oryza indica*), carrying the resistance gene *Pi54,* at 48 hours post inoculation (hpi). *Pi54* encodes a nucleotide binding site-leucine rich repeat (NBS-LRR) domain with a small zinc finger domain, and was previously reported to be expressed

constitutively at a basal level in both resistant transgenic as well as susceptible native rice lines up to 48 hpi (Gupta et al., 2012). The phenotypic reactions and transcriptome profiles allowed us to identify the resistant background and the genes and biological processes which were altered during the interaction between *M. oryzae, Pi54*, genetic backgrounds and high temperature. We also measured the levels of salicylic acid (SA), hydrogen peroxide (H_2O_2), peroxidase (POX) and phenylalanine ammonia lyase (PAL) in attempts to determine whether gene expression data correlate with defense related biochemical changes. The results of these studies are included in chapter 2.

The second objective of this work was to simultaneously determine the transcript profiles of *M. oryzae in planta* expressed genes and rice defense response at high temperature using the *japonica* cv. Nipponbare and *M. oryzae* isolate TAN211.16. TAN211.16 was selected for transcriptome sequencing because it evoked consistent disease reaction scores on most of the monogenic lines tested in the greenhouse. We examined the transcript profiles of TAN211.16 and Nipponbare at 28°C and 35°C to identify the significant biological processes and genes that relate to pathogen infection, survival and adaptation to the host environment at 48 hpi. We searched for genes encoding for known pathogenicity factors, the secretome and/or effectors, transcription factors, primary metabolism and secondary metabolism and compared their induction during infection at 35°C to infection at 28°C. On the other hand, activated signaling pathways associated with defense response in rice were examined to understand the gene expression differences that occur during infection at 28°C compared to 35°C. The results of these studies are included in Chapter 3.

M. oryzae is relatively less studied in East Africa, but considered a threat to rice production. In the third objective, we were interested in understanding the population structure and active evolutionary forces acting on *M. oryzae* populations in East Africa. We used isolates collected in 2009 and 2011 from three East African countries: Rwanda, Uganda and Tanzania. For comparative purposes, isolates from West Africa and the Philippines were included. A total of 88 isolates were subjected to AFLP analysis. The data were used to estimate gene diversity, genetic distances, genetic differentiation and to make indirect measures of gene flow between local and/or regional population groups. The pathogenicity and mating type distribution for the isolates analyzed were also determined. The results of this study are included in chapter 4.

The last part of this dissertation constitutes the general discussion. The summary of the main findings and potential contributions of this research work to the scientific community are also presented at the end.

Literature review

Rice blast disease

Rice blast, caused by *M. oryzae,* is a filamentous heterothallic ascomycete in the order Diaporthales and family Magnaporthaceae (Cannon, 1994). The naming "*Magnaporthe grisea*" was previously used to encompass all isolates infecting rice and other grasses (Bar, 1977). However, the name *M. grisea* was recently changed to *M. oryzae* based on gene tree topology derived from sections of actin, beta-tubulin, and calmodulin gene sequences, and the inability of isolates infecting rice to interbreed with *Digitaria* isolates (Couch and Kohn, 2002). This was consistent with previous reports that *M. oryzae* is adapted to rice, and probably did not co-evolve with other graminaceous species (Kato et al., 2000). Moreover, high pathogenicity levels on the tracked host and reduced virulence on closely related hosts was indicative of host-specialization (Couch et al., 2005).

Magnaporthe oryzae is present in almost every rice growing area in the world. The disease has been reported to cause yield losses from the hot and dry climate of California and Iraq (Ou, 1985; Greer et al., 1997) to the cool temperate continental climate of Italy. Yield losses of 10%–30% are typical, although regional epidemics can lead to losses ranging from 70%–80% when predisposing factors favor epidemic development (Piotti et al., 2005). *Magnaporthe oryzae* is polycyclic, with several generations in a single rice crop cycle. Crop debris and infected seeds are the most common sources of primary inoculum, while secondary spread occurs through splash or wind dispersed conidia following foliar infections. The disease is favored by frequent occurrence of cloudy days with humidity ranging from 80%–100%. Rice is most susceptible when young plants hold 3 to 4 leaves and during flowering. Infection of rice plants starts with the landing of airborne conidia on the rice leaf cuticle, followed by germination by producing a germ tube which elaborates into an appressorium (Howard and Valent, 1996). When appressorium is fully developed, turgor generated force ruptures the leaf cuticle and an infection peg emerges from its base, which penetrates the leaf surface. The infection peg differentiates into a series of bulbous, branched infectious hyphae soon after plant infection. Four to five days after infection, first necrotic lesions appear simultaneously with aerial conidiophores. The lesions progress and coalesce to form larger lesions which sporulate after six to ten days (Wang et al., 2005). Sporulation is highly favored by the presence of moisture on infected leaf surfaces and by temperatures ranging from 25°C–30°C. Cloudy days and extended periods of high humidity also favor sporulation. All foliar tissues and panicles are subject to infection. The leaf lesions are diamond-shaped, dusty

grayish with a pale chlorotic margin and a necrotic centre and can be longer than 1 cm (Figure 1.1; Wilson and Talbot, 2009), whereas panicle/stem lesions are mainly necrotic. A recent report also shows that *M. oryzae* attacks the roots (Sesma and Osbourn, 2004). However, the root symptom development studies have received less attention.

Pathogenicity factors and effector molecules of *M. oryzae*

Pathogenicity is the ability of an organism to cause disease or harm the host. This ability represents genetic components of the pathogen that promote a compatible host-pathogen interaction. *Magnaporthe oryzae* is classified as a hemibiotroph whereby an initial biotrophic phase, characterized by penetrating the host cell without killing, is followed by a necrotrophic phase, characterized by secreting enzymes and probably toxins that kill and degrade host tissues. This infection strategy is accomplished by employing several factors to colonize and infect rice, for review see (Fernandez and Wilson, 2014a). Successful infection is initiated by a thigmotropic response to a hard surface, which is regulated by regulator of G protein signaling (*Rgs1*; Liu et al., 2007). A hard and hydrophobic surface also activates G protein-coupled receptor protein *Pth11* (DeZwaan et al., 1999). Both *Rgs1* and *Pth11*, in the presence of cyclase-associated protein (*Cap1*), activate adenylate cyclase *Mac1* via G protein signaling. Activated *Mac1* generates cyclic adenosine monophosphate (cAMP), a process that activates cAMP-dependent protein kinase A (*cPKA*) required for initiation of appressorium formation. Recruitment of mitogen activated protein kinase (*Pmk1*), which acts downstream of *Mst11*, *Mst7* and an adaptor protein *Mst50* (Wilson and Talbot 2009; Li et al., 2012), is required for full appressorium formation. Besides this, two proteins, *MoMsb2* and *MoSho1*, are reported to act upstream of *Mst11* as hydrophobicity and cutin monomer sensors (Liu et al., 2011). Moreover, two intermediate proteins orthologuous to *Ras1* and *Ras2*, which are localized beneath *MoMsb2* and *MoSho1*, are non-covalently associated with *Mst11* (Li et al., 2012). Existence of *Mgb1*, a Gβ subunit, upstream of *Pmk1* is also reported, and apparently acts as a link between cAMP signaling and MAPK pathway (Nishimura et al., 2003; Fernandez and Wilson, 2014a).
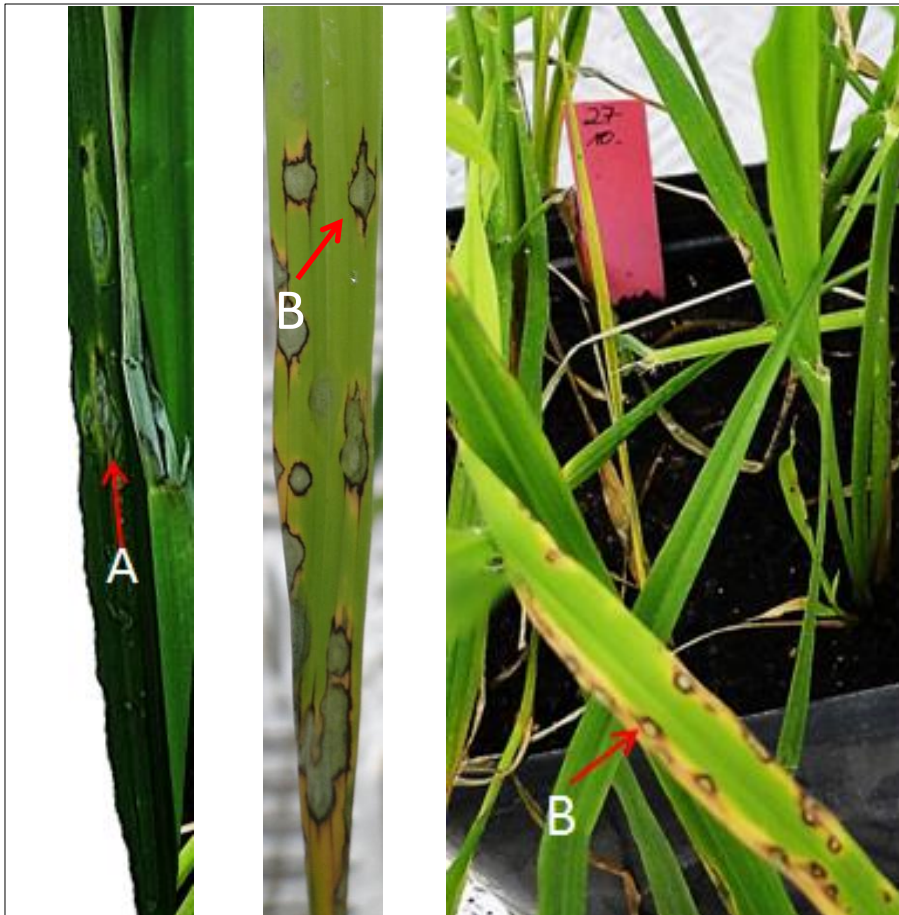
Figure 1.1: Typical rice blast lesions on rice leaf sheath (A) and leaves (B) on 5 weeks grown plants in the greenhouse. The arrows indicate the lesions.

The transcription factor *Mst12*, a homologue of the yeast *STE12*, is reported to be a *Pmk1* downstream target required for penetration and invasive growth (Park et al., 2002). A MADS-box transcription factor, *MoMcm1* was recently shown to form a heterodimeric complex with *Mst12* in activating components required for infection (Zhou et al., 2011). These multiple events suggest that the infection-related morphogenesis in *M. Oryzae* is highly regulated, and multiple steps are required for the development of the penetration peg and successful penatration of host tissues.

Differentiation of the infection peg into infection hyphae requires *PLS1*, which encodes a putative tetraspanin protein (Clergeot et al., 2001). *PLS1* is apparently involved in signal transduction essential for reorganization of actin at the base of the appressorium and directing mechanical pressure at the pore (Clergeot et al., 2001; Talbot, 2003). A list of other pathogenicity proteins involved in surface sensing, appressorium formation and the subsequent phases of *M. oryzae* infection is provided in Figure 1.2.

Upon plant penetration, and the subsequent invasive growth, *M. oryzae* secretes proteins into the host cell, some of which are categorized as effectors. Effectors are generally defined as pathogen derived proteins and small molecules directed towards manipulation of host cell structure and function, either by facilitating infection (toxins and virulence factors) or by activating defence response (elicitors and avirulence factors) (Kamoun, 2006). About 1306 genes coding for putative secreted proteins have been predicted from *M. oryzae* genome (Zhang and Xu, 2014). Effector delivery into host cells is accomplished by fungal hyphal modification into: (1) a biotrophic interfacial complex (BIC), which forms in primary hyphae as they enter each host cell and (2) host-derived extra invasive hyphal membrane (EIHM) surrounding bulbous invasive hyphae (Fernandez and Wilson, 2014a).
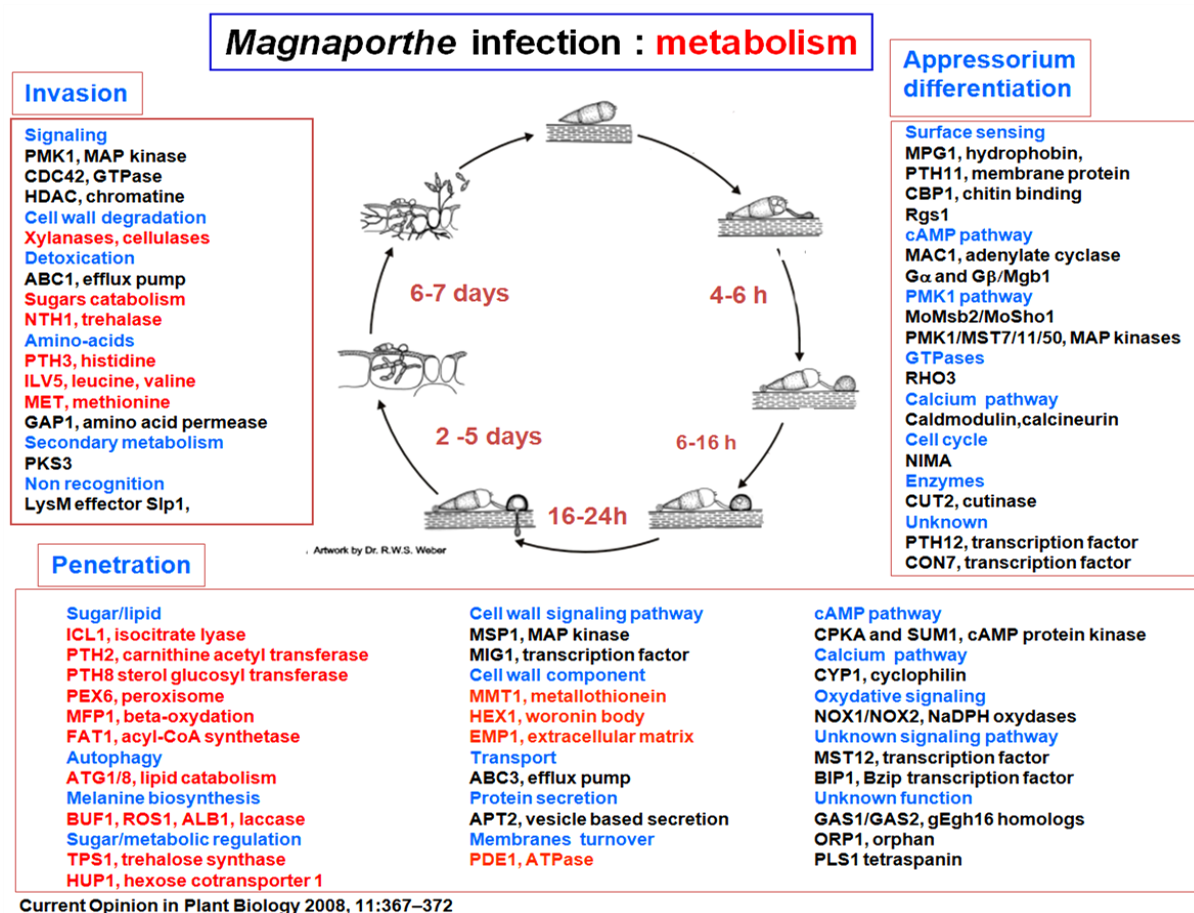
Figure 1.2: *Magnaporthe oryzae* infection cycle accompanied with pathogenicity proteins involved in each stage; from appressorium differentiation to invasion. Reprinted with permission and support from Marc Henri LEBRUN, INRA-CPP

Two types of effectors are distinguished in *M. oryzae* based on their localization in plant cells: (1) cytoplasmic effectors, including *Avr-Pita*, *PWL1*, *PWL2*, *BAS2*, and *Avr-Piz-t*, which accumulate in the BIC before being delivered into plant cells, and (2) apoplastic effectors

such as *BAS4*, *Avr1-CO39* and *Slp1*, which are dispersed in the extracellular space between the fungal cell wall and EIHM (Zhang and Xu, 2014) where they either interact with plant derived defence proteins or prevent fungal structures from being recognized by the host defences.

Previous reports have shown that apoplastic effectors require the conventional Golgi-mediated secretion pathway, while cytoplasmic effectors require BIC associated pathway involving the exocyst components *Exo70* and *Sec5* for their secretion into host cells (Giraldo et al., 2013). However, unlike in oomycetes where cytoplasmic effectors are modular proteins with defined signal peptide motifs for secretion (Schornack et al., 2009), the specific protein motifs or sequences specifying localization in *M. oryzae* effectors are still elusive. Hence, predicting localization based on amino acid sequence is presently a challenge. Nonetheless, it is hypothesized that effector trafficking may depend on rice cell types, protein size and conserved fungal mechanisms to recognize plasmodesmata for the movement of effector proteins and spreading of invasive hyphae (Zhang and Xu, 2014). Validation of these hypotheses will provide more insights into *M. oryzae* infection process.

Variability and population structure studies on *M. oryzae*

Magnaporthe oryzae is highly variable with a potential to evolve relatively quickly and adapt to changes in environmental conditions and host resistance (Huang et al., 2014). Genetic variability is correlated with high levels of genetic instability of traits such as pathogenicity, morphology and fertility (reviewed in Scheuermann et al., 2012). Variation in pathogenicity is attributed to genomic alterations that lead to loss of function of avirulence effectors, including point mutations, especially repeat-induced point mutations (Fudal et al., 2009), insertions of transposable elements, or deletions of entire genes (De Wit et al., 2009). Some of the avirulence genes are located in telomeric and sub-telomeric regions, as is the case of *Avr-Pita*, *AvrMedNoï-1, AvrKu86-*1, *Avr-Piz*, *Avr-Pii*, *Avr-Pi15*, *Avr-Pit* and *Avr-Pia* (Scheuermann et al., 2012). Deletions in these regions results in the loss of *Avr* genes, leading to virulence gain (Orbach et al., 2000). As suggested previously, such mutations could also be the major cause of genetic diversity within populations from one region (Tharraeu et al., 2009).

Several molecular typing techniques have been used to understand *M. oryzae* population structure, including MGR 586 repetitive DNA sequence (Hamer et al., 1989), *Pot2* (Kachroo et al., 1994), Randomly amplified polymorphic DNA (RAPD) (Rathour et al., 2004; Sere et

al., 2007), amplified fragment length polymorphism (AFLP) (Nguyen et al., 2006), simple sequence repeats (SSRs) (Brondani et al., 2000), and pathogenicity tests on differential sets of rice varieties (Levy et al., 1991). These studies have revealed several clonally derived lineages, as well as genetic variability associated with race diversity. Regional clustering of populations has been observed, for instance genotypes from Europe are very similar and are distinct from genotypes from Madagascar, which likewise form one cluster (Tharraeu et al., 2009). Alternatively, evidence has shown that *M. oryzae* populations are more diverse in Asia, where rice cultivation has been going on for several years, compared to Europe and East Africa where rice cultivation is relatively recent. This is probably due to the abundance of several and diverse rice cultivars and a heterogeneous environment, which prevents clonal expansion of lineages. In the Himalayas and parts of China, where there is high diversity of rice, both mating types of *M. oryzae* are present (Rathour et al., 2004), which suggests that sexual reproduction could be still contributing to genetic diversity in those areas. However, there are suggestions that in some areas where rice cultivation and favorable weather conditions enable the fungus to survive in the form of mycelia during many fallow seasons, mutations that remove sexual reproduction could be fixed because of high energy costs associated with this character (Zeigler, 1998). The fungus, therefore, propagates asexually by means of conidia. Indeed some of the rice growing areas, including USA, Europe, and Africa, have been shown to have near monomorphic populations (Xia et al., 1993; Xia et al., 2000; Roumen et al., 1997; Takan et al., 2011), suggesting that asexual reproduction is a dominant phenomenon in these regions, and that different mechanisms are acting to create genetic variability in *M. Oryzae.* Alternative causes of genetic variation, such as parasexual recombination (Noguchi, 2011) and mutation, could be contributing to genetic diversity observed in such regions. There is, however, no evidence to support these hypotheses, and further studies are warranted.

Management of rice blast

Rice blast management includes various methods such as chemical, cultural and cultivar resistance or a combination of the three. Chemical control has long been viewed as a last resort to control rice blast. Where necessary, several fungicides have been shown to be effective, including tetrachlorophthalide, tebuconazole + trifloxystobin and propiconazole (Ghazanfar et al., 2009). In cultural control, burning of diseased straw and stubble to minimize carryover of inoculum to the next season crop (Kato, 2001), planting healthy seeds, nitrogen fertilizer management, crop rotation and flooding reduce the amount of inoculum

available for subsequent disease development. However, host genetic resistance remains a reliable strategy that combines both economic viability and environmental safety aspects.

Genetic resistance to rice blast in rice

Rice blast resistance is classified into two types: i) complete or true (qualitative) and ii) partial or field resistance (quantitative) (Ezuka 1972). Complete resistance, induced by incompatible interaction, is usually controlled by a major gene, whereas partial resistance is generally non-race specific and polygenic (Kiyosawa 1981). Partial resistance, also called basal or horizontal disease resistance is sometimes referred to as pathogen-associated molecular pattern (PAMP)-triggered immunity (PTI), and is considered as the primary facet of active plant defence. Major gene resistance, also called effector-triggered immunity (ETI) mostly relies on the endogenious NB-LRR protein products encoded by resistance (R)-genes. Major gene resistance is generally not durable, and usually breaks down a few years after introduction into commercial varieties, whereas partial resistance is preferred because it is thought to lead to durable resistant cultivars (Mackill and Bonman 1992). However, major gene resistance is now effectively being deployed through pyramiding of several R-genes in the same cultivar, which increases resistance durability and spectrum. Moreover, combining several R-genes with horizontal resistance has been hypothesized to be the most promising approach to develop durable resistance in rice (Jena and Mackill 2008).

PTI is mediated by pattern recognition receptors (PRRs) that recognize PAMPs. Generally, PTI and ETI trigger similar defence responses, but ETI is much faster and quantitatively stronger (Wei et al., 2013). In addition, ETI is an efficient defence system for more progressed infections, as it is able to guard against weak points or even setting up decoys to confuse invaders. On the other hand, PTI is important for non-host resistance and for basal immunity in susceptible host plant cultivars. Both PTI and ETI are often activated preceding pathogen recognition. Following pathogen recognition, a cascade of signal transduction pathways, which require regulators such as hydrogen peroxide, salicylic acid (SA), jasmonic acid (JA), ethylene (ET), abscisic acid, mitogen activated protein kinases and transcriptional factors initiate PTI or ETI, depending on the pathogenicity factors recognized by the plant. Subsequently, downstream defence responses which include programmed cell death leading to the hypersensitive response (HR), production of antimicrobial secondary metabolites (e.g., phytoalexins), pathogenesis-related (PR) proteins (e.g., chitinases and glucanases) and cell-wall strengthening occur (Vergne et al., 2008). The hallmark of ETI in plant defense is the

hypersensitive response (HR), which is largely derived from membrane localized NADPH oxidases.

Over 85 blast resistance genes have been identified in rice (Valent and Khang, 2010; Huang et al., 2014), 22 of these have been cloned (Luo et al., 2012). Furthermore, near-isogenic lines with single genes for resistance have been developed in the genetic backgrounds of the *O. indica* variety CO39, *O. japonica* variety Li-Jiang-Xin-Tuan-He-Gu (LTH) and a universal susceptible line US2 (Kobayashi et al., 2007). These isogenic lines are useful for identification of the blast races, monitoring of shifts in blast races and determining plant-specific resistance in rice breeding (Telebanco-Yanoria et al., 2010; Koide et al., 2011).

Previous studies have reported the molecular processes mediated by R genes and partial resistance genes during blast infection using differential expression studies: e.g., rice carrying the R gene *Pi33* infected with *M. oryzae* strain carrying the avirulence gene *ACE1* (Vergne et al., 2007), resistant vs. susceptible NILs differing for the introgression of the *Pi-k* gene (Li et al., 2006), *Pi54* activation of multiple defense mechanisms in rice (Gupta et al., 2012) and rice early defense response to *M. oryzae* in a compatible and incompatible interaction (Wei et al., 2013). The molecular function of some R genes in rice defense responses is well documented (Dai et al., 2007; Miah et al., 2010). The functional domain positioning is probably the reason behind several R genes identified in rice. One of the well-known functional domain positioning examples is the recognition of *M. oryzae* effector, *AVR-Piz-t* by the R gene *Piz-t*, which adopts a six-stranded β-sandwich structure and contains a single disulphide bond. In addition, the direct binding of *AVR-Pik* to *Pik-1* by interacting with Heavy-Metal Associated domain (HMA; also known as RATX1) of *Pik-1* is another domain positioning example that could be different from some R genes. Thus, the functional domain positioning underlying effector binding could be causing defence-related differences between R genes.

Partial resistance/PTI is conferred by QTLs, and several blast resistance QTLs have been mapped (reviewed in Liu et al., 2010); the genes underlying two of them, *pi21* and *Pb1*, have been cloned (Fukuoka et al., 2009; Hayashi et al., 2010). In addition, transcript profiling of temperate *japonica* Italian rice cultivars with contrasting response to *M. oryzae* infection using RNA-sequencing (RNA-Seq) was recently carried out in an effort to establish a more meaningful picture of durable resistance in rice (Bagnaresi et al., 2012). These studies

allowed for the identification of the main biological processes and functional categories of defense related genes responsive to *M. oryzae* in genotypes with contrasting resistance. Alternatively, in a study involving transgenic plants carrying *Xa26* (also known as *Xa3*), it was found that the background of *japonica* variety Mudanjiang 8 showed increased resistance to eight *Xoo* strains as compared to the gene donor of *indica* variety Minghui 63 (Sun et al., 2004). These findings were later confirmed by Cao et al (2007), who found that the genetic background of *japonica* rice enhanced *Xa3* mediated resistance more than the background of *indica* rice. Genetic characterization studies have also suggested that *indica* varieties have more complicated blast resistance patterns than *japonica* varieties (Shang et al., 2009). Moreover, different *indica* backgrounds appear to have a significant influence on the function of *R* genes (Cao et al., 2007). Although much is already known about the influence of genetic background on plant response to pathogens, an initial step will be to refine this knowledge further and determine the influence of environmental factors on host genetic background-pathogen interaction. In order to address this question, a well characterized pathosystem is required. As reported earlier, the rice-*Magnaporthe oryzae* pathosystem is an ideal model in this regard.

References

Bagnaresi, P., Biselli, C., Orrù, L., Urso, S., Crispino, L., Abbruscato, P., Piffanelli, P., Lupotto, E., Cattivelli1, L. and Valè, G. (2012) Comparative transcriptome profiling of the early response to *Magnaporthe oryzae* in durable resistant vs susceptible rice (Oryza sativa L.) genotypes. PLoS One 7, e51609.

Banniza, S., Sy, A.A., Bridge, P.D., Simons, S.A. and Holderness, M. (1999) Characterization of populations of Rhizoctonia solani in paddy rice fields in Cote d' Ivoire. Phytopathology, 89, 414-420.

Barr, M. (1977) *Magnaporthe*, Telimenella and Hyponectria (Physosporellaceae). Mycologia, 69, 952-966.

Bokszczanin, K.L., Fragkostefanakis, S., Bostan, H., Bovy, A., Chaturvedi, P., Chiusano, M.L., Firon, N., Iannacone, R., Jegadeesan, S., Klaczynskid, K., Li, H., Mariani, C., Müller, F., Paul, P., Paupiere, M., Pressman, E., Rieu, I., Scharf, K.D., Schleiff, E., Van Heusden, A.W., Vriezen, W., Weckwerth, W. and Winter, P. (2013) Perspectives on deciphering mechanisms underlying plant heat stress response and thermotolerance. Frontiers in Plant Science 4, 315

Bonman, J.M. and MacKill, D.J. (1988) Durable resistance to rice blast disease. Oryza 25, 103-110.

Brondani, C., Brondani, R., Garrido, L.D. and Ferreira M. (2000) Development of microsatellite markers for genetic analysis of Magnaporthe grisea. Genetics and Mol. Bio. 23, 753-762.

Cannon, P. (1994) The newly recognized family Magnaporthaceae and its interrelationships. Systema Ascomycetum 13, 25-42.

Chen, C., Lian, B., Hu, J., Zhai, H., Wang, X., Venu, R.C., Liu, E., Wang, Z., Chen, M., Wang, B., Wang, G.L., Wang, Z. and Mitchell, T.K. (2013) Genome comparison of two Magnaporthe oryzae field isolates reveals genome variations and potential virulence effectors. BMC Genomics 14, 887.

Clergeot, P.H., Gourges, M., Cots, J., Laurans, F., Latorse, M.P., et al., (2001) PLS1, a gene encoding a tetraspanin-like protein, is required for penetration of rice leaf by the fungal pathogen Magnaporthe grisea. Proc Natl Acad Sci USA 98, 6963-6968.

Couch, B.C. and Cohn, L.M. (2002) A multilocus gene genealogy concordant with host preference indicates segregation of a new species, Magnaporthe oryzae from M. grisea. Mycologia 94, 683-693.

Couch, B.C., Fudal, I., Lebrun, M.H., Tharreau, D., Valent, B., van Kim, P., Notteghem, J.L., et al., (2005) Origins of host-specific populations of the blast pathogen Magnaporthe oryzae in crop domestication with subsequent expansion of pandemic clones on rice and weeds of rice. Genetics 170, 613–630.

Dai, Y., Jia, Y., Correll, J.C., Wang, X. and Wang, Y. (2010) Diversification and evolution of the avirulence gene ARV-Pita1 in field isolates of Magnaporthe oryzae. Fungal Genet Biol 47, 973e980.

Dean, R.A., Talbot, N.J., Ebbole, D.J., Farman, M.L., Mitchell, T.K., Orbach, M.J., Thon, M., Kulkarni, R., Xu, J.R., Pan, H.Q., Read, N.D., Lee, Y.H., Carbone, I., Brown, D., Oh, Y.Y., Donofrio, N., Jeong, J.S., Soanes, D.M., Djonovic, S., Kolomiets, E., Rehmeyer, C., Li, W.X., Harding, M., Kim, S., Lebrun, M.H., Bohnert, H., Coughlan, S., Butler, J., Calvo, S., Ma, L.J., Nicol, R., Purcell, S., Nusbaum, C., Galagan, J.E., and Birren, B.W. (2005) The genome sequence of the rice blast fungus Magnaporthe grisea. Nature 434, 980-986.

DeWit, P.J.G.M., Mehrabi, R., van den Burg, H. and Stergiopoulos, I. (2009) Fungal effector proteins: past, present and future. Molecular Plant Pathology 10, 735–747.

DeZwaan, T.M., Carroll, A.M., Valent, B. and Sweigard, J.A. (1999) Magnaporthe grisea Pth11p is a novel plasma membrane protein that mediates appressorium differentiation in response to inductive substrate cues. Plant Cell 11, 2013–2030.

Ezuka, A. (1972) Field resistance of rice varieties to rice blast disease. Rev Plant Prot Res 5,1–21

Fernandez, J. and Wilson, R.A. (2014a) Cells in cells: morphogenetic and metabolic strategies conditioning rice infection by the blast fungus Magnaporthe oryzae. PLoS ONE 9, e87300.

Fudal, I., Collemare, J., Bohnert, H.U., Melayah, D. and Lebrun, M.H. (2007) Expression of Magnaporthe grisea avirulence gene ACE1 is connected to the initiation of appressorium-mediated penetration. Eukaryotic cell 6 no 3, 546.

Fukuoka, S., Saka, N., Koga, H., Ono, K., Shimizu T., et al., (2009) Loss of function of a proline-containing protein confers durable disease resistance in rice. Science 325, 998–1001.

Fukuoka, S., Saka, N., Koga, H., Ono, K., Shimizu, T., Ebana, K., Hayashi, N., Takahashi, A., Hirochika, H., Okuno, K. and Yano, M. (2009) Loss of function of a proline-containing protein confers durable disease resistance in rice. Science 325, 998–1001.

Garber, M., Grabherr, M.G., Guttman, M. and Trapnell, C. (2011) Computational methods for transcriptome annotation and quantification using RNA-seq. Nature Methods 8, 469–477.

Ghazanfar, M.U., Wakil, W., Sahi, S.T. and Saleem-il-Yasin. (2009). Influence of various fungicides on the management of rice blast disease. Mycopath. 7(1), 29-34.

Giraldo, M.C., Dagdas, Y.F., Gupta, Y.K., Mentlak, T.A., Yi, M., et al., (2013) Two distinct secretion systems facilitate tissue invasion by the rice blast fungus Magnaporthe oryzae. Nat Commun 4, 1996.

Gousseau, H.D.M., Deverall, B.J. and Mclntosh, R.A. (1985) Temperature-sensitivity of the expression of resistance to Puccinia graminis conferred by the Srl5, SrVh and Srl4 genes in wheat. Physiological Plant Pathology 27, 335 43.

Greer, C.A. and Webster, R.K. (2001) Occurrence, Distribution, Epidemiology, Cultivar Reaction, and Management of Rice Blast Disease in California. Plant Dis 85, 1096-1102.

Gupta, S. K., Rai, A.K., Kanwar, S.S., Chand, D., Singh, N. K., et al., (2012) The single functional blast resistance gene Pi54 activates a complex defence mechanism in rice. J Exp Bot 63, 757-772.

Hamer, J., Farral, L., Orbach, M., Valent, B. and Chumley, F.G. (1989) Host species-specific conservation of a family of repeated DNA sequences in the genome of a fungal plant pathogen. Proceedings of the National Academy of Sciences of the United States of America 86, 9981-9985.

Hayashi, N., Inoue, H., Kato, T., Funao, T., Shirota, M., et al., (2010) Durable panicle blast-resistance gene Pb1 encodes an atypical CC-NBS-LRR protein and was generated by acquiring a promoter through local genome duplication. The Plant Journal 64, 498–510.

Hayashi, N., Inoue, H., Kato, T., Funao, T., Shirota, M., Shimizu, T., Kanamori, H., Yamane, H., Hayano-Saito, Y., Matsumoto, T., Yano, M. and Takatsuji, H. (2010) Durable panicle blast-resistance gene Pb1 encodes an atypical CC-NBS-LRR protein and was generated by acquiring a promoter through local genome duplication. Plant J 64, 498-510.

Hepworth, N., and Goulden, M. (2008) Climate change in Uganda: Understanding the implication and appraising the response. LTS International Edinburgh.

Howard, R. and Valent B. (1996) Breaking and entering: Host penetration by fungal rice blast pathogen Magnaporthe grisea. Annual Review of Microbiology 50, 491-512.

Huang, J., Si, W., Deng, Q., Li, P. and Yang, S. (2014) Rapid evolution of avirulence genes in rice blast fungus Magnaporthe oryzae. BMC Genet 15, 45.

International Rice Genome Sequencing Project (IRGSP). (2005) The map-based sequence of the rice genome. Nature 436,793-800.

IPCC: Intergovernmental Panel on Climate Change. (2007) Climate change 2007: The physical science basis. Summary for policymakers. Contribution of working group I and II to the third assessment report of the IPCC. IPCC Secretariat, Geneva, Switzerland.

Jena, K.K. and Mackill, D.J. (2008) Molecular markers and their use in marker-assisted selection in rice. Crop Sci 48, 1266-1276.

Jorgensen, T.H. (2012) The effect of environmental heterogeneity on RPW8-mediated resistance to powdery mildews in Arabidopsis thaliana. Ann Bot 109, 833-842.

Wu, J., Kou, Y., Bao, J., Li, Y., Tang, M., Zhu, X., Ponaya, A., Xia, G., Li, J., Li, C., Song, M., Joseph, C., Deng, Q., Lu, G., Jeon, J., Naqvi, N. and Zhou, B. (2015): Comparative genomics identifies the Magnaporthe oryzae avirulence effector AvrPi9 that triggers Pi9-mediated blast resistance in rice. New phytologist 206, 1463-1475.

Juroszek, P. and von Tiedemann, A. (2012) Climate change and potential future risks through wheat diseases. Eur J Plant Pathol 36, 21–33.

Kachroo, P., Leong, S. A. and Chattoo, B. B. (1995) Mg-SINE: a short interspersed nuclear element from the rice blast fungus, Magnaporthe grisea. Proc Natl Acad Sci USA 92, 11125-11129.

Kachroo, P., Leong, S. and Chattoo, B. (1994) Pot2, an inverted repeat transposon from the rice blast fungus Magnaporthe grisea. Molecular and General Genetics 245(3), 339-348.

Kamoun, S. (2006) A catalogue of the effector secretome of plant pathogenic oomycetes. Annu Rev Phytopathol 44, 41-60.

Kato, H. (2001). Rice blast disease - An Introduction. Pesticide Outlook, 23-25.

Kato, H. and Kozaka, T. (1974) Effects of temperature on lesion enlargement and sporulation of Pyricularia oryzae in rice leaves. Phytopathology 64, 828-830.

Kato, H., Yamamoto, M., Yamaguchi-Ozaki, T., Kadouchi, H., Iwamoto, Y., Nakayashiki, H., Tosa,Y., Mayama, S. and Mori N. (2000) Pathogenicity, mating ability and DNA restriction fragment length polymorphisms of Pyricularia populations isolated from Gramineae, Bambusideae and Zingiberaceae. Plants Journal General Plant Pathology 66(1), 30-47.

Kawahara, Y., Oono, Y., Kanamori, H., Matsumoto, T., Itoh, T. and Minami, E. (2012) Simultaneous RNA-Seq analysis of a mixed transcriptome of rice and blast fungus interaction. PloS One 7, e49423.

Kihoro, J., Njoroge, J. B., Murage, H., Ateka, E. and Makihara, D. (2013) Investigating the impact of rice blast disease on the livelihood of the local farmers in greater Mwea region of Kenya. SpringerPlus 2, 308

Kiyosawa, S. (1981) Gene analysis for blast resistance. Oryza 18, 196-203.

Kobayashi, N., Telebanco-Yanoria, M.J., Tsunematsu, H., Kato, H., Imbe, T. and Fukuta, Y. (2007) Development of new sets of international standard differential varieties for blast resistance in rice (Oryza sativa L.). JARQ 41, 31-37.

Koide,Y., Telebanco-Yanoria, M.J., Peña, F.D., Fukuta, Y. and Kobayashi, N. (2011) Characterization of rice blast isolates by the differential system and their application for mapping a resistance gene. Pi19 (t) J Phytopathol 159, 85e93.

Laine, A.L. (2007) Pathogen fitness components and genotypes differ in their sensitivity to nutrient and temperature variation in a wild plant–pathogen association. Journal of Evolutionary Biology 20, 2371–2378.

Leung, H., Borromeo S., Bernardo, M. A. and Notteghem, J. L. (1988) Genetic analysis of virulence in the rice blast fungus Magnaporthe grisea. Phytopathol 78, 1227-1233.

Levy, M., Romao, J., Marchetti, M. A. and Hamer, J. E. (1991) DNA fingerprinting with dispersed repeated sequence resolves pathotype diversity in the rice blast fungus. Plant Cell 3, 95-102.

Li, Q., Chen, F., Sun, L., Zhang, Z., Yang, Y., et al., (2006) Expression profiling of rice genes in early defence responses to blast and bacterial blight pathogens using cDNA microarray. Physiological and Molecular Plant Pathology 68, 51–60.

Li,G., Zhou, X. and Xu, J.R. (2012) Genetic control of infection-related development in Magnaporthe oryzae. Curr Opin Microbiol 15, 678–684.

Liu, H., Suresh, A., Willard, F.S., Siderovski, D.P., Lu, S., et al., (2007) Rgs1 regulates multiple G alpha subunits in Magnaporthe pathogenesis, asexual growth and thigmotropism. Embo Journal 26, 690–700.

Liu, J., Wang, X., Mitchell, T., Hu, Y., Liu, X., Dai, L. and Wang, G.L. (2010) Recent progress and understanding of the molecular mechanisms of the rice-Magnaporthe oryzae interaction. Molecular Plant Pathology 11, 419-427.

Liu, W., Zhou, X., Li, G., Li, L., Kong, L., et al., (2011) Multiple plant surface signals are sensed by different mechanisms in the rice blast fungus for appressorium formation. PLoS Pathog 7, e1001261.

Luo, S., Zhang, Y., Hu, Q., Chen, J., Li, K., Lu, C., Liu, H., Wang, W. and Kuang, H. (2012) Dynamic nucleotide-binding site and leucine-rich repeat-encoding genes in the grass family. Plant Physiol 159, 197-210.

Luo, Y., Teng, P.S., Fabellar, N.G. and TeBeest, D.O. (1998) The effects of global temperature change on rice leaf blast epidemics: a simulation study in three agroecological zones. Agriculture Ecosystems and Environment 68, 187–196.

Mackill, D.J. and Bonman, J.M. (1992) Inheritance of blast resistance in near-isogenic lines of rice. Phytopathology 82, 746-749.

Miah, G., Rafii, M.Y., Ismail, M.R., Puteh, A.B., Rahim, H.A., Asfaliza, R. and Latif, M.A. (2013) Blast resistance in rice: a review of conventional breeding to molecular approaches. Mol Biol Rep. 40, 2369–2388.

Nguyen, T., Bigirimana, J., Roumen, E., Van Der Straeten, D. and Hofte, M. (2006) Molecular and pathotype analysis of the rice blast fungus in North Vietnam. European Journal of Plant Pathology 114, 381–396.

Nishimura, M., Park, G. and Xu, J.R. (2003) The G-beta subunit MGB1 is involved in regulating multiple steps of infection-related morphogenesis in Magnaporthe grisea. Mol Microbiol 50, 231–243.

Noguchi, M. (2011) Parasexual recombination in Magnaporthe oryzae. Japan Agricultural Research Quarterly 45(1), 39-45.

Orbach, M., Farrall, L., Sweigard, J., Chumley, F. and Valent, B. (2000) A Telomeric avirulence gene determines efficacy for the rice blast resistance gene Pi-ta. The Plant Cell 12(4), 2019-2032.

Ou, S.H. (1985) Rice Diseases, 2nd ed. Kew, Surrey, U.K. Commonwealth Mycological Institute.

Palloix, A, Ayme, V and Moury, B. (2009) Durability of plant major resistance genes to pathogens depends on the genetic background, experimental evidence and consequences for breeding strategies. New Phytol. 183, 190-199.

Pangga, I.B., Hanan, J. and Chakraborty, S. (2011) Pathogen dynamics in a crop canopy and their evolution under changing climate. Plant Pathology 60, 70-81.

Park, G., Xue, G.Y., Zheng, L., Lam, S. and Xu, J.R. (2002) MST12 regulates infectious growth but not appressorium formation in the rice blast fungus Magnaporthe grisea. Mol Plant Microbe Interact 15, 183–192.

Piotti, E., Rigano, M.M., Rodino, D., Rodolfi, M., Castiglione, S., Picco, A.M. and Sala, F. (2005) Genetic Structure of Pyricularia grisea (Cooke) Sacc. Isolates from Italian Paddy Fields. J. Phytopathol 153, 80-86.

Rathour, R., Singh, B., Sharma, T. and Chauhan, R. (2004) Population Structure of Magnaporthe grisea from North-western Himalayas and its implications for blast resistance breeding of rice. Journal of Phytopathology 152(5), 304–312.

Scheuermann, K.K., Raimondi, J.V., Marschalek, R., de Andrade, A. and Wickert, E. (2012) Magnaporthe oryzae genetic diversity and its outcomes on the search for durable resistance. In Caliskan, M. (Ed.), The molecular basis of plant genetic diversity (pp. 331-356). InTech.

Schornack, S., Huitema, E., Cano, L.M., Bozkurt, T.O., Oliva, R., et al., (2009) Ten things to know about oomycete effectors. Mol Plant Pathol 10, 795–803.

Séré, Y., Onasanya, A., Afolabi, A., Mignouna, H. and Akator, K. (2007) Genetic diversity of the blast fungus, Magnaporthe grisea (Hebert) Barr, in Burkina Faso. African Journal of Biotechnology 6(22), 2568-2577.

Sesma, A. and Osbourn, A. (2004). The rice leaf blast pathogen undergoes developmental processes typical of root-infecting fungi. Nature 431, 582-586.

Shang, J., Tao, Y., Chen, X., Zou, Y., Lei, C., Wang, J., Li, X., Zhao, X., Zhang, M., Lu, Z., Xu, J., Cheng, Z., Wan, J. and Zhu, L. (2009) Identification of a new rice blast resistance gene, Pid3, by genome-wide comparison of paired NBS-LRR genes and their pseudogene alleles between the two sequenced rice genomes. Genetics, 182, 1303–1311.

Soanes, D.M., Chakrabarti, A., Paszkiewicz, K.H., Dawe, A.L. and Talbot, N.J. (2012) Genome-wide transcriptional profiling of appressorium development by the rice blast fungus Magnaporthe oryzae. PLoS Pathog 8, e1002514.

Talbot, N.J. (2003) On the trail of a cereal killer: exploring the biology of Magnaporthe grisea. [Review] Annu Rev Microbiol 57, 177-202.

Telebanco-Yanoria, M.J., Koide, Y., Fukuta, Y., Imbe, T., Kato, H., Tsunematsu, H. and Kobayashi, N. 2010. Development of near-isogenic lines of Japonica-type rice variety Lijiangxintuanheigu as differentials for blast resistance. Breed Sci 60, 629e638.

Tharraeu, D., Fudal, I., Andriantsimialona, D., Santoso, Utami, D., Fournier, E., Lebrun M-H. and Nottéghem J.L. (2009) World Population Structure and Migration of the Rice Blast Fungus, Magnaporthe oryzae. Advances in Genetics, Genomics and Control of Rice Blast Disease Part III, 209-215.

Urashima, A.S. (2001) Variation in virulence in the rice blast fungus Magnaporthe grisea in São Paulo State. Pesq agropec bras Brasília37, 109-115.

Valent, B. and Khang, C.H. (2010) Recent advances in rice blast effector research. Current Opinion in Plant Biology 13, 434–441.

Vergne, E, Ballini E, Marques S, Mammar BS, Droc G, Gaillard S, Bourot S, DeRose R, Tharreau D, Notteghem J-L et al., 2007. Early and specific gene expression triggered by rice resistance gene Pi33 in response to infection by ACE1 avirulent blast fungus. New Phytologist 174, 159–171.

Vergne, E., Grand, X., Ballini, E., Chalvon, V., Saindrenan, P., Tharreau, D., Nottéghem, J.L., Morel, J.B., et al., (2010) Preformed expression of defence is a hallmark of partial resistance to rice blast fungal pathogen Magnaporthe oryzae. BMC Plant Biology 10, 206.

Wang, Z.Y., Jenkinson, J., Holcombe, L., Soanes, D., Veneault-Fourrey, C. and Bhambra, G. (2005) The molecular biology of appressorium turgor generation by the rice blast fungus Magnaporthe grisea. Biochemical Society Transactions 33 part 2, 384-388.

Wei, T., Ou, B., Li, J., Zhao, Y., Guo, D., et al., (2013). Transcriptional Profiling of Rice Early Response to Magnaporthe oryzae Identified OsWRKYs as Important Regulators in Rice Blast Resistance. PLoS ONE 8, e59720.

Wilson, R.A. and Talbot, N.J. (2009) Under pressure: investigating the biology of plant infection by Magnaporthe oryzae. Nat Rev Microbiol 7, 185-195.

Xue, M.F., Yang, J., Li, Z.G., Hu, S.N.A., Yao, N., Dean, R.A., Zhao, W.S., Shen, M., Zhang, H.W., Li, C., et al., (2012) Comparative analysis of the genomes of two field isolates of the rice blast fungus Magnaporthe oryzae. PLoS Genet 8, e1002869.

Yoshida, K., Saitoh, H., Fujisawa, S., Kanzaki, H., Matsumura, H., Tosa, Y., Chuma, I., Takano, Y., Win, J., Kamoun, S., et al., (2009) Association genetics reveals three novel avirulence genes from the rice blast fungal pathogen Magnaporthe oryzae. Plant Cell 21(5), 1573-1591.

Zeigler, R. (1998) Recombination in Magnaporthe grisea. Annual Reviews of Phytopathology 36, 249-275.

Zhang, S. and Xu, J.R. (2014) Effectors and Effector Delivery in Magnaporthe oryzae. PLoS Pathog 10, e1003826.

Zhou, X., Liu, W., Wang, C., Xu, Q., Wang, Y., Ding, S. and Xu, J. R. (2011) A MADS-box transcription factor MoMcm1 is required for male fertility, microconidium production and virulence in Magnaporthe oryzae. Mol Microbiol 80, 33–53.

Chapter 2: Rice NILs carrying *Pi54* in LTH and Co39 backgrounds confer resistance to *Magnaporthe oryzae* at 35°C but show contrasting reactions at 28°C*

.First, third and last authors: Division of Plant Pathology and Crop Protection, Department of Crop Sciences, Georg-August-University Göttingen, Germany; second author: Erfurt University of Applied Sciences, Horticulture - Plant Production and Climate Change, Germany; fourth author: Africa Rice Center, P.O Box 33581, Dar es Salaam, Tanzania.

Introduction

Global climate models project an increase in average global temperatures by 2 to 5°C until the end of this century (Bokszczanin and Fragkostefanakis, 2013). In the past three decades the average global surface temperatures were reported to have increased by 0.2°C per decade, and eleven out of twelve years registered as the warmest in history since 1850, occurred between 1995 and 2006 (Ghini et al., 2008). Knowledge on the mechanisms underlying the effect of high temperature (HT) on plant pathogen interaction is however limited, and has been largely contrasting. For instance, HT suppressed the resistance of wheat to *Puccinia graminis tritici* (Harder et al., 1979) and the resistance of soybean to *Phytophthora sojae* (Gijzen et al., 1996). The amount of *EDS1* and *PAD4* transcripts was also reported to be temperature dependent in Arabidopsis, with lower accumulation at 28°C than at 22°C (Yang and Hua, 2004). Conversely, the yellow rust resistance gene *Yr36* was reported to be up-regulated at HT, leading to full or partial resistance against stripe rust (*Puccinia striiformis*) in spring wheat (Fu et al., 2009). High temperature also positively modulated *Xa7* and *Rp1-D21* mediated resistance in rice (Webb et al., 2010) and maize (Negeri et al., 2013), respectively. Thus, plant response to both HT and pathogen stress, when occurring simultaneously, can be varied in multiple ways.

Magnaporthe oryzae is the most destructive pathogen of rice, a staple crop for over half of the world's population (Xue et al. 2012). The primary breeding tool in rice blast management is to introduce resistance (R) genes into elite rice cultivars. During the past 25 years, genetic and molecular analysis of resistant donors has led to identification and mapping of more than 100 major blast resistance (R) genes; 22 of these genes have been cloned and used for crop protection against *M. oryzae* (Zhang et al., 2015). Some of these R genes have been reported

to confer broad-spectrum resistance against *M. oryzae* strains tested under normal growth conditions (Liu et al., 2002; Jiang et al., 2012). However, the potential of rice and the introgressed R genes to adapt to both HT and *M. oryzae* stresses remains to be elucidated.

In the present study two rice NILs having Co39 (*Oryzae sativa-indica*, CO) and LTH (*O. sativa-japonica*, LT) as genetic backgrounds, and carrying the R gene (*Pi54*) were used to determine the response of rice to HT and Mo infection. *Pi54* possesses a nucleotide binding site-leucine rich repeat (NBS-LRR) domain in addition to a small zinc finger domain, and was previously reported to be constitutively expressed at a basal level in both resistant transgenic as well as susceptible rice lines up to 48 hpi (Gupta et al., 2012).

Results

Phenotypic performance of infected plants after high temperature exposure

We investigated the interaction between rice and *M. oryzae* under the normal growth temperature of 28°C and a warmer temperature of 35°C. Two rice genotypes, Li-Jiang-Xin-Tuan-He-Gu (LT; *Oryza japonica*) and Co39 (CO; *Oryza indica*) carrying *Pi54* R gene, were used. At 28°C, CO had a severe disease phenotype and displayed lesions within 5 days post inoculation (dpi), while LT exhibited reduced lesion sizes (Figure 2.1a). *Pi54*-associated lesion development was rarely observed in the plants grown and inoculated at 35°C. To exempt any direct effect of HT on the pathogen, such plants were grown at 35°C for 7 d prior to Mo inoculation, where after all procedures were carried out at identical temperature conditions (28°C). Pre-inoculation exposure to 35°C induced a delay in disease progress and typical HR lesions in both NILs (Figure 2.1b). To further investigate HT modulation of plant defence, the level of callose deposition in plants subjected to 35°C and inoculated with Mo was compared with that in plants grown and inoculated at 28°C. Ample callose deposition was observed in LT than CO at 28°C. At 35°C, a stronger induction of callose accumulation and intense cell wall fluorescence of the attacked epidermal cells was detected in both NILs (Figure 2.2).

Transcription profiles of CO and LT infected with *M. oryzae* at 28°C and 35°C

To determine temperature-induced transcriptome changes, genome-wide gene expression patterns were investigated in CO and LT using mRNA-Seq following exposure of rice plants to 35°C and Mo. An overview of the sequential steps from sample collection to data analysis

is provided in Figure 2.3a. Three biological replicates of each treatment were sequenced, yielding an average of 69,315,066 single-end reads. More than 80% of the total reads reached the quality scores at Q20 (Phred score), although a reduced number of quality reads was found in plants treated with double stress involving high temperature and *M. oryzae* infection (Figure 2.3b). To obtain the expression profiles and predict gene structures, the sequenced reads were mapped against the Ensembl cDNA release 16 for the *Oryza sativa* genome. Using Samtools generated BAM files as input, the R/Bioconductor environment was employed to calculate gene expression levels. We included both unique and multireads in the analysis to avoid undercounting genes with closely related paralogs. A false discovery rate (FDR) of 0.05 was set for the calling of differentially expressed genes (DEGs). The number of DEGs in infected rice (CO+28°C+Mo, LT+28°C+Mo, CO+35°C+Mo LT+35°C+Mo) was significantly higher than in rice plants subjected to only high temperature (CO+35°C and LT+35°C) (Additional file S1a-f). A considerable number of significantly regulated genes was shared by all the infected rice samples (3,557 genes), irrespective of the temperature treatment (Figure 2.4a). A total of 600 significantly regulated genes were shared between high temperature stress and *M. oryzae* infection (Additional file S2). A large number of DEGs (2,394) was shared between LT and CO in response to high temperature (Figure 2.4b). From the up-regulated temperature responding genes, 3,459 were exclusive to LT, 750 were found only in CO, and 969 were identified in both genotypes. From the down-regulated genes, 1,778 and 737 were identified as LT and CO-specific, respectively, and 1,400 were repressed in both genotypes. Hierarchical clustering analysis on the log2 transformed fold change values showed substantial transcriptional profile variation (Figure 2.4c). The response to only high temperature was distinct, and clustered separately, from infected samples.

Gene ontology enrichment analysis of DEGs from infected samples at both temperatures

Gene ontology (GO) categories were assigned to significant DEGs using the goseq R package, which requires the input of gene lengths based on the median length of transcripts associated with each locus (Young et al., 2010). We used the DEG estimates from DESeq analysis as input files for goseq. We found 34, 37, 35 and 30 GO terms overrepresented in CO+28°C+Mo, CO+35°C+Mo, LT+28°C+Mo and LT+35°C+Mo, respectively, with more than 4-fold increased enrichment value at a FDR value of ≥0.05 (Figure 2.5, Additional file S3a-d). The GO terms: defense response to the fungus, incompatible interaction (GO:0009817) and flavonoid biosynthetic process (GO:0009813) were unique to

CO+35°C+Mo, LT+28°C+Mo and LT+35°C+Mo. Response to biotic stimulus (GO:0009607) and heat acclimation (GO:0010286) were more enriched in LT than in CO. Diterpene phytoalexin metabolic process (GO:0051501), carbon utilization (GO:0015976) and cellular response to calcium ions (GO:0071277) were common to both backgrounds. When we analyzed only gene sets that are up-regulated in CO+35°C+Mo and LT+35°C+Mo, oxidation-reduction process was consistently significant in both backgrounds (Figure 2.6). However, cellular metabolic process, protein ubiquitination, carbon utilization, and response to salicylic acid stimulus were more enriched in CO+35°C+Mo, whereas response to salt stress, transmembrane transport, response to cadmium ion, cilliary or flagella motility, response to bacterium and cellular protein metabolic process were significantly enriched in LT+35°C+Mo. Down-regulated genes in both genetic backgrounds were mainly involved in photosynthesis (GO:0009765), citrate transport (GO:0015746) and chlorophyll biosynthetic process (GO:0015995). Our data show that many different pathways were involved and critical processes for the protection of the plant from stress such as oxidation-reduction process were highly enriched.

Gene expression profiles in LT and CO in response to only high temperature (35°C)

Heat stress presents an added degree of complexity in plant defense response to pathogen attack, as the response to heat is apparently controlled by largely different signaling pathways, and may interact positively or negatively with pathogen defense. We observed a significant overlap between genes induced and repressed by heat stress and genes induced by pathogen infection (Figure 2.4c). Since temperature-induced resistance to *M. oryzae* was more pronounced in CO than in LT, we studied high temperature responding genes and enriched GO terms in CO in contrast to LT. We found 145 significantly enriched GO terms (FDR≤0.05) in CO compared to 7 in LT (Table S1). The GO categories that were specifically enriched in CO in response to high temperature included starch biosynthetic process (GO:0019252), sucrose transport (GO:0015770), phosphatidylinositol metabolic process (GO:0046488) and galactolipid biosynthetic process (GO:0019375). GO analysis of LT DEGs revealed significant enrichment of pseudouridine synthesis (GO:0001522), RNA modification (GO:0009451) and flavonoid biosynthetic process (GO:0009813). Oxidation-reduction process (GO:0055114), zinc ion homeostasis (GO:0055069) and phenylpropanoid metabolic process (GO:0009698) were enriched in both backgrounds (Figure S1).

Among the defense response genes up-regulated in response to only high temperature, NB-ARC (LOC_Os11g45190) and PR6 (RBBI2-0; LOC_Os01g03680) were >34-fold induced in both backgrounds (Figure 2.7). Some NBS-LRR genes (e.g., LOC_Os11g45180, LOC_Os11g44960 and LOC_Os11g45050) were specifically induced in CO, whereas *Pit* (LOC_Os01g05620), NBS-LRR (LOC_Os01g05600) which shares 92% sequence homology with *Pit* and a putative stripe rust resistance protein *Yr10* homolog (LOC_Os12g17090) were induced in LT but not in CO. In the GO term, response to heat GO:0009408, twenty two transcripts were induced in LT compared to only six in CO. Genes encoding for small HSPs e.g., *HSP16.9A* (LOC_Os01g04370) were highly expressed in LT, whereas LOC_Os08g26230 and a heat shock protein 83 (*HSP90*; LOC_Os04g01740) exhibited higher induction in CO than in LT. Sequence alignment of LOC_Os08g26230 using Beijing Genomics Institute Rice Information System (BGI-RIS) revealed a 94% identity to BGIOSGA000853 with Serine/threonine-protein kinase activity. Several genes in the GO term, response to oxidative stress, showed contrasting expression patterns. For example, some peroxidases (e.g., LOC_Os04g59200 and LOC_Os08g41090), oxidoreductases (e.g., aldo/keto reductase; LOC_Os10g02490) and metallothionein-like protein 3B (e.g., LOC_Os05g11320) were strongly induced in LT than CO, whereas peroxidases (e.g., LOC_Os03g55410 and LOC_Os06g20150) were more induced in CO than in LT. Genes encoding for cytochrome P450 (e.g., LOC_Os01g36294) and CASP-like protein (LOC_Os03g60250) were induced by high temperature stress in both genetic backgrounds. In the GO term "response to hormone stimulus", SAM dependent carboxyl methyltransferase (LOC_Os06g13310), *OsGH3.2* (LOC_Os01g55940), 2OG-Fe (II) oxygenase domain containing protein (LOC_Os06g07914) were specifically up-regulated in CO but not in LT. Genes encoding for cytokinin-O-glucosyltransferase (e.g., LOC_Os02g51930) were strongly induced in both backgrounds. A transcription factor *OsIAA13* - Auxin-responsive Aux/IAA gene family member (LOC_Os03g53150) and C2H2 zinc finger proteins (LOC_Os06g34400) involved in zinc ion binding were up-regulated >60-fold in LT than CO. In addition, *PTAC12* (LOC_Os01g56350) involved in a plastid-encoded bacterial-type RNA polymerase (PEP) dependent transcription, pentatricopeptide repeat (PPR) containing proteins (e.g., LOC_Os03g11690 and LOC_Os03g55840), phosphoenolpyruvate/phosphate translocator (*OsPPT2*; LOC_Os08g25624) involved in dihydroxyacetone phosphate transport and a membrane localized proton-dependent oligopeptide transporter (LOC_Os01g65140) were stronger induced in LT than CO. Furthermore, a putative DNA-binding bifunctional nuclease 1 (OsBBD1; LOC_Os01g50622) involved in abscisic acid-derived callose deposition was

induced >100-fold in LT than CO. In contrast, splicing factor U2af small subunit A (LOC_Os09g31482) involved in mRNA processing, proliferating cell nuclear antigen (PCNA; LOC_Os02g56130), glucose-6-phosphate 1-dehydrogenase (LOC_Os03g20300) and expressed protein (LOC_Os06g20270) were strongly induced in CO than LT. In addition, terpene synthase (LOC_Os04g27430), and DUF6 containing protein (LOC_Os04g34530) which shares 88% sequence homology with Walls Are Thin1 (*WAT1*) were stronger induced in CO than LT.

Expression of peptidyl-prolyl isomerase is elevated in response to 35°C plus *M. oryzae* infection

To investigate the effect of rising temperature and *M. oryzae* infection on both LT and CO, we examined highly induced genes in CO+35°C+Mo and LT+35°C+Mo treatments. Among the genes with significant up regulation were genes encoding for peptidyl-prolyl isomerase (*PPIase*, LOC_Os04g28420), *HSFA2* (LOC_Os03g53340), photosystem II 10 kDa polypeptide/ chloroplast (LOC_Os07g05360), S-adenosyl-L-methionine benzoic acid/salicylic acid carboxyl methyltransferases and expressed proteins (e.g., LOC_Os09g13440). Perhaps the most compelling observation was the significantly higher expression of peptidyl-prolyl isomerases (*OsFKBP65*) in CO+35°C+Mo and LT+35°C+Mo. *OsFKBP65* belongs to a class of FK506-binding proteins (FKBPs) with a cis/trans isomerase enzyme activity, some of which can operate as molecular chaperones. *OsFKBP65* is a duplicate form of *OsFKBP64* both of which were reported as up-regulated by heat treatment (Magiri et al., 2006). *OsFKBP65* and *OsFKBP64* are orthologous to Arabidopsis *AtFKBP65* (*ROF2*) and *AtFKBP62* (*ROF1*) (Aviezer-Hagai et al., 2007). *OsFKBP65* was induced >100-fold in CO+35°C+Mo and LT+35°C+Mo, while *OsFKBP64* (LOC_Os08g41390) was only slightly up-regulated (7-fold in CO and 4.5 in LT). The high induction of *OsFKBP65* was further confirmed by qRT–PCR in all samples (Figure 2.8).

Differentially expressed resistance (R) gene and R gene analogues (RGAs)

Nucleotide-binding and leucine-rich repeat (NB–LRR) R proteins are important for rice resistance response to biotic challenges, including infection with the rice blast fungus (Okuyama et al. 2011). In our dataset, 61 and 75 genes encoding for R like proteins were up-regulated (>4 fold) in LT+28°C+Mo and CO+28°C+Mo, respectively (additional file S4). The number, however, decreased to 50 and 63 in LT+35°C+Mo and CO+35°C+Mo, respectively.

Database similarity searches indicated that the highly up-regulated R like genes in LT+35°C+Mo and CO+35°C+Mo were identical to *RPM1* (LOC_Os08g16070 and LOC_Os11g11770), *PibH8* (LOC_Os08g42700), *Xa1* (LOC_Os04g53160), putative pleiotropic drug resistance proteins (*PDR4/PDR8*; LOC_Os01g42410 and PDR like ABC transporter; LOC_Os11g37700), *RPR1* (LOC_Os11g12000) and *RPS2* encoding genes (e.g., LOC_Os01g72680 and LOC_Os04g43440). In plants grown at 28°C, LOC_Os11g45060 was induced 168 and 117-fold in LT and CO, respectively. The gene LOC_Os04g41370, which shares 63% homology with *Pi54* (4.1e-30), was 39 and 17-fold up-regulated in CO and LT, respectively, at 28°C, but its expression was lower (11-fold in CO and 8-fold in LT) at high temperature. We tested the expression of *Pi54* (LOC_Os11g42010) using qRT-PCR (Figure 2.9). *Pi54* was expressed to a greater extent at 24 hpi than at 48 hpi. This probably explains why it was undetected in our samples at 48 hpi. *Pi54* also exhibited sensitivity to high temperature with reduced expression at 35°C in both backgrounds.

Respiratory burst resistance components

Reactive oxygen species (ROS) play a significant role in plant defense against pathogen attack through the establishment of hypersensitive response (HR). The cell membrane NADPH oxidases (Noxs) are major sources of reactive oxygen species (ROS) under both normal and stress conditions in plants. Oxidative stress gene, OsNox9 (LOC_Os12g35610) was stronger induced in LT compared to CO at both temperatures, whereas NADPHoxi (RbohD) was stronger induced in CO than LT, with a stronger induction at 35°C compared to 28°C. To elucidate on this finding, we investigated H_2O_2 production in the leaves infiltrated with diaminobenzidine (DAB). Interestingly, intense brown precipitation was observed in all infected plants, and we were unable to convincingly demonstrate any difference in H_2O_2 production between plants infected at 28°C and 35°C. We further quantified the accumulation of H_2O_2 in plants exposed to 35°C and *M. oryzae* infection in comparison with plants exposed to 28°C. In accordance with callose deposition, both NILs had significantly higher H_2O_2 levels during Mo infection of plants pre-exposed to 35°C (Figure 2.10A). H_2O_2 levels were also consistently higher in LT than CO at 28°C.

Both NADPH oxidases and cell wall peroxidases are known to be mediators of ROS production in response to pathogen attack. More than 20 peroxidase genes were differentially expressed in response to infection compared to <10 in response to high temperature

(additional file S5). Some peroxidase encoding genes were background specific in expression. In the case of LT, LOC_Os04g59200 was >80-fold up-regulated in response to both temperature and infection, while LOC_Os04g59160 was >100-fold up-regulated in CO at 28°C. LOC_Os04g59190 and LOC_Os01g73200 were expressed in both backgrounds during infection, with a significantly higher up-regulation in CO than in LT. These observations were confirmed by a significant increase in POX activity in CO compared to LT during infection at 28°C, 48 hpi (Figure 2.10B). However, at 24 hpi, both backgrounds showed increased POX activity in response to Mo. Moreover, POX activity was consistently higher in both backgrounds when subjected to only high temperature, indicating similar temperature sensitivities with respect to POX activity.

Hormone signaling pathway in relation to high temperature induced resistance

Plant hormones are key signaling molecules in response to stress. Three hormones are of particular significance in plant response to pathogen infection: salicylic acid (SA), jasmonic acid (JA) and ethylene (ET). The phenolic phytohormone, SA, has beneficial effects on plant growth and development under stress conditions (Awasthi et al., 2015). The biosynthesis of SA and other phenolics involved in plant resistance requires the activity of phenylalanine ammonia-lyase (PAL), the first enzyme of the phenylpropanoid pathway (Duan et al., 2014). To determine whether gene expression mirrored SA levels, we compared the levels of free SA and PAL activity in LT and CO plants exposed to 28°C and 35°C at 24 and 48 hpi. Free SA was consistently higher in CO than LT in plants grown and inoculated at 28°C (Figure 2.11). Surprisingly, free SA significantly increased in both NILs after exposure to 35°C, although this increase did not last longer in LT. At 48 hpi free SA declined sharply in LT compared to CO; the decline was substantially contrastive at 35°C than at 28°C. There was a comparably similar pattern in PAL activity in LT plants exposed to 35°C (Figure 2.12). Although PAL activity was higher in LT than CO at 24 hpi at both temperatures, there was a sharp decline of PAL activity in LT plants exposed to 35°C and Mo at 48 hpi, when compared to that of CO plants.

Genes encoding for SA conversion to MeSA, e.g., S-adenosyl-L-methionine: benzoic acid/salicylic acid carboxyl methyltransferase (SAMT) were highly induced in plants pre-exposed to 35°C than 28°C (additional file S6) prior to *M. oryzae* infection. SAMT genes with greater induction included *OsBISAMT1* (LOC_Os11g15040), LOC_Os06g13560 and

LOC_Os11g15300. *OsBISAMT1* was also up-regulated >80-fold in response to high temperature in both backgrounds. Analyses of *OsBSMT1* expression in wild-type rice plants under various stress conditions was reported to be regulated by jasmonic acid (JA) signaling pathway in rice (Zhao et al. 2010). Although genes encoding for proteins in the jasmonic acid synthesis and signaling pathway were highly induced in both backgrounds, including *LOX2* like genes (e.g., LOC_Os08g39840 and LOC_Os08g39850), 12-oxophytodienoate reductases (e.g., LOC_Os06g11200 and LOC_Os06g11240), allene oxide synthase (LOC_Os02g12680) and *OsMYB4* (LOC_Os02g41510), there is little evidence supporting their relevance in *OsBSAMT1* expression. Previous studies have shown that SA and MeJA conditionally regulate *PDF1.2* expression through their activity on *NPR1* (Mur et al. 2006). However, Jasmonate O-methyltransferases (e.g., LOC_Os06g21820) which catalyze the conversion of JA to MeJA and jasmonate induced jacalin-like lectin (LOC_Os12g14440) that mediates broad spectrum resistance were highly induced in LT than CO. As reported earlier, LT had lower levels of SA compared to CO, suggesting that the positive interaction between MeJA and SA likely occurs at relatively lower levels of SA.

In the ethylene signaling and biosynthetic pathway, we detected >100-fold higher induction of a putative constitutive stress-response transcriptional coactivator multiprotein bridging factor 1c (*MBF1c*; LOC_Os06g39240) at 35°C than at 28°C in CO, but consistent expression levels were observed in LT at both temperatures. Genes encoding for 1-aminocyclopropane-1-carboxylic acid (ACC) synthase (e.g., *ACS6*; LOC_Os04g48850), a key enzyme in ethylene synthesis, were >90 times up-regulated in CO than LT at both temperatures. In addition, elevated transcript levels of flavonol synthase, a rice ortholog of *DMR6* (LOC_Os03g03034) involved in the last step of ethylene synthesis was detected in both backgrounds but with a stronger induction in CO than LT.

Many genes involved in gibberellins pathway (e.g., *GID1L2*; LOC_Os03g57640), auxin (e.g., auxin efflux carrier; LOC_Os09g31478) and abscicic acid (e.g., *HVA22* (LOC_Os11g05800) were strongly induced in response to Mo, irrespective of the temperature treatment. However, genes encoding for auxin (e.g., OsIAA13) and cytokinin suppressors and ABA responsive genes (e.g., GEM; LOC_Os02g42430) were strongly induced in plants exposed to 35°C.

Activated signaling pathways involved in rice defense against pathogen attack

Receptor like kinases (RLK)

About 1,100 RLKs that are involved in numerous cellular signaling and developmental events have been reported in rice (Kawano and Shimamoto 2013). Our transcriptome analysis revealed a large number of genes encoding putative receptor kinases (Additional file S7). Within the highly expressed genes, 19 DEGs were annotated as cysteine rich (CRKs), 64 wall associated kinases (OsWAK), 24 SHR5-RLKs, 2 LRRs, 19 S-locus/domain-like receptor protein kinases, 10 senescence-induced receptor-like serine/threonine-protein kinases, 10 Ser/Thr receptor-like kinases and 78 generally annotated as RLKs. The cysteine-rich RLKs (CRKs) represent a prominent subfamily of transmembrane-anchored RLKs, 263 of which are found in rice (Wrzaczek et al., 2010). The CRK encoding genes (e.g., *CRK5*; LOC_Os04g56430 and LOC_Os04g25060), were >60-fold induced in response to *M. oryza* infection. S-locus-like receptor protein kinases (e.g., LOC_Os12g03640) were induced >65-fold in LT than in CO, whereas lectin-like receptor kinase encoding genes, e.g., LOC_Os07g03780, LOC_Os02g42780 and LOC_Os11g03820, were strongly induced in CO than LT. Genes encoding for wall-associated receptor kinase-like (e.g., *OsRLCK146*; LOC_Os04g30060) and wall-associated receptor kinase 3 (LOC_Os04g30110) were induced in response to *M. oryzae* and high temperature. *OsWAK80*, *OsWAK60* and *OsWAK47* were >50-fold up-regulated in both backgrounds, but with a higher induction in CO than in LT. Three SHR5-receptor-like kinase encoding genes, LOC_Os05g17604, LOC_Os05g16430 and LOC_Os05g16920 were up-regulated >50-fold in both backgrounds. Moreover, LOC_Os05g16430 was induced >20-fold in response to only high temperature, suggesting its involvement in heat stress response. Most SHR5 proteins possess leucine-rich repeats (LRR) extracellular domain, placing these receptors into the LRR-RLK family. Interaction network search using PlaNet showed that LOC_Os05g16920 falls in the same interaction network with LOC_Os05g17604 and cytochrome P450 (LOC_Os08g39660), both of which were highly expressed in this study. Cytochromes P450 are mainly involved in alleviating oxidative stress, and activation of allene oxide synthases (*AOS*). This may suggest that SHR5 proteins perceive oxidative stress signals, and probably act upstream of several signalling molecules, including JA.

Calcium, calcium-dependent protein kinases

Cytoplasmic calcium participates in numerous events including signaling, cell membrane permeability and cell wall formation. Calcium metabolism is associated with ROS signaling, and ROS are apparently required to prime Ca^{2+} influx after elicitation (Torres et al., 2006). Several of Ca^{2+} binding protein encoding genes, showed reduced expression at high temperature when compared to their expression in response to *M. oryzae* infection. However, induction of calreticulins (e.g., LOC_Os04g32950) and EF-Hand type family proteins (e.g., LOC_Os03g29770) at 35°C than 28°C was observed in both backgrounds, and may suggest a possible role in in heat stress response. Plants exposed to double stress involving high temperature and *M. oryzae* infection showed a high induction of calcineurin B (LOC_Os01g41510). Calcineurin B controls responses to stresses, including ion and thermal stresses, to adapt cell growth and proliferation to environmental stresses. With respect to the genetic background, we detected several up-regulated genes involved in calcium signaling during *M. oryzae* infection (additional file S8). At 28°C, *OsCML21* (LOC_Os05g24780) and *OsCML14* were induced >70-fold in both backgrounds, with >20-fold higher induction in LT than in CO. Putative sodium/calcium exchanger proteins encoding genes (e.g., LOC_Os12g42910 and LOC_Os05g51610) were more up-regulated in LT than in CO. In addition, RelA/SpoT protein (LOC_Os07g42160), which hydrolyses the nucleotide alarmone ppGpp, regulator of cellular metabolism in response to changing environmental conditions was also strongly induced in LT than CO. In contrast, genes encoding for *OsCML26*, *OsCML25* and *OsCML20* showed higher induction in CO than in LT. Furthermore, *OsCML15*, *OsCML4* and *OsCML31* were stronger induced in CO than in LT at both temperatures.

Mitogen activated protein kinases (MAPKs)

In rice-*M. oryzae* interaction, MAPKs play a significant role in signaling pathways leading to plant defence. More than 17 MAPKs (OsMPKs) with conserved protein kinase domains I–XI and an activation T-loop of either TEY or TDY motifs have been found in rice (Sheikh et al., 2013). In this study, we detected a significant transcript accumulation of six MAPK encoding genes during infection, including *OsMEK5, OsMEK1, OsMPK1, OsMPK5, OsMPK12* and *OsMPK13*. Interestingly, *OsMEK5* (LOC_Os06g09190) was >100-fold up-regulated in CO+28°C+Mo, but was relatively suppressed in CO+35°C+Mo. This suppression was probably crucial for effective defense response. *OsMPK1* (LOC_Os01g32660) was also up-

[36]

regulated 6-fold in CO+28°C+Mo compared to only 4-fold in LT+28°C+Mo. Protein serine/threonine kinase genes (e.g., *OsNPK4*; LOC_Os01g50420 and *WEE1*; LOC_Os02g04240) were induced >60-fold in response to infection at both temperatures. *OsMAPK5* was up-regulated >16-fold in CO during infection at both temperatures but not in LT. *OsMPK12* (LOC_Os06g49430) was induced 13-fold in CO+35°C+Mo compared to 6-fold in CO+28°C+Mo. Conversely, *OsMPK13* (LOC_Os02g04230) was >20-fold induced in CO+28°C+Mo compared to 12-fold in CO+35°C+Mo. *OsMEK1* (LOC_Os01g32660) was 5-fold induced in CO+35°C+Mo but not in CO+28°C+Mo. *OsMEK1* is lately expressed in response to fungal elicitors and was shown to accumulate in cells inoculated with the avirulent strain of *M. oryzae* (Kim et al., 2000). Expression of these genes was relatively lower in LT at both temperatures. Taken together, differential expression of MAPK encoding genes between LT and CO indicates a significant background influence on their role.

Transcription factors (TFs) induced during high temperature stress

A total of 2,478 non-redundant set of rice TFs compiled from the Plant Transcription Factor Databases are available in RiceSRTFDB (Priya and Jain 2013). So far, 84 families have been classified based on their domain composition following the rules for each family. TFs exhibited complex expression patterns in response to temperature and *M. oryzae* in both backgrounds (additional file S9). The majority of TFs were activated in response to *M. oryzae* compared to high temperature, indicating that the critical transcriptional changes occurred more predominantly in response to pathogen stress than in heat stress. *MYB* was the largest group induced in plants subjected to 35°C, and this was consistent with a high frequency (>90%) of *cis*-elements for water stress (MYBCORE) and dehydration stress (MYB1AT) response in both sense and antisense strands of most temperature stress responsive DEGs. Among *MYB* genes induced were the *R1-MYB/MYB-like* subfamily genes (e.g., LOC_Os01g60850, LOC_Os03g55840 and LOC_Os01g74600), which were common to both backgrounds but were highly induced in LT than CO. Two *AP2-EREBP* genes with the cis acting element GCC-Box (AGCCGCC); *AP2/ERF-138* (LOC_Os09g11480) and LOC_Os05g45954 were induced >5 fold in LT but not in CO. Among *WRKY* genes, *OsWRKY111* (LOC_Os05g50700) was strongly induced in both backgrounds. The *SWIB/MDM2* complex (LOC_Os03g55310) involved in chromatin remodeling, bZIP genes (e.g., *bZIP62*; LOC_Os07g48660 and LOC_Os05g16640) and *OsMADS25* (LOC_Os04g23910) were >20-fold induced in LT but not in CO. Our dataset also showed

overlap in the induction of members of homeobox (HB), bHLH, NAC families, and genes that encode zinc-coordinating elements like C2H2, C2H2 CO-like, C3H, GATA, GT (trihelix DNA binding proteins) and histone H2A in response to high temperature.

Homeobox (HB), bZIP, AP2-EREBP and MYB transcription factor encoding genes are highly induced during *M. oryzae* infection

Homeobox is a highly conserved domain in plants, animals and fungi, and their role in maintenance of shoot apical meristem and epidermal development has been demonstrated (Sentoku et al., 2000). In rice, a well-characterized TF in this group is *OsBHID1* which encodes a BELL type homeodomain protein (Luo et al., 2005). *OsBHID1* was reported to be rapidly induced by BTH and *M. oryzae*. In our dataset we instead found a high induction of *HOX24* and a putative Ser/Thr-rich protein T10 in DGCR region (LOC_Os09g15480) in LT+28°C+Mo (additional file S9). *HOX24* belongs to the HD-Zip family of HD proteins, characterized by an additional leucine zipper motif adjacent to the HD which facilitates homo- and heterodimerization of the transcriptional regulators (Johannesson et al., 2001). *HOX24* shares 65% homology with Arabidopsis *ATHB-6* which was identified as a negative regulator of ABA signal pathway (Himmelbach et al., 2002). *ATHB-6* interacts with abscisic acid insensitive 1 (*AB1*), an upstream phosphatase. In our dataset we instead found higher induction of a putative *bZIP* transcription factor, *ABA INSENSITIVE 5* (*ABI5*) in LT but not in CO. ABA and OPDA act synergistically to increase levels of *ABI5* (Dave et al. 2011). *ABI5* is also up-regulated in the ped3 allele, which in turn leads to higher levels of polygalacturonase inhibiting proteins (Kanai et al., 2010). The higher induction of *OsBURP16* (LOC_Os10g26940) in LT compared to CO is however intriguing. *OsBURP16* belongs to 21 PG1-β-like sub family of *BURP* genes and encodes a putative PG1-β-subunit 22 precursor in rice which was previously reported to be up-regulated by ABA treatment (Ding et al., 2009). PG1s decrease pectin content and cell adhesion and increases abiotic stress sensitivity in rice. The inhibition of PG1 is not well understood. However, internal dynamics leading to inhibition could probably involve *ABI5* in the induction of PG1 inhibitors. Another ABA responsive *OsBURP* gene (*OsBURP05;* LOC_Os04g14990) from the RD22-like subfamily was induced >100 times higher in CO than LT. RD22 is expressed in response to drought stress, and appears to play a different role from *OsBURP16*.

We also detected a significant induction of *HBP-1b* (LOC_Os01g06560) in both backgrounds. In addition, four of the *MYB* genes, *MYB-1, MYB-101, MYB-120* and LOC_Os02g07170, were more induced in LT, while *MYB-33* and LOC_Os02g07170 showed >100-fold induction in CO. The basic helix-loop-helix encoding gene *bHLH25*, and auxin response genes *OsSAUR2* and *OsSOUR15* were strongly induced in CO than in LT. *WRKY* genes that showed high induction in LT during *M. oryzae* infection included *OsWRKY55*, *OsWRKY62*, *OsWRKY28* and *OsWRKY71*, whereas *OsWRKY32, WRKY97, OsWRKY28, OsWRKY27* and *OsWRKY84* showed higher induction in CO.

Aspartic proteinases and antimicrobial compounds are highly up-regulated during *M.oryzae* infection.

Plant aspartic proteinases (APs) have several functions in plants, including protein processing and/or degradation during plant senescence, stress response, programmed cell death, and reproduction. In this study, the putative aspartic proteinase nepenthesin encoding genes (e.g., LOC_Os10g39260 and LOC_Os10g39300) showed >100-fold induction in CO as compared to <100-fold in LT (additional file 10). Both genes are designated as signal peptides in the TIGR database and appear to be homologous. The signal peptides encoded by these genes are involved in hydrolase activity and fall in the super family of acid proteases. The increase in their transcript levels suggests a significant role in rice response to *M. oryzae*. On the other hand, defensins (e.g., *DEFL9*; LOC_Os06g22919 and *DEFL49*; LOC_Os04g31250), thionins (e.g., LOC_Os07g24820), lipid transfer proteins LTPs (e.g., LOC_Os10g36070, LOC_Os10g36090 and LOC_Os10g36100), ligatoxin A (e.g., LOC_Os07g46950) and *BBTIs* were >20 fold induced in LT+35°C+Mo and CO+35°C+Mo, suggesting their involvement in rice defense. Genes involved in folate deglutamylation, ubiquitination and subsequent proteasomal degradation of target proteins, including gamma-glutamyl hydrolase (LOC_Os05g44130), *SKP1-like protein 1B* (LOC_Os10g30200) and cullin (*CUL1*; LOC_Os01g70920) that perceive JA-Ile or giberellin in the nucleus and direct targeted degradation of transcriptional repressors, were stronger induced in CO than LT at high temperature. In contrast, RING-H2 finger proteins encoding for E3 ubiquitin ligase (LOC_Os05g40020), *OsFtsH6 FtsH* protease (LOC_Os06g12370) involved in oxygenic photosynthesis, peptidase C19, ubiquitin carboxyl-terminal hydrolase 2 and *OsFBO10* involved in signaling were strongly induced in LT than in CO in response to high temperature.

Transcriptional regulation of the TCA cycle, carbon and amino acid metabolism

Under stressful conditions, plant cells must maintain a balance between energy generation and synthesis of structural biomolecules to meet the demands. The glyoxylate shunt in the TCA cycle is of primary importance for the conversion of stored lipids to carbohydrates that serve as an alternative carbon source during stress. Two enzymes: isocitrate lyase and malate synthase are involved in glyoxylate shunt pathway, and contribute to the synthesis of cell components such as cell-wall polysaccharides, nucleotides, and amino acids (Mizuno et al., 2012). In this study, isocitrate lyase (*ICL1*) and malate synthase encoding genes, LOC_Os07g34520 and LOC_Os04g40990, were >100-fold up-regulated in both backgrounds during *M. oryzae* infection (Additional file S11). In addition, genes encoding for bifunctional monodehydroascorbate reductase (e.g., LOC_Os11g05520) and dehydrogenase E1 component (e.g., LOC_Os04g02900) were strongly induced in both backgrounds. Genes encoding for citrate synthase, dihydrolipoyl dehydrogenase and aconitate hydratase showed contrasting expression in LT and CO.

Plant defence response requires an abundant supply of energy derived from carbohydrate metabolism. Genes encoding for starch mobilization, including alpha-amylase (*Amy3*; LOC_Os08g36910), were >60-fold induced in both backgrounds during *M. oryzae* infection. UDP-glucoronosyl (LOC_Os09g34250) and UDP-glucosyl transferases (LOC_Os02g10880) were induced >10-fold in response to high temperature and *M. oryzae* infection in CO and LT, respectively.

Amino acid metabolism genes encoding for asparagine synthetase, a crucial enzyme in primary nitrogen metabolism, alanine-glyoxylate aminotransferase, isovaleryl-CoA dehydrogenase and 2-aminoethanethiol dioxygenase were >40-fold induced in both CO and LT in response to *M. oryzae* infection, whereas fumarylacetoacetase, 2-isopropylmalate synthase B and D-3-phosphoglycerate dehydrogenase were up-regulated in response to high temperature.

Photosynthesis and lipid metabolism

Genes involved in photosynthesis and chlorophyll biosynthesis are mostly down-regulated in many plant microbe interaction studies, especially in HR associated plant defence responses (Berger et al., 2007). However, in this study we detected a high induction (>50-fold) of photosystem II 10 kDa polypeptide encoding genes (e.g., LOC_Os07g05360 and

[40]

LOC_Os07g05365) during high temperature stress and *M. oryzae* infection (Additional file 12). The other genes that were highly induced include glycolate oxidase (*GLO3*; LOC_Os04g53210), a key enzyme in photorespiration, catalyzing the oxidation of glycolate to glyoxylate. Several cytochrome P450s (e.g., LOC_Os02g36280) were also induced >100-fold during *M. oryzae* infection in both backgrounds. Genes encoding for oxygen evolving enhancer protein 3 (*OEE3*; LOC_Os02g36850) required for photosystem II assembly/stability, chloroplastic group IIA intron splicing facilitator (*CRS1*; LOC_Os07g30670) involved in chloroplast protein translation and 2Fe-2S iron-sulfur cluster binding protein (LOC_Os07g30670) were >30-fold induced in LT than in CO in response to high temperature. A putative photosystem Q (LOC_Os10g21192) and a photosynthetic reaction center protein (LOC_Os10g39880) were specifically induced in CO at high temperature.

Lipid metabolism is important in the biosynthesis of precursors for plant cuticle synthesis, plant hormones and cell membranes. Interestingly, most genes in the lipid metabolic pathway were either not expressed or down-regulated in plants subjected to 35°C. Nonetheless, we detected a slight induction of a putative flavonol sulfotransferase (LOC_Os12g17160) in both backgrounds in response to high temperature. One GDSL like gene (LOC_Os01g11730) was highly induced (>100-fold) in both backgrounds, but to a higher level in LT than CO. In contrast, putative lipase encoding genes (e.g., LOC_Os06g10850) were more induced in CO than LT. Genes encoding for omega-6 fatty acid desaturase (LOC_Os07g23410), male sterility protein 2 (fatty acid reductase 1; LOC_Os08g44360), diacylglycerol acyltransferase (LOC_Os09g33530) and thioesterase family protein (LOC_Os09g33530) were highly induced in response to *M. oryzae* infection at both temperatures.

Expression of PR genes

Pathogenesis related (PR) proteins are rapidly induced by pathogenic infection through the coordinated action of SA, JA and ET signaling pathways. We found a significant overlap in transcript accumulation of several PR encoding genes between CO and LT. At 35°C, without *M. oryzae* inoculation, we detected a significant induction of several PR6 genes including *RBBI2-0, RBBI2-1, OsOC-6, OsOC-1* and *OsWIP1-1*, in both backgrounds (Figure 2.13). Conversely, PR3 (*CHIT17*; LOC_Os05g33130) and PR2 (*Gns6*; LOC_Os01g71350) were significantly induced in CO but not in LT, whereas PR-5 (*TLP-D34*; LOC_Os12g43380) was >10-fold induced in LT but not in CO.

In plants inoculated with *M. oryzae*, allergen V5/Tpx-1 related family protein encoding genes were the most highly induced in both CO and LT (>100-fold). Two of these genes, LOC_Os07g03319 and LOC_Os07g03499, were highly induced in LT, while LOC_Os07g0336, LOC_Os07g03279 and LOC_Os07g03458 were highly induced in CO. On the other hand, we detected high induction of *PR-1a* like genes (e.g., LOC_Os07g03580 and LOC_Os07g03730) in CO more than in LT. High induction (>70-fold) of glucan endo-1,3-beta-glucosidases (e.g., *Gns12*; LOC_Os07g35350, *Gns14*; LOC_Os07g35350), *OsPR4b* and *OsPR4c* was detected in both backgrounds, irrespective of the temperature treatment. Transcript accumulation of the gemine like protein (GLP) encoding genes overlapped between the two backgrounds. *GLP1* (LOC_Os04g22080) was >160-fold expressed in LT but was not significantly expressed in CO. In contrast, LOC_Os08g13440 was >200-fold induced in CO compared to only 31-fold in LT. There was, as well, an overlap in the expression of PR-5 encoding genes. PR5 like genes, LOC_Os12g43380, LOC_Os12g43390 and LOC_Os12g43410, were significantly induced in both backgrounds but to a lesser extent in LT than in CO. Conversely, a subtilisin-like serine proteinase, *OsSub13*, belonging to a class of pathogenesis-related proteins (Jorda and Vera 2000), and a protein-disulfide isomerase (*OsPDIL1-1*), involved in the biosynthesis of a group of plant defense peptides called cyclotides (Jennings et al., 2001), were more induced in LT than in CO. Expression of glycosyl hydrolase (GH) genes encoding for β-1,3 glucanases, including LOC_Os01g71830, LOC_Os01g71340 and LOC_Os01g71650, was detected in both CO and LT. Acidic endochitinase (CHIT) encoding genes (e.g., LOC_Os05g15880, LOC_Os11g47500 and LOC_Os06g25010) were the most consistently expressed among the CHIT genes up-regulated, and were equally expressed in LT and CO at both temperatures during pathogen infection. In addition, transcript accumulation of *CHIT14, CHIT15* and *CHIT16* was also detected in both backgrounds. Our results demonstrated that the expression pattern of PR genes in LT and CO infected samples is somewhat similar, although the level of induction is variable. On the other hand, high temperature affected the transcription of PR genes in both backgrounds, but the magnitude also varied with the genetic background.

Expression of genes involved in secondary metabolism during pathogen infection

Secondary metabolism, including the production of phytoalexins, plays a significant role in plant defense against pathogens. We analyzed transcripts from both genetic backgrounds for up-regulated DEGs involved in the various metabolic pathways in response to high

temperature and *M. oryzae* infection. The expression of blast-responsive genes encoding almost all of the biosynthesis enzymes of diterpenoid phytoalexins was either lower or down-regulated in plants exposed to only high temperature. However, activated secondary metabolism sub pathways included the phenylpropanoid, flavonoid and terpenoid metabolites (Additional file S13). Among the phenylpropanoids, hydroxycinnamoyl-CoA-shikimate (HCT; LOC_Os11g07960), caffeoyl-3-O-methyltransferase (LOC_Os08g38910) and cinnamyl alcohol dehydrogenase 6 (LOC_Os09g23550) were up-regulated (>4-fold). Phenyalanine ammonia lyase (PAL) encoding genes were down-regulated at high temperature, except *PAL2* (LOC_Os02g41670) that showed a >5-fold induction, with significantly higher induction in CO than LT. This is consistent with the higher PAL activity in CO plants pre-exposed to 35°C at 48 hpi reported earlier. During *M. oryzae* infection, genes encoding for O-methyltransferase (OMT), including flavonoid-7-OMT (LOC_Os09g17560) and putative O-methyltransferase ZRP4 (LOC_Os10g02880) were highly induced in LT but not in CO. In contrast, LOC_Os12g13800 was highly up-regulated in CO (>100-fold at 35°C, 37-fold at 28°C), but not in LT. *M. oryzae* infection also increased transcript levels of terpene synthase genes (LOC_Os08g07100, LOC_Os04g27190 and LOC_Os04g27670) oryzalexin biosynthesis genes, *ent*-kaurene synthase (*OsKSL8*; LOC_Os11g28530 and *OsKSL10*; LOC_Os12g30824), momilactones biosynthesis genes, *ent*-copalyl diphosphate synthase (*OsCPS4*; LOC_Os04g09900), (*OsKSL4*; LOC_Os04g10060) and *CYP99A2* (LOC_Os04g10160), and phytocasanes biosynthetic gene, *OsKSL7* (LOC_Os02g36140). Additionally, genes encoding for O-hydroxycinnamoyl transferase (LOC_Os04g56910), putative flavanone 3-hydroxylase (LOC_Os10g40934), putative transferase family proteins (LOC_Os08g02030 and LOC_Os04g56910), caffeoyl-CoA-O-methyltransferase (LOC_Os08g38920) putative decarboxylase (LOC_Os08g04540) and chalcone and stilbene synthases (LOC_Os07g34260) were highly induced in both backgrounds during *M. oryzae* infection.

Validation of differential Gene Expression of known temperature and infection responsive rice genes by qRT-PCR

The expression profiles of known responsive rice genes were validated by checking their up regulation at high temperature and during high temperature pathogen interaction (Figure 2.14). The response of all the measured genes was similar but the magnitude of response was greater in RNA-Seq. This analysis also confirmed the high induction of OsBISAMT1,

OsFKBP65 (Figure 2.8) and OsWRKY71 in plants pre-exposed to 35°C prior to infection compared to 28°C.

Discussion

In this study, we used two rice genetic backgrounds carrying *Pi54* with a general hypothesis that elevated temperature would weaken rice defenses and cause enhanced pathogen susceptibility, irrespective of the genetic background in which the R gene is introgressed. The two genotypes showed contrasting reaction to *M. oryzae* at 28°C, with CO displaying a more severe disease phenotype than LT. In accordance with restricted lesions sizes observed on infected leaves of LT, intense callose deposits and cell wall florescence were observed in LT than CO, indicating that *Pi54* was more effective in LT than in CO at 28°C. This is consistent with the previous reports that *Pi54* induces callose deposition (Gupta et al., 2012); although a substantial background influence was detected in this study. Surprisingly, a resistant response was observed in both backgrounds at high temperature. This led us to conclude that resistance in CO background is apparently more temperature dependent than in LT, and that similarities could probably exist between high temperature stress upstream signals and those associated with resistant defense response to *M. oryzae* infection. Indeed, we detected intense cell wall florescence and elevated levels of H_2O_2 in both backgrounds at 35°C, suggesting that induction of ROS and callose may be the first line of defense in plants pre-exposed to high temperature. Intriguingly, HT induced rice defense responses to Mo in both NILs were contrasted by a decrease in *Pi54* expression at HT, suggesting that this HT effect enhances plant resistance by either increasing the baseline levels of endogenous *Pi54* downstream products thereby decreasing its expression or act independent of *Pi54*. Thus, it was critical to identify genetic factors that reinforce plant defenses against pathogens at HT. Therefore, an RNA-Seq analysis was carried out to determine whether and how HT and Mo infection alters the transcriptome in the two contrasting NILs.

Our data showed a substantially higher number of DEGs in *M. oryzae* infected rice than in rice subjected to only high temperature, suggesting that rice-*M. oryzae* interaction involved more genome transcriptional regulation than the rice-high temperature interaction. In addition, the response to only high temperature was distinctively different, and clustered separately from both 35°C-plus-*M. oryzae* and 28°C-plus-*M. oryzae* treatments. However, combining both stresses sequentially, by exposing plants to high temperature followed by *M. oryzae*

infection (35°C-plus-*M. oryzae*), induced both heat and pathogen stress response genes, although disproportionately, suggesting a possible crosstalk between the responses elicited by the two stresses. Our study identified 600 common genes in both high temperature and *M. oryzae* stress conditions. These genes may form a basis for further investigation of crosstalk between abiotic and biotic stress responses. Several genes of unknown function were also induced in plants exposed to high temperature and *M. oryzae* infection (Figure 2.15), some of them may be a target for further investigations. However, several of the defense response genes showed lower induction in plants subjected to 35°C-plus-*M. oryzae* compared to plants inoculated at 28°C, suggesting that coping with two energetically demanding processes simultaneously prompts the plant to trade off some biochemical processes.

Gene ontology analyses revealed some similarities in the DEGs from both backgrounds during *M. oryzae* infection and in response to high temperature stress. A large part of the modulated transcriptome was devoted to control the main metabolic processes (e.g., oxidation-reduction reactions, photosynthesis, defence response to fungus, carbohydrate, lipid and cellular homeostasis) in both backgrounds. Redox reactions are the basis for many biochemical pathways related to the plants ability to cope with ROS. A stronger enrichment of oxidation-reduction reaction in both genetic backgrounds suggests similarities in oxidative stress response. Heat acclimation was higher enriched in LT compared to CO, suggesting that cellular processes related to heat stress response were more affected in LT compared to CO. In addition, the GO terms pseudouridine synthesis and RNA modification were specific to LT at high temperature (Appendix 2, Figure S1). Pseudouridines (Ψ) have been reported to enhance thermodynamic stability of RNA duplexes through substitution of Ψ for U (Kierzek et al. 2014). The significant enrichment of GO:0001522 in LT, suggests a crucial role of pseudouridines in thermo protection of rice cells. The significant enrichment of defense response to fungus, incompatible interaction in LT compared to CO in response to *M. oryzae* infection at 28°C, suggests defense related transcription enhancement in LT than CO, and may be a reason for the differential disease phenotypes between the two genetic backgrounds at 28°C.

Genes encoding for heat stress response proteins (e.g., *OsFKBP65*) were among the top up-regulated genes in all treatments, and likely perform defense roles in both abiotic and biotic stresses. There are 29 FKBP loci in the rice genome, however, the specific induction of *OsFKBP65* suggests its crucial role in both thermotolerance and pathogen defense. Bissoli et

al. (2012) suggested that ROF2, an orthologue of OsFKBP65, regulates intracellular acid stress, resulting from protein denaturation, by activating H$^+$ extrusion. The same authors showed that over-expression of ROF2 activates K+ uptake. Indeed we found >100-fold induction of a putative potassium transporter encoding gene (LOC_Os03g37930) suggesting a possible involvement of OsFKBP65 in K+ uptake. FKBPs are also implicated in tobacco and wheat disease resistance (Shumilina et al., 2006). A recent study by Narsai et al. (2013) showed overrepresentation of peptidyl isomerases in rice against bacterial and parasitic infection. Consistent with this, a PPI was detected among the four genes induced by SA-analogue in wild-type *Arabidopsis*, which failed to accumulate in *wrky33* mutants (Qiu et al., 2008). We speculate that *OsFKBP65* may be a downstream target of SA. *OsFKBP65* could also interact with *HSFA2* to regulate small HSPs in heat stress response. Previous studies have shown that OsFKBP65 is orthologous to Arabidopsis AtFKBP62 (ROF1), which positively modulates heat tolerance by interacting with AtHSP90.1 and increasing AtHsfA2-mediated accumulation of small HSPs (Meiri and Breiman, 2009; Bissoli et al., 2012). Several HSP encoding genes such as *HSP81-1*, HSP70s, *OsDjC10* and small HSPs were induced in high temperature treated plants, suggesting that the aformentioned studies are consistent with the high induction of *OsFKBP65* in this study. Other genes expressed in response to heat stress included several PPR repeat containing proteins, which have been reported to mediate specific RNA processing events including RNA editing, transcript processing, and translation initiation (Kotera et al., 2005). The C2H2-type of zinc finger proteins (e.g., LOC_Os06g34400), which are perceived to constitute a redundant family of transcriptional regulators in plants with 94 so far reported in the *O. indica* rice genome and 113 in *O. japonica,* were also strongly induced in response to high temperature. These proteins regulate target gene expression through DNA binding and have been reported in response to pathogens (Kim et al., 2004). Thus, this C2H2-type of zinc finger proteins may be important in both high temperature and *M. oryzae* defense response.

Several R genes and pleiotropic drug resistance (PDR)-ABC transporters were stronger induced in plants exposed to *M. oryzae* infection than high temperature in this study. The co-localization of some of these induced RGAs, PDRs and R genes, e.g., PDR4/PDR8 (LOC_Os01g42410) RPS2 (LOC_Os01g72680), *Pit* (LOC_Os01g05620 and LOC_Os01g05600) on chromosome 1; LOC_Os04g41370*, RPS2* (LOC_Os04g43440) and Xa1 (LOC_Os04g53160) on chromosome 4; RGAs (LOC_Os11g45190, LOC_Os11g45180, LOC_Os11g44960, LOC_Os11g45060 and LOC_Os11g45050), PDR like ABC transporter

(LOC_Os11g37700), RPM1 (LOC_Os11g11770), RPR1 (LOC_Os11g12000) and *Pi54* (LOC_Os11g42010) on chromosome 11, suggests that their expression could be in concert with *Pi54* defense response. Pleiotropic drug resistance genes are induced by ABA, SA and JA in rice (Moons, 2008), which suggests that PDRs and plant defense response, probably involving R genes, are somewhat connected. The ABC transporters have been also reported to be involved in the efflux of an antimicrobial diterpenoid compound, sclareol, on to the leaf surfaces of tobacco, and defense response in Arabidopsis involving inhibition of hypersensitive cell death during pathogen defense (Kobae et al., 2006). It is likely that these ABCs transfer defense proteins, including antimicrobial peptides to the apoplast, and probably regulate cell death in rice-*M. oryzae* interaction. The exact mechanism by which these interactions happen in association with R genes needs further investigation.

Genes involved in ABA signaling pathway were also significantly induced in this study. For instance, a putative DNA-binding protein encoding gene *OsBBD1* involved in ABA-derived callose deposition was induced in both backgrounds at high temperature, but with a stronger induction in LT than CO. Consistent with this, a strong induction of OsBURP16 was observed in LT during *M. oryzae* infection. OsBURP16 belongs to PG1-β-like subfamily of the BURP family genes induced by ABA, and was recently reported to decrease pectin content in rice leaves (Liu et al., 2013). We speculate that OsBURP16 could probably contribute to damage-associated molecular patterns (DAMPs) commonly referred to as oligogalacturonides (OG), which invoke OG-induced callose deposition through OsBBD1. In fact, a DNA/RNA nuclease has been reported to regulate ABA-dependent stimulation of callose deposition during *Botrytis cinerea* infection (You et al., 2010). Luna et al. (2010) also showed that callose-promoting growth conditions significantly enhanced levels of basal and PAMP-induced H_2O_2, and indicated that callose deposition is preceded by PAMP triggered H_2O_2. Hence, the observed variation in callose deposition in LT and CO probably correlates with the timing and levels of H_2O_2 accumulation. This is consistent with the stronger induction of OsNox9 in LT than in CO at 28°C, but detectable in CO at 35°C. On the other hand, ABA induced callose deposition has been shown to be more suppressed at 5% compared to 1% sucrose (Luna et al., 2010). Our data show that genes involved in carbohydrate metabolism leading to sugar accumulation are more induced in CO than LT, suggesting that higher sugar levels could be have a negative impact on callose induction in CO than LT. This is also substantiated by the stronger induction of glucose-6-phosphate 1-dehydrogenase (G6PDH) in CO compared to LT. G6PDH supplies reducing energy to cells by maintaining the level of the

co-enzyme nicotinamide adenine dinucleotide phosphate (NADPH). The NADPH in turn maintains the level of the antioxidant enzyme glutathione. Besides this, PAMP induced callose was shown to be higher under environmental growth conditions that induced ROS accumulation (reference there in). Hence, the high activity of antioxidants in CO at 28°C likely compromises ROS induced callose deposition. The production of callose is essential for many physiological processes in addition to innate immunity, such as regulation of cell-to-cell movement of molecules, cell plate formation, formation and closure of sieve pores, guard cell wall thickening and establishment of distinct cell cortex domains, which may provide an explanation as to why the rate of callose formation is necessary and faster at high temperatures. In this context, induction of callose by *M. oryzae* infection in plants treated with high temperature could be associated with increased ROS production and ABA activity. Consistent with this, reduction in sucrose levels as a result of repression of photosynthesis in abiotic stress treated plants further enhances callose deposition. Callose may restrict the fungus to the substomatal space, isolating and possibly starving the fungus. Because ABA induces the transcription of PG1 genes, it is possible that OGs generated from the activity of PG1s invoke intracellular production of JA via the octadecanoid pathway. This is consistent with previous reports (Howe and Schaller, 2008).

Alternatively, it has been shown that ABA binding inhibits the activity of PP2C phosphatases that in turn represses the activity of sucrose non-fermenting 1 (SNF1)-related kinase to relieve repression of key transcription factors (Cutler et al., 2010). Indeed most calcium/calmodulin dependent protein kinases (SNF1-related) were suppressed at high temperature, indicating that ABA played a crucial role in modulating these kinases. On the other hand, LecRLKs have been reported to confer rice resistance to *M. oryzae*, bacterial blight and insect parasites (Singh et al., 2012). The *Nicotiana attenuata* lectin receptor kinase1 (LecRK1) was identified to be involved in the mechanism used by plants to suppress the *Manduca sexta*-triggered accumulation of salicylic acid (Bonaventure 2011), suggesting independent signaling from SA. LecRLKs are carbohydrate binding receptors, and this might suggest that OGs are the most likely ligands, and is consistent with a strong induction of a jacalin-like lectin (LOC_Os12g14440) that mediates broad spectrum resistance in LT but not in CO.

Although we detected increased levels of SA in CO at both temperatures, and in LT at high temperature, there is no complete picture of SAR action in rice. Studies show that SA plays a protective role against oxidative stress than defense against pathogens (Iwai et al., 2007). Our

data shows decreased levels of SA in LT compared to CO at 28°C, suggesting that SA may not provide sufficient protection against *M. oryzae* at 28°C. Indeed SA has been reported to poorly induce PR gene expression and resistance to *M. oryzae* infection (reference therein). Moreover, R gene mediated resistance in *M. oryzae* infected young rice plants occurs independent of SA (Iwai et al., 2007). Thus, the induction of OsBISAMT1, which converts SA to MeSA, appears to suggest that MeSA could probably participate in a defence response pathway leading to seedling resistance in rice rather than SA. Previous reports have suggested that JA probably antagonizes SA by modulating biosynthesis and activity BSMT1 (Chen et al., 2003). Although MeSA has been reported not to induce a defense response (Seskar et al., 1998), a link between MeSA, lipid derivatives and apoplastic lipid transfer proteins has been reported (Park et al., 2007), indicating that MeSA probably interacts with JA and JA derivatives. Considering that jasmonate-O-methyltransferase, an enzyme that catalyzes the conversion of JA to MeJA was highly induced in LT than CO; it is possible that the lipid derivative that interacts with MeSA is methyl jasmonate (MeJA). MeJA and certain jasmonoyl-amino acid conjugates (e.g., JA-Ile) are potent elicitors of defense gene expression (Howe and Schaller, 2008), and a strong induction of jasmonate-O-methyltransferase in LT but not in CO suggests the involvement of MeJA in rice defence response.

However, there may be additional signals from HT eventually eliciting defence responses to Mo in CO, which could be explained by other mechanisms. The increased transcript levels of *MBF1c* in CO plants exposed to 35°C compared to 28°C may be one other mechanism suggestive of priming towards effective resistance response. Constitutive expression of *MBF1c* in transgenic Arabidopsis plants was previously shown to increase resistance against bacterial infection, heat and osmotic stress by partially activating the ethylene-response signal transduction pathway (Suzuki et al., 2008). Ethylene burst being one of the earliest events in HR (Seo et al., 2011), we speculate that the up-regulation of *MBF1c* in plants exposed to 35°C partially compensates for the reduced resistance at 28°C through amplification of the ET signaling pathway. Coupled with this, an increased transcript level of *ERF5*, an orthologue of Arabidopsis *ERF96* was detected in our dataset. *ERF96* is up-regulated by ACC, a process that is repressed by SA. The increased transcript levels of this gene, as well as methionine derivatives (e.g., SAMTs) and defensins suggest that ET, in addition to JA, are the major players in the response of HT pre-treated plants to Mo.

Besides this, genes encoding for various kinds of other defence related transcription factors such as U2 small nuclear ribonucleoprotein auxiliary factor (*U2AF*), WRKYs, zinc finger

RING type, OsEREBPs, MYBs, HB, bHLH, zinc finger (ZF) family and basic region/Leu zipper motif (bZIP) family were induced in response to HT and Mo. *U2AF* plays a crucial role in the recognition of a 3′-splice site which contributes to the fine-tuned control of pre-mRNA splicing. *U2AF* was expressed in all treatments and could be an important candidate to explore the crosstalk between HT and pathogen response. Increased expression of OsWRKY IIa encoding genes was also detected in response to *M. oryzae*. OsWRKY IIa have been reported to interact or play an indirect role in transcriptional activation of defense-related gene expression by interacting with other regulatory proteins or form combinatorial dimers themselves to regulate target gene expression (Peng et al., 2010). In this study, OsWRKY55 was stronger induced in LT than in CO, indicating that this gene could probably have a positive role in rice defense against *M. oryzae.* This is consistent with the previous reports (Wei et al. 2013). Alternatively, *OsWRKY84* was strongly induced in CO+35°C+Mo than CO+28°C+Mo. *OsWRKY84* was previously reported to be over-expressed in response to xylanases in suspension-cultured rice cells. *M. oryzae* is known to induce endoxylanases for horizontal expansion in infected leaves (Nguyen et al., 2011). Since the functional role of *OsWRKY84* is not well understood, it would be a potential target for further investigation. Induction of OsIAA13, which participates in blocking auxin signaling by repressing auxin response factor (ARF) function as a transcriptional regulator (Kitomi et al., 2012), suggests transcriptional reprogramming towards enhanced heat tolerance, and indirectly pathogen resistance. We also detected increased expression of histone H2A encoding genes. H2As have specialized roles through alterations they create in chromatin stability and folding (Ausio and Abbott, 2002). Their expression reflects a specialized role in plants during high temperature stress, when stability of major cellular functions is required. Interestingly, genes encoding for Histone H2A were not expressed during *M. oryzae* infection, suggesting a more significant role in heat stress compared to pathogen stress.

Downstream of TFs could be several genes encoding for defensins, GDSL LIPASE-LIKE 1, thionins, LTPs, PR6, GLPs, and membrane attack complex component/perforin/complement C9 (LOC_Os05g48360), which were stronger induced in CO+35°C+Mo than CO+28°C+Mo. These proteins have fungicidal activity, and could confer resistance through membrane permeabilization of fungal tissues. Several proteinases and proteinase inhibitors induced in this study could also probably play important roles in protein breakdown and recycling, as well as, control of proteolysis by allowing selective mobilization of proteins during stress. However, the stronger induction of these proteases in a relatively susceptible interaction

(CO+28°C+Mo) compared to a resistant response (LT+28°C+Mo, CO+35°C+Mo LT+35°C+Mo) is intriguing, and could probably suggest that these proteinases play a role in *M. oryzae* successful colonization of the host.

Genes involved in primary metabolism, secondary metabolism and PRs were more induced in response to *M. oryzae* than high temperature. Genes involved in photosynthesis were also suppressed at high temperature. However, genes encoding for photosystem II 10 kDa polypeptides were induced at all conditions, suggesting that these proteins probably play a significant role in protecting rice PSII from oxidative perturbations induced by heat stress and pathogen infection.

Overall, the present biochemical and transcriptome analysis provided a broad insight into biological processes potentially involved in rice response to HT and Mo, including representatives of all major classes of defence genes. We have shown that rice lines carrying *Pi54* respond to Mo by rapid induction of callose and H_2O_2, and that these resistance mechanisms are amplified at HT. Coupled with this, our analyses show that MeSA, MeJA and ET have a role in enhancing defence response to Mo after HT treatment. Crosstalk among these pathways appears to be a key defence mechanism against Mo. Other than these molecules, increased expression of genes in the Auxin, ABA and gibberellin signaling pathways was also detected. However, increased expression of negative regulators of these pathways such as *OsIAA13, OsGH3.2, OsGH3.5, ARF19*, *ERF5,* and *OsBBD1* involved in ABA-derived callose deposition, suggests that internal dynamics are involved in fine-tuning the negative defence responses associated with this hormones. For instance, *ARF19* is induced by either IAA or ethylene treatments, but could be inactivated by the binding of *OsIAA13* to decrease its sensitivity to auxin. *GH3* genes encode IAA-conjugating enzymes, which could also act as feedback regulators by reducing free auxin levels. Thus, multiple regulatory pathways coupled with genetic background factors are involved in achieving potentially effective resistance in plants exposed to elevated temperatures. We have not linked our transcriptome analysis with functional analysis. It is possible that temperature might significantly modify post-transcriptional regulation. Thus, the effects of temperature on plant defense related genes identified in this study may require further investigation at the post transcriptional level. Equally, we do not know how much callose is required to completely restrict the pathogen, and whether temperatures of 35°C would produce the same results in plants without R gene mediated resistance. Nonetheless, the interaction between high

temperature and *M. oryzae* infection widens our understanding of how more than one stress factor and the genetic background influence rice defense responses.

Materials and Methods

Plant and fungal material and rice blast inoculation

Two genotypes, Li-Jiang-Xin-Tuan-He-Gu (LT, *Oryza japonica*) and Co39 (*Oryza indica*) carrying the Pi54 R gene, were used as hosts in this experiment. LT is widely identified as a genetic background for the development of NILs, whereas Co39, a short duration *O. indica* cultivar from India with high susceptibility to tropical blast isolates, was recently introduced as a second background for the development of NILs. The plants were grown in the greenhouse at 27±2°C with a photoperiod of 14 h for 21 days and then transferred to growth chambers at 28°C and 35°C for 7 days. After high temperature exposure, all plants were kept at 28°C for inoculation to allow fungal infection at equal conditions. The fungal strains were cultured on V8 agar plates at 25°C. Inoculation was performed using a blast isolate, TAN211.16, from Tanzania. The inoculated plants were incubated for 24 h at 28°C and 90% relative humidity in the dark and then transferred back to 12 h of light for additional 24 h before leaf sampling. Some plants were maintained at 35°C and 28°C after inoculation for disease assessment. Leaf blast was assessed from 4 to 12 days after inoculation. Disease assessment was repeated two times to confirm the presence of lesions. The area under the disease progress curve (AUDPC) was calculated using the trapezoidal method.

Illumina HiSeq2000 Sequencing

The RNAseq gene expression analysis experiment was designed as a three-factor experiment with eight treatments: (1) LT+35°C+Mo; (2) LT+28°C+Mo; (3) LT+35°C; (4) LT+28°C; (5) CO+35°C+Mo; (6) CO+28°C+Mo; (7) CO+35°C; (8) CO+28°C. These treatments represent the genetic background (LT or CO), temperature (28°C and 35°C) and *M. oryzae* inoculation (Mo). The experiment included three biological replicates. Each sample represented leaf material from five plants. Total RNA was isolated using Trizol reagent (Invitrogen, Carlsbad, CA) according to the manufacturer's instructions. The integrity of each RNA sample obtained was examined by Agilent Lab-on-a-chip technology using the RNA 6000 Nano LabChip kit and a Bioanalyzer 2100 (Agilent Technologies, Palo Alto, CA). Two micrograms of total RNA were subjected to library preparation using the 'TruSeq RNA Sample preparation v2 Guide' following the manufacturer's instructions. Briefly, the poly-A containing mRNAs

were purified by using poly-T oligo-attached magnetic beads and then fragmented. The first and second cDNA strands were synthesized, end repaired, and adaptors were ligated after adenylation at the 3'-ends. cDNA fragments containing adaptors on both ends were selectively enriched by 15 cycles of PCR amplification. The indexed Illumina libraries were validated for fragment size using the Agilent High-Sensitivity cDNA chip on 2100 Bioanalyzer. Libraries were clustered for sequencing using Illumina cBOT Cluster generation system and TrusSeq v3 chemistry. Fifty bp single-end sequencing was performed on the HiSeq2000 using three barcoded libraries per lane.

Preprocessing, Mapping, and analysis of illumina reads and subsequent gene expression data

Sequence images were transformed with Illumina software BaseCaller to bcl files, which were demultiplexed to fastq files with CASAVA v1.8.2 allowing for one mismatch in the indices. Sequences were aligned by Bowtie2 v2.0.2 to the Ensembl cDNA release 16 for *Oryza sativa*. Subsequently, conversion and sorting of the resulting sam files to sorted bam files was conducted with samtools 0.1.18 followed by counting the reads to each gene. Data was preprocessed and analysed in the R/Bioconductor environment loading DESeq, lattice, estrogen, gplots and colorRamps, biomaRt packages. After filtering the genes exceeding more than 50 counts for at least one sample, normalization (via Trimmed Mean and Median-values), estimation of dispersions and testing for differentially expressed genes based on a $\chi2$ likelihood ratio test, assuming negative binomial data distribution were computed via DESeq. Candidate genes were filtered to a minimum of 4x fold change and FDR-corrected P-value<0.05. Gene annotation was conducted using Ensembl Biomart via R. Functional association enrichment analysis was conducted via the R package goseq. RPKM values were calculated via CLC Genomics Workbench software (CLC Bio, Swansea, UK). We generated hierarchical clustering heatmaps using Multi experiment Viewer (MEV TM4 Microarray Software Suite, v4.9; Dana-Farber Cancer Institute) using average linkage Pearson correlation hierarchical clustering. The identification of cis elements was performed using Osiris software (available at http://www.bioinformatics2.wsu.edu/cgi-bin/Osiris/cgi/home.pl), which searches known cis elements from PLACE - Plant Cis-acting Regulatory DNA Elements (Higo et al., 1999) database. In order to verify if the elements were not randomly presented, a Z test was performed. The probability (p) for each motif was obtained and the elements with p-values equal to or less than 0.05 were considered as non-random. Cis elements with higher occurrence among up-regulated DEGs were identified.

Histochemistry and microscopy

Callose staining was carried out according to the method of Hao et al. (2008), with minor modifications. Briefly, leaf sections were destained by boiling in methanol:acetic acid (3:1) at 72°C and rinsed first in 50% ethanol and then in water. The destained leaves were stained for 1 h at room temperature in a solution containing 0.1% (w/v) aniline blue in 0.15M K_2HPO_4 and examined under the UV epifluorescence microscope. Diaminobenzidine (DAB) staining of hydrogen peroxide was carried out according to Thordal-Christensen et al. 1997 with some modifications. Briefly, destained leaf sections were immersed in 1 mg ml^{-1} DAB solution and incubated in the dark overnight. The leaf sections were rinsed in double distilled water before microscopic examination.

Measurement of hydrogen peroxide (H_2O_2)

Leaf samples were collected 24 and 48 hai and immediately ground in liquid nitrogen. The ground powder was extracted in 5% w/v metaphosphoric acid. The samples were centrifuged at $5000 \times g$ for 60 min. The supernatant was adjusted to pH 6.5 using 1 M tricine in 6 M NaOH, and the initial amount of NADH was measured at 340 nm (OD_1) using SPECORD 40 (Analytik, Jena, Germany). Horseradish peroxidase ($350\mu l$ l^{-1}; 2500 U ml^{-1}) dissolved in 25mM sodium phosphate buffer (pH 7.0) was added and the mixture was incubated at room temperature. The absorbance changes at 340 nm were measured at 25°C, 60 min after the addition of horseradish peroxidase (OD_2). The H_2O_2 contents were determined by a calibration curve using known amounts of H_2O_2 and expressed as micromoles per gram of fresh weight (FW).

Guaiacol peroxidase and PAL activity

Fresh leaf samples weighing 300 mg were homogenized in 3 ml of cold 100mM Na-phosphate buffer (pH 7.0). The homogenates were centrifuged at 5000 x g for 30 min, and the dialyzed enzyme extracts were used for the assay. Assay mixture in a total volume of 3 ml contained 100 mM Na-phosphate buffer (pH 7.0), 50μl of 20mM guaiacol solution, 30 μl of 12.3mM hydrogen peroxide and 50 μl of enzyme extract. Increase in absorbance was measured at 420 nm (extinction coefficient of 26.6 mM_1 cm_1) at 30 s intervals up to 3 min, using SPECORD 40, Analytikjena AG (Germany). Enzyme specific activity was expressed as mKatal. PAL activity was determined according to Ueno et al. (2011).

Salicylic acid determination

Accumulation of salicylic acid (SA) was examined through high performance liquid chromatography (HPLC) analysis. SA extraction was carried out according to a modified method of Kamble and Bhargava (2007) with minor modifications. Briefly, 300mg of ground leaf tissue was homogenized in 3 ml acetone and centrifuged at 3800 x g for 60min in a refrigerated centrifuge (Sigma 4K10). For determination of free SA, the supernatant was transferred to a new tube and acetone was evaporated at 35°C for about 2 hours. The dry residue was dissolved in HPLC grade water and partitioned against an equal volume of ethyl acetate. The ethyl acetate layer was evaporated to dryness at 35°C, and the residue was finally dissolved in 500μl of HPLC grade methanol. SA samples were subjected to HPLC separation using a C18 (LiChrospher 100 Merck) reverse phase column (25cmx4mm id), at a flow rate of 1ml min^{-1} in a gradient program for the solvents: (A) 20mM NaAc and (B) methanol. SA was detected using a fluorescence detector with excitation and emission wavelengths of 315 and 405nm, respectively.

Real-time RT-PCR analysis

Total RNA was isolated using Trizol reagent (Invitrogen, Gaithersburg, MD, USA) according to the manufacturer's instructions. Relative gene expression was determined by quantitative real time PCR (RT-PCR) on a Bio-Rad CFX384 real time system using SYBR Green dye (Bio-Rad, California, USA). The primer efficiency was determined and taken into account when evaluating the qRT-PCR data. The data were normalized to the geometrical mean of a reference gene (LOC_Os07g02340), previously found to show a stable expression pattern across biotic and abiotic stress (Narsai et al. 2010). The Pfaffl method was used to analyse the qRT-PCR data in Microsoft Excel, and the calculated values were expressed relative to the control. Primer sequences are listed in (Additional file S14).

Acknowledgement

running illumina sequencing. Our sincere thanks are expressed to Dagmar Tacke, Marian Süß and Daniel Kretzschmar for their technical support.

References

Ausio, J., and Abbott, D. W. 2002. The many tales of a tail: carboxyl-terminal tail heterogeneity specializes histone H2A variants for defined chromatin function. Biochemistry 41:5945-5949.

Aviezer-Hagai, K., Skovorodnikova, J., Galigniana, M., Farchi-Pisanty, O., Maayan, E., Bocovza, S., Efrat, Y., von Koskull-Doring, P., Ohad, N. and Breiman, A. 2007. Arabidopsis immunophilins ROF1 (AtFKBP62) and ROF2 (AtFKBP65) exhibit tissue specificity, are heat-stress induced, and bind HSP90. Plant Mol. Biol. 63:237-255.

Berger S, Benediktyová Z., Matous K., Bonfig K., Mueller M. J., Nedbal L., Roitsch T. 2007. Visualization of dynamics of plant-pathogen interaction by novel combination of chlorophyll fluorescence imaging and statistical analysis: differential effects of virulent and avirulent strains of *P. syringae* and of oxylipins on *A. thaliana*. J Exp Bot. 58:797–806.

Bieri, S., Mauch, S., Shen, Q. H., Peart, J., Devoto, A., Casais, C., Ceron, F., Schulze, S., Steinbiss, H. H., Shirasu, K., et al. 2004. RAR1 positively controls steady state levels of barley MLA resistance proteins and enables sufficient MLA6 accumulation for effective resistance. Plant Cell 16:3480-3495.

Bissoli, G., Niñoles, R., Fresquet, S., Palombieri, S., Bueso, E., Rubio, L., García-Sánchez, M. J., Fernández, J. A., Mulet, J. M., and Serrano, R. 2012. Peptidyl-prolyl *cis-trans* isomerase ROF2 modulates intracellular pH homeostasis in Arabidopsis. Plant J. 70:704-716.

Bonaventure, G. 2011. The Nicotiana attenuata Lectin Receptor Kinase 1 is involved in the perception of insect feeding. Plant Signal Behav. 6:1-4.

Chen, F., D'Auria, J. C., Tholl, D., Ross, J. R., Gershenzon, J., Noel, J. P., and Pichersky, E. 2003. An *Arabidopsis thaliana* gene for methylsalicylate biosynthesis, identified by a biochemical genomics approach, has a role in defense. Plant J. 36:577-588.

Cheong, Y. H., Moon, B. C., Kim, J. K., Kim, C. Y., Kim, M. C., Kim, I. H., Park, C. Y., Kim, J. C., Park, B. O., Koo, S. C., Yoon, H. W., Chung, W. S. et al. 2003. BWMK1, a rice mitogen-activated protein kinase, locates in the nucleus and mediates pathogenesis-related gene expression by activation of a transcription factor. Plant Physiology 132:1961-1972.

Cutler, S. R., Rodriguez, P. L., Finkelstein, R. R., and Abrams, S. R. 2010. Abscisic acid: emergence of a core signaling network. Annu. Rev. Plant Biol. 61:651-679.

Dave, A., Hernández, M. L., He, Z., Andriotis, V. M. E., Vaistij. F. E., Larson, T. R., and Graham, I. A. 2011. 12-Oxo-phytodienoic acid accumulation during seed development represses seed germination in *Arabidopsis*. Plant Cell. 23:583-599.

Ding, D., Zhang, L., Wang, H., Liu, Z., Zhang, Z. and Zheng, Y. 2009. Differential expression of miRNAs in response to salt stress in maize roots. Ann. Bot. 103:29-38.

Eitzinger, J., Orlandini, S., Stefanski, R., and Naylor, R. E. L. 2010. Climate change and agriculture: introductory editorial. J. Agri. Sci. Cambridge 148:499-500.

Elmore, J.M., Lin, Z-J.D., and Coaker G. 2011. Plant NB-LRR signaling: upstreams and downstreams. Current Opinion in Plant Biology 14:365-371.

Fu, D. L., Uauy, C., Distelfeld, A., Blechl, A., Epstein, L., Chen, X., Sela, H., Fahima, T., and Dubcovsky, J. 2009. A Kinase-START Gene confers temperature-dependent resistance to wheat stripe rust. Science 323:1357-1360.

Ghini, R., Hamada, E., and Bettiol, W. 2008. Climate change and plant diseases. Sci. Agric. (Piracicaba, Braz.) 65:98-107.

Gupta, S. K., Rai, A. K., Kanwar, S. S., Chand, D., Singh, N. K., et al. 2012. The single functional blast resistance gene *Pi54* activates a complex defense mechanism in rice. J Exp. Bot. 63:757-772.

Himmelbach, A., Hoffmann, T., Leube, M., Hohener, B., Grill, E. 2002. Homeodomain protein ATHB6 is a target of the protein phosphatase ABI1 and regulates hormone responses in Arabidopsis. EMBO J. 21:3029-3038.

Howe, G. A., and Schaller A. 2008. Direct defense in plants and their induction by wounding and insect herbivores. In: Schaller A. (Editor) Induced plant resistance to herbivory, Springer Science + Business Media B.V. 7-29.

Iwai, T., Seo, S., Mitsuhara, I., and Ohashi, Y. 2007. Probenazoleinduced accumulation of salicylic acid confers resistance to Magnaporthe grisea in adult rice plants. Plant Cell Physiol. 48:915-924.

Jennings, C., West, J., Waine, C., Craik, D., and Anderson, M. 2001. Biosynthesis and insecticidal properties of plant cyclotides: The cyclic knotted proteins from *Oldenlandia affinis.* Proc. Natl. Acad. Sci. USA. 98:10614-10619.

Johannesson, H., Wang, Y., and Engstrom, P. 2001. DNA-binding and dimerization preferences of Arabidopsis homeodomain-leucine zipper transcription factors in vitro. Plant Mol. Biol. 45:63-73.

Jorda, L., and Vera, P. 2000. Local and systemic induction of two defense-related subtilisin-like protease promoters in transgenic *Arabidopsis* plants. Luciferin induction of PR gene expression. Plant Physiol. 124:1049-1057.

Jorgensen, T. H. 2012. The effect of environmental heterogeneity on RPW8-mediated resistance to powdery mildews in *Arabidopsis thaliana*. Ann. Bot. 109:833-842.

Jung, K. H., Gho, H. J., Giong, H. K., Chandran, A. K., Nguyen, Q. N., Choi, H., Zhang, T., Wang, W., Kim, J. H., Choi, H. K., and An, G. 2013. Genome-wide identification and analysis of *Japonica* and *Indica* cultivar-preferred transcripts in rice using 983 Affymetrix array data. Rice 6:19.

Kanai, M., Nishimura, M., and Hayashi, M. 2010. A peroxisomal ABC transporter promotes seed germination by inducing pectin degradation under the control of ABI5. Plant J. 62:936-947.

Kawano, Y., and Shimamoto, K. 2013. Early signaling network in rice PRR-mediated and R-mediated immunity. Curr. Opin. Plant Biol. 16:496-504.

Kierzek, E., Malgowska, M., Lisowiec, J., Turner, D. H., Gdaniec, Z. and Kierzek, R. 2014. The contribution of pseudouridine to stabilities and structure of RNAs. Nucl. Acids Res. 42:3492-3501.

Kim, C. Y., Lee, S. H., Park, H. C., Bae, C. G., Cheong, Y. H., Choi, Y. J., Han, C., Lee, S. Y., Lim, C. O. and Cho. M. J. 2000. Identification of rice blast fungal elicitor-responsive genes by differential display analysis. Mol. Plant Microbe. Interact. 13:470-474.

Kim, H. S., and Delaney, T. P. 2002. Over-expression of *TGA5*, which encodes a bZIP transcription factor that interacts with NIM1/NPR1, confers SAR-independent resistance in Arabidopsis thaliana to Peronospora parasitica. Plant J. 32:151-163.

Kim, S. H., Hong, J. K., Lee, S. C., Sohn, K. H., Jung, H. W., and Hwang, B. K. 2004. CAZFP1, Cys2/His2-type zinc-finger transcription factor gene functions as a pathogen-induced early-defense gene in Capsicum annuum. Plant Mol. Biol. 55:883-904.

Kim, S. T., Cho, K. S., Yu, S., Kim, S. G., Hong, J. C., Han, C. D., Bae, D. W., Nam, M. H., and Kang, K. Y. 2003. Proteomic analysis of differentially expressed protein induced by rice blast fungus and elicitor in suspension-cultured rice cells. Proteomics 3:2368-2378.

Kitomi, Y., Inahashi, H., Takehisa, H., Sato, Y., and Inukai Y. 2011. OsIAA13-mediated auxin signaling is involved in lateral root initiation in rice. Plant Sci. Int. J. Exp. Plant Biol. 201190:116-122.

Kobae, Y., Sekino, T., Yoshioka, H., Nakagawa, T., Martinoia, E., and Maeshima M. 2006. Loss of AtPDR8, a plasma membrane ABC transporter of Arabidopsis thaliana, causes hypersensitive cell death upon pathogen infection. Plant Cell Physiol. 47**:** 309-318

Koo, Y. J., Kim, M. A., Kim, E. H., Song, J. T., Jung, C., Moon, J. K., Kim, J. H., Seo, H. S., Song, S. I., Kim, J. K., Lee, J. S., Cheong, J. J., and Choi, Y. D. 2007. Overexpression of salicylic acid carboxyl methyltransferase reduces salicylic acid-mediated pathogen resistance in Arabidopsis thaliana. Plant Mol. Biol. 64:1-15.

Kotera, E., Tasaka, M., and Shikanai, T. 2005. A pentatricopeptide repeat protein is essential for RNA editing in chloroplasts. Nature 433:326-30.

Liu, H., Ma, Y., Chen, N., Guo, S., Liu, H., Guo, X., Chong, K., and Xu, X. 2013. Overexpression of stress-inducible OsBURP16, the β-subunit of polygalacturonase 1, decreases pectin content and cell adhesion and increases abiotic stress sensitivity in rice. Plant Cell and Environ. 37:114-1158

Luna, E., Pastor, V., Robert, J., Flors, V., Mauch-Mani, B., and Ton, J. 2011. Callose deposition: a multifaceted plant defense response. Mol Plant Microbe Interact. 24:183-193.

Luo, H., Song, F., and Zheng, Z. 2005. Overexpression in transgenic tobacco reveals different roles for the rice homeodomain gene OsBIHD1 in biotic and abiotic stress responses. J.Exp. Bot. 56:2673-2682.

Magiri, E N., Farchi-Pistany, O., Avni, A., and Breiman, A. 2006. The expression of the large rice FK506 binding proteins demonstrate tissue specificity and heat stress responsiveness. Plant Sci. 170:695-704.

Mizuno, H., Kawahigashi, H., Kawahara, Y., Kanamori, H., Ogata, J., Minami, H., Itoh, T., and Matsumoto, T. 2012. Global transcriptome analysis reveals distinct expression among duplicated genes during sorghum-interaction. BMC Plant Biol. 29:12:121.

Moons, A. 2008. Transcriptional profiling of the PDR gene family in rice roots in response to plant growth regulators, redox perturbations and weak organic acid stresses. Planta 229:53-71.

Mur LA, Kenton P, Atzorn R, Miersch O, Wasternack C. 2006. The outcomes of concentration-specific interactions between salicylate and jasmonate signaling include synergy,antagonism, and oxidative stress leading to cell death. Plant Physiology. 140:249–262.

Narsai, R., Wang, C., Chen, J., Wu, J., Shou, H., and Whelan, J. 2013. Antagonistic, overlapping and distinct responses to biotic stress in rice (*Oryza sativa*) and interactions with abiotic stress. BMC Genomics. 14:93.

Negeri, A., Wang, G-F., Benavente, L., Kibiti, C. M., Chaikam, V., Johal, G., and Balint-Kurti, P. 2013. Characterization of temperature and light effects on the defense response phenotypes associated with the maize *Rp1-D21* autoactive resistance gene. BMC Plant Biol. 13:106.

Niinemets, U. 2010. Responses of forest trees to single and multiple environmental stresses from seedlings to mature plants: past stress history, stress interactions, tolerance and acclimation. Forest Ecology and Management 260:1623-1639.

Noutoshi, Y., Ito, T., Seki, M., et al. 2005. A single amino acid insertion in the WRKY domain of the Arabidopsis TIR-NBS-LRR-WRKY-type disease resistance protein SLH1

(sensitive to low humidity 1) causes activation of defense responses and hypersensitive cell death. Plant J. 43:873-888.

Okuyama, Y., Kanzaki, H., Abe, A., Yoshida, K., Tamiru, M., Saitoh, H., Fujibe, T., Matsumura, H., Shenton, M., Galam, D.C., Undan, J., Ito, A., Sone, T., and Terauchi, R. 2011. A multifaceted genomics approach allows the isolation of the rice Pia-blast resistance gene consisting of two adjacent NBS-LRR protein genes. Plant J. 66:467-479.

Park, H. L., Lee, S. W., Jung, K. H., Hahn, T. R., and Cho, M. H. 2013. Transcriptomic analysis of UV-treated rice leaves reveals UV-induced phytoalexin biosynthetic pathways and their regulatory networks in rice. Phytochemistry. 96:57-71

Park, S.W., Kaimoyo, E., Kumar, D., Mosher, S., and Klessig, D.F. 2007. Methyl salicylate is a critical mobile signal for plant systemic acquired resistance. Science 318:113-116.

Priya, P., and Jain, M. 2013. RiceSRTFDB: A database of rice transcription factors containing comprehensive expression, cis-regulatory element and mutant information to facilitate gene function analysis. Database 2013: article ID bat027.

Qiu J. L., Fiil, B. K., Petersen, K., Nielsen, H. B., Botanga, C. J., Thorgrimsen, S., et al. 2008. Arabidopsis MAP kinase 4 regulates gene expression through transcription factor release in the nucleus. EMBO J. 27:2214-2221.

Rabbani, M. A., Maruyama, K., Abe, H., Khan, M. A., Katsura, K., Ito, Y., Yoshiwara, K., Seki, M., Shinozaki, K., and Yamaguchi-Shinozaki, K. 2003. Monitoring expression profiles of rice genes under cold, drought, and high-salinity stresses and abscisic acid application using cDNA microarray and RNA get-blot analyses. Plant Physiol. 133:1755-1767

Ren, D., Yang, H., and Zhang S. 2002. Cell death mediated by MAPK is associated with hydrogen peroxide production in Arabidopsis. J. Biol. Chemistry 277:559-565.

Reyna, N. S., and Yang, Y. 2006. Molecular analysis of the rice MAP kinase gene family in relation to Magnaporthe grisea infection. Mol. Plant-Microbe. Interact. 19:530-540.

Rojas, C. M., and Mysore, K. S. 2012. Glycolate oxidase is an alternative source of H2O2 production during plant defense responses and functions independently from NADPH oxidase. Plant Signaling & Behavior 7:752-755

Sentoku, N., Sato, Y., and Matsuoka, M. 2000. Overexpression of rice OSH genes induces ectopic shoots on leaf sheaths of transgenic rice plants. Dev. Bio. 220:358-364.

Seo, S., Mitsuhara, I., Feng, J., Iwai, T., Hasegawa, M., and Ohashi, Y. 2011. Cyanide, a co-product of plant hormone ethylene biosynthesis, contributes to the resistance of rice to blast fungus.Plant Physiol. 155:502-514.

Shah, F., Huang, J., Cui, K., Nie, L., Shah, T., Chen, C., and Wang, K. 2011. Impact of high-temperature on rice plants and its trait related to tolerance. J. Agri Sci. 149:545-549.

Sheikh, A. H., Raghuram, B., Jalmi, S. K., Wankhede, D. P., Singh, P., and Sinha, A. K. 2013. Interaction between two rice mitogen activated protein kinases and its possible role in plant defense. BMC Plant Biol. 13:121.

Shimizu, T., Lin, F., Hasegawa, M., Okada, K., Nojiri, H., and Yamane, H. 2012. Phytoalexin Sakuranetin in Rice Enzyme in Biosynthesis of Flavonoid Naringenin 7- *O*-Methyltransferase, a Key Enzyme in Biosynthesis of Flavonoid Phytoalexin Sakuranetin in Rice. J. Biol. Chem. 287:19315-19325.

Shumilina, D. V., Il'ina, A. V., Kulikov, S. N. and Dzhavakhiya, V. G. 2005. Elicitor activity of MF-3 protein from *Pseudomonas fl uorescens* and combination of MF3-protein with chitosan in different host-pathogen pairs. Adv. Chitin Sci. 8:275-278.

Singh, P., Kuo, Y. C., Mishra, S., Tsai, C. H., Chien, C. C., Chen, C. W., Desclos-Theveniau, M., Chu, P. W., Schulze, B., Chinchilla, D., Boller, T., and Zimmerli, L. 2012. The lectin receptor kinase-vi.2 is required for priming and positively regulates Arabidopsis pattern-triggered immunity. Plant Cell 24:1256-1270.

Suzuki, N., Bajad, S., Shuman, J., Shulaev, V., and Mittler, R. 2008. The transcriptional co-activator MBF1c is a key regulator of thermotolerance in Arabidopsis thaliana. J. Biol. Chem. 283:9269-9275.

Torres, M. A., Jones, J. D., and Dangl, J. L. 2006. Reactive oxygen species signaling in response to pathogens. Plant Physiol 141:373-378.

Umemura, K., Satou, J., Iwata, M., Uozumi, N., Koga, J., Kawano, T., Koshiba, T., Anzai, H., and Mitomi, M. 2009. Contribution of salicylic acid glucosyltransferase, OsSGT1, to chemically induced disease resistance in rice plants. The Plant J. 57:463-472.

Ueno, M., Kumura, Y., Ueda, K., Kihara, J., and Arase S. 2011. Indole derivatives enhance resistance against the rice blast fungus *Magnaporthe oryzae*. J. Gen. Plant Pathol. 77:209-213.

Webb, K. M., Ona, I., Bai, J., et al. 2011. A benefit of high temperature: increased effectiveness of a rice bacterial blight disease resistance gene. New Physiol. 185:568-576.

Wei, T., Ou, B., Li, J., Zhao, Y., Guo, D., et al. 2013. Transcriptional Profiling of Rice Early Response to *Magnaporthe oryzae* Identified OsWRKYs as Important Regulators in Rice Blast Resistance. PLoS ONE 8:e59720.

Wrzaczek, M., Brosché, M., Salojärvi, J., Kangasjärvi, S., Idänheimo, N., Mersmann, S., Robatzek, S., Karpiński, S., Karpińska, B., and Kangasjärvi, J. 2010. Transcriptional regulation of the CRK/DUF26 group of receptor-like protein kinases by ozone and plant hormones in Arabidopsis. BMC Plant Biol. 10:95.

Xiao, S. Y., Brown, S., Patrick, E., Brearley, C., and Turner, J. G. 2003. Enhanced transcription of the *Arabidopsis* disease resistance genes RPW8·1 and RPW8·2 via a salicylic acid-dependent amplification circuit is required for hypersensitive cell death. Plant Cell 15:33-4.

Yan, G. P., and Chen, X. M. 2008. Identification of a quantitative trait locus for high-temperature adult-plant resistance against Puccinia striiformis f. sp hordei in 'Bancroft' barley. Phytopathol. 98:120-127.

Yang, S. H., Hua, J. 2004. A haplotype-specific resistance gene regulated by BONZAI1 mediates temperature-dependent growth control in Arabidopsis. Plant Cell 16:1060-1071.

You, M. K., Shin, H. Y., Kim, Y. J., Ok, S. H., Cho, S. K., Jeung, J. U., Yoo, S. D., Kim, J. K., and Shin, J. S. 2010. Novel bifunctional nucleases, OmBBD and AtBBD1, are involved in abscisic acid-mediated callose deposition in Arabidopsis. Plant Physiol. 152:1015-1029.

Young, M. D., Wakefield, M. J., Smyth, G. K., and Oshlack, A. 2010. Gene ontology analysis for RNA-seq: accounting for selection bias. Genome Biol. 11:R14.

Zhang, S., Chen, C., Li, L., Meng, L., Singh, J., Jiang, N., Deng, X-W., He, Z.H., and Lemaux, P.G. 2005. Evolutionary Expansion, Gene Structure, and Expression of the Rice Wall-Associated Kinase Gene Family. Plant Physiol. 139:1107-1124.

Zhao, N., Guan, J., Ferrer, J. L., Engle, N., Chern, M., Ronald, P., Tschaplinski, T. J., and Chen, F. 2010. Emission, biosynthesis and regulation of insect-induced methyl salicylate and methyl benzoate from rice. Plant Physiol. Biochem. 48:279-287.

Figures
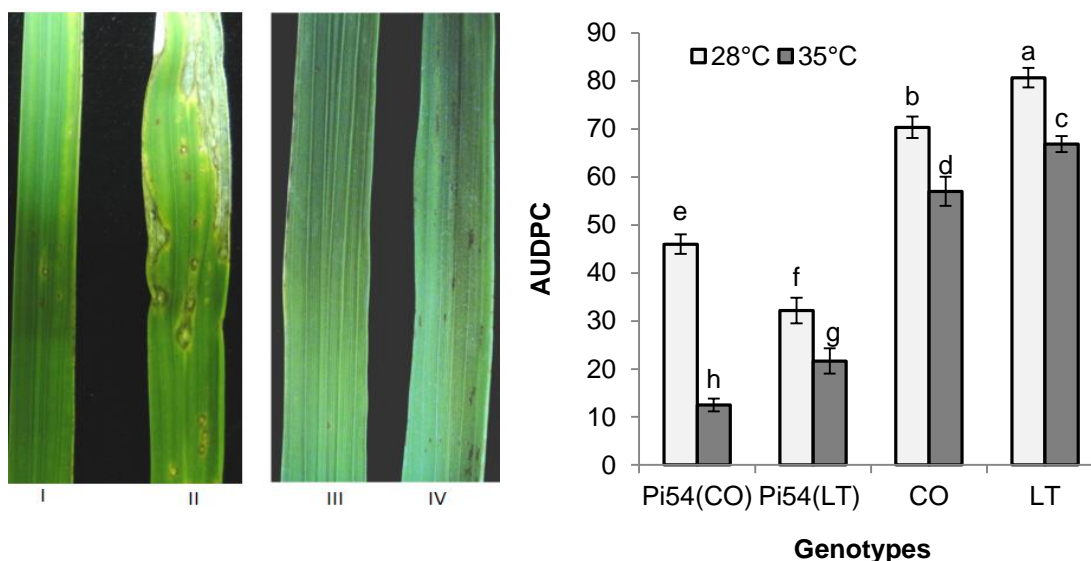
Figure 2.1a: Disease phenotypes of *M. oryzae* on Pi54(LT) (I & III) and Pi54(CO) (II & IV) at 28°C and 35°C, 5 dpi. I and II represent disease phenotype at 28°C, and III and IV represent disease phenotype in plants pre-exposed to 35°C prior to inoculation at 28°C.

Figure 2.1b: Disease progress of *M. oryzae* on Pi54(CO) and Pi54(LT) carrying R gene Pi54, and their background parents LTH (LT) and CO39 (CO) at 28°C and 35°C. Same letters above standard error bars indicate no significant difference (P<0.05). The genetic backgrounds are indicated as LT and CO.
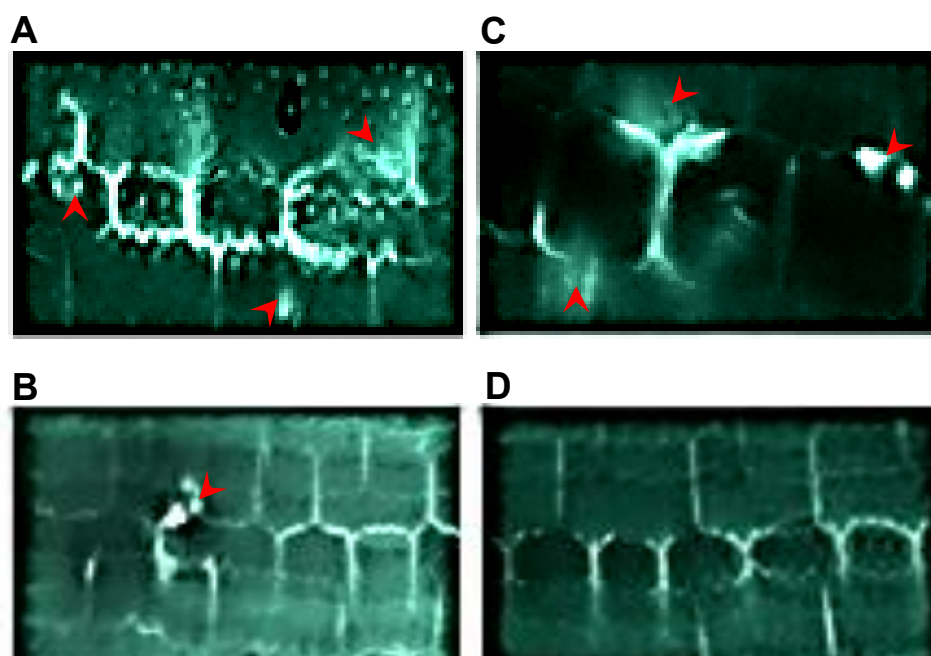
Figure 2.2: Callose deposition due to anilin blue staining of epidermal cells of LT (A and B) and CO (C and D) 48 hrs after inoculation with *M. oryzae*. A and C represent plants grown at 35°C for 7 days before inoculation, and B and D plants grown at 28°C before inoculation. Callose deposits appear more pronounced at 35°C compared to 28°C in both genetic backgrounds. LT shows more intense cell wall florescence than CO at both temperatures.
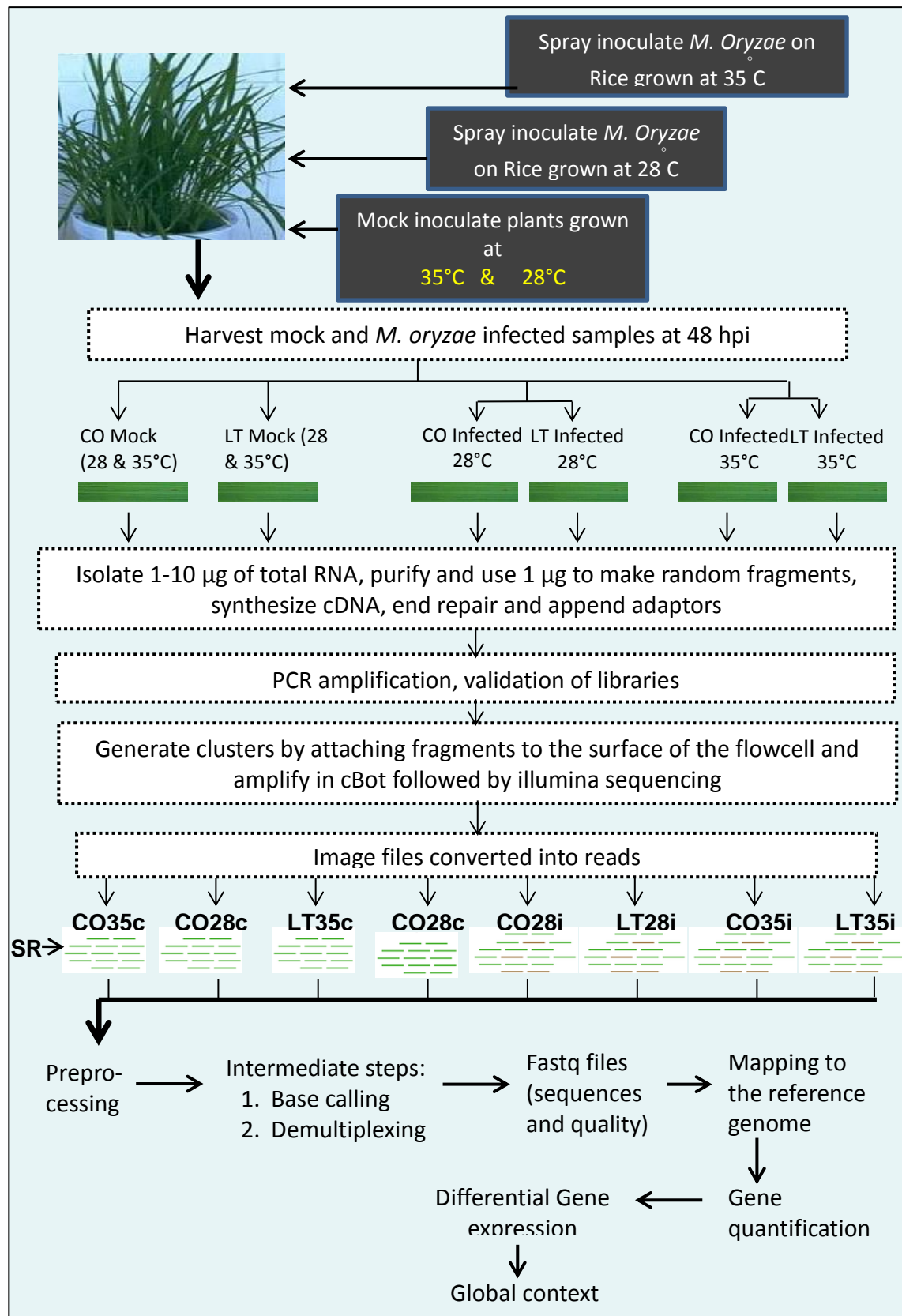
Figure 2.3a: Overview of the steps involved the mRNA isolation, illumina sequencing, preprocessing, mapping, and analysis of illumina reads and subsequent gene expression data. LT and CO represent genetic backgrounds carrying *Pi54* and exposed to 35°C and 28°C. Both genetic backgrounds were subjected to mock and *M. oryzae* inoculation. The mRNA reads were mapped to the Ensembl cDNA release 16 for *Oryza sativa*. SR-sequenced reads

[64]
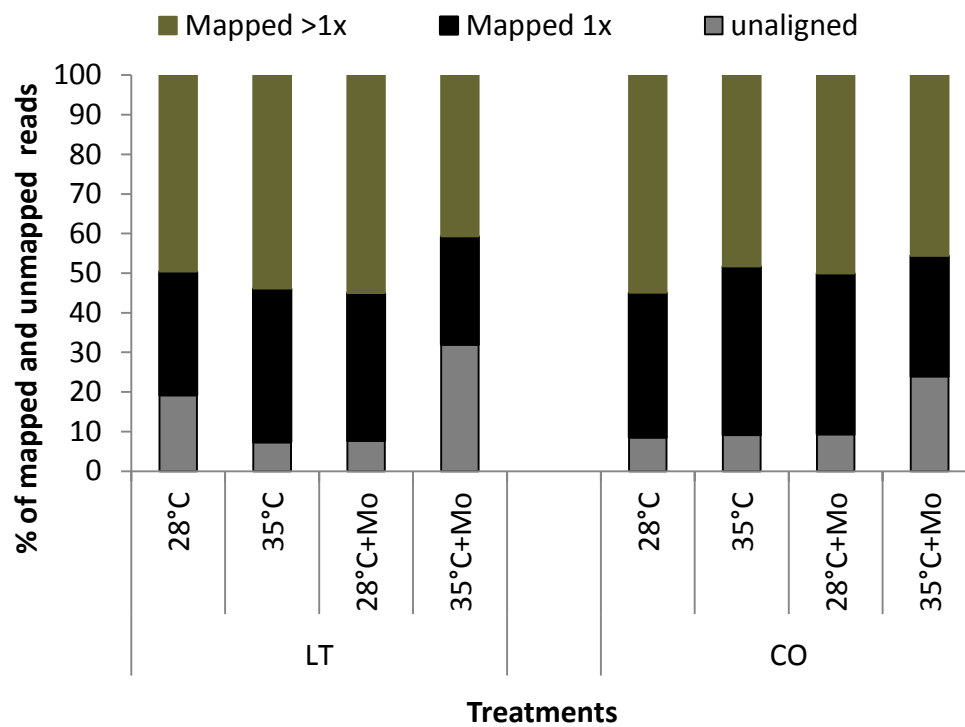
Figure 2.3b: Summary of the alignment statistics of the read mapping onto the reference genome, Ensembl cDNA release 16 for *Oryza sativa,* is presented in clustered stacked columns. Grey represents percentage of unmapped reads, black represents unique reads and green represents non unique reads. LT and CO are the genetic backgrounds carrying Pi54 and exposed to 35°C and 28°C. Mo: *M. oryzae* infection.
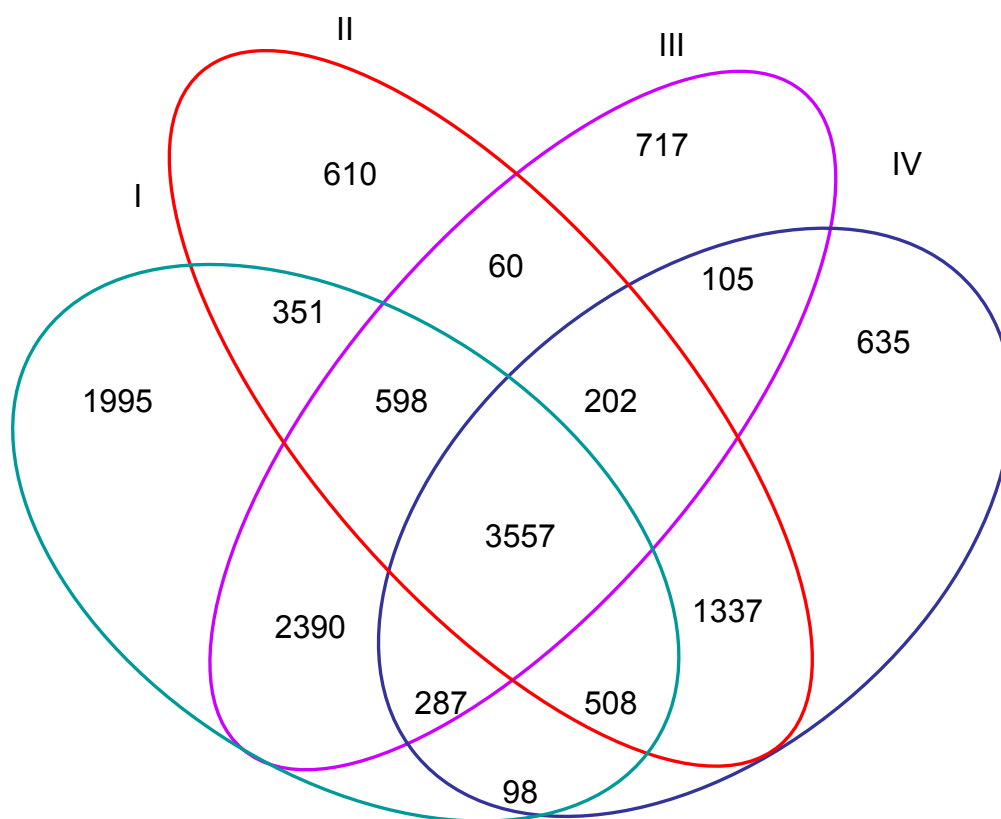
Figure 2.4a: Venn diagram analysis of the differentially expressed genes (fold change 4; FDR, 0.05) in (I) CO+28°C +Mo, (II) LT+28°C +Mo, (III) CO+35°C+Mo and (IV) LT+35°C +Mo.
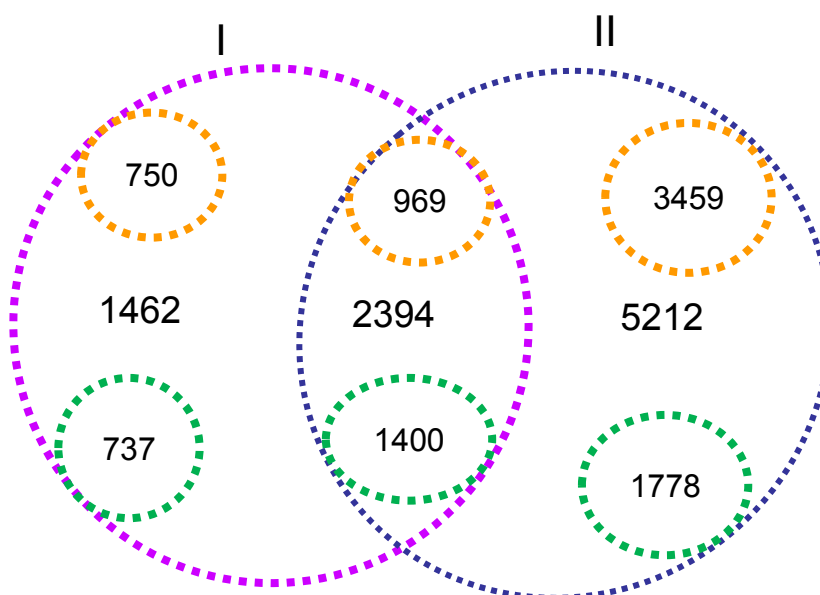
Figure 2.4b: Venn diagram analysis of the differentially expressed genes (fold change 4; FDR, 0.05) in (I) CO+35°C, (II) LT+35°C. The numbers in the orange circles represent the specific and shared up regulated genes in the respective treatments while those in the green circles represent specific and shared down regulated genes.
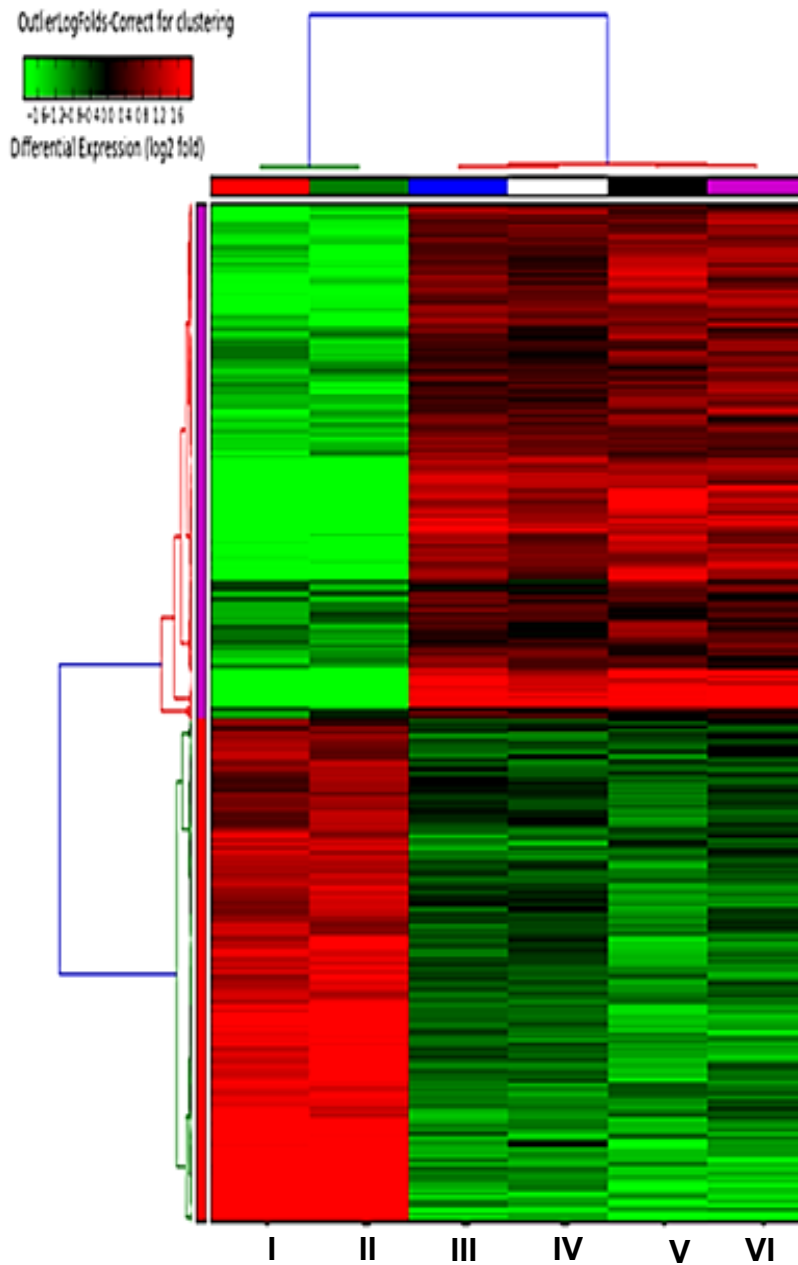
Figure 2.4c: Heat map showing the gene expression clusters and sample clusters. The color bar represents the log2 of fold change values compared to mock, ranging from green to red. Samples I, II, III, IV, V and VI represent CO+35°C, LT+35°C, LT+28°C+Mo, LT+35°C+Mo, CO+28°C+Mo and CO+35°C+Mo, respectively.
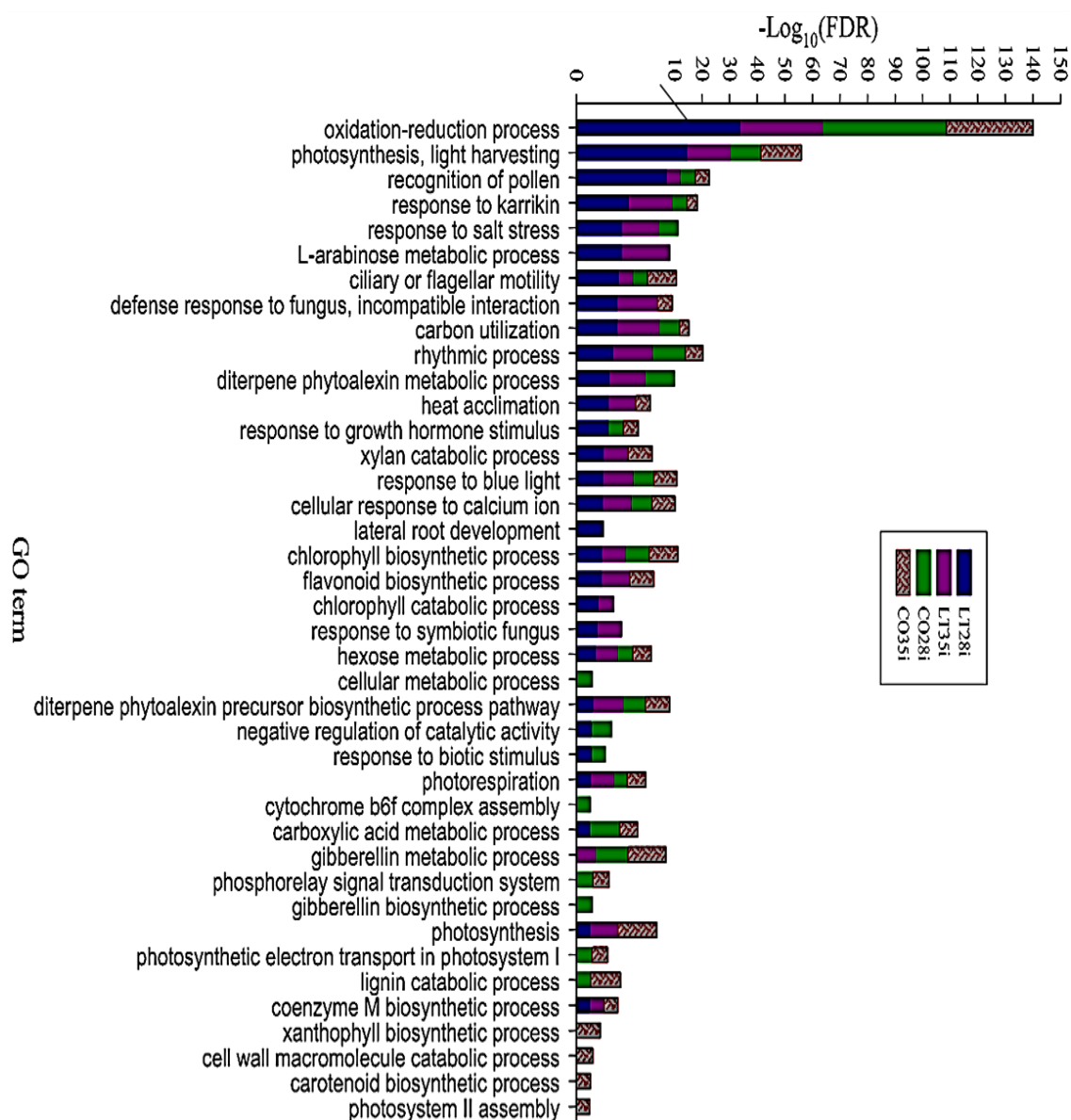
Figure 2.5: Significant Gene Ontology (GO) enriched terms from differentially expressed genes in infected samples (fold change 4; FDR 0.05); blue bars, LT+28°C+Mo; purple bars, LT+ 35°C +Mo; green bars, CO+28°C +Mo; red stripe bars, CO+35°C +Mo.
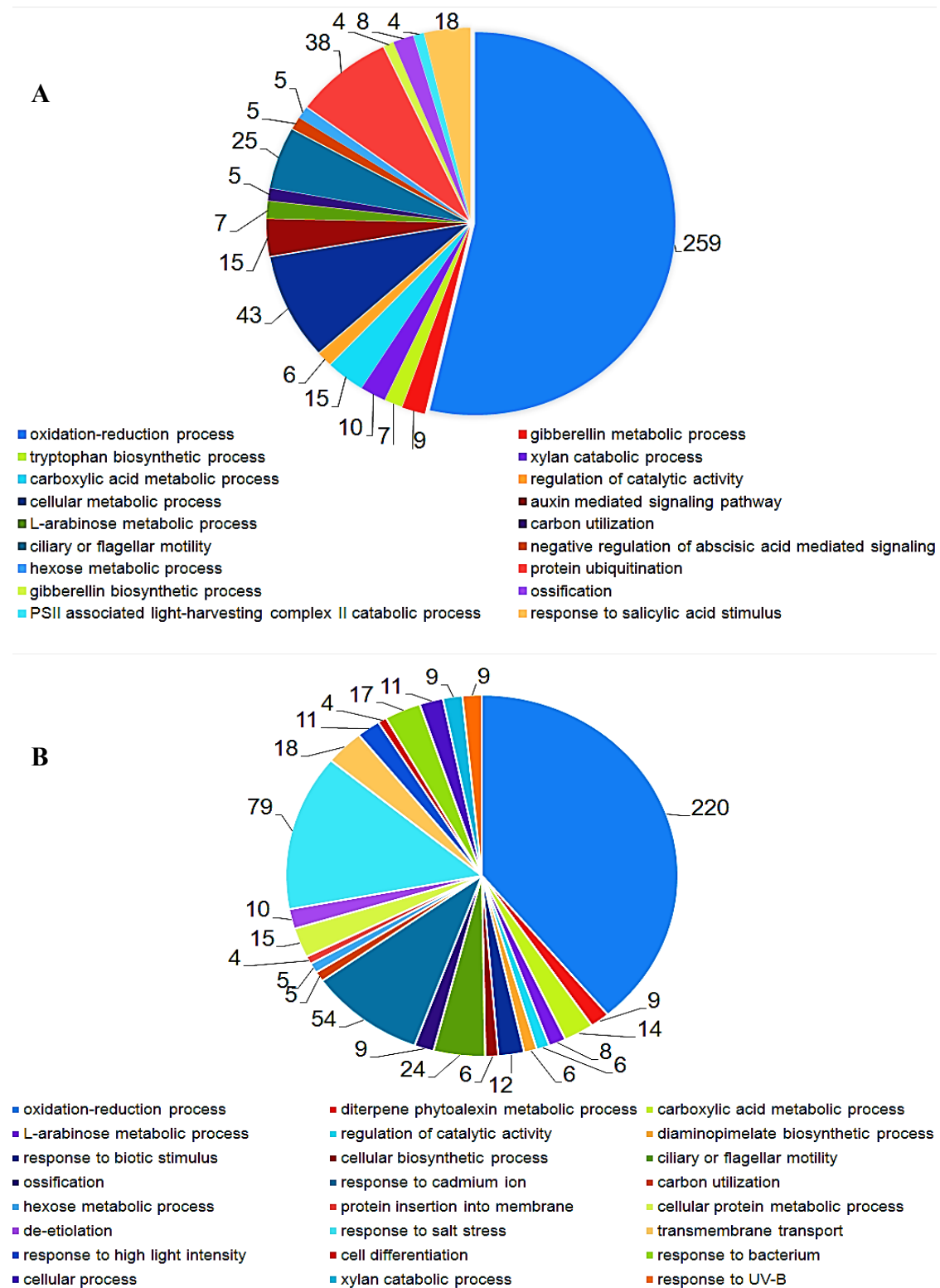
Figure 2.6: Classification of up regulated DEGs into biological processes. (A) experiment comparing RNA derived from CO+35°C+Mo to that derived from its control (CO+28°C) and B comparing sample LT+35°C +Mo to its control (LT+28°C). Only significantly enriched GO terms are presented based on over represented P-value of <0.05. The numbers represent the fraction of genes enriching the specific GO term represented in the legend.
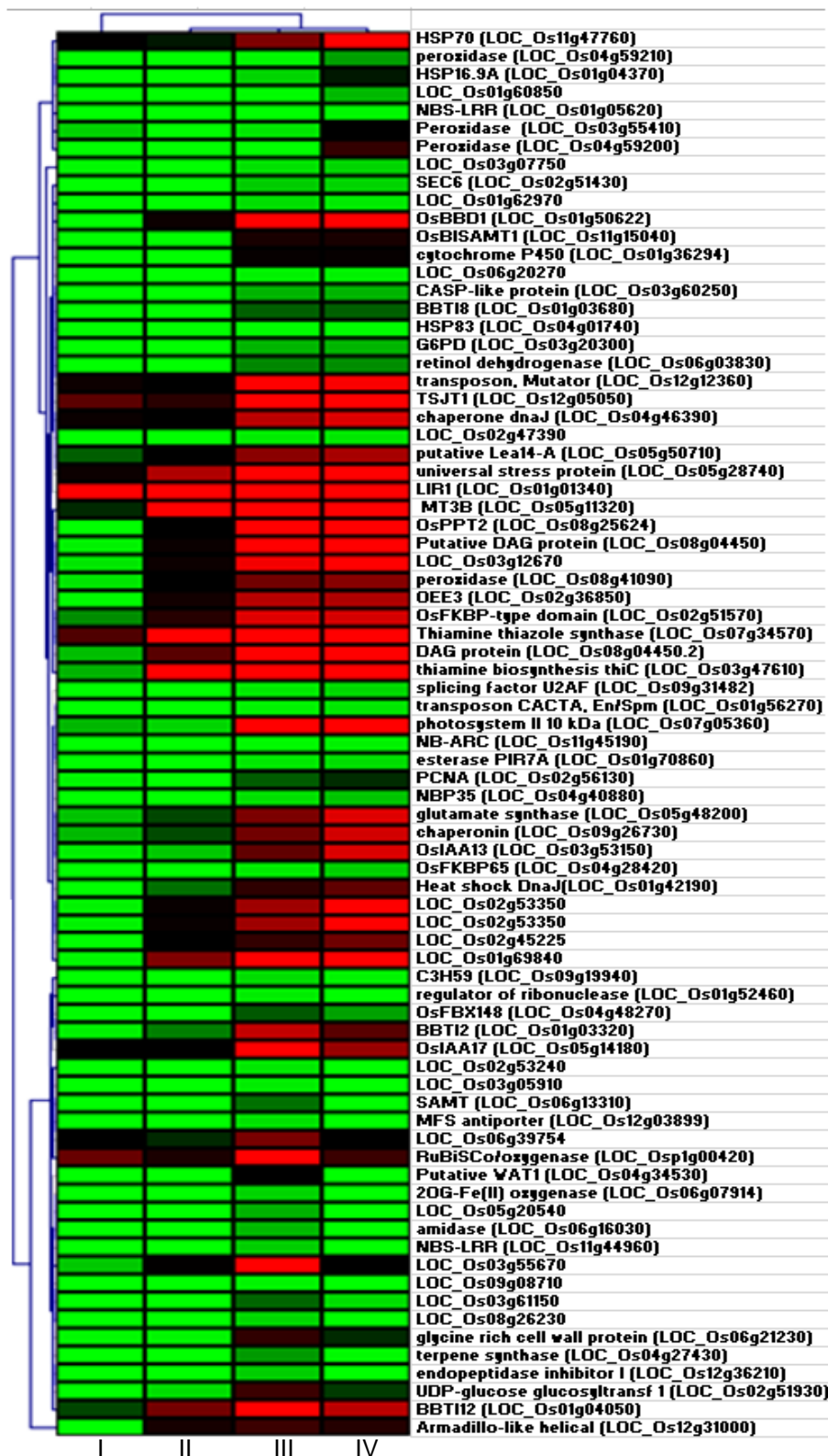
Figure 2.7: Expression profile matrix of highly induced genes in CO relative to other treatments in response to only high tempretature, made by hierarchical clustering. The treatments I-IV indicated below the cluster analysis represent LT+28°C, CO+28°C, CO+35°C and LT+35°C. On the left side of the cluster analyses the cluster dendogram is shown.
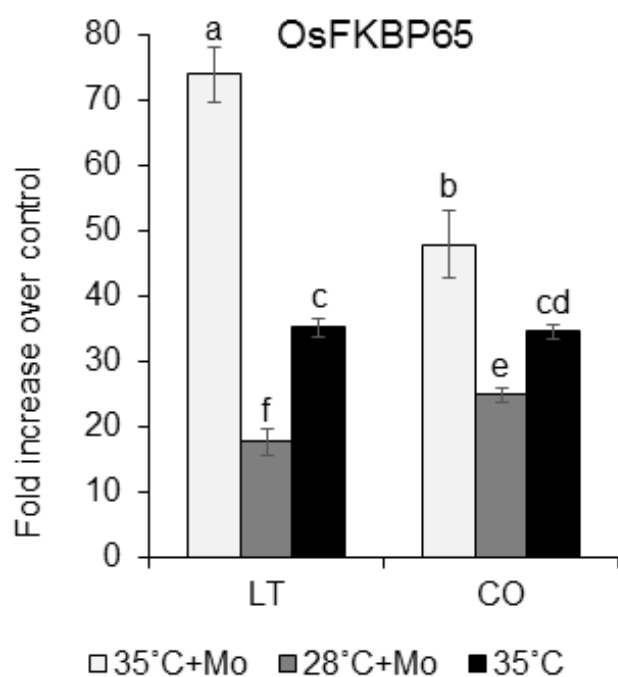
Figure 2.8: The effect of temperature, on transcript levels of OsFKBP65 in LT and Co genetic backgrounds. The samples were taken at 48 hours after inoculation.. Mock and high temperature samples were taken at 0 hpi. Data are presented as mean fold increase over control ± standard deviation. Same letters above standard error bars indicate no significant difference at P<0.05.
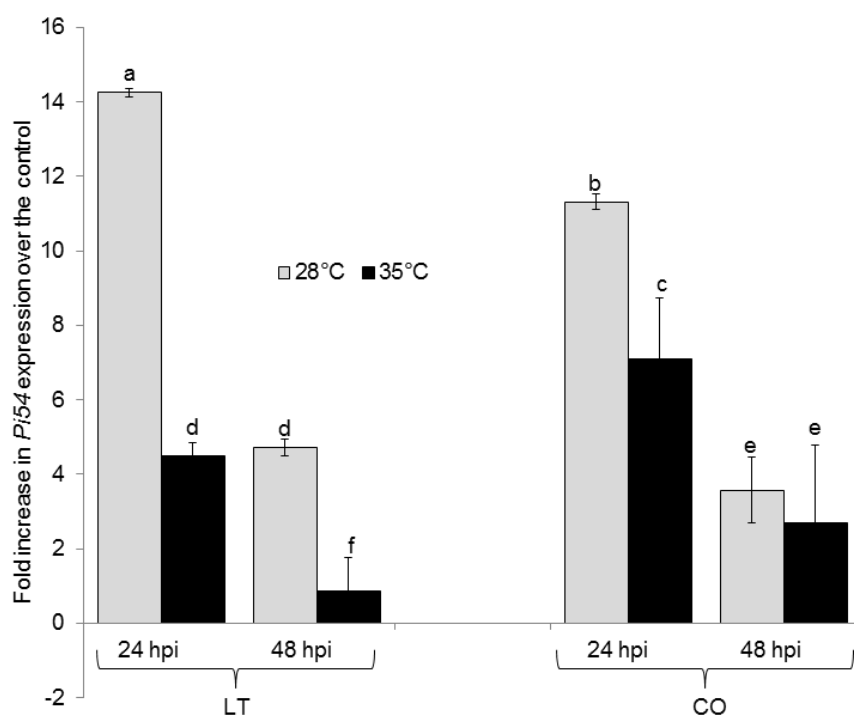
Figure 2.9: The effect of temperature, on transcript levels of *Pi54* in LT and Co genetic backgrounds. The samples were taken at 24 and 48 hours after inoculation (hpi). Mock and high temperature samples were taken at 0 hpi. Data are presented as mean fold increase over control ± standard deviation. Same letters above standard error bars indicate no significant difference at P<0.05.
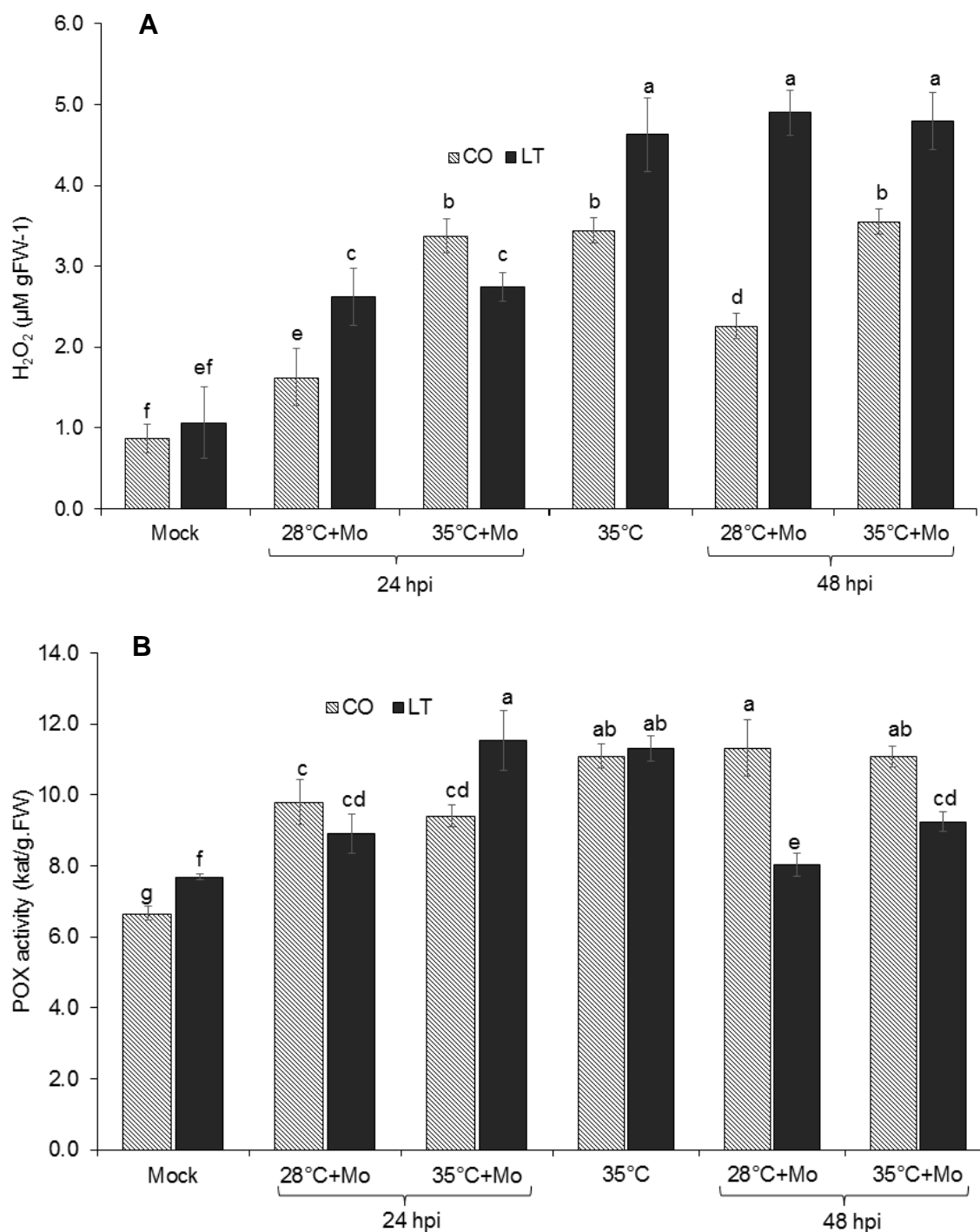
Figure 2.10: Hydrogen peroxide (H_2O_2) quantification in micromoles per gram (A) and POX activity measure in mkatal (kat) per gram (B) of fresh leaf tissue weight (FW) collected from healthy (Mock), *M. oryzae* inoculated (28°C+Mo), high temperature (35°C), and high temperature plus *M. oryzae* inoculated (35°C+Mo). The samples were taken at 24 and 48 hours after inoculation (hpi). Mock and high temperature samples were taken at 0 hpi. One katal (kat) corresponds to the quantity of enzyme activity that transforms 1 mol S^{-1} of substrate. Data are presented as mean ± standard deviation. Different letters denote significant differences at P ≤ 0.05.
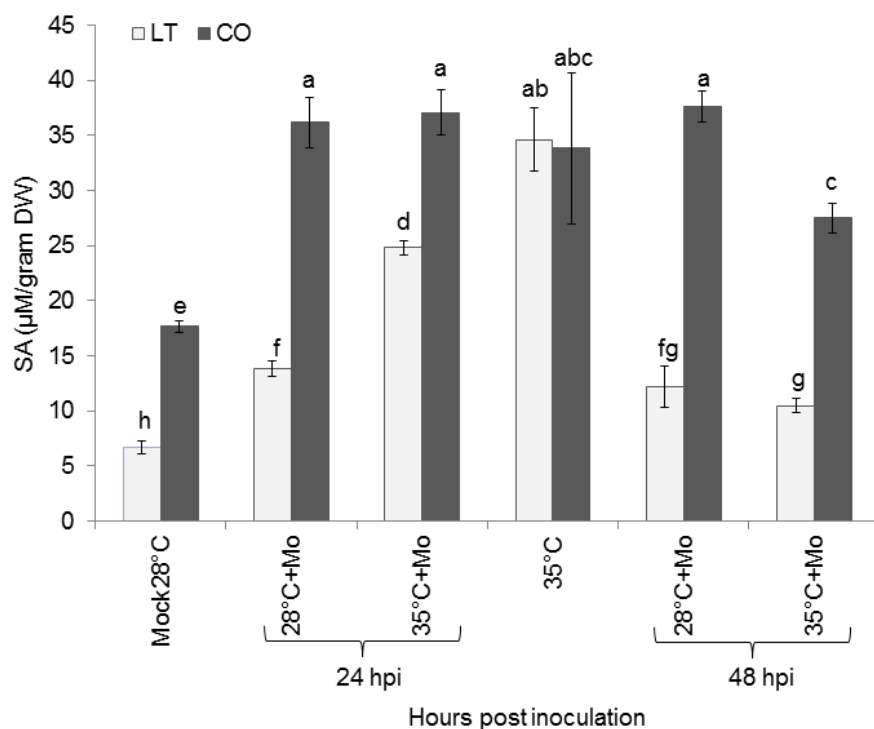
Figure 2.11: Comparison of SA accumulation in CO and LT at 28°C and 35°C. Mock28^{o}C and 35°C, represent mock samples exposed to 28°C and 35°C without pathogen inoculation. 28°C+Mo and 35°C+Mo represent samples exposed to 28°C and 35°C prior to *M. oryzae* inoculation. Sampling was done at 24 and 48 hours post inoculation. Different letters denote significant differences at P ≤ 0.05.
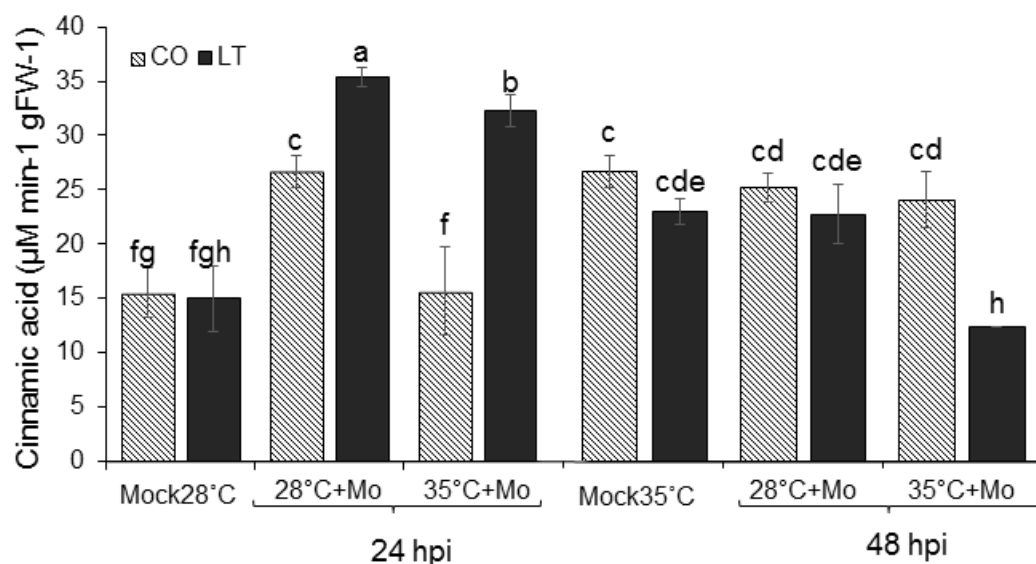
Figure 2.12: PAL activity expressed as micromolar change in cinnamic acid per minute and gram of fresh leaf tissue weight (FW) collected from healthy (Mock28°C), *M. oryzae* inoculated (28°C+Mo), high temperature (Mock35°C), and high temperature plus *M. oryzae* inoculated (35°C+Mo). The samples were taken at 24 and 48 h after inoculation (hpi). Mock and high temperature samples were taken at 0 hpi. Data are presented as mean ± standard deviation. Different letters denote significant differences at P ≤ 0.05.
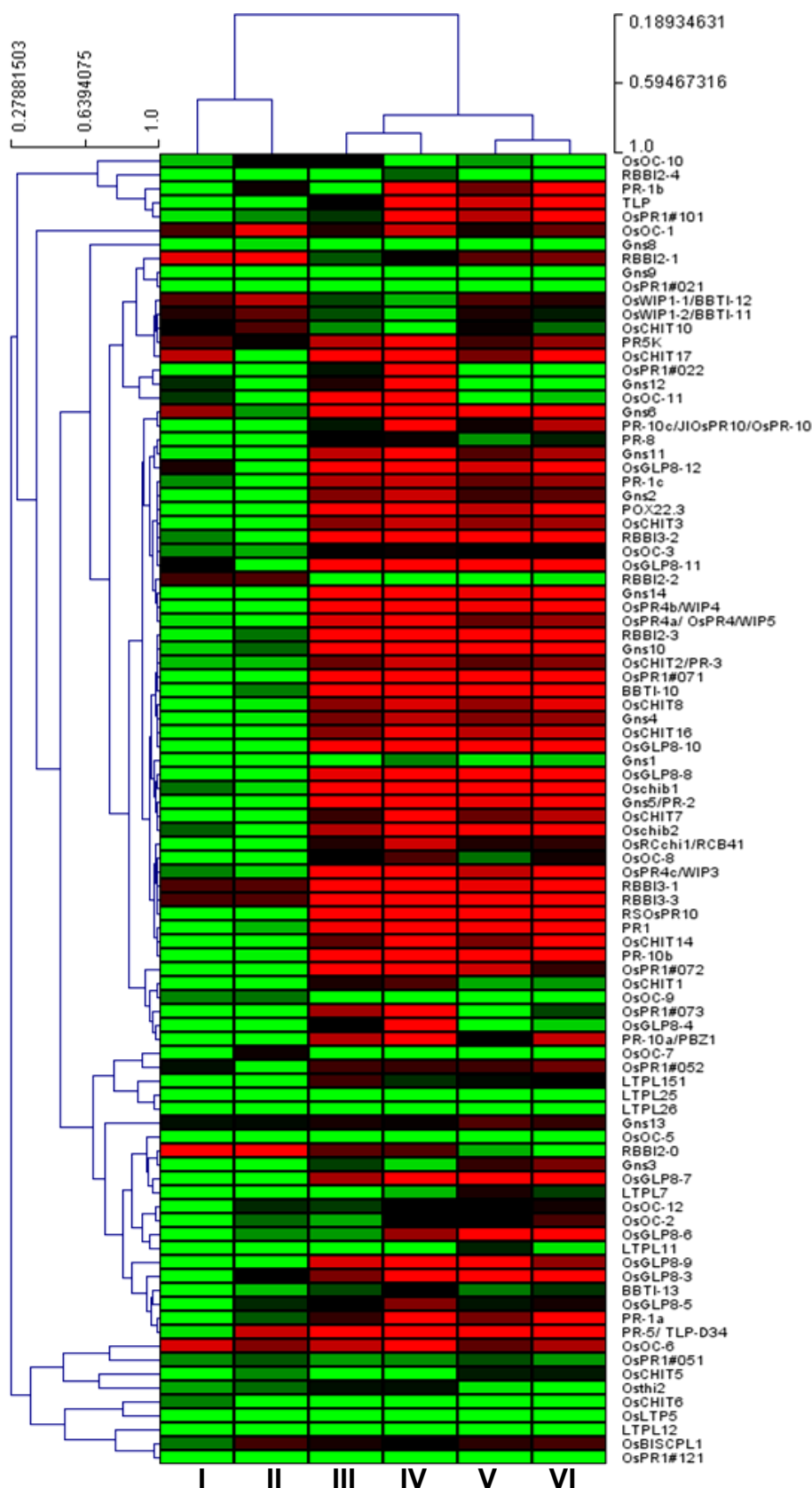
Figure 2.13: Heat map view of the previously reported PR genes differentially expressed in the six treatments I; CO+35°C, II; LT+35°C, III; CO+35°C +Mo, IV; CO+28°C +Mo, V; LT+35°C +Mo, VI; LT+28°C +Mo. Cluster analysis of expression profiles of the 78 genes. Red indicates higher expression while green represents lower expression.
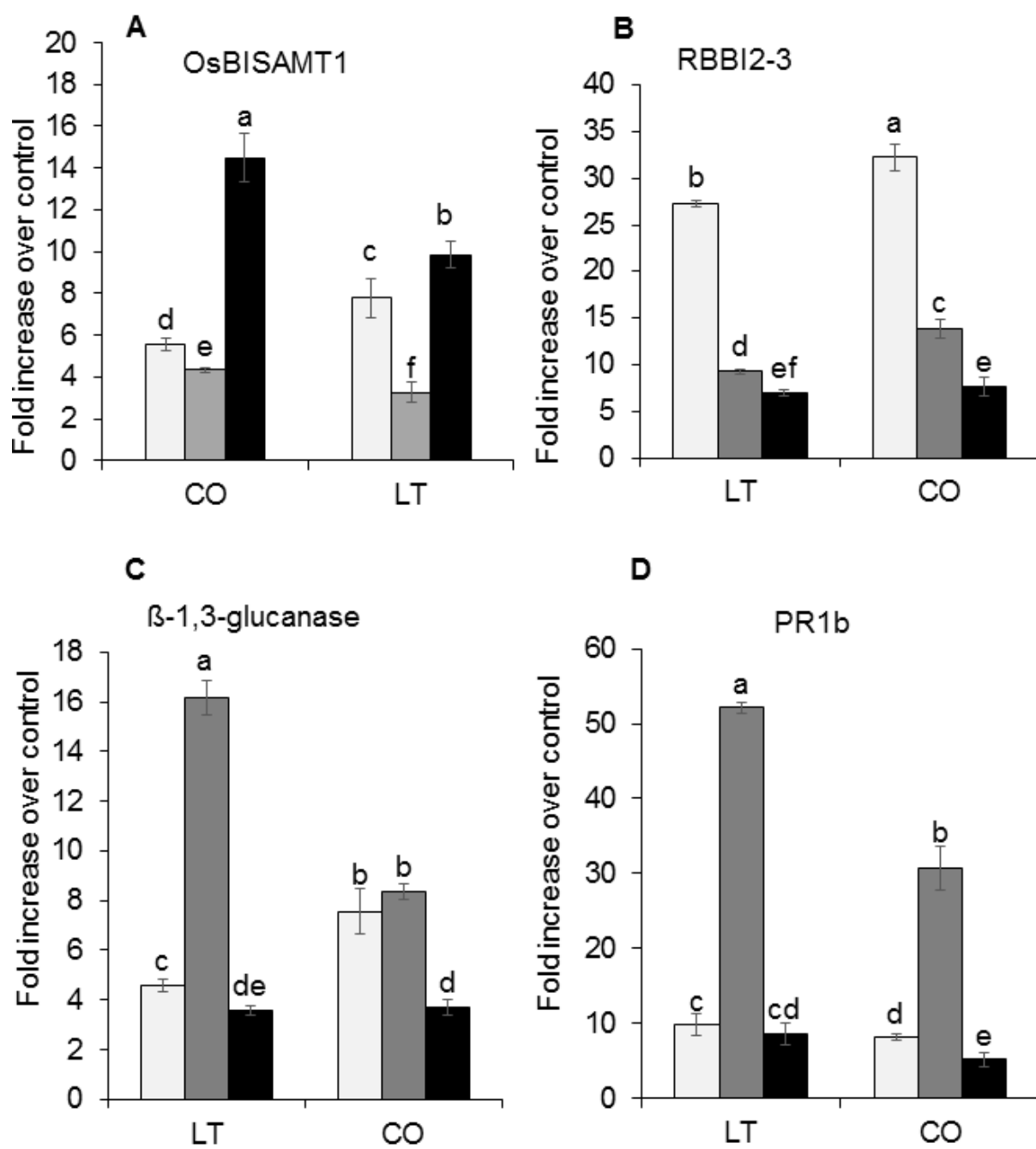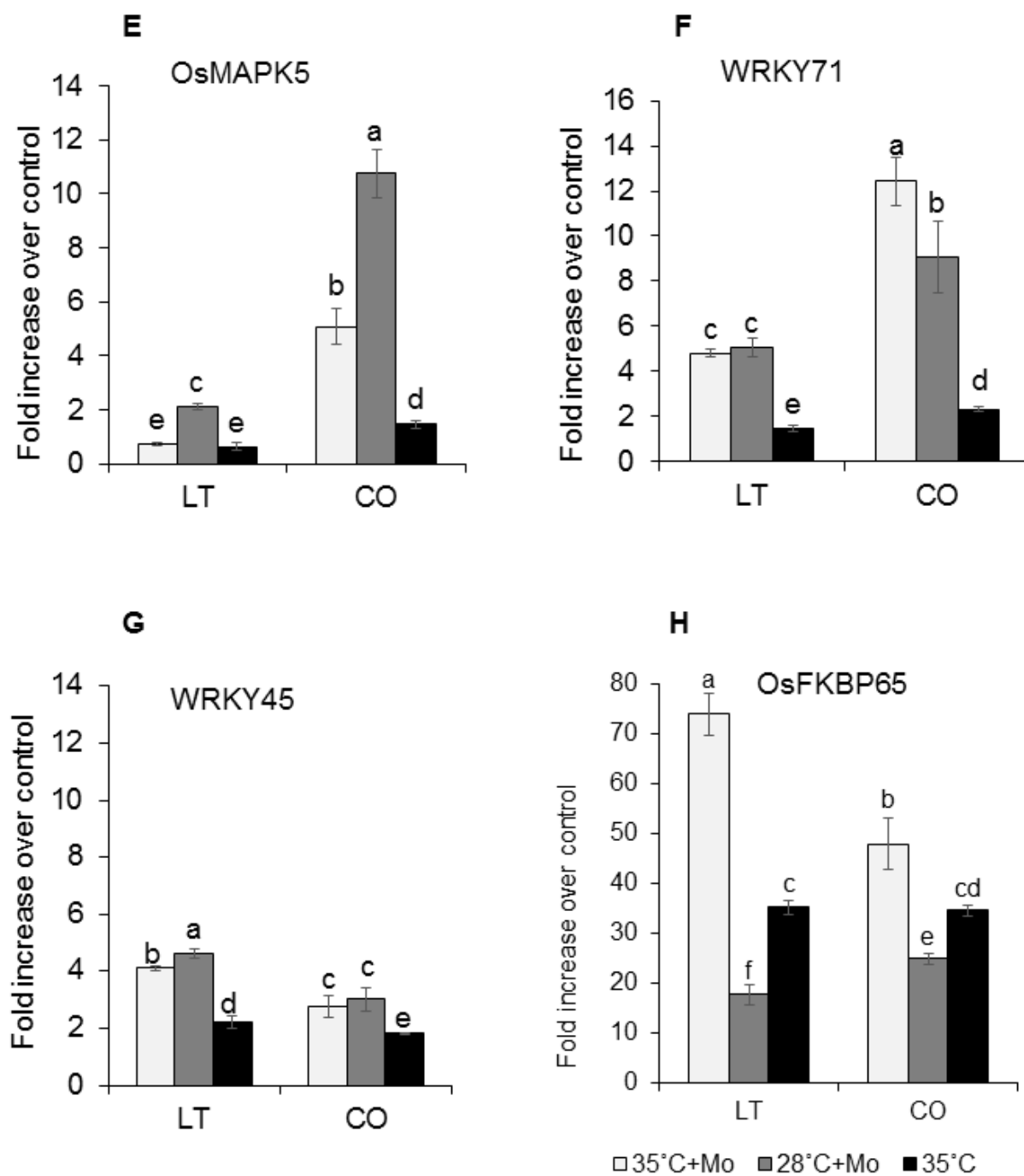
Figure 2.14: Selected differentially expressed genes in all the treatments whose transcription in rice leaves was evaluated by qRT-PCR, relative to mock28 treatment. Bars represent means (three replicates for expression level ± SD).
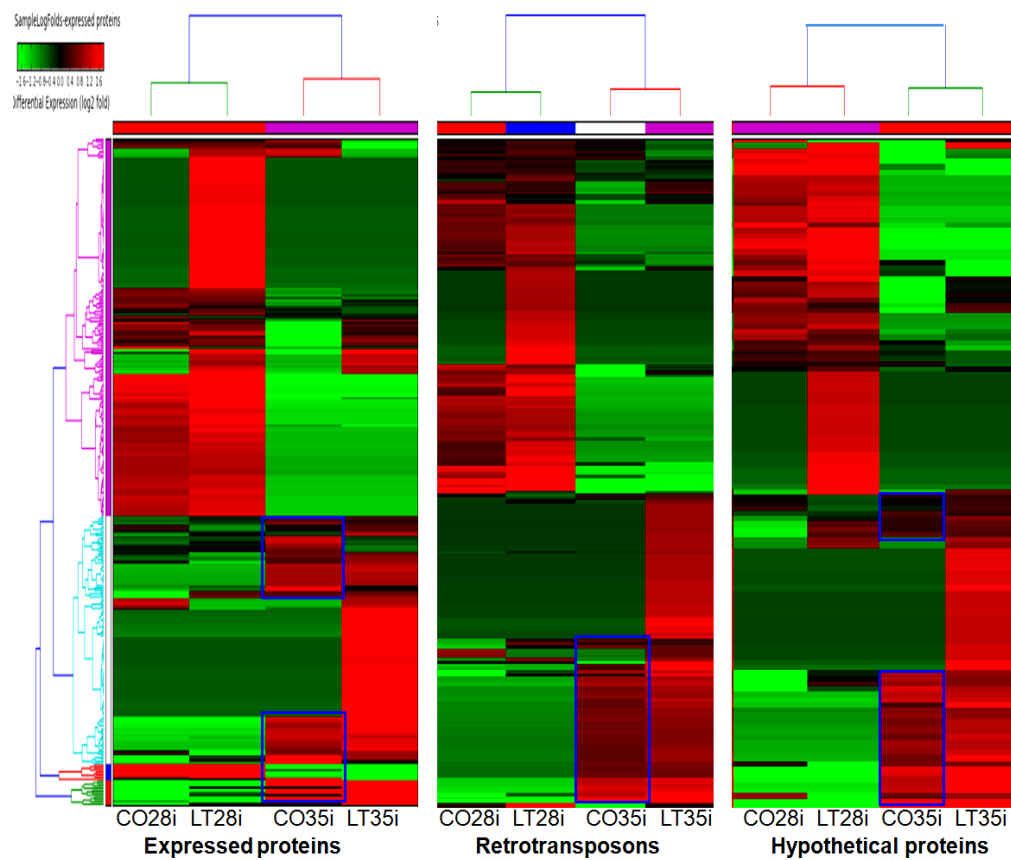
Figure 2.15: Heat map view of differentially expressed genes encoding for expressed proteins, retrotransposons and hypothetical proteins. Genes highlighted with a blue rectangle may be positive regulators of plant resistance at high temperature. CO28i, LT28i, CO35i and LT35i represent CO and LT plants infected with *M. oryzae* at 28°C and 35°C, respectively. Red indicates higher expression while green represents lower expression.

Chapter 3: Transcript profiles of *Magnaporthe oryzae* in planta expressed genes and rice defense response genes in plants pre-exposed to high temperature

First, third and last authors: Division of Plant Pathology and Crop Protection, Department of Crop Sciences, Georg-August-University Göttingen, Germany; second author: Georg-August-University Göttingen, CLB-Tropical and Subtropical Agriculture and Forestry, Germany; fourth author: Africa Rice Center, P.O Box 33581, Dar es Salaam, Tanzania.

Introduction

Temperature is arguably the most important environmental factor that influences plant pathogen interaction (Gregory et al., 2009). Temperature changes have the potential to alter the incidence and severity of plant disease epidemics and disease pressures, as well as to reshape the co-evolutionary relationships between plants and pathogens (Garrett et al., 2006). With the recent manifesting effects of climate change, it is expected that warmer temperatures will affect the biological processes leading to pathogenicity in most plant pathogens. This has been evident in some pathosystems; for instance, in wheat, studies have demostrated that higher mean temperatures correlated with hightened susceptibility to *Cochliobolus sativus* (Sharma et al., 2007). Although the optimal temperature range of 12–25°C used for wheat is considerably lower compared with an optimal temperature range of 28–32°C for rice, tropical and sub-tropical species have a narrow temperature range for growth and are likely to be more sensitive to changes in temperature (Ghini et al., 2011a). Thus, shifts in temperature may favor infection by some hemibiotrophic and necrotrophic pathogens.

Magnaporthe oryzae is conceivably the most important pathogen in global rice production. Annual rice harvest losses attributed to this disease range from 10–30%, which is enough to feed 60 million people (Dean et al., 2012). The pathogenesis of *M. oryzae* is complex and a myriad of factors associated with virulence have been implicated. Several signal transduction events have been reported to modulate appressorium formation, penetration, and infectious growth (Wilson and Talbot, 2009). Even though the current knowledge of *M. oryzae* pathogenesis is extremely insightful, the role of environment on the pathogenesis of this pathogen is incomplete. Plants pathogen interaction is not a static phenotype, but is shaped by

broad aspects of host and pathogen physiology, which are shaped by both genetic and environmental variations that often interact in nonlinear ways. Indeed, previous work has demonstrated that the influence of temperature on both pathogen fitness and host resistance affects blast pathogen infection, latency, lesion growth and sporulation, and has a significant role in blast epidemics (Ou, 1985; Teng, 1994). Hashioka (1950) reported an increase in the number of days required for rice blast infection when temperature is increased from 19 to 32°C. In a study conducted on lesion development as a function of temperature, Kato and Kozaka (1974) showed that high alternating temperatures of 32/25°C and 32/20 °C resulted in initial rapid lesion growth, with a leveling off after 15 days. Moreover, warmer temperatures have been reported to induce severer blast epidemics in the cool subtropics than in the warm, humid subtropical regions, such as southern China, the Philippines and Thailand (Luo et al., 1998). Thus, temperature may shape the host phenotype and pathogen growth by either directly affecting pathogen growth or indirectly by its effect on host immunity. The pattern in which these temperature effects occur is not well understood. Obviously, rice blast like any other pathogen may alter primary and secondary metabolism, virulence factor production and infection efficiency when the normal growth temperature is altered (Ullrich et al., 1995; Budde and Ullrich, 2000). However, the success of infection will depend on the level at which the elevated temperature modulates both components of the pathosystem.

Here, we analyzed the effect of elevated temperature on the transcriptomes of rice and *M. oryzae* simultaneously using RNAseq. We used Nipponbare, the cultivar with available sequenced genome, to determine whether the infection process of *M. oryzae* is temperature-controlled. A comprehensive search for temperature regulated genes in *M. oryzae* and Nipponbare was carried out to gain fundamental insights into the major molecular adjustments in the pathogen and the host during *M. oryzae* infection at elevated temperature.

Results

Effect of temperature on in planta fungal growth

We investigated the interaction between rice and *M. oryzae* under normal growth temperature of 28°C and a warmer temperature of 35°C using Nipponbare rice cultivar as a host. Plants pre-exposed to 35°C had a severe disease phenotype, and displayed lesions within 4 days post inoculation (dpi). Alternatively, disease development was slow and mild in plants grown and inoculated at 28°C (Figure 3.1a). We used a quantitative real-time polymerase chain reaction

(qPCR) to quantify *M. oryzae* biomass in infected leaf tissues of Nipponbare using *Pot2* primers, *pfh2a* and *pfh2b*, 48 hours after inoculation of plants exposed to 35°C and 28°C. In accordance with the disease severity observed on infected leaves, the relative fungal biomass, as indicated by the DNA quantity of *Pot2*, was significantly higher in Nip35i than Nip28i (Figure 3.1b).

RNAseq data analysis

We analyzed the transcriptomes of Nipponbare and *M. oryzae* exposed to 35°C and 28°C simultaneously using RNA-seq. Two biological replicates of each treatment were sampled at 48 hpi and sequenced (see materials and methods). We obtained an average of 57,550,449 and 58,189,196 mixed transcriptome and the reference fungal reads, respectively, after raw reads filtering. Reads were aligned to *Oryza sativa* (ENSEMBL) and *Magnaporthe oryzae* 70-15 (Broad institute) genomes using Bowtie2 v2.0.2. More than 90% (53,843,253) of the mixed transcriptome reads mapped to Nipponbare genome. Reads that did not map onto the Nipponbare genome were mapped to the reference genome of isolate 70–15, and SAM files were generated using samtools 0.1.18. To improve on the genome coverage, the fungal reads that could not be aligned to 70–15 were recombined with the mapped fungal read SAM files to guide assembly, and later processed with the *de-novo* assembler and re-mapped using CLC Genomics Workbench with default parameters i.e. two mismatches, minimum length fraction 0.9, minimum similarity fraction 0.8 and maximum hits for a read of 10. We obtained an average of 1.83% (1,053,057) reads that mapped to the fungal genome. To assess biological variation between replicates, we compared the read clustering pattern in all biological samples. Our experiments showed high levels of correlation for biological replicates (Pearson's Correlation Coefficient >0.90; Figure 3.2).

Transcript profiles of *M. oryzae* and rice during infection at 28 and 35°C

Differentially expressed genes (DEGs) in Nip28i, Nip35i and Nip35c were grouped, based on reads per kilobase of exon model per million mapped reads (RPKM) values. We used a minimum of four-fold expression based on RPKM ratio to represent significant differentially expressed genes (DEGs), for either up or down regulation. From the significant fungal DEGs, 556 were exclusive to Nip35i, 519 were found only in Nip28i, and 4302 were detected in both treatments (Figure 3.3a; additional file S1). From the up-regulated fungal DEGs, 549 and 443 were identified as Nip35i and Nip28i-specific, respectively, and 1620 were up regulated in

both treatments. We detected 143 and 212 down regulated DEGs as Nip35i and Nip28i-specific, respectively, and 2542 were down regulated in both treatments. To determine the fungal DEGs which differed significantly between Nip35i and Nip28i, the SAM files were analysed using SeqSolve software and Fisher's exact test was used test the level of significance between genes expressed in Nip35i and Nip28i. Direct visualization of significance and magnitude of differences in gene expression between Nip35i and Nip28i is presented using a volcano plot (Figure 3.3b). On the other hand, the rice response to pathogen infection and high temperature also showed differences among Nip28i, Nip35i and Nip35c treatments. A larger number of plants DEG (6458) were obtained in the comparison of Nip35i vs Nip28c, compared to 6013 in Nip28i vs Nip28c (Additional file S2). Among the differentially expressed rice genes responding to only high temperature (Nip35c vs Nip28c), 561 were up regulated and 763 were down regulated. From the anaylsis of DEGs between high temperature and *M. oryzae* infection, 1625 genes were exclusive to Nip35i, 1329 were found only in Nip28i, 420 were specific to Nip35c, whereas 652 were common to the three treatments (Figure 3.3c). The rice genes described throughout the text are provided in additional file S2.

Transcriptional changes in *Magnaporthe oryzae*

GO annotations of fungal *in planta* induced genes

Induced DEGs with at least 5 unique reads and more than 4 fold change expression in Nip35i and Nip28i, based on RPKM ratios, were selected for Gene Ontology (GO), Clusters of orthologous genes (COG) and Kyoto Encyclopedia of Genes and Genomes (KEGG) pathway representation using Fisher's Exact Test in DAVID database (Huang da et al., 2009b). The GO terms were categorized based on enrichment in biological processes (BP), cellular component (CC) and molecular function (MF). In the BP category, highly enriched subcategories in Nip35i were growth or development of symbiont on or near the host, regulation of transcription, carbohydrate transport, regulation of RNA metabolic process, oxidation reduction, ribosomal biogenesis and response to cAMP (Figure 3.4). In the CC domain, most of the up regulated DEGs were deemed intrinsic and integral to the cell membrane. The predominant annotations in the MF domain were transition metal ion binding, transcription regulator activity, electron carrier activity and peptidase activity. Terms related to interaction with host via secreted substance and secondary metabolic processes were more enriched in Nip28i than Nip35i. Terms related to transcription regulator activity, transition

metal ion binding, peptidase activity and ATPase activity were highly enriched in Nip35i than Nip28i. Fatty acid metabolism and inorganic ion transport and metabolism COG group were the most highly enriched among COGs at both temperatures. Cell division and chromosome partitioning was specific to Nip35i, whereas carbohydrate transport and metabolism was highly enriched in Nip28i. The enrichment in the KEGG pathways was also influenced by temperature. In Nip35i, genes involved in N-glycan biosynthesis, meiosis and cell cycle were dominant, whereas valine, leucine and isoleucine degradation and starch and sucrose metabolism were dominant in Nip28i. Fatty acid metabolism was enriched in both treatments.

High temperature influence on Known pathogenicity genes

To predict *M. oryzae* pathogenicity genes affected by temperature, we performed BLASTp analysis of fungal DEGs against the pathogen-host interaction gene database (PHI database). Forty-four induced genes encoding for pathogenicity proteins were represented in both Nip35i and Nip28i, whereas 18 and 8 were identified as Nip35i and Nip28i-specific, respectively (Table S1). Among the 44 genes detected, MAS3 (MGG_12337), ribonuclease T2 (MGG_10510), PWL1, PWL2, Avr-Pita1, MoHox7, CUT1 (MGG_09100) and GAS2 (MGG_04202) were >60-fold up regulated at both temperatures but with a higher induction in Nip35i than Nip28i. Isocitrate lyase (ICL), calcium-transporting ATPase 3, MAC1, MoRgs5 (MGG_08735) and ABC proteins also showed increased abundance in Nip35i than in Nip28i. Moreover, Moatg11, HDL1, MoSFl1 and ERG2 were specifically induced in Nip35i. In contrast, endo-1,4-beta-xylanases (MGG_09098) and endoglucanase II (MGG_04547) were more induced in Nip28i than Nip35i. In addition, endo-1,4-beta-xylanases (XYL2; MGG_01542 and MGG_14243) and MoRgs6 were >70-fold induced in Nip28i but not in Nip35i. All genes previously reported to mediate docking and fusion of vesicles with the plasma membrane target site (Giraldo et al., 2013), were not significantly expressed, except polarisome component (Spa2; MGG_03703), which was induced 4-fold in Nip35i but not in Nip28i.

Analysis of *M. oryzae* secretome during infection at high temperature

About 1306 genes coding for putative secreted proteins have been predicted from *M. oryzae* genome (Zhang and Xu, 2014). However, the functional analysis of most *M. oryzae* secreted proteins is a pending challenge. In this study, we predicted transcripts categorized as signal peptides in the secretome of *M. oryzae* by analyzing a set of translated gene sequences using

SignalP4.1 (Bendtsen et al., 2004), which detects the presence of a signal peptide in the amino terminus of a protein. We detected 367 and 342 signal peptides in Nip28i and Nip35i, respectively (Additional file S3). These signal peptides were analyzed using Phobius (Kall et al., 2007) and TMHMM (Krogh et al., 2001) to identify and remove proteins with TM helices, whereas proteins with mitochondrial signal peptides were identified using TargetP. Thereafter, a total of 189 induced genes encoding secreted proteins were detected, 36 of which were exclusive to Nip28i, 23 were specific to Nip35i, and 130 were identified in both treatments (additional file S4).

To gain insight into the functional categories of secreted proteins, their protein sequences were analyzed in order to identify PFAM domain categories associated with each induced gene (Finn et al., 2010). InterPro Scan was then used to confirm the distribution of recognizable protein domains among signal peptide sequences. The most frequently represented protein domains were glycosyl hydrolases, domains of unknown function (DUFs) and peptidases (Figure 3.5). To identify RxLR motifs that are thought to be required for host translocation of effectors, amino acid sequences of the secreted proteins were subjected to motif analysis using FuzzPro, a tool from EMBOSS package (Rice et al., 2000). A stringent analysis, which predicts RxLR patterns between initial 30–60 amino acids and appearing after the observed signal cleavage site (30 amino acids from the start), did not indicate any evidence of RXLR sequence presence in *M. oryzae* signal peptides. A less stringent approach, where any protein with RxLR motif and signal peptide cleavage site, without TM domain, identified 11 proteins with RxLR motifs in both Nip35i and Nip28i (Table 1), most of which were cell wall degrading glycosyl hydrolases. Interestingly, we detected a conserved hypothetical protein (MGG_14055) in this category, which was strongly induced in Nip35i but not in Nip28i. BLASTp homology search indicated that MGG_14055 shares 58% homology with β-xylosidase from *Leptosphaeria maculans* and 57% with *Bipolaris sorokiniana*. It also showed 56% identity to glycosyl hydrolase 39 of *Trichoderma atroviride*, *Bipolaris zeicola*, *Bipolaris oryzae* and *Bipolaris maydis*. Consistent with this, Pfam domain searches indicated that MGG_14055 encodes a protein with glycosyl hydrolase 39 domain. We conducted multiple sequence alignment on all the putative secreted proteins using Phylogeny.fr platform (Dereeper et al., 2008). Three major clusters were formed with branch support values >50 (Figure 3.6).

Expression of peptidases

Sequences of predicted secreted proteins were subjected to MEROPS Batch Blast analysis (Rawlings et al., 2010) to identify potential peptidases expressed during infection at high temperature. We detected 15 and 14 up-regulated peptidase encoding genes in Nip35i and Nip28i, respectively (Table 2). Among the prominent genes were MGG_00230, carboxypeptidase S1 (MGG_03995), GAS2/MAS3 (MGG_04202) and epoxide hydrolase 2 (MGG_09603). Lipase 1, categorized as peptidase family S9 was also detected in both Nip35i and Nip28i. On the other hand, tripeptidyl-peptidase 1 (MGG_07404), phosphatidylethanolamine-binding protein (MGG_06844) and lipase 2 (MGG_02130) were strongly induced in Nip35i but not in Nip28i, whereas endoprotease endo-Pro-*Aspergillus niger* (MGG_02275) was specific to Nip28i.

Table 1: Predicted genes of *M. oryzae* with RxLR in their protein sequences

Feature ID	Description	Log2FC		
		Nip35i	Nip28i	
MGG_14055	conserved hypothetical protein	10.69	-	SignalP-noTM
MGG_01885	beta-glucosidase 2	6.27	4.48	SignalP-noTM
MGG_03257	plasma alpha-L-fucosidase	4.93	3.65	SignalP-noTM
MGG_11210	beta-glucosidase 1	4.09	2.30	SignalP-noTM
MGG_10414	cholinesterase	4.07	3.37	SignalP-noTM
MGG_08088	conserved hypothetical protein	3.46	2.71	SignalP-noTM
MGG_09246	oryzin	3.46	3.14	SignalP-noTM
MGG_09732	feruloyl esterase	2.79	2.90	SignalP-noTM
MGG_03761	conserved hypothetical protein	2.29	-	SignalP-noTM
MGG_04078	WSC domain-containing protein	2.25	-	SignalP-noTM
MGG_00202	conserved hypothetical protein	2.12	-	SignalP-noTM
MGG_00042	alpha-L-fucosidase precursor	-	3.27	SignalP-noTM
MGG_01396	periplasmic beta-glucosidase	-	2.80	SignalP-noTM
MGG_01876	chitinase 3	-	6.18	SignalP-noTM
MGG_08487	cellobiose dehydrogenase	-	3,52	SignalP-noTM

Increased expression levels of previously identified and novel secreted proteins of *M. oryzae* at 35°C

Magnaporthe oryzae virulence is highly variable and has been associated with diverse enzyme activities, including glycosyl hydrolases, peptidases and lipases among others. Among the genes previously reported, four biotrophy-associated secreted proteins (BAS1–4) identified by Mosquera et al. (2009) were induced >100-fold in both Nip35i and Nip28i, but with a higher expression level in Nip35i than Nip28i.

Table 2 Peptidase like genes of *M. oryzae* induced during infection at 35°C and 28°C

Feature ID	Description	Nip35i Log2FC	Nip28i Log2FC
MGG_00230	98% AVR-Pita2	13.20	13.09
MGG_08416	lipase 1	10.88	11.50
MGG_03995	carboxypeptidase S1	10.50	9.02
MGG_09603	epoxide hydrolase 2	1030	10.50
MGG_07844	maltose permease	9.88	8.18
MGG_07584	conserved hypothetical protein	9.62	9.92
MGG_04202	MAS3 protein	9.50	10.63
MGG_02201	endothiapepsin	9.26	7.45
MGG_03468	intracellular hyphae protein 1	8.43	7.48
MGG_07404	tripeptidyl-peptidase 1	8.18	0.00
MGG_06844	conserved hypothetical protein	7.88	0.00
MGG_02130	lipase 2	7.56	0.00
MGG_01885	beta-glucosidase 2	6.27	0.00
MGG_01369	alpha/beta hydrolase fold-3 domain-containing protein	4.40	0.00
MGG_04618	amidophosphoribosyltransferase	2.58	0.00
MGG_02275	endoprotease Endo-Pro-Aspergillus niger	0.00	7.65
MGG_09716	carboxypeptidase A2 precursor	0.00	4.52
MGG_10744	beta-lactamase family protein	0.00	3.22
MGG_02987	para-nitrobenzyl esterase	0.00	2.92
MGG_07789	3-phytase	0.00	2.63

Among the genes previously published by Kawahara et al. (2012) as candidate novel fungal effectors, MGG_09379, MGG_10705, MGG_10004, MGG_12655, MGG_10080, MGG_09628, MGG_09629 and MGG_08715 were strongly induced in both Nip35i and Nip28i. In addition, two putative secreted proteins with LysM domains, annotated as intracellular hyphae protein 1 (MGG_03468 and Slp1; MGG_10097) were >30-fold induced in both Nip35i and Nip28i. MGG_10097 was not expressed in mycilia and appears to be exclusively expressed *in planta*. In addition, a conserved hypothetical protein (MGG_02405) also with LysM domain was induced >3-fold in Nip35i than Nip28i. A histidine phosphatase superfamily protein encoding gene (3-phytase A; MGG_15390) was also induced >100-fold in both Nip35i and Nip28i, but with a higher induction in Nip35i. Alternatively, several genes showed specificity in expression. For instance, MGG_11009, a putative cell wall galactomanno (GM) protein, which shares 99% sequence identity with hydrophobic surface binding protein A (HsbA) was >100-fold induced in Nip35i but not in Nip28i. Additional noteworthy genes with a >30-fold induction in Nip35i compared to Nip28i were MGG_13116, Cupredoxin (MGG_08291), W rich C domain containing protein (MGG_04263) and polygalacturonase A (MGG_08938).

Induction of genes containing partial sequences of Avr genes

A total of 7 *Avr* genes have been cloned in *M. oryzae*, including AvrPi-ta, Avr1-CO39, ACE1, AvrPiz-t, AvrPii, AvrPia, and AvrPik/km/kp (Li et al., 2012). We performed database similarity searches using the several predicted and hypothetical proteins present in our dataset to identify sequences belonging to Avr genes. Among the strongly induced genes, AVR-Pita1 (MGG_15370), MGG_00230 and MGG_16175 with 98% and 95% sequence identity to AVR-Pita2, respectively, MGG_16585 and MGG_18041 with 99% and 100% sequence identity to Avrpiz-t were induced >100-fold in Nip35i compared to Nip28i. In addition, the gene MGG_15972 with 99% identity to AvrPik/kp/km was >100-fold induced in Nip35i compared to Nip28i. Some genes shared partial sequence identity to known Avr genes and transposable elements. For example, MGG_16585 shared 99% partial sequence identity with both Avrpiz-t and AVR-Pita1 whereas MGG_15972 was 99% identical to AvrPik/kp/km, AvrPi7, flanked by 3% coverage of 98% sequence from *Pot2*. MGG_16570 shared 92% sequence homologywith Avrpiz-t and AVR-Pita1 and was induced exclusively in planta. The presence of genes with Avr identical sequences interrupted with transposable elements is consistent with the previous report (Li et al., 2012). Disease resistance response is regulated by plant resistance (R) genes whose products directly or indirectly recognize products of the corresponding pathogen avirulence (Avr) genes. To find out whether the presence of these putative Avr transcripts corresponded with the R genes currently used as differentials, we tested 32 differential lines against TAN211.16. Interestingly, *Piz-t* was highly resistant at both 28°C and 35°C (Figure 3.7). The other lines with increased resistance included Pita-2, Pii and Pi9.

Effect of high temperature stress on lipid metabolism of *M. oryzae* during infection

M. oryzae mobilizes lipid bodies for the synthesis of glycerol through lipolysis, especially during appressorium formation (Wilson and Talbot, 2009). *M. oryzae* possesses 19 genes that encode intracellular lipases, and that degrade and utilize intracellular lipids, most of which have not been functionally characterized. We detected a high induction of lipase 1 (MGG_08416), with >100-fold higher expression in Nip28i than in Nip35i (additional file S1). Transcription of other lipases, including lipase 4 (MGG_00314) and MGG_09839 was detected in both Nip28i and Nip35i. However, secreted lipase family protein (MGG_04257) was >40-fold higher induced in Nip35i than in Nip28i. Among the genes involved in the synthesis of the cell membrane components, non-specific lipid-transfer protein

(MGG_02409), 7-dehydrocholesterol reductase (MGG_03765) that catalyzes the last step of cholesterol biosynthesis, fatty acid-binding protein (MGG_07337) and fatty acid synthase S-acetyltransferase (MGG_04775) that catalyzes fatty acid synthesis intermediates from acetyl-CoA were >15-fold up-regulated in both Nip35i and Nip28i. In addition, a putative lipid phosphate phosphatase 1 (LPP; MGG_14955) was strongly induced in both Nip35i and Nip28i, but with a higher induction in Nip35i. In contrast, glycerol-3-phosphate acyltransferase (MGG_01894) required for phospholipid biosynthesis and mannosylinositol phosphorylceramide (MIPC) synthase (MGG_13744) that catalyzes the synthesis of sphingolipids were specifically induced in Nip35i, whereas a conserved hypothetical protein (MGG_15479) encoding for esterase, SGNH hydrolase-type domain containing protein was induced 55-fold in Nip28i but down-regulated in Nip35i.

Very long chain fatty acids have been reported to accumulate in fungal cells with a disrupted acyl-CoA synthetase, FAT1 (Oh et al., 2008). We detected 21-fold and 11-fold induction of long chain fatty acyl-CoA synthetase (MGG_08257) in Nip35i and Nip28i, respectively, suggesting higher fatty acid catabolism during infection at $35^{o}C$ than at $28^{o}C$. Indeed several genes involved in the initial step of fatty acid β-oxidation, including acyl-CoA dehydrogenase (MFP1; MGG_03418), which encodes a multifunctional β-oxidation protein, isocitrate lyase (MGG_04895) and malate synthase (MGG_02813) of the glyoxylate cycle, peroxisomal acetyl carnitine transferase (PTH2; MGG_01721) and MgPex6 (MGG_00529) required for peroxisome biogenesis were more induced in Nip35i than Nip28i. In contrast, mitochondrial β-oxidation protein enoyl-CoA hydratase (MGG_08775) required for neutralizing host defenses at the post-penetration stage was induced in both Nip35i and Nip28i.

Effect of high temperature stress on carbohydrate metabolism of *M. oryzae* during infection

Growth of *M. oryzae* in the plant host involves utilization of carbohydrate carbon sources, including glucose and glycerol. Storage carbohydrates include glycogen and polyols, whereas chitin, glucans and xylans are primary constituents of the fungal cell wall. We searched for carbohydrate metabolism encoding genes using the CAZy annotation pipeline (http://www.cazy.org), and compared the genes presented in *M. oryzae* inventory to the genes expressed in our study. We detected 216 genes in our dataset, 174 of which were common to both Nip35i and Nip28i (Additional file S5). Glycosyl hydrolases (GHs), glycosyltransferases

(GTs) and carbohydrate esterases (CEs) were the most abundant in our dataset. Among the GHs, MAS3 featured as the most prominent in this category. Three GH43 genes (MGG_09098, MGG_00570 and MGG_00574) also exhibited high induction during infection at both temperatures. Among the CEs, ferulic acid esterase A (MGG_10040), acetylxylan esterase 2 (MGG_15403) and fungal cellulose binding domain-containing protein (MGG_01403) were induced >50-fold at both temperatures.

Chitin is a microfibrillar b-1,4-linked homopolymer of N-acetylglucosamine (GlcNAc) synthesized by polymerase activity of chitin synthases. A putative chitin deacetylase (MGG_09159), which catalyzes the conversion of chitin to chitosan was up-regulated >60-fold in both Nip28i and Nip35i. In contrast, two chitinases (acidic mammalian chitinase; MGG_04732 and chitinase 1; MGG_05533) were more induced in Nip35i than Nip28i, whereas a hypothetical protein (MGG_05351) with a chitin-binding, type 1 domain was >100-fold up-regulated in Nip28i than Nip35i. Among the genes that exhibited specific expression, GH3 genes (e.g., MGG_08985 and MGG_01885), were specific to Nip35i, whereas GH7 exoglucanase 1 (MGG_10712) and GH10 endo-1,4-beta-xylanase (Xyl2; MGG_01542) were strongly induced in Nip28i. Genes encoding for pectin degrading enzyme (e.g., PL1; MGG_07566) were more induced in Nip28i, although PL4 (MGG_06041) was more induced in Nip35i than Nip28i. The expression of other genes involved in the utilization of non-preferred carbon sources, including genes encoding for alcohol dehydrogenase 1, galactose oxidase, levanase, NADP-dependent alcohol dehydrogenase 6, and a hypothetical protein (MGG_10051) which shares 72% sequence identity with cellobiose dehydrogenase, also showed significant up regulation (>70-fold) in both Nip35i and Nip28i. In addition, mannosyl-oligosaccharide 1,2-alpha-mannosidase IC (MGG_00994) and cytochrome P450 for alkane assimilation (MGG_05908) were also strongly induced at both temperatures. In contrast, a gene involved in sugar alcohol degradation (alcohol oxidase; MGG_09072) was >100-fold induced in Nip35i than Nip28i. Also present were genes involved in building fungal glycoproteins and other cell wall components, including mannosyl-oligosaccharide 1,2-alpha-mannosidase IB, chitobiosyldiphosphodolichol beta-mannosyltransferase, dolichyl-di-phosphooligosaccharide-protein glycotransferase and dolichyl pyrophosphate Glc1Man9GlcNAc2 alpha-1,3-glucosyltransferase. These genes were highly induced in Nip35i than Nip28i.

Stress and secondary metabolism induced genes during infection at high temperature

Genes involved in stress and defence responses have been shown to be differentially expressed during infection in *M. oryzae* (Rauyaree et al., 2004). In this study, highly up regulated genes in relation to high temperature stress included DnaJ domain-containing proteins (MGG_14699; 33-fold), chaperone protein dnaJ 2 (MGG_07502; 8-fold), heat shock factor protein HSF24 (MGG_03242; 6-fold), HSP40 (*SCJ1;* MGG_07502, 8-fold), HSP70 domain containing protein (MGG_09631; 24-fold) and methyltransferase (MGG_05053; 67-fold). In addition, a putative DnaJ domain-containing protein (MGG_03581), a flocculation suppression protein (MGG_06971), predicted protein (MGG_06486) and mitochondrial chaperone (MGG_14588) were more induced in Nip35 than Nip28i. *SCJ1* was previously reported to be induced together with LHS1 during vegetative growth and conidiation (Yi et al., 2009), suggesting its involvement in *M. oryzae* pathogenicity. We used the cytochrome P450 database (FCPD) pipeline (http://p450.riceblast.snu.ac.kr/) to identify cytochrome P450 encoding genes. Prominent genes identified in this category included averantin oxidoreductase (MGG_10070), pisatin demethylase (MGG_05235), metalloproteinase (MGG_15370) and epoxide hydrolases (e.g., MGG_03070 and MGG_09603). Additional noteworthy genes were ent-kaurene oxidases (e.g., MGG_02294), CYP589A1 (MGG_12497), polyketide synthase (MGG_00241), citrinin polyketide synthase (MGG_10011) and CYP611A1 (MGG_10355) (Additional file S6). In contrast, two cytochrome P450s (CYP563A1; MGG_07593 and CYP608A1; MGG_04337) were induced in Nip35i but not in Nip28i. Both genes putatively encode for cytochrome P-450 monoxygenases required for isotrichodermin C-15 hydroxylation in trichothecene biosynthesis. A high induction of pentalenene synthase (MGG_10671), phenylacetone monooxygenase (MGG_00824) and geranylgeranyl pyrophosphate synthetase (MGG_03432) was also detected in both Nip35i and Nip28i, suggesting that their function is independent of high temperature effect. Peroxidases have been suggested to be integral components of antioxidant defense system in *M. Oryzae* (Egan et al., 2007; Fernandez and Wilson, 2014b). We searched the Fungal Peroxidase Database (fPoxDB) for peroxidase encoding genes and found 27 putative peroxidases in *M. oryzae* genome. Among them, *MoCCP2* (MGG_10368), *MoVPX1* (MGG_02210) and *CATA* (MGG_10061) were more induced in Nip35i than Nip28i. In addition, thioredoxin peroxidase (MGG_07503), oxidoreductase (MGG_02115), L-ascorbate oxidase (MGG_14307) were stronger induced in Nip35i than Nip28i, suggesting an adaptive response to the ROS environment in plants, probably induced in response to high temerature.

Alternatively, MoHPX2 was highly induced in Nip28i but was not significantly induced in Nip35i.

Genes encoding for 2-oxoglutarate-dependent ethylene/succinate-forming enzyme (MGG_10266) and 1-aminocyclopropane-1-carboxylate deaminase (MGG_02812) were also higher induced in Nip35i than in Nip28i. In addition, salicylate hydroxylases (e.g., MGG_03764 and MGG_10012) and 2,3-dihydroxybenzoic acid decarboxylase (MGG_03793) required for SA degradation and conversion of 2,3-dihydroxybenzoic acid to catechol, respectively, were induced >100-fold in both Nip35i and Nip28i. The gene encoding for general amino acid permease (GAP1; MGG_07606), previously shown to be down-regulated in the study of Mathioni et al. (2012), was up and down-regulated in Nip35i and Nip28i, respectively.

Magnaporthe oryzae induced genes encoding for transport proteins

Fungal pathogenesis requires active translocation of various molecules, including water, amino acids, proteins, soluble carbohydrates, fatty acids, and enzymes, and removal of antifungal plant defense compounds. Our data revealed differential expression of genes encoding various transporters, including ATP-binding cassette (ABC) and major facilitator (MFS) transport proteins and ion transporters (Additional file S7). From the up regulated ABC transporters, multidrug resistance protein CDR1 (MGG_07848) was strongly induced in both Nip35i and Nip28i. The same was true for ABC-type Fe^{3+} transport system (MGG_10060). In contrast, ABC transporter CDR4 (*ABC1;* MGG_13624), previously reported to be strongly induced by azole fungicides and the rice phytoalexin sakuranetin (Oh et al., 2008) was induced in Nip35i but not in Nip28i. Among the major facilitator superfamily (MFS) genes, two genes (MGG_00144 and MGG_01877) were strongly induced (>100-fold) in Nip35i but not in Nip28i. Other MFS encoding genes (e.g., MGG_06794 and MGG_02167), which were previously reported to share homology with toxin efflux pumps and multidrug transporters (Oh et al., 2008), were >30-fold induced in Nip35i than Nip28i. We further found that malic acid transport protein (MGG_09085), inorganic phosphate transporter PHO84 (MGG_03299), ammonium transporter 1 (MGG_04576), phosphate transporter (MGG_04251), urea active transporter (MGG_09063), aquaporins and oligopeptide transporter 2 (MGG_08984) were more induced in Nip35i than in Nip28i. Furthermore, the major myo-inositol transporter iolT (MGG_08776) and calcium-transporting

ATPase 3 (MGG_10730) were induced >20-fold in Nip35i compared to Nip28i, which suggests that these genes play a role in plant infection at high temperature. In contrast, the MFS gene encoding for H(+)/hexose cotransporter 1 (HUP1; MGG_08617) involved in sugar transport was >100-fold induced in Nip28i compared to Nip35i. Other noteworthy genes up-regulated at both temperatures included a quinate permease (MGG_07779), a lactose permease (MGG_00085), two maltose permeases (MAL31; MGG_07844 and MAL61; MGG_08266), peroxisomal 2,4-dienoyl-CoA reductase (SPS19; MGG_05138.6), an aquaporin-9 (AQY2; MGG_13615), glycerol kinase (GUT1 MGG_10005) and a sorbose reductase (SOU1; MGG_07883). The induction of these genes is consistent with the previous report (Mathioni et al., 2012).

Regulation of transcription factors in *M. oryzae* during infection at high temperature

A list of all *M. oryzae* transcription factors expressed in this study was identified using InterPro terms associated with DNA-binding motifs as described by Park et al. (2013). Using InterPro domain classification, we identified fungal-specific Zn2Cys6 and C2H2 zinc finger as dominant TF genes expressed during infection (Additional file S8). All *M. oryzae* TFs present in the Fungal Transcription Factor Database (FTFD, http://ftfd.snu.ac.kr) were also analyzed for domain categrization. From the 120 TFs identified as up regulated, 112 and 89 were expressed in Nip35i and Nip28i, respectively. A hypothetical protein with Homeodomain (MGG_09628) was induced >100-fold at both temperatures. Two C2H2 zinc finger (MGG_10280 and MGG_10276) and a winged helix repressor (MGG_08377) were specifically induced *in planta*. In contrast, a nucleic acid-binding, OB fold (MGG_04335) was induced >100-fold more in Nip35i than Nip28i, whereas for C2H2 zinc finger (MGG_15489) the opposite was true. In addition, two Zn2Cys6 genes (MGG_02879 and MGG_00049) and C2H2 zinc finger (MGG_04546) were >50-fold induced in Nip35i, but not in Nip28i. One TF, previously reported to be a general regulator controlling multiple processes in *M. oryzae*, MGG_00021 (Park et al., 2013), was more induced in Nip28i than Nip35i. Conversely, the *MST12* (MGG_12958) transcription factor that was previously reported to be regulated by *PMK1* during penetration and invasive growth, and Ste50 (MGG_05199), an adaptor protein for the upstream components of the *PMK1-MST7-MST11* cascade, were slightly induced (>4-fold) in Nip35i, but not in Nip28i. Additional noteworthy genes that were highly induced in Nip35i than Nip28i were cutinase transcription factor 1 beta (MGG_08199), transcriptional activator xlnR (MGG_02880), and several genes of unknown function with Zn2Cys6 domain,

including MGG_08777 and MGG_07368. Interestingly, two TF genes (MGG_00080 and MGG_10575) were strongly down-regulated at high temperature (>100-fold). The functional role of these genes remains ellusive.

Temperature-responsive, promoter motifs identified for induced genes specific to Nip35i

We analyzed the upstream intergenic sequences of genes with >15-fold up-regulation that were specifically expressed during infection at high temperature to identify motifs that correlate with temperature-dependent changes using the MEME algorithm. MEME analysis returned three motifs with E-value <0.1. Motif 1 was enriched with tyrosine kinase phosphorylation site between amino acids 33-40 and casein kinase II phosphorylation site 34-37. Motif 2 consisted of protein kinase C phosphorylation site 32-34, N-myristoylation sites 23-28 and 28-33 and casein kinase II phosphorylation site 43-46. Motif 3 consists of N-glycosylation site 7-10 and N-myristoylation site 15-20. Motif 2 and Motif 3 were the most abundant in the upstream regions of genes showing significant enrichment (Figure 3.8).

Rice plant reactions in response to HT and M. oryzae infection

GO enrichment and transcript abundance in rice during *M. oryzae* infection

On the basis of GO categories, rice transcripts were assorted into several biological categories using AgriGO. Parametric analysis of gene set enrichment (PAGE) tool was used to identify GO terms significantly associated with Nip35c, Nip35i and Nip28i versus Nip28c comparisons. PAGE method is based on central limit theorem, and considers gene expression level using a two-tailed test to count Z scores. The up-regulated transcripts were grouped into 21 GO terms in infected samples (Nip28i and Nip35i) and 16 categories in Nip35c vs Nip28c (Figure 3.9). The prominent categories in all the treatments were related to metabolic process, followed by response to stimulus, response to stress and protein modification process. To identify common transcriptional changes due to temperature effect and *M. oryzae* infection, the gene expression profiles obtained from Nip35c and Nip35i were compared to Nip28i. Among the genes with >40-fold induction in both Nip35c and Nip35i, were genes encoding for peptidyl-prolyl isomerase (OsFKBP65; LOC_Os04g28420), photosystem II 10 kDa polypeptide chloroplast precursor (LOC_Os07g05360), S-adenosyl-L-methionine benzoic acid/salicylic acid carboxyl methyltransferase (OsBISAMT1; LOC_Os11g15040) and expressed protein (LOC_Os09g13440), which is consistent with our previous findings.

Activated signaling pathways involved in rice defense against pathogen attack at high temperature

Plant defense response genes are transcriptionally activated by pathogens depending on specific environmental conditions. In this study, we detected several genes involved in recognition (receptors), signaling, transcription modulation and downstream cascades associated with plant defense. We detected 204 receptor like kinases, among which SHR5 genes (e.g., LOC_Os08g10310) were induced >100-fold in both Nip35i and Nip28i. LOC_Os08g10310 was slightly induced (12-fold) in Nip35c, suggesting that SHR5 is relatively more responsive to *M. oryzae* infection than high temperature. Additional noteworthy genes were wall-associated receptor kinase-like 22 (LOC_Os10g07556), receptor protein kinase-like (LOC_Os10g05570), LOC_Os05g16930, OsWAK89a, OsWAK95, OsWAK88, OsWAK80, OsWAK71, OsWAK37, OsWAK38 and CRK5 (LOC_Os04g56430). LOC_Os05g16930 shares 85% sequence identity with *Oryza brachyantha* LRR receptor-like serine/threonine-protein kinase, and was specifically induced in Nip35i.

In rice-*M. oryzae* interactions, MAPKs play significant roles in transducing defense signals to downstream targets. We detected induction of OsMPK13 (LOC_Os02g04230) and OsMPK5 in both Nip35i and Nip28i. Both genes have been shown to be induced by ACC and *M. oryzae* infection (Reyna and Yang, 2006), and are markers for negative plant resistance in rice. Also prominent were calcium response signaling genes, including OsCML25, OsCML26, calmodulin binding proteins (e.g., LOC_Os11g44700 and LOC_Os11g44630), which were up regulated >50-fold during *M. oryzae* infection. These genes were undetected in samples exposed to only high temperature, except OsCIPK4 (LOC_Os12g41090).

One important feature of plant response to stress is cell wall modification. We detected 501-fold and 184-fold induction of a beta-expansin gene (LOC_Os06g47360) in Nip35i and Nip28i, respectively. Another expansin gene (LOC_Os09g29710) was 84-fold and 40-fold induced in Nip35i and Nip28i, respectively. Expansins have the ability to induce extension of cell walls and enhance stress relaxation (Valdivia et al., 2007). NCBI BLAST search comparisons of LOC_Os06g47360 revealed high sequence similarity with blight-associated protein p12, which was previously associated with citrus blight (Ceccardi et al., 1998).

During plant pathogen interaction, pathogens that successfully elude the first layer of defense secrete effectors that deregulate PTI. To counteract this, plant resistance (R) proteins recognize effectors and activate effector-triggered immunity. Genes encoding for coiled-coil motif nucleotide binding site–leucine-rich repeat (CC-NBS-LRR) proteins (e.g., LOC_Os04g25900) and NBS-ARC RPM1 like encoding gene (LOC_Os08g16070) were up-regulated >100-fold in Nip35i, but not in Nip28i. LOC_Os04g25900 was previously shown to be induced in rice challenged with Brown plant hopper (Kamolsukyunyong et al. 2013), and is apparently induced by ethylene.

The expression of genes encoding for ROS producing enzymes was evidently lower in response to both high temperature and infection. Alternatively, the induction of genes encoding for ROS scavenging enzymes, including peroxidases, cytochrome P450s, thioredoxins, catalase isozyme B, glutaredoxin and glutathione S-transferases was evident at both temperatures.

Hormone signaling pathway in relation to high temperature in Nipponbare

Phytohormones regulate plant resistance through mediation of signaling pathways in response to environmental stresses. The role of salicylic acid (SA), ethylene (ET) and jasmonic acid (JA)-mediated signaling in response to pathogen infection is well documented (Denancé et al., 2013). SA is also a key mediator of high temperature response in plants (Bita and Gerats, 2013). We previously reported that MeSA is emitted in response to both high temperature and *M. oryzae* infection (Onaga et al., unpublished), which is consistent with the results of this study. We also indicated that MeSA was not an inducer of a defense response, but probably invokes the JA pathway to boost rice defense against *M. oryzae*. Indeed, we detected >50-fold induction of 12-oxophytodienoate reductase (LOC_Os06g11210), LOXC2 (LOC_Os08g39850), AOS (LOC_Os03g12500), LOX2 (LOC_Os08g39840) and several other LOX and AOS, but we did not detect MeJA production related genes as previously found in our study involving R genes. We also detected two BRASSINOSTEROID INSENSITIVE 1 (BRI1)-associated receptor kinase 1 encoding genes (LOC_Os11g31540 and LOC_Os11g31530), which were >100-fold induced. BRI1s are members of the leucine-rich repeat RLK (LRR-RLK) family that perceive signals from brassinosteroids (BRs), a steroid hormone that regulates a wide range of developmental and physiological processes in plants (Tang et al., 2010). BRs induce the expression of 12-oxophytodienoate reductase and 1-

aminocyclopropane-1-carboxylate synthase (Nakashita et al., 2003). This is consistent with a strong induction of ET associated genes, including 1-aminocyclopropane-1-carboxylate oxidase (LOC_Os08g30100; 405-fold), naringenin,2-oxoglutarate 3-dioxygenase (LOC_Os04g49194; 286-fold and LOC_Os04g49210; 172-fold), ACC (LOC_Os04g48850) and ERF1 (LOC-Os09g39850 and LOC_Os03g64260), and the JA biosynthesis pathway enzyme 12-oxophytodienoate reductase. Other noteworthy genes were flavonol synthase/flavanone 3-hydroxylase (DMR6), regulators of auxin signaling such as OsIAA25, OsGH3.2 and OsIAA13 and SMALL AUXIN-UP RNA genes (OsSAUR26, OsSAUR20, OsSAUR24, OsSAUR25 and OsSAUR2).

Induced transcription factors in rice during M. oryzae infection at 35 and 28°C

Transcription factors (TFs) play an essential role in modulating defense, hormone and growth related genes. Superfamily TFs, including WRKYs, MYBs, bHLH and C2H2 were significantly expressed in this study. Among the WRKYs, OsWRKY84, WRKY47, WRKY49, WRKY107, WRKY19 were >50-fold induced in Nip35i. Six MYB genes, LOC_Os11g01480, LOC_Os12g01490, LOC_Os08g33150, LOC_Os09g23620, LOC_Os05g37060 and MYB4 (LOC_Os02g41510) showed >20-fold induction in both Nip35i and Nip28i. Induction of OsMYB4 is consistent with our previous study (Onaga et al., unpublished). We also detected up regulation of several pentatricopeptide PPR repeat containing proteins, including LOC_Os03g55840 and LOC_Os11g37330, which share structural identity with some of the MYB encoding genes. The induction of genes encoding for AP2 domain containing proteins (e.g., OsEREBP1; LOC_Os09g39850, LOC_Os03g08470 and LOC_Os03g08460) is consistent with our previous findings, and is apparently associated with the increase in the amount of the JA precursor 12-Oxo-phytodienoic acid (OPDA) in the ethylene-JA interplay against pathogen infection. Other up regulated TFs include ZOS8-14 - C2H2 zinc finger protein (LOC_Os08g44830; 97-fold), CCT/B-box zinc finger protein (LOC_Os02g49230; 92-fold) and core histone H2A (LOC_Os03g06670; 15-fold). Besides this, we detected >100-fold induction of putative aspartic proteinase nepenthesin encoding genes (LOC_Os10g39300, LOC_Os10g39260 and LOC_Os07g34850). These genes were induced in concert with defensin and thionin encoding genes, including DEFL9 (LOC_Os06g22919).

Genes involved in secondary metabolism in rice response to pathogen attack

We detected several genes involved in secondary metabolism, some of which were documented in our previous study (Onaga et al., unpublished). Our data exhibited a significant induction (>100-fold) of hydroxycinnamoyl-CoA shikimate (HCT) encoding genes (e.g., LOC_Os04g56910, LOC_Os10g23310 and LOC-Os09g37200) and a putative mannitol dehydrogenase (LOC_Os09g23530). HCT is a key enzyme in the conversion of *p*-coumaroyl CoA to *p*-coumaroyl shikimic acid and caffeoyl CoA during lignin biosynthesis. Mannitol dehydrogenase is involved in the conversion of intermediates, including conferaldehyde to monilignols such as coniferyl alcohols. Also prominently expressed was LOC_Os08g34790, which encodes an AMP-binding domain-containing protein, a close homologue of 4-coumaroyl-CoA synthase 2 (4CL) involved in the conversion of *p*-coumaric acid to *p*-coumaroyl CoA. A number of caffeoyl-CoA 3-O-methyltransferase putative encoding genes, including LOC_Os09g30360 and LOC_Os08g05790, were also up regulated. Interestingly, most PAL encoding genes (PAL2; LOC_Os02g41670, LOC_Os05g35290 and LOC_Os02g41680) were expressed, but kept lower in Nip35i than in Nip28i, suggesting that high temperature affected PAL gene expression, and this is consistent with our previous findings. Genes involved in phytoalexin biosynthesis, including putative Anthranilate N-hydroxycinnamoyl/benzoyltransferase 3 (LOC_Os08g01950), diterpene cyclase genes, OsKSL4 (LOC_Os04g10060), OsKSL7 (LOC_Os02g36140) and OsKSL8 (LOC_Os11g28530) were >20-fold induced during *M. oryzae* infection at both temperatures. The same was true for OsKSL10 (LOC_Os12g30824), OsCPS4 (LOC_Os04g09900) and OsCPS2 (LOC_Os02g36210). Other genes induced >20-fold included chalcone and stilbene synthases (LOC_Os07g34190 and LOC_Os07g34260). Cytochrome P450 genes involved in phytoalexin biosynthesis (Park et al., 2013), such as CYP99A2 (LOC_Os04g10160), CYP99A3 (LOC_Os04g09920), CYP76M8 (LOC_Os02g36070) and CYP71Z7 (LOC_Os02g36190), were induced >100-fold in response to *M. oryzae* infection but were not detected in plants exposed to only high temperature. The same was true for the sex determination protein tasselseed-2 (LOC_Os04g10010), a homolog of dehydrogenase gene involved in phytoalexin biosynthesis.

Expression of pathogenesis related (PR) genes

To identify PR genes specifically induced in Nip35c, Nip35i and Nip28i, we examined our data using known PR genes reported in literature. We detected higher induction of PR3

(CHIT17; LOC_Os05g33130) and β-1,3-glucanase (Gns6; LOC_Os01g71350) in response to only high temperature. In addition, a cupin domain containing protein (OsGLP8-12; LOC_Os08g13440), thaumatin-like protein 1(PR5K; LOC_Os03g14050), PR10-b (LOC_Os12g36850), WIP3 (OsPR4c; LOC_Os11g37950) and WIP4 (OsPR4b; LOC_Os11g37960) were induced >5-fold in response to only high temperature. To determine the PR gene expression changes in response to both high temperatures and *M. oryzae* infection, the genes expressed in Nip35i were compared with genes induced in Nip28i. Of the 112 PR genes identified from literature, 42 were up regulated in Nip35i as compared to 39 in Nip28i. A similar number of genes (n = 6) were down regulated in both treatments. The genes LOC_Os10g11500 similar to PR1-a, PR2 (Gns5; LOC_Os01g71340), PR8 (Gns11; LOC_Os07g35480) were induced >50-fold in Nip35i but not in Nip28i. Transcript levels for the cupin domain containing proteins, including OsGLP8-10 (LOC_Os08g09060), OsGLP8-9 (LOC_Os08g09040), OsGLP8-8 (LOC_Os08g09020), OsGLP8-5 (LOC_Os08g08990) were >100-fold induced in Nip35i compared to Nip28i. In addition, the genes PR1 (LOC_Os07g03730), PR8 (Oschib2; LOC_Os10g28120) and PR2 (Gns10; LOC_Os01g51570) were also >100-fold induced in Nip35i than in Nip28i. On the other hand, OsGLP8-12 (LOC_Os08g13440) was >100-fold induced in Nip28i compared to Nip35i. Similarly, OsGLP8-3 (LOC_Os08g08970) was induced 137-fold in Nip28i but not in Nip35i.

Confirmation of genes of interest using qPCR

To confirm our RNA-Seq findings using a different assay, we probed 4 genes from the fungus (MAS3, BAS1, aquaporin 9 and BAS3) and 5 genes from the plant (OSFKBP65, LOC_Os06g37224, cytochrome P450, PR1b and β-1,3-glucanase) using qPCR. Expression levels were highly correlated across all targets, though the magnitude was slightly higher in RNA-seq than qPCR. Results of qPCR analysis are presented in Figures 3.10 and 3.11. Details on the primer probe sets for these genes are provided in (Additional file S9).

Discussion

Although temperature has long been reported to be an important component of plant disease development, at present knowledge on the mechanisms underlying the effect of elevated temperature on plant pathogen interaction is limited. Therefore, it is important to gain in-depth knowledge about the complexity of transcriptional regulation in *M. oryzae* and rice

during high temperature stress using advanced technologies. We performed RNA-seq analysis to explore the transcriptional variations in *M. oryzae* and rice at 35°C and 28°C in an attempt to understand fungal pathogenic and plant defense mechanisms modulated during infection at high temperature. Interestingly, *in planta* fungal biomass was significantly higher in Nip35i than Nip28i, suggesting that by 48 hpi, *in planta* fungal biomass was consistent with the rate of lesion expansion observed in Nip35i. This result suggested that high temperature increased the rate of colonization of the plant tissues by the pathogen. Thus, it was critical to identify genetic factors that facilitate rapid colonization of the host and the corresponding genetic responses exhibited by the plant host against the pathogens at HT. Therefore, an RNA-Seq analysis was carried out to gain a deeper understanding of the genes that are regulated during host pathogen interaction at high temperature. We identified a total of 5377 differentially-regulated transcripts from *M. oryzae*, 4302 of which were commonly regulated at both temperatures, suggesting that transcriptional signatures in Nip35i and Nip28i were largely similar. However, most up-regulated fungal genes were stronger induced in Nip35i than Nip28i. A stronger transcript accumulation during infection at 35°C suggested that there was potentially increased protein synthesis activity to facilitate pathogen adaptation to the host environment, which was probably altered by high temperature treatment.

Given that fungal induction of virulence factors is necessary for successful colonization of the host, we searched for pathogenicity related genes in the PHI database. Many pathogenicity genes previously reported, including MAS3 (MGG_12337), PWL2, PWL1, ribonuclease T2, MoHox7, AVR-Pita and (BAS1-4) (Kawahara et al., 2012) were induced, but with a stronger induction in Nip35i compared to Nip28i. In addition, two genes, MGG_16585 and MGG_15972 with 99% partial sequence identity to Avrpiz-t and AvrPik/kp/km, respectively, were stronger induced during infection at 35°C than at 28°C. MAS3 is tentatively assigned to GH125 family of α-mannosidases in the CAZy database. Fungal cell walls contain high levels of mannoproteins (glycosylphosphatidylinositol anchored) which are synthesized through glycosylation by addition of mannose to their serine or threonine amino acid residues through mannosyltransferase activity, and further processing by mannosidases (Oh et al., 2008). The entire process aids in stabilizing the cell wall either during invasive growth or during appressorium expansion. The high induction of MAS3 at both temperatures might suggest that this gene is crucial to *M. oryzae* invasive growth. Mannose uptake and utilization is also likely to be controlled by MGG_00994. MGG_00994 is a secreted alpha-1,2-mannosidase capable of hydrolyzing alpha-1,2 linked mannobiose. Although this gene was previously shown not to

be important for *M. oryzae* pathogenicity (Zhou et al., 2009), its expression in concert with other secreted proteins suggests that it probably plays a role in the modification of fungal cell walls during invasive growth in rice plants.

The role of pathogenicity effectors: Avr-Pita, Pwl1, Pwl2, Avr-Piz-t and AvrPik/kp/km is well documented (Fernandez and Wilson, 2014a). We found increased transcript levels of genes encoding for these effectors at elevated temperature, which suggests that increased levels of these effectors may be required for pathogenesis at elevated temperatures. Ribonuclease T2 enzymes are reported to be involved in turning over ribosomal RNA to maintain cellular homeostasis, tRNAs cleavage, pathogenicity, phosphate scavenging and nitrogen storage (MacIntosh, 2011). In *M. oryzae*, tRNAs cleavage was recently proposed to restrict protein synthesis during appressorium formation in order to direct cellular metabolism towards colonization (Nunes et al., 2011). Although the role of ribonuclease T2 in conferring such functions remains to be understood, the increased expression of its encoding gene may imply a potential role in enhanced protein synthesis during colonization.

Several secreted putative effectors, previously reported (Mathioni et al. 2011; Kawahara et al. 2012) were more induced at 35°C than 28°C. Among which, MGG_00230, which shares 98% partial sequence identity with AVR-Pita2 was strongly induced in both Nip35i and Nip28i. Furthermore, three secreted protein encoding genes with LysM domains, MGG_03468, Slp1 (MGG_10097) and MGG_02405, were induced in both Nip35i and Nip28i. Slp is crucial for suppression of PAMP triggered immunity (Zhang and Xu, 2014). Protein sequence alignment indicated more conserved signatures between MGG_03468 and Slp1. However, Slp1 had more deletions than MGG_03468 and MGG_02405, indicating that it may be a novel derivative different from the other two. Nevertheless, the high induction of MGG_03468 and Slp1 suggests synergistic or complementary roles in suppressing PAMP triggered immunity.

Phylogenetic relationship of the top 50 secreted proteins in this study formed three major clusters, indicating a possible similarity between the known and unknown secreted proteins. Several of these proteins could potentially represent new virulence factors active in host plant colonization. For instance, MGG_11009 is a putative cell wall galactomanno (GM) protein, which shares 99% identity with hydrophobic surface binding protein A (HsbA). Hydrophobins form protective surface coatings for fungi and reduce water surface tension, both of which are needed for growth delimitation of aerial structures such as hyphae and

conidiospores (Ohtaki et al., 2006). The same authors demonstrated that HsbA recruits CutL1 to the PBSA surface for consequent hydrolysis. Cutinases were previously shown to be necessary for carbon acquisition during subcuticular growth of *Venturia inaequalis* (Koller et al., 1991). Although the link between HsbA and cutinases is not clear, we speculate that in a stressful environment, there is a possibility of interaction between the two proteins. Moreover, cutinases are probably crutial to *M. oryzae* pathogenicity at high temperature. GMs have also been reported to exist in a glycosylphosphatidylinositol membrane-bound form (Morelle et al., 2005), which might provide a stable association with the lipid bilayer during infection. Another gene, MGG_14055, which shares sequence similarity with genes encoding for β-Xylosidases was strongly induced at 35°C. Xylans are the most abundant hemicelluloses in plants. The complete degradation of hemicellulose requires complementary activity of hemicellulolytic enzymes, including endo-1, 4-L-xylanases, for the hydrolysis of xylan backbone, and L-xylosidases for the cleavage of xylooligomers to free xylose (Czjzek et al., 2005). The expression of β-Xylosidases in Nip35i might suggest a probable form of a backup system for the pathogen to degrade the plant cell wall at high temperature.

To further clarify the differences between *M. oryzae* infection at 35°C and 28°C, we looked for genes encoding for enzymes involved in lipid metabolism. Several genes involved in the initial step of fatty acid β-oxidation, including MFP1, ICL, PTH2, MgPex6, ECH1 and lipases were more induced in Nip35i than Nip28i. Initial steps of infection may depend on metabolism of stored lipids via the glyoxilate pathway to produce glucose that supports fungal development. The induction of β-oxidation genes suggests generation and conversion of acetyl CoA to canitine intermediates for energy production during host invasion. Indeed, PTH2 was previously reported to be required for *M. oryzae* pathogenesis, whereas MgPEX6 was reported to be necessary for lipid body degradation during pathogenesis (Reviewed in Fernandez and Wilson, 2014a). Moreover, ECH1 was reported to be important in neutralizing host defenses at post-penetration stage. Increased expression of genes encoding for these proteins at high temperature suggests that their transcript accumulation is necessary for *M. oryzae* infection at high temperature. Alternatively, the role of *M. oryzae* lipases in pathogenicity is intriguing. Deletion of individual lipase encoding genes has been reported to be less effective in reducing *M. oryzae* pathogenesis (Wang et al., 2007). However, their induction in this study may be linked to enhanced biomass accumulation during *M. oryzae* infection at high temperature as previously reported (Maia et al., 1999). We also detected a strong induction of LPP. LPPs have been reported to be involved in dephosphorylation of

lysophosphatidic acid (LPA), sphingosine 1-phosphate (S1P) and related substrates to control intracellular lipid metabolism and signaling (Sigal et al., 2005). The high induction of this gene is likely crutial to *M. oryzae* lipid biosynthesis during infection.

Several genes involved in carbohydrate metabolism, including GH43, GH7, GH10, PL1, PL4 and CEs were less affected by high temperature, and showed similar induction on Nip35i and Nip28i. Of particular interest was the induction of CEs and PLs. The induction of genes encoding for these enzymes likely contributes to deacetylation of chitin and degradation of pectin, respectively, during *M. oryzae* infection. However, increased expression levels of genes involved in the utilization of non-preferred carbon sources was detected in Nip35i, and may probably suggest disperate measures by the pathogen to ensure rapid colonization of the host. For instance, cellobiose dehydrogenase (CDH) is an extracellular hemoflavoenzyme produced by several cellulose degrading fungi (Baminger et al., 1999), whereas alcohol dehydrogenase I (MGG_03880), aldehyde dehydrogenase (MGG_00719) and a NADP-dependent alcohol dehydrogenase 6 (MGG_00246), are involved in ethanol degradation for the production of acetyl-CoA. Due to reduced photosynthetic activity in the plants in response to high temperature, it is possible that a shift in the glycolytic pathway could occur to produce ethanol. This shift likely plays a significant role during infection, and is consistent with the strong induction of ICL and malate synthase, the two enzymes that are necessary for glyoxylate shunt. Increased expression of stress response genes was also detected in this study, including genes involved in alternative pathways for detoxification, and secondary metabolism. Excessive ROS production in the fungal cells has been reported to induce accumulation of aldehydes and alcohols (Asiimwe et al., 2012). The induction of alcohol dehydrogenases and aldehyde dehydrogenases could also suggest a detoxification strategy instead of nutrient aquisition from alcohols and aldehydes.

Increased transcript levels of GUT1, which is a key regulator in the conversion of glycerol to glycerol-3-phosphate (G3P) was detected among *in planta* expressed genes. Previous reports have shown that fungal glycerol metabolism during host invasion plays an important role in the establishment of infection, including growth and conidiation *in planta* (Venugopal et al., 2009). Both glycerol and mannose may be a source of carbon *in planta*, in a likely event of a shift in the glycolytic pathway, and is consistent with a stronger induction of manose utilization enzymes previously discussed. This is also consistent with the lower induction of hexose uptake protein (HUP1) in Nip35i, which could be a strategy for rapid transition to

necrotrophy during stress. As discussed before, high temperature probably invokes reorganisation of energy supplies in the plant thereby reducing nutrient availability to the pathogen at the biotrophic phase forcing the fungus to rapidly activate necrotrophic phase processes, which dramatically induces necrosis, as observed in Nip35i diseased phenotypes.

Stress related genes, including genes involved in secondary metabolism were also more induced in Nip35i than Nip28i. For instance, averantin oxidoreductase, a key enzyme in the hydroxylation of averantin during aflatoxin biosynthesis; pisatin demethylase, which detoxifies pisatin and functions as virulence factor in *Fusarium solani* (Khan et al. 2003); and epoxide hydrolases, which have been reported to be enhanced at acidic pH and glucose (Morisseau and Hammock, 2013) were strongly induced in Nip35i. In addition, metalloproteinases, which deactivate proteinaceous substrates and contribute to cell wall degradation by targeting structural proteins such as hydroxyproline-rich glycoproteins (Dunasevsky et al., 2007) were strongly induced in Nip35i. The induction of these genes at high temperature suggests that a similar strategy could be employed by *M. oryzae* during host colonization. Several other genes in cytochrome P450 gene families, including CYP563A1 and CYP608A1, were stronger induced in Nip35i than Nip28i, suggesting enhanced detoxification activity in *M. oryzae* during host colonization at high temperature.

Interestingly, several genes encoding for enzymes involved in ethylene and gibberellin synthesis were also detected. For instance, ent-kaurene oxidase (MGG_02294), which catalyzes oxidation of the 4-methyl group of ent-kaurene producing kaurenoic acid, a key step in gibberellin (GA) biosynthesis, and 2-oxoglutarate-dependent ethylene/succinate-forming enzyme participates in ethylene biosynthesis were highly induced during *M. oryzae* infection at both temperatures. Induction of these genes might as well suggest a counter defense strategy against plant induced defence pathways associated with these molecules. Similarly, SA degradation enzyme encoding genes were strongly induced, which, as well, suggests a dampening effect on SA signaling.

Among the ABC transporters, an orthologue of CDR1 was strongly induced at both temperatures. ABC transporters are known to detoxify antifungal compounds produced by the plant cells, and a strong induction of CDR1during *M. oryzae* infection is consistent with previous reports (Mathioni et al., 2011). Some ABC transporters may facilitate the aquisition of nutrients from the host during *in planta* growth, and this may be consistent with the

induction of ABC-type Fe^{3+} transport system in this study. Alternatively, the higher induction of MFS encoding genes in Nip35i than in Nip28i indicates that these monooxygenases may take part in intracellular pathways required for temperature adaptation or in detoxification of plant derived antifungal molecules. MFS proteins have been implicated in transmembrane transport of a wide range of substrates (Law et al., 2008). Similarly, a strong induction of genes encoding for aquaporin water channels that prevent osmotic damage of cells suggests potential induction of mechanisms leading to dessication tolerance during *M. oryzae inplanta* growth.

To colonize host plants successfully, pathogens must overcome the ROS toxic environment in the plant. Most antioxidative enzymes were less induced in this study, and is consistent with previous reports (Egan et al., 2007). However, we detected a higher induction of *MoCCP2* (MGG_10368), *MoVPX1* (MGG_02210) and *CATA* (MGG_10061) in Nip35i than Nip28i. Alternatively, *MoHPX2* was highly induced in Nip28i but was not significantly induced in Nip35i. The differential induction of these peroxidases suggests that antioxidation is regulated by temperature stress during *M. oryzae* infection. Coupled with this, the differential enrichment of casein kinase II site, which flanks di-leucine motifs that are present in transmembrane proteins in humans (Mauxion et al., 1996), in genes specifically induced in Nip35i suggest alternative antioxidative pathways in *M. oryzae*. Di-leucine-based motifs and tyrosine motifs mediate endocytosis of cell surface proteins. Moreover, tyrosine phosphorylation motifs are present in protein kinase C (PKC), which is a key mediator of ROS activation of protein kinase D leading to cell survival under oxidative stress (Döppler and Storz, 2007). This signaling pathway could be important for survival under oxidative stress in *M. oryzae*.

The enrichment of N-glycosylation in Motif 3 was consistent with enrichment of the KEGG pathway, N-Glycan biosynthesis and the higher induction of asparagine synthase in Nip35i than Nip28i. *N*-linked glycans attached to nitrogen of asparagine requires participation of dolichol phosphate for N-lycosylation, which is consistent with the induction of dolichyl lipids in Nip35i. N-glycosylation confers stability or correct folding of secreted glycoproteins, and likely plays a key role during infection at high temperature.

A large number of TF genes were commonly regulated, suggesting that the same transcription regulators probably control infection, although the level of induction varies with the external

plant stress environment. Among the transcription factors identified in this study, a homeodomain like (MGG_09628), which was previously reported (Kawahara et al., 2012), showed the strongest induction at both temperatures, whereas a nucleic acid-binding, OB-fold (MGG_04335) was strongly induced in Nip35i. In addition, two Zn2Cys6 genes (MGG_02879 and MGG_00049) and C2H2 zinc finger (MGG_04546) were >10-fold induced in Nip35i, but not in Nip28i, suggesting that these TFs are probably crucial to *M. oryzae* adaptation to elevated temperature during host colonization.

To explore how rice transcriptome is altered in response to both *M. oryzae* and temperature, we searched for genes involved in various biological pathways in our dataset. The GO analysis exhibited common enrichment in metabolism, response to stress and response to stimuli in both high temperature and *M. oryzae* stress response genes. A clear difference observed in this study was the rapid symptome development in Nipponbare at high temperature, as opposed to our previous findings with R genes (Onaga et al., unpublished). We previously reported that high temperature might offer the rice plants an advantage by priming SA conversion to MeSA which prods the JA and ET induction. In this study, most genes involved in hormonal pathways, including OsBISAMT1 were up-regulated. However, we found that genes encoding for jasmonate O-methyltransferase were not significantly expressed in Nipponbare. The same was true for naringenin 7-*O*-methyltransferase (NOMT; LOC_Os12g13800), a positive regulator of sakuranetin biosynthesis (Shimizu et al. 2012), which is regulated by JA (Rakwal et al., 1999). NOMT was induced in Nip28i but was not detected in Nip35i suggesting that high temperature compromised its expression. Consistent with this, LOC_Os09g17560, previously reported as one of the genes encoding for OsOMT involved in sakuranetin biosynthesis (Park et al., 2013) was also missing. Incidentally, the absence of these genes corresponded with the strong induction of *M. oryzae* ABC transporter (*ABC1;* MGG_13624), previously reported to be strongly induced by azole fungicides and the rice phytoalexin sakuranetin (Oh et al., 2008), in Nip35i but not in Nip28i. Given that *ABC1,* which is responsible for regulating intracellular levels of cytotoxic or xenobiotic compounds, was more induced at elevated temperature, the suppression of OsOMT genes in Nip35i could have probably compromised resistance in Nip35i, The same was found for a multiprotein bridging factor 1c (MBF1c) which was strongly induced in our previous study. Moreover, heat shock transcription factor A2 (HsfA2) which was strongly induced in our previous study, was equally suppressed in Nipponbare, further suggesting compromised stress response. We also studied ABA associated callose deposition genes. Although OsBBD1

(LOC_Os01g50622), which is involved in abscisic acid-derived callose deposition was significantly induced in this study, we speculate that callose deposition alone may not stop the fungus from colonizing the rice plants. Besides this, two Homeobox genes (LOC_Os09g15480 and Hox24; LOC_Os02g43330), which were highly induced in LT in our previous study were not detected in Nipponbare.

On the other hand, a stronger induction of expansins in this study compared to our previous study likely affected the integrity of the cell wall. In fact expansins were previously reported to increase rice susceptibility to *Xanthomonus oryzae* (Ding et al., 2008). GH3.8 (LOC_Os07g40290), which was shown to regulate expression of expansins by the same authors, was not detected in Nipponbare, when compared to our previous study. Remarkably, expansin genes were expressed in concert with pectin methylesterase (LOC_Os09g39760; 61-fold) and von Willebrand factor type A (LOC_Os11g45990; 36-fold). Pectin methylesterase is induced in Arabidopsis upon infection and is necessary for a successful colonization by necrotrophic pathogens (Raiola et al., 2011). These cell wall modifications at high temperature likely favored host colonization, and could be compounded by pathogen induction of polygalacturonase A (MGG_08938) and pectate lyase B genes during infection. A significant alteration in transcription factor genes was also observed. We previously reported a strong induction of OsWRKY55 and OsWRKY32 in LT and CO, respectively, and several other WRKYs reported to play complementary roles in a defense response (Peng et al., 2010). These genes were not significantly induced in Nip35i, suggesting that several downstream genes modulated by these TFs were either not expressed or less induced. This is consistent with the reduction of the transcriptome in Nipponbare by almost one third when compared to our previous study.

Taken together, our data highlight how elevated temperature shapes plant pathogen interaction. We show that elevated temperature increases the rate of colonization of the plant tissues by the pathogen when high temperature treated plants are inoculated with *M. oryzae* and kept at $28^{o}C$ for 24 hpi prior to re-exposure to $35^{o}C$. This is contrary to our previous findings, and indicates that the putative mechanisms that enhance resistance at elevated temperature are largely complex. It is not unexpected that some of the specific defences might play an important role in offsetting resistance suppression at elevated temperatures even at reduced transcript levels, while the non-specific defence system adapts. Thus, identifying stable R genes and understanding the mechanism associated with stable resistance at elevated

temperatures could provide further insight into the mechanism relevant for improving rice in a changing climate. Several *M. oryzae* genes were highly induced at high temperature. Thus, blast epidemics are likely to occur in some rice production areas, especially where conducive temperatures for infection alternate with elevated temperatures.

Materials and Methods

Plant and fungal material preparation

A compatible Tanzanian fungal strain (TAN211.16) and *Oryza sativa* L. ssp. *japonica* cv. Nipponbare were used in this study. TAN211.16 was collected in 2011 from infected rice fields in Kyela, Tanzania. This strain was selected for transcriptome sequencing because it was aggressive on most of the isogenic lines tested. The strain is currently maintained at the Division of Plant Pathology and Crop Protection, Goettingen University, Germany as APP number 1177. The genome of the rice cultivar Nipponbare is sequenced and available as a reference for genomic studies. The plants were grown and maintained in the greenhouse at a temperature of 27±3°C with a photoperiod of 14 hours for 18 days. Prior to inoculation, seedlings were transferred from the greenhouse to the growth chambers maintained at 28°C and 35°C for additional 7 days. Inoculated plants were kept at 28°C in the dark for 24 hours to allow for fungal infection. Thereafter, plants were returned to respective temperature chambers (28°C and 35°C) for additional 24 hours prior to sample collection. We obtaine fungal mycilia by growing the fungus in 250 ml of a medium containing $3gL^{-1}$ of glucose, $3gL^{-1}$ of casamino acids and $3gL^{-1}$ of yeast extract. The culture was incubated at 25°C under continuous rotation at 100 rpm for 24 h. The procedure was repeated for additional 24 h by blending the first culture with a fresh medium. Mycelium was collected by filtration and stored at -80°C for RNA extraction. Inoculation and symptom evaluation was carried out as previously described (Onaga et al., 2015).

Sample preparation mRNA extraction and sequencing

Infected leaves from each treatment were sampled from four plants in two replicates and immediately frozen in liquid nitrogen. Leaf samples infected with *M. oryzae* at 28°C and 35°C are designated as Nip28i and Nip35i, respectively. Samples collected before inoculation are designated as Nip28c, Nip35c and Fungus. Infected leaf samples were collected at 48 hours post inoculation (hpi). We chose to examine 48 hpi because this is the most likely stage at which several fungal effectors, including those that culminate into effector triggered

immunity (ETI) are abundantly secreted. Total RNA was extracted with Trizol reagent (Invitrogen, Carlsbad, CA) according to the manufacturer's instructions. Four micrograms of total RNA were subjected to library preparation using the "TruSeq RNA Sample preparation v2 Guide" following the manufacturer's instructions. Libraries were amplified by 15 cycles of PCR, and concentration and size were assayed on a 2100 Bioanalyzer (Agilent). Libraries were clustered for sequencing using Illumina cBOT Cluster generation system and TrusSeq v3 chemistry. Fifty bp single-end sequencing was performed on the HiSeq2000. Sequence images were transformed with Illumina software BaseCaller to bcl files, which were demultiplexed to fastq files with CASAVA v1.8.2 allowing for one mismatch in the indices. The mixed transcriptome was alligned to the respective genomes of both organisms using Bowtie2 v2.0.2, first to the rice genome followed by *M. oryzae* genome. The reads that did not map on to the rice genome were considered to have come from *M. oryzae,* and were mapped onto the reference genome of isolate 70–15. Unmapped *M. oryzae* reads were recombined with the mapped read SAM files to guide assembly, and later processed with the *de-novo* assembler using CLC Genomics Workbench. The resulting sam files from the respective genome mappings were converted to sorted bam files using samtools 0.1.18. Further processing was conducted as previously described (Onaga et al. unpublished). GO analysis of fungal DEGs was conducted using the DAVID functional annotation tool (Dennis et al., 2003), while plant genes were analyzed using the hypergeometric statistical method with Hochberg FDR adjustment in the AgriCO website (http://bioinfo.cau.edu.cn/agriGO/analysis.php webcite) as described elsewhere (Du et al., 2010). Upstream protein sequences were analyzed for enriched motifs using the MEME algorithm. Motifs were visualized with Weblogo (Crooks et al., 2004). Maximum Likelihood based phylogenetic relationship between protein sequences of genes encoding putative secreted proteins were analysed on the Phylogeny.fr platform (Dereeper et al., 2008).

Relative real-time qRT-PCR

To confirm the results of RNA-seq analysis, we determined the expression levels of 10 DEGs by qRT-PCR. Total RNA (1.0 μg) was used to synthesize cDNA using the iScript™ Reverse Transcription Supermix for RT-qPCR (BioRad). Following the instruction manual, the reverse transcription conditions were: 5 min at 25 °C, 30 min at 42 °C and finally 5 min at 85 °C. Primers were designed using the software Primer3Plus (http://www.bioinformatics.nl/cgi-bin/primer3plus/primer3plus.cgi/). Candidate reference genes [(actin, beta tubulin, elongation

factor and expressed protein (LOC_Os07g02340)] were selected from previous reports (Narsai et al., 2010), and tested for stability. The reference genes, LOC_Os07g02340 (for rice) and Actin (for the fungal genes), were used in subsequent RT-qPCR reactions based on their stable expression in all treatments. Gene-specific primers were used for amplification of the target genes using iQ SYBR Green supermix on the thermal cycler CFX384 (BioRad) under the following conditions: 3 min at 95 °C (1 cycle), 15 s at 95 °C and 5 s at 62 °C (50 cycles) and a melting curve from 60 to 95 °C in triplicates (all from Bio-Rad). The relative expression was computed as previously described (Pfaffl, 2001). Fungal quantification was performed using primers reported in Harmon et al. (2003), which amplify a 687bp region of repetitive DNA fragment *Pot2*. About 100 copies of *Pot2* are reported to be present per genome of *M. oryzae* (Kachroo et al., 1994).

Acknowledgement

References

Asiimwe, T., Krause, K., Schlunk, I. and Kothe, E. (2012) Modulation of ethanol stress tolerance by aldehyde dehydrogenase in the mycorrhizal fungus *Tricholoma vaccinum*. *Mycorrhiza* **22**, 471–484.

Baminger, U., Nidetzky, B., Kulbe, K.D. and Haltrich, D. (1999) A simple assay for measuring cellobiose dehydrogenase activity in the presence of laccase. *J. Microbiol. Methods*, **35**, 253-259.

Bendtsen, J.D., Nielsen, H., von Heijne, G. and Brunak, S. (2004) Improved prediction of signal peptides: SignalP 3.0. *J. Mol. Biol.* **340**, 783-795

Bita, C.E. and Gerats, T. (2013) Plant tolerance to high temperature in a changing environment: scientific fundamentals and production of heat stress-tolerant crops. *Front. Plant Sci.* **4**, 273.

Budde, I.P. and Ullrich, M.S. (2000) Interactions of *Pseudomonas syringae* pv. *glycinea* with host and non-host plants in relation to temperature and phytotoxin synthesis. *Mol. Plant–Microbe Interact.* **13**, 951-961.

Ceccardi, T.L., Barthe, G.A. and Derrick, K.S. (1998) A novel protein associated with citrus blight has sequence similarities to expansin. *Plant Mol. Biol.* **38**, 775–783.

Crooks, G.E., Hon, G., Chandonia, J.M. and Brenner, S.E. (2004) WebLogo: a sequence logo generator. *Genome Res.* **14**, 1188–1190.

Czjzek, M., David, A.B., Bravman, T., Shoham, G., Henrissat, B. and Shoham, Y. (2005) Enzyme–substrate complex structures of a GH39 b-xylosidase from *Geobacillus stearothermophilus*. *J. Mol. Biol.* **353**, 838–846.

Dean, R., van Kan, J.A.L., Pretorius, Z.A., Hammond-Kosack, K.E., Di Pietro, A., Spanu, P.D., Rudd, J.J., Dickman, M., Kahmann, R., Ellis, J. and Foster, G.D. (2012) The top 10 fungal pathogens in molecular plant pathology. *Mol. Plant Pathol*. **13**, 414–430.

Denancé, N., Sánchez-Vallet, A., Goffner, D. and Molina, A. (2013) Disease resistance or growth: the role of plant hormones in balancing immune responses and fitness costs. *Front Plant Sci.* **24**, 155.

Dereeper, A., Guignon, V., Blanc, G., Audic, S., Buffet, S., Chevenet, F., Dufayard, J.-F., Guindon, S., Lefort, V., Lescot, M., Claverie, J.-M. and Gascuel, O. (2008) Phylogeny.fr: robust phylogenetic analysis for the non-specialist. *Nucleic Acids Res.* **36**, W465-9.

Ding, X., Cao, Y., Huang, L., Zhao, J., Xu, C., Li, X. and Wang, S. (2008) Activation of the indole-3-acetic acid-amidosynthetase GH3-8 suppresses expansin expression and promotes salicylate- and jasmonate-independent basal immunity in rice. *Plant Cell* **14**, 228–240.

Döppler, H. and Storz, P. (2007) A novel tyrosine phosphorylation site in protein kinase D contributes to oxidative stress-mediated activation. *J Biol Chem.* **282**, 31873–31881.

Doyle, E.L. (2006) Computational and experimental analysis of TAL effector-DNA binding. *PhD thesis. Iowa State University, Ames, Iowa.*

Du, Z., Zhou, X., Ling ,Y., Zhang, Z. and Su, Z. (2010) agriGO: a GO analysis toolkit for the agricultural community. *Nucleic Acids Res*. **38,** W64-W70.

Dunasevsky, Y.E., Matveeva, A.R., Beliakova, G.A., Domash, V.I. and Belozersky, M.A. (2007) Extracellular alkaline proteinase of *Colletotrichum gloeosporioides*. *Biochemistry,* **72**, 345-350.

Egan, M.J., Wang, Z.Y., Jones, M.A., Smirnoff, N. and Talbot, N. J. (2007) Generation of reactive oxygen species by fungal NADPH oxidases is required for rice blast disease. *Proc. Natl. Acad. Sci. U S A.* **104**, 11772-11777.

Fernandez, J. and Wilson, R.A. (2014b) Characterizing roles for the glutathione reductase, thioredoxin reductase and thioredoxin peroxidase-encoding genes of *Magnaporthe oryzae* during rice blast disease. *PLoS ONE* **9**, e87300.

Fernandez, J. and Wilson, R.A. (2014a) Cells in cells: morphogenetic and metabolic strategies conditioning rice infection by the blast fungus *Magnaporthe oryzae*. *Protoplasma* 251:37–47.

Finn, R.D., Mistry, J., Tate, J., Coggill, P., Heger, A., Pollington, J.E., Gavin, O.L., Gunasekaran, P., Ceric, G., Forslund, K., Holm, L., Sonnhammer, E.L.L., Eddy, S.R. and Bateman, A. (2010) The Pfam protein families database. *Nucleic Acids Res.* **38**, D211–D222.

Garrett, K.A., Dendy, S.P., Frank, E.E., Rouse, M.N. and Travers, S.E. (2006) Climate change effects on plant disease: Genomes to ecosystems. *Ann. Rev. Phytopathol.* **44**, 489-509.

Giraldo, M.C., Dagdas, Y.F., Gupta, Y.K., Mentlak, T.A., Yi, M., Martinez-Rocha, A.L., Saitoh, H., Terauchi, R., Talbot, N.J. and Valent, B. (2013) Two distinct secretion systems facilitate tissue invasion by the rice blast fungus *Magnaporthe oryzae*. *Nat. Commun.* **4**, 1996.

Gregory, P.J., Johnson, S.N., Newton, A.C., Ingram, J.S.I. (2009) Integrating pests and pathogens into the climate change/food security debate. *J. Exp. Bot.* **60**, 2827-2838.

Hashioka, Y. (1950) Studies on the mechanism of prevalence of the rice blast disease in the tropics.*Technical Bulletin No. 8. Taiwan Agricultural Research Institute*.

Huang, D.W., Sherman, B.T. and Lempicki, R.A. (2009b) Systematic and integrative analysis of large gene lists using DAVID bioinformatics resources. *Nature Protocols* **4**, 44-57.

Kall, L., Krogh, A. and Sonnhammer, E.L. (2007) Advantages of combined transmembrane topology and signal peptide prediction - the Phobius web server. *Nucleic Acids Res,* **35**, W429-432.

Kamolsukyunyong, W., Sukhaket, W., Ruanjaichon, V., Toojinda, T. and Vanavichit, A. (2013) Single-feature polymorphism mapping of isogenic rice lines identifies the influence of terpene synthase on brown planthopper feeding preferences. *Rice,* **6**, 18.

Kato, H. and Kozaka, T. (1974) Effects of temperature on lesion enlargement and sporulation of Pyricularia oryzae in rice leaves. *Phytopathol.* **64**, 828-830.

Kawahara, Y., Oono, Y., Kanamori, H., Matsumoto, T., Itoh, T., Minami, E. (2012) Simultaneous RNA-Seq analysis of a mixed transcriptome of rice and blast fungus interaction. *PloS One,* **7**, e49423.

Khan, R., Tan, R., Mariscal, A.G. and Straney, D. (2003) A binuclear zinc transcription factor binds the host isoflavonoid-responsive element in a fungal cytochrome p450 gene responsible for detoxification. *Mol. Microbiol.* **49**, 117–130.

Koller, W., Parker, D.M. and Becker, C.M. (1991) Role of cutinase in the penetration of apple leaves by *Venturia inaequalis*. *Phytopathology,* **81**, 1375–1379.

Krogh, A., Larsson, B., von Heijne, G. and Sonnhammer, E.L. (2001) Predicting transmembrane protein topology with a hidden Markov model: Application to complete genomes. *J. Mol. Biol.* **305**, 567-580.

Li, P., Bai, B., Zhang, H-Y., Zhou, H. and Zhou, B. (2012) Genomic organization and sequence dynamics of the *AvrPiz-t* locus in *Magnaporthe oryzae. J. Zhejiang Univ Sci B.* **13**, 452–464.

Luo, Y., Teng, P.S., Fabellar, N.G. and TeBeest, D.O. (1998) The effects of global temperature change on rice leaf blast epidemics: a simulation study in three agroecological zones. *Agri., Ecosys. and Environ.* **68**, 187–196

MacIntosh, G.C. (2011) RNase T2 Family: Enzymatic properties, functional diversity, and evolution of ancient ribonucleases In: Nicholson, A.W. (ed.), Ribonucleases, *Nuc. Acids and Mol. Biol.* **26**.

Maia, M. de M.D, Morais, M.M.C. de, Morais, Jr. M.A. de, Melo, E.H.M. and de Lima Filho, J.L. (1999) Production of extracellular lipase by the phytopathogenic fungus *Fusarium solani* FS1. *Revista de Microbiologia.* **30**, 304-309.

Mosquera, G., Giraldo, M.C., Khang, C.H., Coughlan, S. and Valent, B. (2009) Interaction transcriptome analysis identifies *Magnaporthe oryzae* BAS1-4 as biotrophy-associated secreted proteins in rice blast disease. *Plant Cell,* **21**, 1273–1290

Mathioni, S.M., Belo, A., Rizzo, C.J., Dean, R.A. and Donofrio, N.M. (2011) Transcriptome profiling of the rice blast fungus during invasive plant infection and *in vitro* stresses. *BMC Genomics,* **14**, 49.

Morisseau, C. and Hammock, B.D. (2013) Impact of soluble epoxide hydrolase and epoxyeicosanoids on human health. *Annu. Rev. Pharmacol. Toxicol.* **53**, 1–3.22

Mauxion, F., Le Borgne, R., Munier-Lehmann, H. and Hoflack, B. (1996) A casein kinase II phosphorylation site in the cytoplasmic domain of the cation-dependent mannose 6-phosphate receptor determines the high affinity interaction of the AP-1 Golgi assembly proteins with membranes. *J. Biol Chem*, **271**, 2171–2178.

Morelle, W., Bernard, M., Debeaupuis, J.P., Buitrago, M., Tabouret, M., and Latgé, J. (2005) Galactomannoproteins of *Aspergillus fumigatus*. *Eukaryot Cell,* **4,** 1308–1316.

Nakashita, H., Yasuda, M., Nitta, T., Asami, T., Fujioka, S., Arai, Y., Sekimata, K., Takatsuto, S., Yamaguchi, I., Yoshida, S. (2003) Brassinosteroid functions in a broad range of disease resistance in tobacco and rice. *Plant J.* **33**, 887–898.

Nguyen, Q.B., Itoh, K., Vu, B.V., Tosa, Y. and Nakayashiki, H. (2011) Simultaneous silencing of endo-b-1,4 xylanase genes reveals their roles in the virulence of *Magnaporthe oryzae*. *Mol. Microbiol.* **81**, 1008–1019.

Nunes, C.C., Gowda, M., Sailsbery, J., Xue, M., Chen, F., Brown, D.E., Oh, Y., Mitchell, T.K., Dean, R. A. (2011) Diverse and tissue-enriched small RNAs in the plant pathogenic fungus, *Magnaporthe oryzae*. *BMC Genomics* **12**, 288.

Oh, Y., Donofrio, N., Pan, H., Coughlan, S., Brown, D., Meng, S., Mitchell, T., and Dean, R. (2008) Transcriptome analysis reveals new insight into appressorium formation and function in the rice blast fungus *Magnaporthe oryzae. Genome Biol.* **9**, R85.

Ohtaki, S., Maeda, H., Takahashi, T., Yamagata, Y., Hasegawa, F., Gomi, K., Nakajima, T. and Abe, K. (2006) Novel hydrophobic surface binding protein, HsbA, produced by Aspergillus oryzae. *Appl. and Envi. Microbiol.* **72**, 2407-2413.

Ou, S.H. (1985) Rice Diseases, 2nd ed. Kew, Surrey, U.K.: *Commonwealth Mycological Institute*.

Park, S-Y., Choi, J., Lim, S-E., Lee, G-W., Park, J., et al. (2013) Global Expression Profiling of Transcription Factor Genes Provides New Insights into Pathogenicity and Stress Responses in the Rice Blast Fungus. *PLoS Pathog.* **9**, e1003350.

Peng, Y., Bartley, L.E., Canlas, P. and Ronald, P.C. (2010) OsWRKY IIa transcription factors modulate rice innate immunity. *Rice*, **3: 36–42.**

Raiola, A., Lionetti, V., Elmaghraby, I., Immerzeel, P., Mellerowicz, E.J., Salvi, G., Cervone, F., Bellincampi, D. (2011) Pectin methylesterase is induced in *Arabidopsis* upon infection and is necessary for a successful colonization by necrotrophic pathogens. *Mol. Plant-Microbe Interact.* **24***, 432–440.

Rauyaree, P., Choi, W., Fang, E., Blackmon, B. and Dean, R.A. (2004) Genes expressed during early stages of rice infection with the rice blast fungus *Magnaporthe grisea. Mol Plant Pathol.* **2**, 347–354.

Reyna, N.S. and Yang, Y. (2006) Molecular analysis of the rice MAP kinase gene family in relation to Magnaporthe grisea infection. *Mol. Plant-Microbe Interact.* **19**, 530-540.

Rice, P., Longden, I. and Bleasby, A. (2000) EMBOSS: the European Molecular Biology Open Software Suite. *Trends Genet.* **16**, 276–277.

Rawlings, N.D., Barrett, A.J. and Bateman, A. (2010) MEROPS: the peptidase database. *Nuc. Acids Res.* **38**, D227-D233.

Sigal, Y.J., McDermott, M.I. and Morris, A.J. (2005) Integral membrane lipid phosphatases/phosphotransferases: common structure and diverse functions. *Biochem. J.* **387**, 281–293.

Sweigard, J.A., Carroll, A.M., Kang, S., Farrall, L., Chumley, F.G. and Valent, B. (1995) Identification, cloning, and characterization of PWL2, a gene for host species specificity in the rice blast fungus. *Plant Cell,* **7**, 1221–1233.

Tang, W., Deng, Z. and Wang, Z.Y. (2010) Proteomics shed light on the brassinosteroid signalling mechanisms. *Curr. Opinion in Plant Biol.* **13**, 27–33.

Teng, P.S. (1994) The epidemiological basis for blast management. In: Zeigler RS, Leong SA, Teng PS. (Eds.), *Rice Blast Disease. IRRI, CAB Int.* 409–433

Ullrich, M., Peñaloza-Vázquez, A., Bailey, A.M. and Bender, C.L. (1995) A modified two-component regulatory system is involved in temperature-dependent biosynthesis of the *Pseudomonas syringae* phytotoxin coronatine. *J Bacteriol.* **157**, 6160-6169.

Valdivia, E.R., Sampedro, J., Lamb, J.C., Chopra, S. and Cosgrove, D.J. (2007) Recent proliferation and translocation of pollen group 1 allergen genes in the maize genome. *Plant Physiol.* **143**, 1269-81.

Venugopal, S.C., Chanda, B., Vaillancourt, L., Kachroo, A. and Kachroo, P. (2009) The common metabolite glycerol-3-phosphate is a novel regulator of plant defense signaling. *Plant Signaling & Behavior*, **4**, 746–749.

Wang, Z.Y., Soanes, D.M., Kershaw, M.J. and Talbot, N.J. (2007) Functional analysis of lipid metabolism in *Magnaporthe grisea reveals a requirement for peroxisomal fatty acid beta-oxidation during appressorium mediated* plant infection. *Mol. Plant Microbe Interact.* **20**, 475–491.

Wilson, R.A. and Talbot, N.J. (2009) Under pressure: investigating the biology of plant infection by Magnaporthe oryzae. *Nat. Rev. Microbiol.* **7**, 185–195.

Yi, M., Chi, M.H., Khang, C.H., Park, S.Y., Kang, S., Valent B. and Lee., Y-H. (2009) The ER chaperone LHS1 is involved in asexual development and rice infection by the blast fungus *Magnaporthe oryzae. Plant Cell,* **21**, 681-695.

Zeigler, R.S., Leong, S.A. and Teng P.S. eds (1994) Rice Blast Disease. *Wallingford, UK: Commonwealth Agricultural Bureau International*.

Zhang, S. and Xu, J-R. (2014) Effectors and effector delivery in *Magnaporthe oryzae. PLoS Pathog.* **10**, e1003826.

Figures
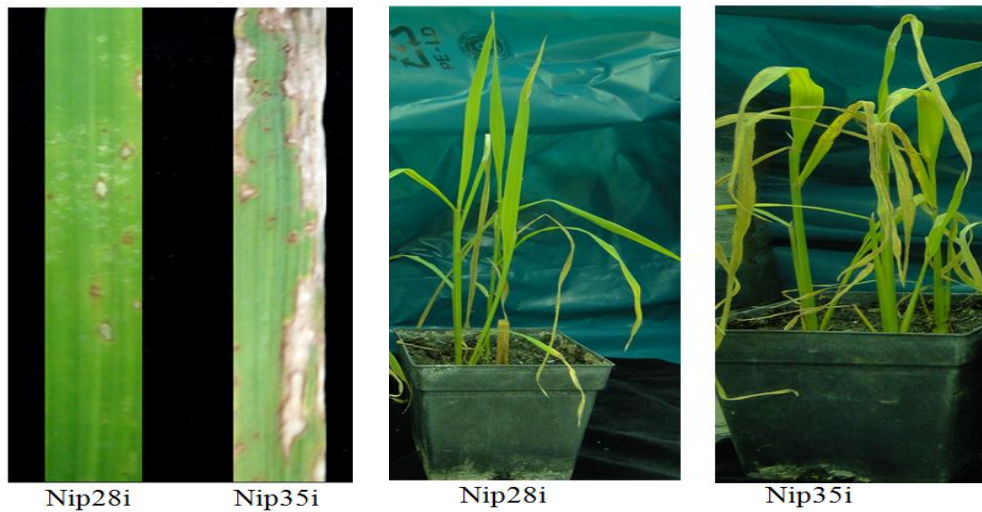
Figure 3.1a: Disease phenotypes of *M. oryzae* on Nipponbare at 28°C (Nip28i) and 35°C (Nip35i) at 5 dpi. Visible symptomes were observed on Nip35i 3dpi which rapidly enlarged, when compared to Nip28i. Nip35i exhibited rapid collapse of the leaf tissue and enlarged grey brown foliar lesions at 5 dpi. Spores from TAN211.16 were spray-inoculated on Nipponbare (five-leaf stage).
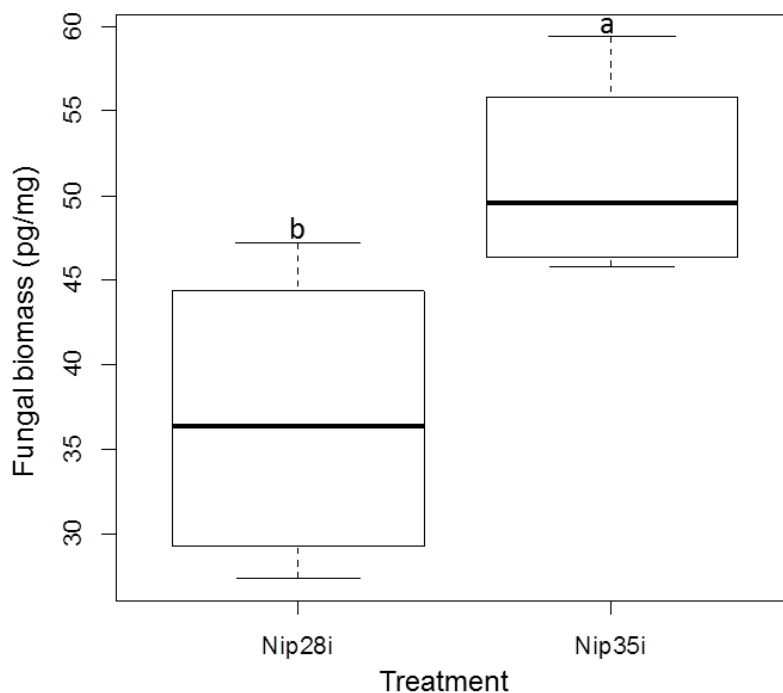
Fig. 3.1b. Quantification of fungal biomass detected by quantitative real-time PCR with primer pair of pfh2a and pfh2b on rice leaves inoculated with *M. Oryzae* at 48 hpi. Data are presented as mean picograms per miligram (pg/mg) fungal DNA ± standard deviation (SD) in 2 replicates. Letters indicate significant differences at $p \leq 0.05$, calculate by Tukey HSD test.
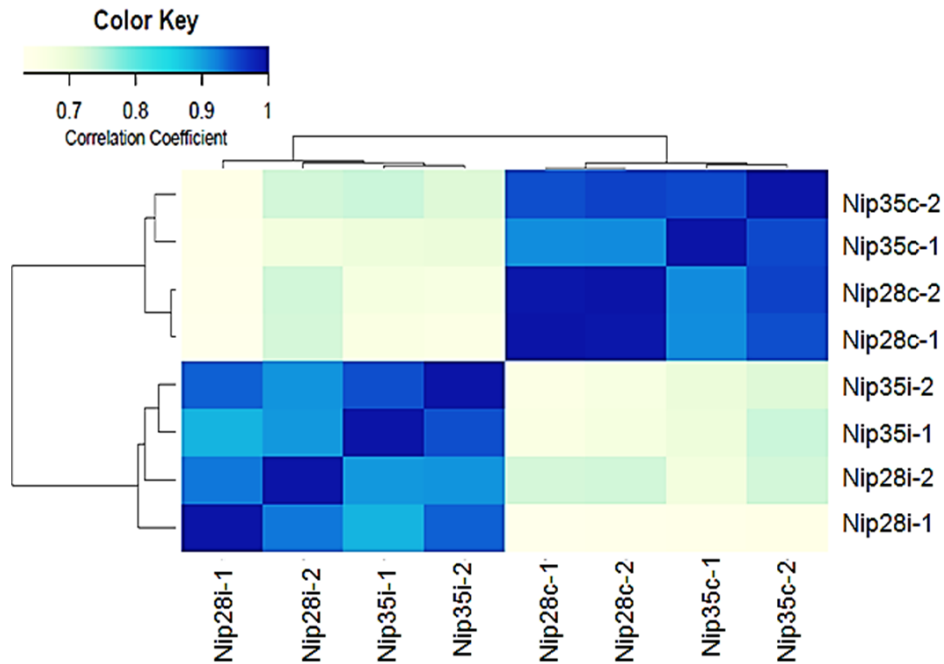
Figure 3.2: Heatmap showing clustering by Euclidean distances between sequenced sample libraries. The darker the color, the closer the two datasets are together. Nip28i and Nip35i represent infected samples at 28°C and 35°C respectively. Nip28c and Nip35c represent uninfected samples at 28°C and 35°C.
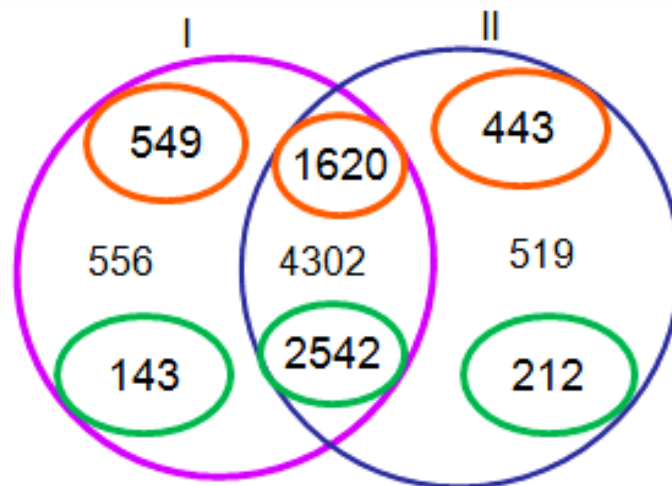
Figure 3.3a: Venn diagram illustrating overlaps between numbers of significant differentially expressed fungal genes (fold change 4; FDR, 0.05) in (I) Nip35i (II) Nip28i. The numbers in the orange circles represent the specific and shared up regulated genes in the respective treatments while those in the green circles represent specific and shared down regulated genes.
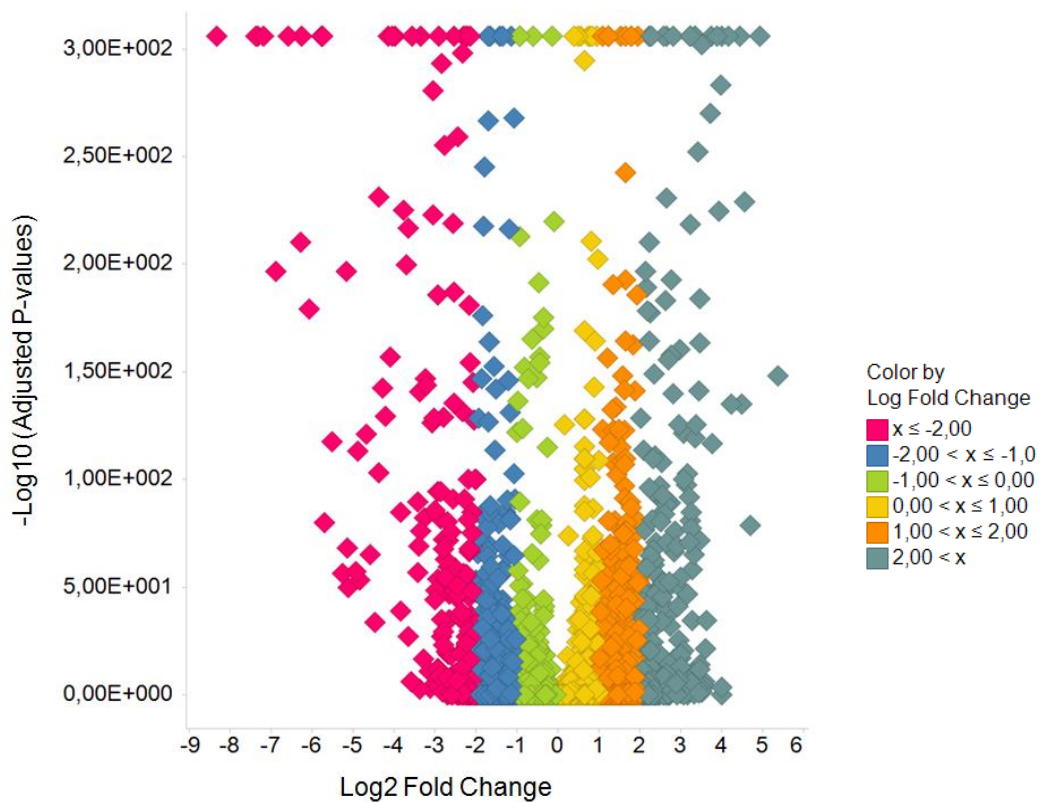
Figure 3.3b: Volcano plot of significance against fold change in fungal *in planta* gene expression, in Nip35i versus Nip28i. The negative $\log_{10}$ of the adjusted *P* values is plotted against the fold change difference of $\log_2$-normalized expression values. Small expression differences are located at the centre of the plot and log fold changes ≥ 2 are located outer part of the plot (see legend). Test-wise threshold of *P*=0·05 was used (corresponding to Fisher's exact test).
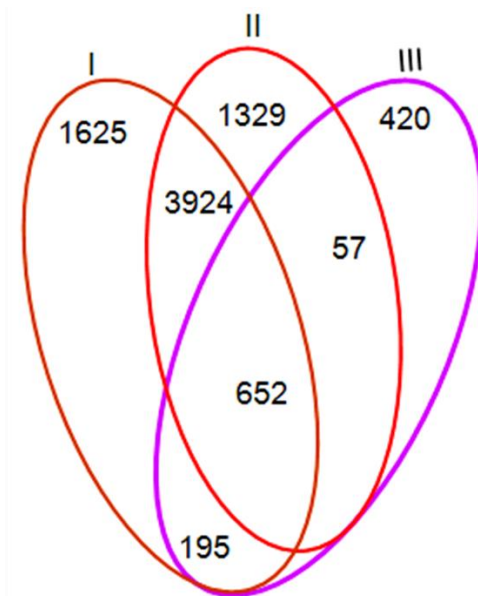
Figure 3.3c: Venn diagram illustrating overlaps between number of significant differentially expressed plant genes (fold change 4; FDR, 0.05) in (I) Nip35i, (II) Nip28i, (III) Nip35c.
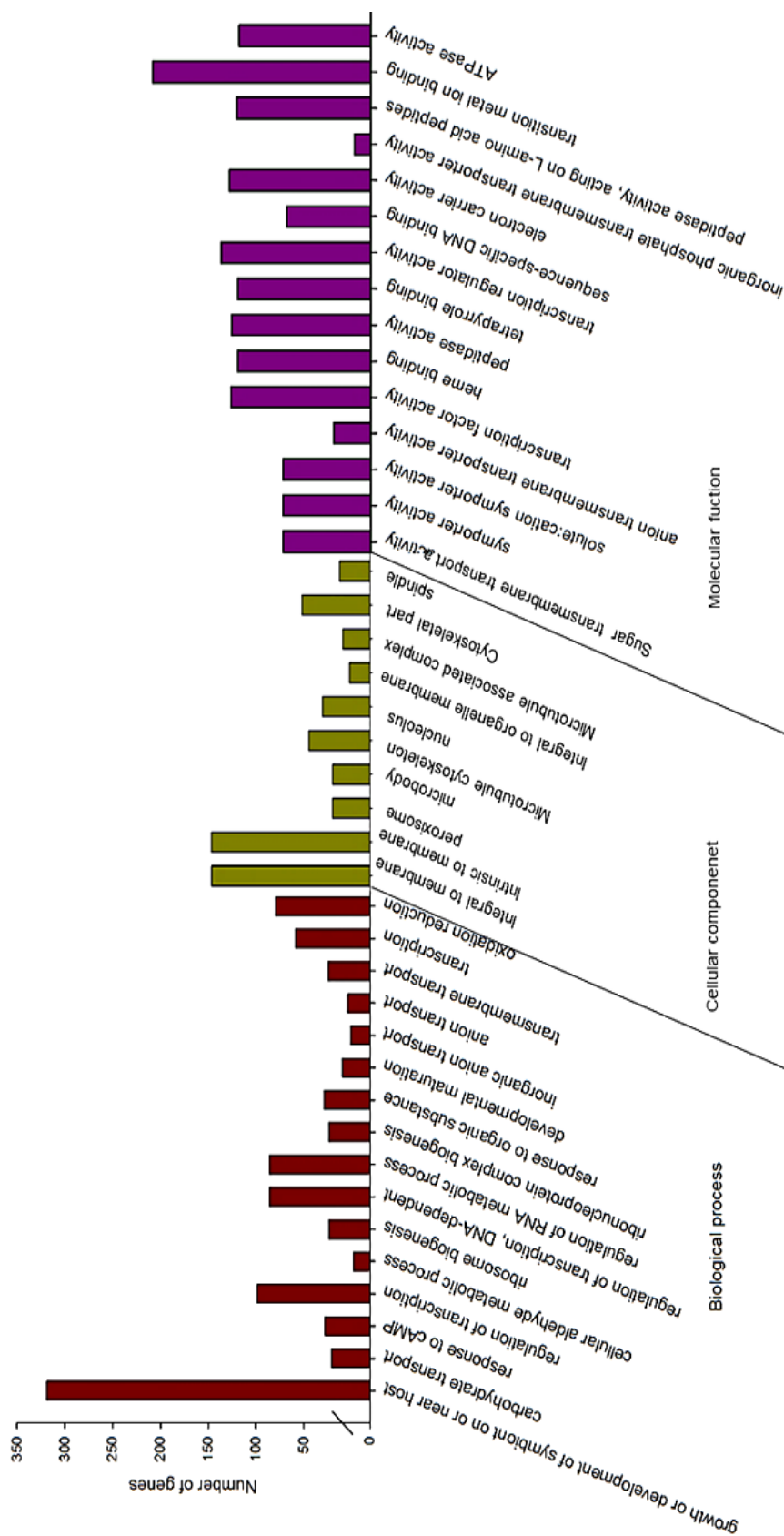
Figure 3.4: Gene Ontology classification of up regulated fungal DEGs in Nip35i (A), categorized into 41 and 39 functional groups of three main categories, respectively: biological process, cellular component and molecular function.
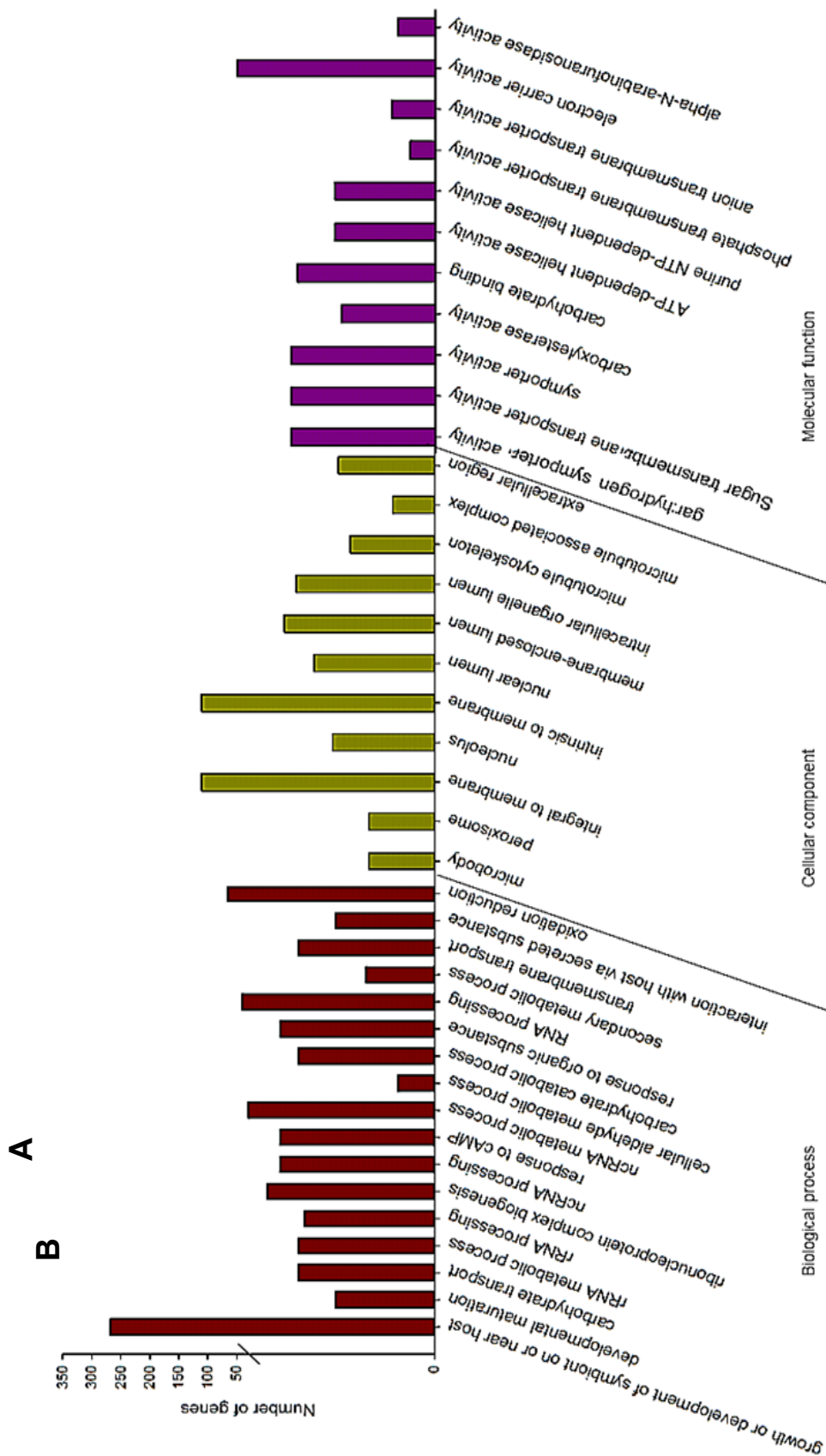
Figure 3.4: Gene Ontology classification of up regulated fungal DEGs in Nip28i (B), categorized into 41 and 39 functional groups of three main categories, respectively: biological process, cellular component and molecular function.
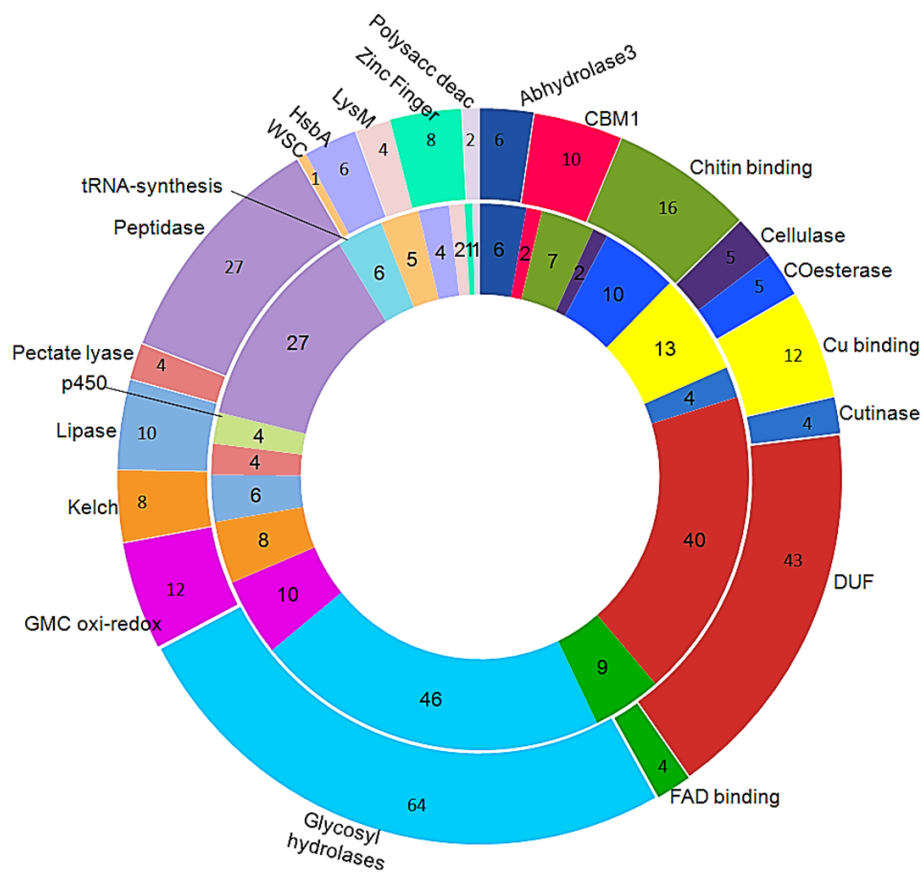
Figure 3.5: Domain classification and comparison of Nip35i (inner circle) and Nip28i (outer circle) putative secreted proteins. In each circle the relative fraction of protein domains (numbers) present in the predicted secreted proteins is presented.
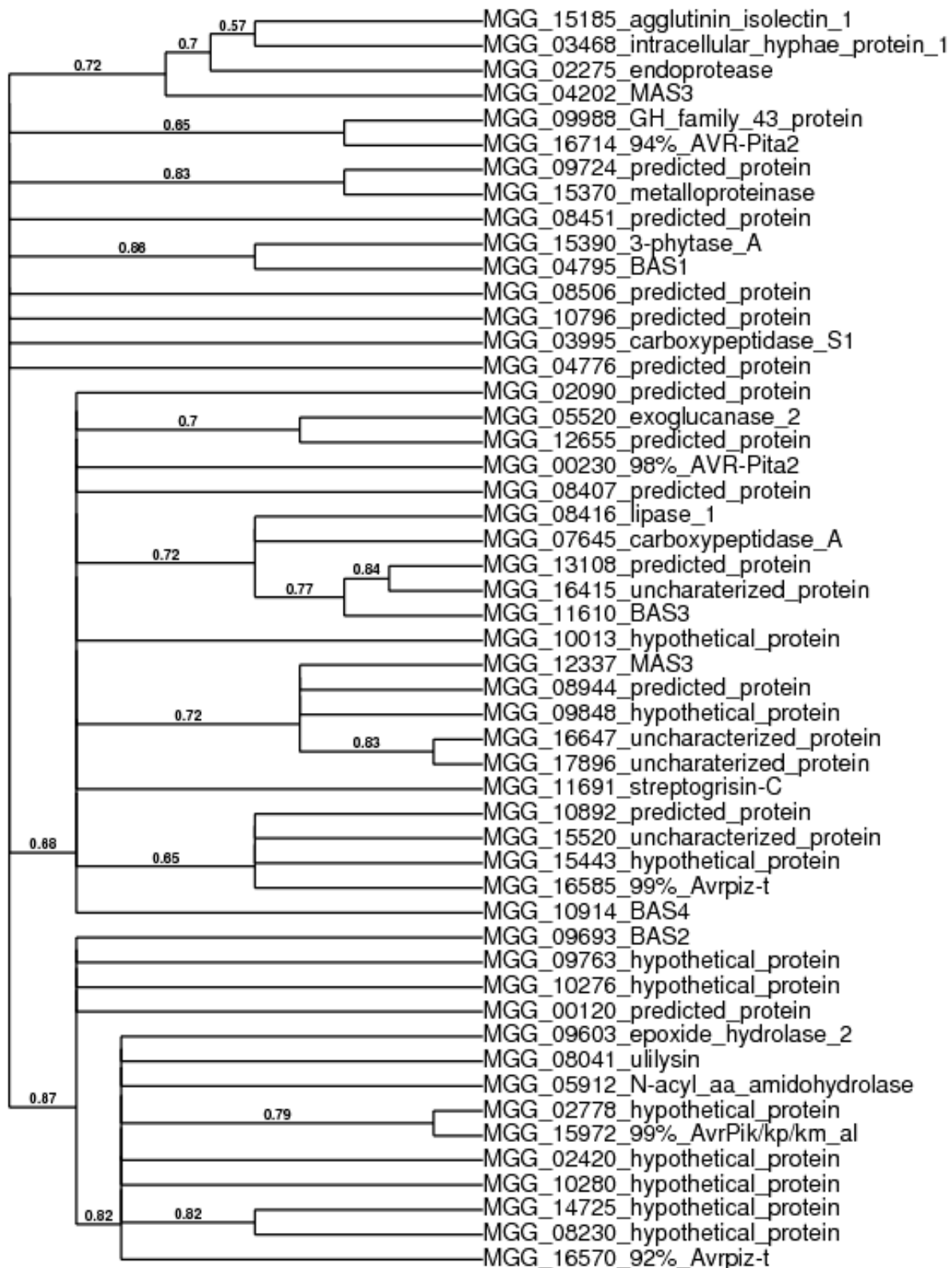
Figure 3.6: Maximum Likelihood based phylogenetic relationship between protein sequences of the top 50 putative secreted proteins induced in planta. Multiple sequence alignment was performed using MUSCLE (v3.7) with default settings, and edition of the phylogenetic tree were performed with TreeDyn (v198.3). The analysis was performed on the Phylogeny.fr platform (Dereeper et al. 2008). The putative secretome formed three major clusters. Branch support values calculated in the bootstrap test (1000 replicates) are shown on the branches.
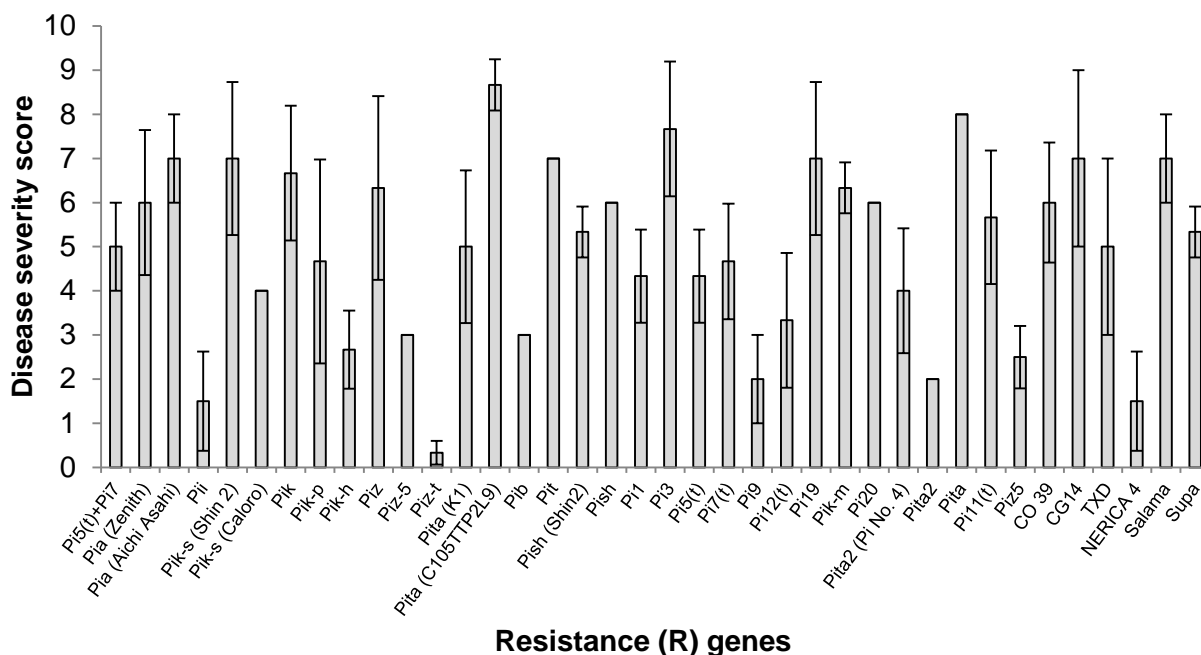
Figure 3.7: Reaction of 32 rice differential lines to TAN211.16. Piz-t was highly resistant to TAN211.16. Data are presented as mean disease severity scores ± standard deviation in 3 replicates.
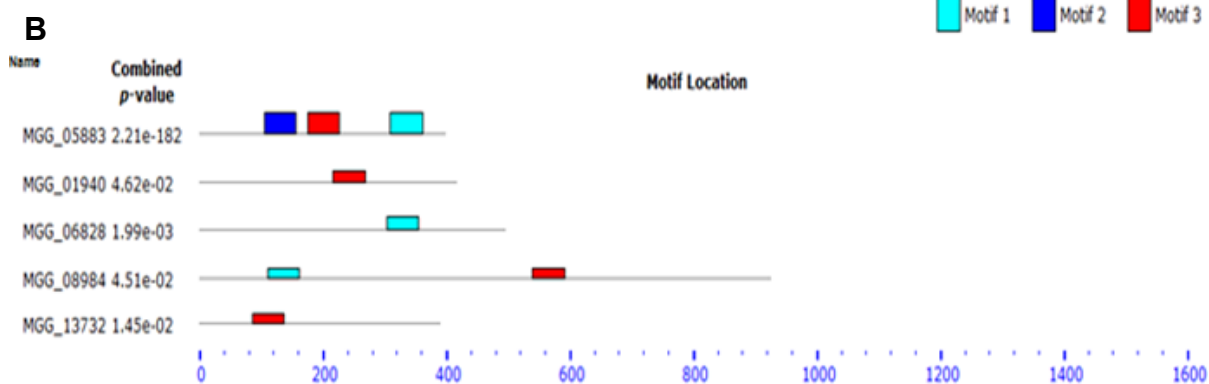
Figure 3.8: MEME searching identified overrepresented motifs in Specific genes up-regulated in NIp35i. Sequence logo of the top scoring MEME result for the top 11 regulated genes by SAM score (A) ; and (B) position and scoring of motif sites (p-value threshold <5e-2) in upstream sequences. The motifs were present in the upstream sequences of10 genes often with multiple instances, as shown by the color blocks depicting motif position within upstream sequences. Only 5 significant genes (>0.05) are presented.
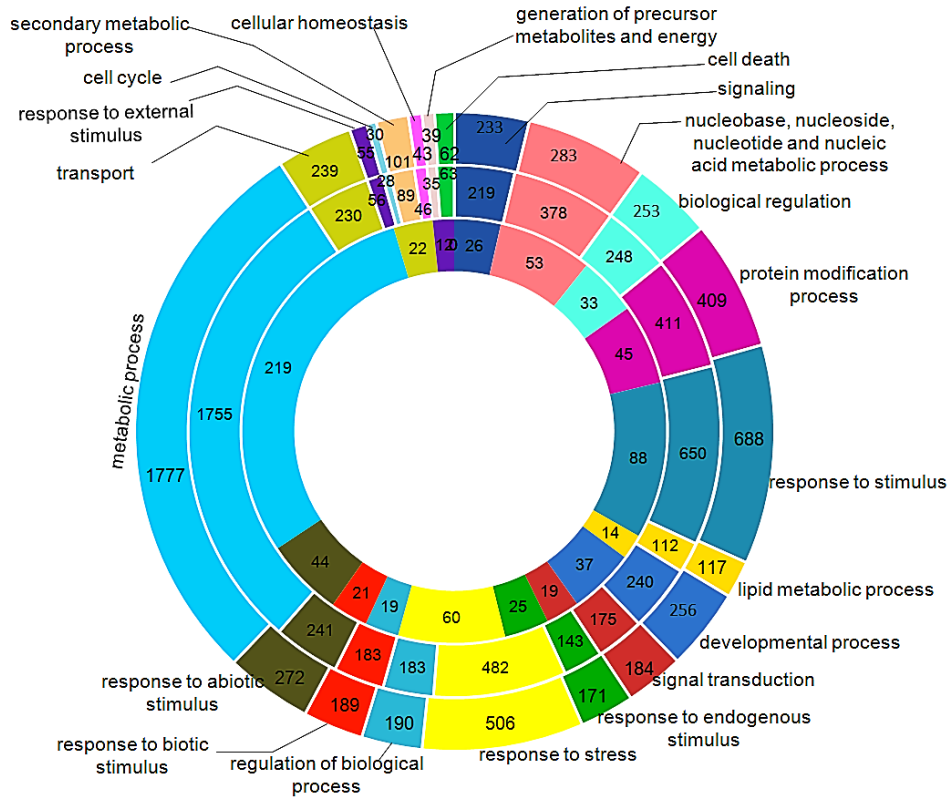
Figure 3.9: Gene Ontology classification of up regulated rice DEGs in Nip35c (inner circle), Nip35i (middle circle) and Nip28i (outer circle), categorized into 23 biological processes. The number of genes enriched in a given biological process is presented in the segments of each circle.
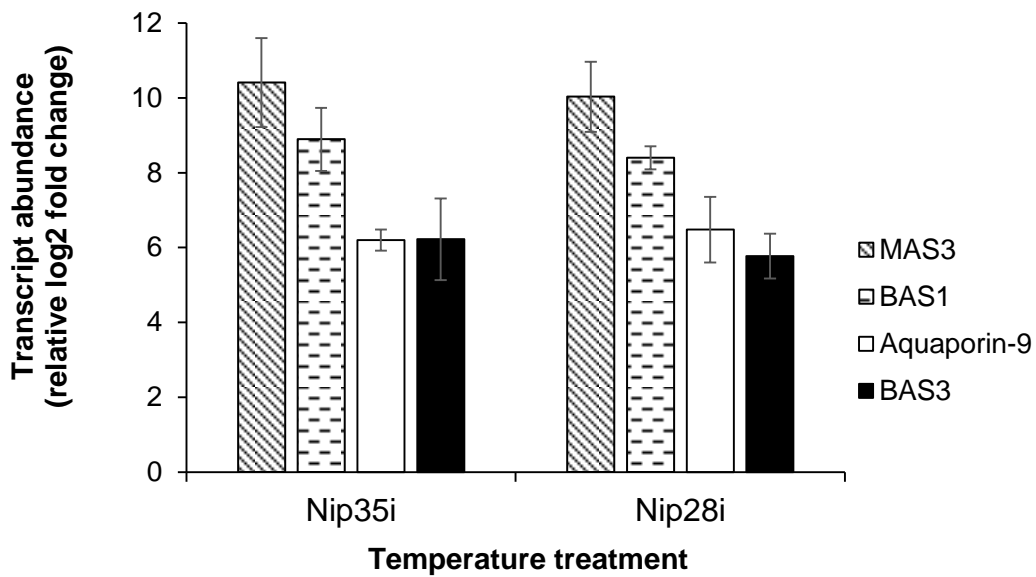
Figure 3.10: qPCR analysis of MAS3, BAS1, aquaporin-9 and BAS3 expression in infected rice leaves exposed to high temperature (Nip35i) and normal temperature (Nip28i). The relative gene transcripts were calculated relative to the fungal control using Pffal method, values are means ±SD.
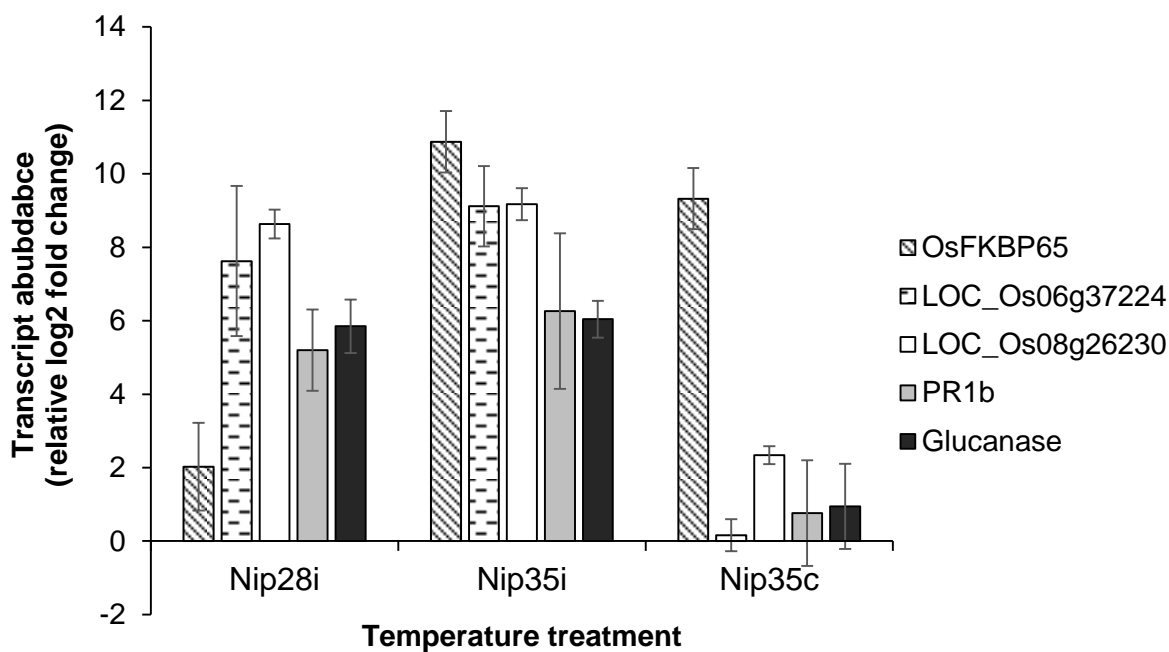
Figure 3.11: qPCR analysis of OsFKBP65, expressed protein (LOC_Os06g37224), Cytochrome P450 (LOC_Os08g26230), PR1b and PAL expression in infected rice leaves exposed to high temperature (Nip35i), normal temperature (Nip28i) and only high temperature without *M. oryzae* infection. The relative gene transcripts were calculated relative to the control (Nip28c) using Pffal method. Values are means ±SD.

Chapter 4: Population structure, pathogenicity and mating type distribution of *Magnaporthe oryzae* isolates from East Africa

Geoffrey Onaga, Kerstin Wydra, Birger Koopmann, Yakouba Séré, and Andreas von Tiedemann

First, third, and fifth authors: Division of Plant Pathology and Crop Protection, Department of Crop Sciences, and second author: CLB-Tropical and Subtropical Agriculture and Forestry, Georg-August-University Göttingen, Germany; and fourth author: Africa Rice Center, P.O. Box 33581, Dar es Salaam, Tanzania.
Accepted for publication 23 March 2015.

ABSTRACT

Onaga, G., Wydra, K., Koopmann, B., Séré, Y., and von Tiedemann, A. 2015. Population structure, pathogenicity, and mating type distribution of *Magnaporthe oryzae* isolates from East Africa. Phytopathology 105:1137-1145.

Rice blast, caused by *Magnaporthe oryzae*, is one of the emergent threats to rice production in East Africa (EA), where little is known about the population genetics and pathogenicity of this pathogen. We investigated the genetic diversity and mating type (MAT) distribution of 88 isolates of *M. oryzae* from EA and representative isolates from West Africa (WA) and the Philippines (Asia) using amplified fragment length polymorphism markers and mating-type-specific primer sets. In addition, the aggressiveness of each isolate was evaluated by inoculating on the susceptible *Oryza sativa indica* 'Co39', scoring the disease severity and calculating the disease progress. Hierarchical analysis of molecular variance revealed a low level of genetic differentiation at two levels (F_{ST} 0.12 and F_{CT} 0.11). No evidence of population structure was found among the 65 isolates from EA, and gene flow among EA populations was high. Moreover, pairwise population differentiation (G_{ST}) in EA populations ranged from 0.03 to 0.04, suggesting that >96% of genetic variation is derived from within populations. However, the populations from Asia and WA were moderately differentiated from EA ones. The spatial analysis of principal coordinates and STRUCTURE revealed overlapping between individual *M. oryzae* isolates from EA, with limited distinctness according to the geographic origin. All the populations were clonal, given the positive and significant index of association (I_A) and standardized index of association (r_d), which indicates a significant ($P < 0.001$) departure from panmixia (I_A and $r_d = 0$). Both MAT1-1 and MAT1-2 were detected. However, MAT1-1 was more prevalent than MAT1-2. Pathogenicity analysis revealed variability in aggressiveness, suggesting a potential existence of different races. Our data suggest that either *M. oryzae* populations from EA could be distributed as a single genetic population or gene flow is exerting a significant influence, effectively swamping the action of selection. This is the first study of genetic differentiation of rice-infecting *M. oryzae* strains from EA, and may guide further studies on the pathogen as well as resistance breeding efforts.

Additional keywords: AFLP.

Rice is a staple food for more than 3 billion people worldwide, and a significant income source to rural communities in developing countries. In East Africa (EA), rice has gained importance only recently. The production area in the three EA countries—Uganda, Rwanda, and Tanzania—increased from approximately 452,000 ha in 1999 to 1,223,910 ha in 2011 (FAOSTAT 2011). This area expansion and the ongoing intensification of rice production could potentially contribute to increased rice supply in the region that was formerly dependent on maize and sorghum as major cereals. However, rice production in EA faces a double burden of destructive diseases and the knowledge gap to cope with disease outbreaks. Among the various diseases, rice blast caused by *Magnaporthe oryzae* is an eminent threat to rice production. In fact, an unexpected blast outbreak was observed in farmers' fields in Kenya in 2009, leading to 48% yield losses (Kihoro et al. 2013). Moreover, field observations in Tanzania, Burundi, and Rwanda indicate the spread of the disease from traditional to new rice-growing areas, a situation that is only anticipated to worsen with increasing temperatures due to climate change (Liu et al. 2010; Mwalyego et al. 2011). How far this spread of the disease in EA indicates the evolution of novel pathotypes and enhancement of population diversity is not known.

Previous studies of genetic variation in *M. oryzae* populations found higher levels of genetic variation in field populations collected from South, East, and Southeast Asia than in other regions (Saleh et al. 2014; Zeigler 1998). However, fewer lineages were detected in the United States (Correll et al. 2009; Levy et al. 1991; Xia et al. 1993, 2000), Europe (Piotti et al. 2005; Roumen et al. 1997), Iran (Javan-Nikkah et al. 2004), Argentina (Consolo et al. 2008), Colombia (Levy et al. 1993; Zeigler 1998), Cuba (Fuentes et al. 2003), and West Africa (Takan et al. 2012), which is probably consistent with the hypothesis that asexual reproduction is dominant in the life cycle of *M. oryzae*. Commonly reported causes of genetic variability in Asian *M. oryzae* populations include high levels of genetic instability of traits such as pathogenicity, morphology, and fertility (Maciel et al. 2014), which could be congruent with the large number of pathotypes in some of the field populations reported.

However, there have been no studies on the genetic structure of the rice infecting *M. oryzae* field populations in EA. Improving our understanding of the genetic diversity, mating type (MAT) distribution, and aggressiveness of this pathogen is the most promising strategy that will provide a basis for implementation of various management approaches, including host plant resistance.

Various methods have been used to study the genetic diversity and population structure in *M. oryzae*, such as MGR 586 repetitive DNA sequence (Borromeo et al. 1993), *Pot2* (Kachroo et al. 1994), randomly amplified polymorphic DNA (RAPD) (Sere et al. 2007), amplified fragment length polymorphism (AFLP) (Thuan et al. 2006), simple sequence repeats (SSR) (Brondani et al. 2000; Saleh et al. 2014), and pathogenicity tests on differential sets of rice genotypes (Levy et al. 1991). From these methods, AFLP and SSR provide more sensitive and reliable analysis for individual genotype profiling. The AFLP technique is particular suitable for genetic diversity analysis due to simultaneous analysis of a large number of

Corresponding author: G. Onaga; E-mail address: gonaga@gwdg.de

polymorphic loci and high reproducibility due to high stringency of polymerase chain reaction (PCR), compared with RAPD (Liu and Cordes 2004). Due to these advantages, AFLP markers have been advocated as a powerful genetic marker system for assessing population structure and individual identity (Gerber et al. 2000).

Our objective here was to assess the extent of genetic variation in EA field populations of *M. oryzae* with AFLP markers, and determine MAT distribution and virulence. The present study provides the first estimates of genetic structure of field populations of *M. oryzae* from EA.

MATERIALS AND METHODS

Sampling, monoconidial isolation, and cultivation of fungal isolates. Isolates were collected in 2009 and 2011 from three EA countries: Rwanda, Uganda, and Tanzania (Fig. 1). For comparative purposes, isolates from West Africa and the Philippines (Asia) were included. Eight sampling points (farmers' fields) per site were considered. One to nine cultivars were sampled per location, with one to five lesion-bearing leaves collected per cultivar and one isolate collected per leaf. The number of sampling points and sites sometimes varied, according to the rice field and disease availability. Prior to isolation, each leaf sample was placed on glass rods in petri dishes with wet filter papers and incubated in continuous fluorescent light for 1 to 2 days at 25°C until conidiophores bearing conidia emerged from stromatal tissue beneath leaf stomata. The sporulating lesions were examined under a stereomicroscope and a group of conidia was aseptically transferred with a transfer needle to V8 agar. The pathogen was identified based on its morphological growth pattern and spore shape. To obtain single conidial isolates, conidia were streaked onto water agar. Individual, germinating conidia were identified with

Fig. 1. Geographic sites of rice fields in East Africa where *Magnaporthe oryzae* strains were sampled. Mean percent disease severity scores (black dots) for the different sampling sites and respective locations are indicated. The size of the dots indicates the level of disease severity.

a stereomicroscope and aseptically transferred and cultured in V8 agar. For long-term storage, each culture was overlaid with several sterilized filter paper sections and incubated at 25°C. After 10 to 12 days of incubation, the colonized filter paper sections were lifted from the agar surface, placed in sterile, empty petri dishes, allowed to dry for 3 days at room temperature, and stored at –20°C.

DNA extraction. In total, 88 isolates of *M. grisea* (Table 1) from the collection stored in the Division of Plant Pathology and Crop Protection, Georg-August University, Goettingen, Germany, were used for AFLP analysis. To obtain mycelia, plugs harvested from 8-day-old cultures were inoculated into a 1,000-ml flask containing 250 ml of liquid Fries medium at room temperature for 7 to 8 days with constant shaking on a rotary shaker. Mycelial mats were harvested, freeze dried, and ground in liquid nitrogen to a fine powder. Approximately 40 mg of the powdered mycelia was used for DNA isolation using a modification of the cetyltrimethylammonium bromide (CTAB) method (Brandfass and Karlovsky 2008), by combining the sodium acetate-sodium dodecyl sulfate with CTAB extraction.

AFLP analysis. AFLP analysis was conducted according to a method modified from Vos et al. (1995). The primary template for preamplification reaction consisted of 125 ng of genomic DNA. Genomic DNA was first digested with 10 U of *Eco*RI at 37°C overnight followed by a second digestion with 5 U of *Tru*I (Fermentas GmbH, St. Leon-Rot, Germany) at 65°C for 2 h. The digested samples were ligated overnight with 1.0 U of T4 DNA ligase (Fermentas GmbH) and 10 µM *Eco*RI and *Tru*I adapters in a final volume of 20 µl at room temperature. The ligation products were diluted 10-fold with ultrapure water and 1 µl of the resulting dilution was used for preselective amplification with *Eco*RI-A and *Tru*I-C primers (10 µM), 10 mM each dNTP, 50 mM MgCl₂, 5 U of Taq DNA polymerase, and 10× *Taq* polymerase buffer (50 mM Tris-HCl [pH 7.5], 50 mM magnesium acetate, and 250 mM potassium acetate) in a total volume of 25 µl. Two replicate AFLP reactions per individual were used to eliminate variation due to anomalous PCR products or artifacts of detection in individual analysis. PCR was performed for 25 cycles, which consisted of 30 s at 94°C, 1 min at 56°C, and 1 min at 72°C in an Eppendorf Master Cycler (Netheler-Hinz GmbH, Hamburg, Germany). The products of the preselective amplification step were diluted 1:10 with ultrapure water and subjected to selective amplification. The amplification reaction mix was similar to the preselective amplification, except that labeled *Eco*RI-ACA-Dy635-5 carboxyfluorescein, *Eco*RI-ACC-Dy750 blue fluorescein, *Eco*RI-AGA-Dy680 green fluorescein (Dyomics, Jena, Germany), and *Tru*I-CCC primers were used. The thermocycler program consisted of two phases. The first phase was performed with a touchdown cycling profile of 12 cycles with a step-down of annealing temperature by 0.7°C/cycle: 30 s at 94°C, 30 s at 65 to 57.3°C, and 1 min at 72°C. The second phase consisted of 23 cycles of 30 s at 94°C, 1 min at 56°C, and 1 min at 72°C.

Preparation of DNA amplification fragments for separation by capillary electrophoresis. The selectively amplified DNA fragments were diluted 1:10 with ultrapure water, and 2.5 µl of each sample was loaded into respective microtiter plate wells. A 30-µl separation solution (formamide incorporated) mixed with a size standard 600 (Beckman Coulter, Fullerton, CA) was added and each well was overlaid with a drop of Sigma mineral oil (M5904). The microtiter plates containing the reaction mixtures were briefly spun and the samples were run in denaturing polyacrylamide gel using an automated DNA sequencer (CEQ 8000 genetic analysis system; Beckman Coulter). The AFLP patterns were captured and peaks were assigned to base pair sizes using the default analysis parameter and analyze the data window in the CEQ System Software. To detect peaks of interest, the slope threshold and the relative peak height threshold were set at 50 and 10, respectively. All peak heights were compared with a reference peak of the same color based on the migration time for each of the dyes used. Further data processing, including background subtraction and signal matching, was
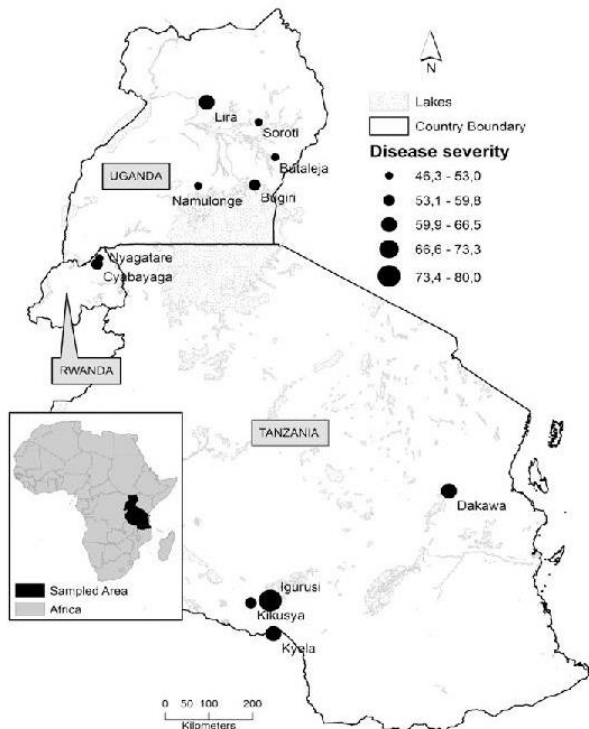
performed according to Weiberg and Karlovsky (2009). The peak data were converted into a binary matrix using the AFLP feature of the CEQ System. The AFLP feature creates bins from fragments with sizes that fall within a user-defined bin width. For each of the possible fragments, a "1" is assigned if a fragment is found in that sample and "0" if the fragment is absent. A table of 1s and 0s is created and exported to an excel spreadsheet. Only PCR fragments that show high reproducibility in the two repeat runs were used for further analyses.

Population genetic structure analysis. The genetic diversity within and between populations was assessed with POPGENE, version 1.3.2 (Yeh and Boyle 1999). Shannon's index (I) and Nei's diversity index (H) were also calculated using the default settings in POPGENE. The genetic differentiation (G_{ST}) among populations was calculated as $G_{ST} = D_{ST}/Ht$. Gene flow (Nm) between any two studied populations was estimated as $Nm = 0.5 (1 - G_{ST})/G_{ST}$. The average allele frequency of alleles unique to one population, across loci ($p[1]$), or private alleles was estimated using GENALEX. We used the *poppr* R package to generate a Maynard Smith index of association (I_A), which assesses multilocus linkage disequilibrium, and another estimator, r_d, to correct for the bias in I_A that may arise due to the influence of increasing number of loci. We estimated multilocus genotypic diversity using Stoddart and Taylor's index G (Stoddart and Taylor 1988), and multilocus genotypic evenness (the distribution of genotypes in a sample) using the index E_5 (Grünwald et al. 2003). Two methods were used to determine population genetic structure. First, the program Tools for Population Genetic Analysis (TFPGA) (Miller 1997) was used to calculate θ, an unbiased estimator of Wright's F_{st}. We calculated 95% confidence intervals around the estimates of θ by bootstrapping with 1,000 replicates. Second, the population genetic analysis program ARLEQUIN 3.5 (Excoffier et al. 2005) was used to assess the interpopulation genetic structure without assuming Hardy-Weinberg equilibrium by performing an analysis of molecular variance (AMOVA).

Cluster analysis of AFLP data. Cluster analysis of the presence (1) or absence (0) data matrix was performed with two methods. We used principle coordinate analysis (PCoA) based on Nei's distances between all pairs of AFLP genotypes using GENALEX 6.2 (Peakall and Smouse 2006; Nei 1978), which generated a two-dimensional principal component analysis plot showing the distribution of *M. oryzae* strains among the studied populations. Second, we used the model-based program STRUCTURE 2.3 (Pritchard et al. 2000), which implements a clustering algorithm based on a Bayesian model to assign individuals to a number of clusters (K) or populations. To estimate the number of Ks, 10 independent runs were performed for each number of possible clusters (K = 1 to 10), without any prior information on the origin of individual isolates. For each run, we used a burn-in period of 1×10^5 iterations followed by a run length of 1×10^5 iterations, using a model with correlated allele frequencies and admixture among populations. The number of populations that best represent the observed data under the model implemented was determined using STRUCTURE output, based on the rate of change in log probability of data (LnP[D]) between successive Ks. The most probable value of K was determined by ΔK, an ad hoc quantity related to the second-order change in the Ln P(D) with respect to the number of clusters inferred by STRUCTURE (Evanno et al. 2005). The estimated membership coefficients for each individual in each cluster in a Q matrix were passed as input to the software package DESTRUCT for visualization.

Pathogenicity assays and statistical analysis. Plant inoculations were performed on short-duration dwarf *Oryza sativa indica* 'Co39', with high susceptibility to tropical blast isolates. The plants were grown in the greenhouse at $25 \pm 5°C$ with a photoperiod of 14 h for 23 days. *M. oryzae* isolates were grown in petri dishes containing V8 agar under 14 h of fluorescent light at 25°C for 12 days. Three days prior to inoculation, cultures were exposed to low levels of visible and near-UV radiation to maximize sporulation.

Conidia were harvested with sterile distilled water and the concentration was adjusted to 1×10^5 conidia/ml after filtration through two layers of Miracloth. Pathogenicity tests were performed by spraying a conidial suspension containing 0.05% Tween 20 onto rice seedlings at four- to five-leaf stages. Inoculated plants were kept in a humidified growth chamber in the dark at 25°C for 24 h, before returning to the greenhouse at $25 \pm 5°C$. Leaf blast was assessed 4 to 12 days after inoculation using a disease evaluation scale from 0 to 9 (Silva et al. 2009). Inoculations were repeated two times using three replicates per repeat to confirm lesion categorization into resistant or susceptible types. Disease severity ratings between the two repeats remained consistent. Violation of assumptions of normality was tested on both datasets using the Shapiro-Wilks test, and the data set with minimal bias in the distribution of residuals was used for calculating the area under the disease progress curve (AUDPC) using the midpoint rule method (Campbell and Madden 1990) in order to compare the different isolates. Analysis of variance for the final rice blast severity (%) and AUDPC was performed using SAS 9.3, and the least significant difference test at 0.05 probability level was used for mean comparisons.

MAT distribution. Two isolates, IN1 (MAT1-1) and OG5 (MAT1-2), kindly provided by Dr. Didier Tharreau (CIRAD, Montpellier, France), were used as testers in this study. DNA of the testers was isolated as described above. Isolates used for MAT determination are indicated in Table 1. Two singleplex PCR amplifications were performed with MAT-specific primers previously used by Consolo et al. (2005): A1 (5′-AGCCTCATCAACGGCAA-3′) and A5 (5′-GGCACGAACATGCGATG-3′) for MAT1-1 and B15 (5′-CTCAATCTCCGTAGTAG-3′) and B16 (5′-ACAGCAGTA TAGCCTAC-3′) for MAT1-2. The PCR had a final volume of 20 µl containing 80 ng of template DNA, 10× *Taq* polymerase buffer (Bioline, Luckenwalde, Germany), 2.5 mM each dNTP, 50 mM $MgCl_2$, *Taq*DNA polymerase at 5 U/µl, and 0.01 mM each primer. Thermal cycling conditions included an initial denaturation step at 95°C for 5 min followed by 30 cycles of 95°C for 45 s, 58 and 62.5°C for MAT1-2 and MAT1-1, respectively, for 1 min, and 72°C for 1 min; and a final elongation step at 72°C for 5 min. PCR products were separated in a 1.2% agarose gel at 66 V for 3 h, stained with ethidium bromide, and photographed.

RESULTS

Genetic diversity and population structure. The three selected AFLP primer combinations generated a total of 289 loci, of which 198 were phylogenetically informative; that is, present or absent in at least two strains, with alleles ranging in size from 60 to 700 bp across all 88 isolates of the five populations. The percentage of polymorphic loci at the population level ranged from 31.3% (West Africa) to 68.7% (Uganda) (Table 2). To distinguish clonal and recombinant structures in all populations, multilocus genotypes (MLG) and I_A were used. We detected clonality in all the populations, given the positive I_A and r_d values (Fig. 2), which indicate a significant ($P < 0.001$) departure from panmixia (I_A and $r_d = 0$). The frequency of MLG in each population was significantly correlated with AFLP loci obtained, indicating widespread linkage disequilibrium. The average gene diversity, Shannon's index, and evenness were estimated to be 0.13, 0.24, and 1, respectively. Private alleles were found in all populations; the highest number was observed in Asia, followed by Uganda.

All populations showed low values of genetic differentiation (G_{ST}), with an overall average among populations of 0.11 (Table 3). Low interpopulation genetic differentiation (θ = 0.078, 95% confidence interval = 0.057 to 0.099) was equally found when the data were analyzed with TFPGA. Moreover, AMOVA, at two hierarchical levels (F_{ST} 0.12 and F_{CT} 0.11), indicated that the populations were not geographically structured. Thus, most of the genetic variation was distributed within populations (88.09%)

[126]

($P < 0.001$, 1,023 nonparametric permutations) rather than among groups (Asia, West Africa, and EA) (10.97%), and no significant variation existed between populations within groups (0.93%) (Table 4). Correspondingly, gene flow between populations was high (>1). Gene flow was highest between Uganda and Rwanda ($Nm = 16.78$), Tanzania and Uganda ($Nm = 13.10$), and Tanzania and Rwanda ($Nm = 10.84$), and was consistent with I_A and population evenness. Tanzania, Uganda, and Rwanda also recorded the highest indices of genetic identity and the lowest levels of genetic distance, corroborating the data obtained for gene flow and genetic differentiation. Conversely, gene flow between Asian and African populations was relatively low.

Cluster analysis. PCoA, based on Nei's genetic distance, grouped the isolates into four main clusters (Fig. 3A). The PCoA captured 54.1% of the total variation in two principal components. The first principal component accounted for 35.7% of the total variation and illustrated the outgroup position of the Philippine isolates (group 1). Group 2 constituted the largest admixed group followed by group 3. Isolates from the various collection sites formed 15 subpopulations (Fig. 3B). Tanzanian subpopulations

were closer to the West African subpopulation, whereas Rwanda and Uganda were found closer to each other. Using STRUCTURE 2.3, Ln probabilities (X|K) for K values (number of assumed populations) of 1 to 10 were calculated, and K = 5 had the highest probability (Fig. 4A). Thus, five genetic groups were resolved (Fig. 4B). The results showed a clear separation of the Philippine isolates from the African groups. Among the African populations, West African isolates were the genetically most homogeneous, which was consistent with the 0 private alleles and the high I_A values observed (Table 2). Populations from Uganda, Tanzania, and Rwanda had a large proportion of admixed individuals, which corroborates the trend observed in the PCoA clustering. Interestingly, we found that variation in AFLP genotypes was not predictive (not correlated) of variation in pathogenicity.

Pathogenicity assays. Isolates varied in pathogenicity, as reflected by the percent leaf area infected (Table 1). At 10 days postinoculation (dpi), 76% of isolates had induced severity scores of ≥50%. The remaining 24% consistently produced restricted lesion sizes. The most virulent isolates were TAN211.8 and 507RWA11 from Tanzania and Rwanda, respectively. The least virulent isolate

TABLE 1. Code, designation, country of origin, site of collection, year of collection, cultivars from which the strains were isolated, mating type, and area under the disease progress curve (AUDPC) obtained from pathogenicity tests

Number	Code	Designation	Country	Site of collection	Cultivar	Mating type	AUDPC[z]
1	1026	501UGA09	Uganda	Tilda, Bugiri	Pusa Basmati	MAT1-2	495.0 de
2	1027	502UGA09	Uganda	Tilda, Bugiri	Pusa Basmati	MAT1-2	480.0 def
3	1028	503UGA09	Uganda	Tilda, Bugiri	Pusa Basmati	MAT1-2	215.0 (2)i–l
4	1029	504UGA09	Uganda	Tilda, Bugiri	Pusa Basmati	MAT1-2	…
5	1030	505UGA09	Uganda	Tilda, Bugiri	Pusa Basmati	MAT1-2	452.5 fgh
6	1031	508UGA09	Uganda	Tilda, Bugiri	Pusa Basmati	MAT1-1	235.0 (2)f–k
7	1032	513UGA09	Uganda	Tilda, Bugiri	Pusa Basmati	MAT1-1	470.0 d–g
8	1033	518UGA09	Uganda	Tilda, Bugiri	Pusa Basmati	MAT1-2	225.0 (2)h–k
9	1035	520UGA09	Uganda	Tilda, Bugiri	Pusa Basmati	MAT1-2	327.5 s–w
10	1037	524UGA09	Uganda	Tilda, Bugiri	Pusa Basmati	MAT1-2	330.0 r–v
11	1106	531UGA11	Uganda	Lira Itek Main Dam	Unknown	MAT1-1	510.0 cd
12	1108	533UGA11	Uganda	Lira Itek Main Dam	Unknown	MAT1-1	155.0 (2)nm
13	1112	537UGA11	Uganda	Soroti-Apalitunga	Unknown	MAT1-1	267.5 (2)a–g
14	1113	538UGA11	Uganda	Soroti-Apalitunga	Unknown	MAT1-1	282.5 yz(2)a–e
15	1114	539UGA11	Uganda	Lira-Abolet	Unknown	MAT1-1	330.0 r–v
16	1116	541UGA11	Uganda	Lira-Abolet	Unknown	MAT1-1	250.0 (2)c–i
17	1117	542UGA11	Uganda	Namulonge	NERICA 4	MAT1-2	387.5 k–p
18	1121	547UGA11	Uganda	Namulonge	NERICA 2	MAT1-1	325.0 s–x
19	1122	548UGA11	Uganda	Namulonge	NERICA 3	MAT1-2	…
20	1123	549UGA11	Uganda	Namulonge	NERICA 4	MAT1-2	332.5 r–u
21	1126	552UGA11	Uganda	Butaleja, Doho Rice Scheme	K98	MAT1-1	197.5 (2)kl
22	1129	556UGA11	Uganda	Namulonge	Pakistan	MAT1-1	…
23	1130	557UGA11	Uganda	Namulonge	Unknown	MAT1-1	265.0 (2)a–h
24	1132	559UGA11	Uganda	Balita-Wakiso	NERICA 4	MAT1-1	412.5 i–m
25	1142	563UGA11	Uganda	Doho-Butaleja	K98	MAT1-1	255.0 (2)b–i
26	1111	536UGA11	Uganda			—	370.0 n–r
27	1092	495UGA11	Uganda			MAT1-1	245.0 (2)e–j
28	1298	Ugm4	Uganda	Doho-Butaleja	K98	MAT1-1	295.0 u–z(2)ab
29	1299	Lira 1-1	Uganda	Lira Itek Main Dam	unknown	MAT1-1	482.5 def
30	1300	Ugm1	Uganda	Doho-Butaleja	K98	MAT1-1	350.0 p–t
31	1301	Ugm2	Uganda	Doho-Butaleja	K98	MAT1-1	…
32	1019	461RWA09	Rwanda	Nyazatare experiment station	Nyiragakara	MAT1-1	…
33	1021	470RWA09	Rwanda	Nyazatare experiment station	Nyiragakara	MAT1-1	250.0 (2)c–i
34	1022	474RWA09	Rwanda	Nyazatare experiment station	Nyiragakara	MAT1-1	400.0 j–m
35	1023	482RWA09	Rwanda	Nyazatare experiment station	Nyiragakara	MAT1-1	220.0 (2)i–l
36	1024	488RWA09	Rwanda	Nyazatare experiment station	Nyiragakara	MAT1-1	437.5 g–j
37	1025	492RWA09	Rwanda	Nyazatare experiment station	Nyiragakara	MAT1-1	310.0 t–z
38	1090	493RWA11	Rwanda	Cyabayaga	Kavamahanga	MAT1-1	370.0 n–r
39	1094	497RWA11	Rwanda	Cyabayaga	Kavamahanga	MAT1-1	357.5 o–s
40	1095	498RWA11	Rwanda	Cyabayaga	Nyiragakara	MAT1-2	285.0 x–z(2)a–e
41	1099	504RWA11	Rwanda	Cyabayaga	Nyiragakara	MAT1-1	182.5 (2)lm
42	1133	505RWA11	Rwanda	Cyabayaga	Yunikeng	MAT1-2	362.5 n–s
43	1147	RWA 11.2	Rwanda	Cyabayaga	Irrigated rice	MAT1-2	422.5 i–l
44	1149	506RWA11	Rwanda	Cyabayaga	Irrigated rice	MAT1-1	360.0 n–s
45	1150	RWA 11.5	Rwanda	Cyabayaga	Irrigated rice	MAT1-1	227.5 (2)g–k
46	1151	RWA 11.6	Rwanda	Cyabayaga	Irrigated rice	MAT1-1	465.0 e–h
47	1152	507RWA11	Rwanda	Cyabayaga	Irrigated rice	MAT1-1	600.0 a

(continued on next page)

[z] Means followed by the same letter are not significantly different from each other.

was 536UGA11 from Uganda, which showed only 30% severity. Ten isolates did not produce any visible symptoms on rice seedlings. The same isolates had low sporulation ability when tested on V8 and oatmeal agar plates, and were not included in the second pathogenicity test. Disease progression varied widely. For all pathogenic isolates, a constant increase in the severity scores was observed from 4 to 10 dpi. By comparison, Tanzania and Rwanda had a larger proportion of the more aggressive isolates than Uganda.

MAT distribution. An assay of 88 isolates, based on MAT-specific PCR primers, revealed the presence of both MAT1-1 and MAT1-2 in EA (Fig. 4; Table 1). In all, 65 isolates from the various collection sites were MAT1-1 and 17 isolates were MAT1-2. The distribution among isolates was 11, 4, and 2 of MAT1-2 type from Uganda, Rwanda, and Tanzania, respectively. Overall, the frequency of MAT1-1 was higher in EA and predominantly the only MAT in most sites. The representative strains from Asia and West Africa were predominantly MAT1-2.

DISCUSSION

We analyzed *M. oryzae* populations from EA and representative isolates from West Africa and the Philippines in attempts to infer genetic variability, MAT distribution, and strain pathogenicity. Our data showed low G_{ST} and pairwise population differentiations among EA populations, suggesting a lack of population structure according to Nei's (1978) classification of population differentiation ($G_{ST} < 0.05$ is low, 0.05 to 0.15 medium, and >0.15 high). The

absence of a population structure often suggests low genetic diversity, largely due to genetically similar populations (Okori et al. 2004). Such populations are either of common origin or restricted distribution, reproduce exclusively asexually, or experience substantial gene flow coupled with genetic drift (e.g., due to limited host availability). However, in populations where mutation rates are high, it has been suggested that the G_{ST} tends to fall back to zero as more novel alleles are added to a population. This happens because of the negative dependence of G_{ST} on diversity (Jost 2008), and may occur in the case of *M. oryzae*, in which considerable genetic variation, even in the absence of sexual reproduction, has been reported (Couch et al. 2005). To circumvent the bias that may probably result due to mutation rates, we related G_{ST} values to other genetic diversity indices. Our data revealed a G_{ST} value of 0.04 (Table 3) among the EA populations, suggesting that 96% of genetic variation is derived from within populations. This is consistent with the low Shannon's indices (0.10 to 0.21) (Table 2). The Shannon's index of 0.21 suggests that more than 78% of the genetic diversity between populations was accounted for by differences between individuals. This result is contrary to the findings of Kumar et al. (1999), where Shannon's diversity indices of 0.89 to 0.92 were found in the Himalayan highly diverse populations of *M. oryzae*. This might be because EA populations represent recent founder populations where only a few generations have passed since colonization.

We used I_A to test the degree of nonrandom association between alleles at different loci (linkage disequilibrium). The I_A calculated

TABLE 1. (*continued from preceding page*)

Number	Code	Designation	Country	Site of collection	Cultivar	Mating type	AUDPC^z
48	1156	508RWA11	Rwanda	Cyabayaga	Irrigated rice	MAT1-1	207.5 (2)j–l
49	1158	510RWA11	Rwanda	Cyabayaga	Irrigated rice	MAT1-1	…
50	1096	500RWA11	Rwanda	Cyabayaga	Irrigated rice	MAT1-2	290.0 v–z(2)abc
51	1159	511RWA11	Rwanda	Cyabayaga	Irrigated rice	MAT1-1	230.0 (2)g–k
52	1163	TAN211.1	Tanzania	Dakawa	Supa	MAT1-1	350.0 p–t
53	1164	TAN211.2	Tanzania	Igurusi	SARO	MAT1-1	495.0 de
54	1165	TAN211.3	Tanzania	Kikusya	Unknown	MAT1-1	…
55	1166	TAN211.4	Tanzania	Kikusya	Unknown	MAT1-2	280.0 yz(2)a–e
56	1167	TAN211.5	Tanzania	Kikusya	Unknown	MAT1-1	280.0 yz(2)a–e
57	1169	TAN211.8	Tanzania	Kikusya	Unknown	MAT1-2	577.5 ab
58	1170	TAN211.9	Tanzania	Kikusya	Unknown	MAT1-1	380.0 m–q
59	1171	TAN211.10	Tanzania	Kyela	V35	MAT1-1	392.5 k–o
60	1172	TAN211.11	Tanzania	Kyela	V36	MAT1-1	350.0 p–t
61	1173	TAN211.12	Tanzania	Kyela	V37	MAT1-1	…
62	1174	TAN211.13	Tanzania	Kyela	V38	MAT1-1	380.0 m–q
63	1175	TAN211.14	Tanzania	Kyela	V39	MAT1-1	380.0 m–q
64	1176	TAN211.15	Tanzania	Kyela	V40	MAT1-1	250.0 (2)c–i
65	1178	TAN211.17	Tanzania	Kyela	V40	MAT1-1	537.5 bc
66	1180	RBELOK-10-7-3	Benin	Lokossa	Unknown	MAT1-2	335.0 r–u
67	1181	RBELOK-10-11-2	Benin	Lokossa	Unknown	MAT1-1	345.0 q–t
68	1182	RBELOK-10-13-3	Benin	Lokossa	Unknown	MAT1-2	245.0 (2)e–j
69	1184	RNIIBAD-09-5-1	Nigeria	Ibadan	Unknown	MAT1-2	245.0 (2)e–j
70	1185	RNIIBAD-09-82-2	Nigeria	Edozhigi	Unknown	MAT1-2	265.0 (2)a–h
71	1187	RNIIBAD-09-82-3	Nigeria	Edozhigi	Unknown	MAT1-2	382.5 l–p
72	1183	RBELOK-1022	Benin	Lokossa	Unknown	MAT1-2	425.0 i–k
73	1179	RBELOK-10-2-4	Benin	Lokossa	Unknown	MAT1-1	447.5 f–i
74	955	43	Philippines	IRRI	Unknown	MAT1-2	447.5 f–i
75	957	AGT211	Philippines	unknown	Unknown	MAT1-2	287.5 w–z(2)a–d
76	958	V86014	Philippines	IRRI	Unknown	MAT1-2	247.5 (2)d–j
77	959	B90289	Philippines	IRRI	Unknown	MAT1-2	312.5 t–z
78	961	M36-1-3-10-1	Philippines	IRRI blast nursery	Unknown	MAT1-2	272.5 z(2)a–f
79	963	C9228-37	Philippines	Caliraya, Laguna	Unknown	MAT1-2	370.0 n–r
80	977	V86010	Philippines	Bo.Bula, Camarines Sur	Unknown	MAT1-2	315.0 t–y
81	969	M39-1-2-21-2	Philippines	IRRI blast nursery	Unknown	MAT1-2	245.0 (2)e–j
82	970	M39-1-3-8-1	Philippines	IRRI blast nursery	Unknown	MAT1-2	275.0 yz(2)a–f
83	973	B90002	Philippines	Caliraya, Laguna	Unknown	MAT1-2	295.0 v–z(2)ab
84	974	M101-1-1-2-9-1	Philippines	IRRI blast nursery	Unknown	MAT1-2	…
85	976	V850256	Philippines	Cavinti, Laguna	Unknown	MAT1-2	310.0 t–z
86	983	Ken53-33	Japan	unknown	Unknown	MAT1-2	302.5 u–z(2)a
87	952	Ca89	Philippines	Cavinti, Laguna	Unknown	MAT1-2	250.0 (2)c–i
88	960	V86046	Philippines	Roxas, Palawan	Unknown	MAT1-2	…

for all populations suggested clonality (Fig. 2), and was consistent with the population evenness and MLG. This indicates widespread linkage disequilibrium and suggests that *M. oryzae* populations from EA are limited to a small number of mostly closely related isolates. A similar pattern was observed with the West African reference collections. In the Asian collection, the number of private alleles was substantially larger, which indicates a greater proportion of diverse alleles compared with EA populations. The relatively short history of rice cultivation and the narrow genetic base of rice germplasm in EA compared with traditional rice-growing areas (e.g., South and Southeast Asia) may be thought of as a contributing factor. Indeed, intensive rice cultivation in EA occurred only recently, when Asian and West African developed varieties were introduced. These introduced cultivars could be causing minor shifts in *M. oryzae* populations already adapted, and may probably take some time for variations to cause a detectable differentiation. In contrast, populations of *M. oryzae* from South and Southeast Asia, where there is a high diversity of rice cultivars, are highly diverse, and clonality is not very obvious (Chen et al. 1995; Kumar et al. 1999; Park et al. 2003).

Exact tests of population differentiation also showed no evidence of differentiation between EA populations (data not shown), which

TABLE 2. Genetic diversity parameters for the East African and representative Asian and West African rice blast strains[z]

Population	N	Gene diversity	Shannon's index	%Pol	I_A	r_d	MLG	Number of private alleles
Tanzania	14.0	0.12	0.19	49.0	4.19	0.05	14.0	2.0
Uganda	31.0	0.12	0.21	68.7	3.76	0.03	31.0	8.0
Rwanda	20.0	0.13	0.21	60.1	7.21	0.06	20.0	5.0
West Africa	8.0	0.09	0.15	31.3	9.94	0.17	8.0	0.0
Asia	15.0	0.13	0.20	48.5	3.93	0.04	15.0	28.0
Mean	...	0.13	0.24	51.52	5.81	0.07	...	...

[z] Abbreviations: N = the number of isolates, %Pol = percentage polymorphism, I_A = index of association, r_d = standardized index of association, and MLG = multilocus genotypes.
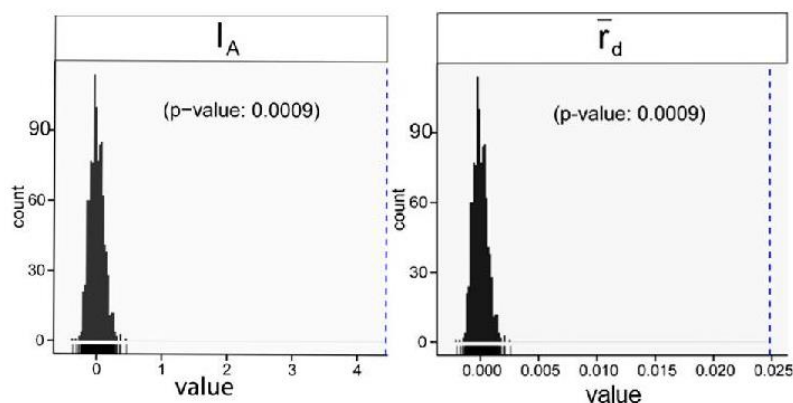
Fig. 2. Visualization of tests for linkage disequilibrium, where observed values (dashed lines) of I_A and r_d are compared with histograms showing results of 999 permutations using the *poppr* R package. All populations were clonal (observed value is significantly different from the expected panmixia).

TABLE 3. Genetic differentiation (G_{ST}), gene flow (Nm), genetic distance (GD), and genetic identity (I) among and between East African *Magnaporthe oryzae* populations and selected Asian and West African groups[z]

Population	G_{ST}					I				
	A	R	U	T	W	A	R	U	T	W
Asia ($n = 15$)	...	0.12	0.09	0.10	0.14	...	0.962	0.971	0.969	0.960
Rwanda ($n = 20$)	3.72	...	0.03	0.04	0.08	0.039	...	0.992	0.987	0.979
Uganda ($n = 31$)	4.79	16.78	...	0.04	0.09	0.030	0.009	...	0.990	0.977
Tanzania ($n = 14$)	4.31	10.84	13.10	...	0.07	0.032	0.013	0.010	...	0.982
West Africa ($n = 8$)	3.04	5.97	5.17	7.06	...	0.041	0.021	0.024	0.017	...
			Nm					GD		

[z] Abbreviations: A = Asia, R = Rwanda, U = Uganda, T = Tanzania, B = Benin, and N = Nigeria. G_{ST} and I are in the upper diagonals in the left and right panels of the table, respectively. Gene flow estimated as $G_{ST} = 0.5(1 - G_{ST})/ G_{ST}$ (Nm); GD is in the lower diagonal of left and right panels, respectively.

TABLE 4. Results of analysis of molecular variance for populations of *Magnaporthe oryzae* sampled from East Africa, West Africa, and Asia

Source of variation	df	Sum of squares	Variance components	Variation (%)
Among groups	2	85.04	1.57Va	10.97
Among populations within groups	4	57.41	0.13Vb	0.93
Within populations	81	1021.25	12.61Vc	88.09
Total	87	1163.71	14.31	...

is consistent with the G_{ST} values. In addition, pairwise comparisons using genetic identity and genetic distances showed low genetic diversity, further indicating that *M. oryzae* populations at the studied sites were relatively homogenous and stable over the study period. Similar population structures have been observed in Europe

(Piotti et al. 2005; Roumen et al. 1997), Iran (Javan-Nikkah et al. 2004), the United States (Correll et al. 2009; Levy et al. 1991; Xia et al. 1993), Argentina (Consolo et al. 2008), Colombia (Levy et al. 1993; Zeigler 1998), Cuba (Fuentes et al. 2003), and West Africa (Takan et al. 2012), in which only a few lineages were detected. Therefore, it appears that either selection pressures have played a weak role in altering allele frequencies or a scenario similar to the aforementioned areas could be shaping the EA populations. Another explanation could be that any selection pressures that exist to influence allele frequencies are not confined to a particular geographic area in EA. On the other hand, *M. oryzae* has been present in EA for over 90 years, and this provides less direct but intriguing evidence that the effect of a colonization bottleneck and subsequent clonal growth could have shaped the EA populations.

The use of hierarchical AMOVA (Table 4) further supports these findings, and corresponds with the strong indication of gene flow detected in this study. Gene flow involves the introduction or reintroduction of genes to a population, and our results indicate that gene flow in EA populations is comparable with that reported for geographically distant wheat blast populations in Brazil (Maciel et al. 2014) and other ascomycete fungi (e.g., *Mycosphaerella graminicola*) (Zhan et al. 2003). This evidence for extensive gene flow in *Magnaporthe oryzae* indicates the ongoing connection between the EA populations, though alternative explanations are also possible. There may be two possible scenarios: either the high gene flow results from the movement of planting materials between these countries or from movement of *M. oryzae* strains to EA via different other routes or at different times but from a common source, homogenizing the effect of gene flow. If germplasm movement is the cause of high gene flow, we speculate that Uganda could represent a focal point from which the pathogen was established first, considering the relatively high gene diversity and the striking admixture (Fig. 4B). However, due to the low sample size of isolates from the other countries studied, such analyses will have to be carefully considered, and continued genetic analysis of additional samples, as they become available, will help to verify this argument. Thus, the genetic clustering observed in our data may reflect either germplasm movement or historical patterns of gene flow that occurred decades ago, which could be both long-lived and able to propagate through asexual reproduction. In both cases, regional efforts to abate disease outbreaks through joint resistance breeding are plausible.

The PCoA, based on Nei's genetic distance, captured only 54.1% of the total variation in two principal components, suggesting limited robustness in the strain grouping. Only the spatial analysis of principal components revealed a slight geographical pattern among the subpopulations. The clustering pattern generated from STRUCTURE 2.3 also did not follow the geographical origin, except for isolates from Philippines, thus supporting the mixed pattern depicted in PCoA. The results obtained from STRUCTURE also show that isolates from Uganda are distributed in all clusters,

Fig. 3. A, Principal coordinate analysis of *Magnaporthe oryzae* isolates from East Africa and representative strains from Philippines and West Africa. The first and second principal coordinates account for 35.73 and 18.37% of the variation, respectively. Numbers 1, 2, 3, and 4 indicate cluster groupings. **B,** Principal coordinate analysis of *M. oryzae* subgroups from East Africa and representative strains from Philippines and West Africa. Isolates from the various collection sites are pooled into 15 subgroups. Subgroups Namulonge, Doho (Butaleja), Lira, and Tilda (Bugiri) represent Uganda; Nyazatara and Cyabayaga represent Rwanda; Dakawa, Kyela, and Kikusya represent Tanzania; Cavinti, IRRI, and Laguna represent Philippines; and Nigeria and Benin represent West Africa.
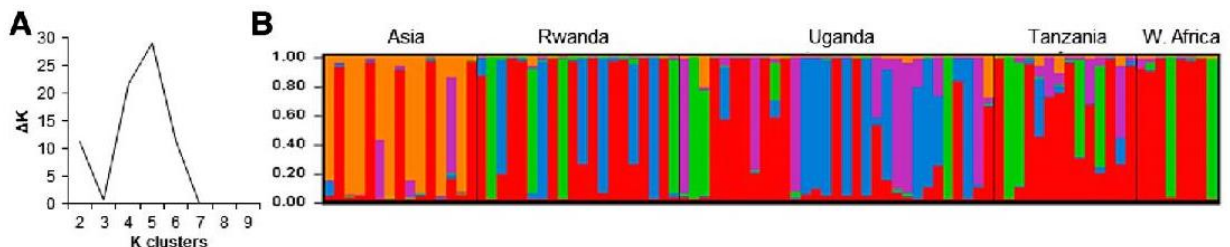
Fig. 4. Graphical representation of the results obtained from STRUCTURE. **A,** The most probable value of K, determined by ΔK for 88 strains (*x*-axis) sorted by membership coefficients (*y*-axis) within clusters (K = 5). **B,** STRUCTURE plot of the 88 isolates with K = 5 clusters. The plot is sorted according to the origin of isolates. Different colors represent genetic groups. Each column represents an individual partitioned into segments representing the estimated coefficients of membership proportions in the five ancestral genetic clusters (genetic groups) inferred with STRUCTURE. The height of the column segments shows the probability of assignment of individual isolates to the genetic groups based on 100,000 runs.

and is consistent with the historical reports of the first detection of the pathogen in Africa (Small 1922), although it would have been present in earlier times than 1921.

Interestingly, both MAT1-1 and MAT1-2 were detected, although with location-specific differences and skewed ratio toward MAT1-1 in all EA populations. Such a skewed pattern of MAT distribution has been also observed in West Africa (Takan et al. 2012). It is common for one MAT to be dominant in field populations, with most of the isolates being male fertile or completely sterile (Tredway et al. 2005). Moreover, recombinants are rarely reported in such scenarios. Whether the EA strains are able to reproduce sexually remains to be determined. However, the skewed distribution of the two MAT and the significant and positive I_A values suggest clonal or mixed reproduction within populations but not sexual reproduction. Thus, we hypothesize that the introduction of isolates with two MAT could have occurred in EA. However, the exact localization of the source population and the time of introduction of both MAT remain to be determined. The difference in MAT distribution between Philippine and most EA isolates suggests that EA isolates could have originated from a source other than the Philippines, which may require a substantially large sample size to verify, including isolates from regions other than the Philippines. Several lines of research that pertain to this issue are in progress that will further our understanding of *M. oryzae* origin and distribution in EA.

In our pathogenicity study, isolates showed differences in severity and disease progress. By comparison of virulence on Co39, Tanzania and Rwanda had a higher percentage of virulent isolates than Uganda. However, the high pathogenic variability was not consistent with the population structure, suggesting that *M. oryzae* populations in EA are dominated by genetically less diverse strains but diverse pathotypes, which is similar to the populations previously reported in Japan (Don et al. 1999) and South Korea (Park et al. 2003). This scenario suggests that pathogenicity is labile to be predicted by linkage with neutral markers in these population samples.

Overall, our results showed low genetic differentiation, skewed distribution of the two MAT, and a possible role of gene flow in *M. oryzae* populations from EA. Either *M. oryzae* could be distributed as a single genetic population in EA or that gene flow is exerting a significant influence, effectively swamping the action of selection. In this way, the alleles present in Tanzania, Uganda, and Rwanda are primarily subsets, with the exception of a few new alleles which could have been created by mutations. These rare alleles could be the reason for the variable pathogenicity observed in EA populations. Although AFLP screens a large number of polymorphic loci, diversity estimates reported in the present study will have to be carefully considered and may need to be confirmed with other marker systems, which could broaden the molecular understanding of the EA pathogen population. Future research should also focus on identifying the source population and study further the evolutionary potential of EA isolates with additional sampling and long-term monitoring. The use of a standard set of differential rice lines with single resistance genes for race differentiation would provide further evidence for pathogenic diversity. The effect of high temperature associated with climate change on recent rice blast outbreaks observed in EA will have to be carefully considered because little is known about the biology of this pathogen in EA.

ACKNOWLEDGMENTS

LITERATURE CITED

Borromeo, E. S., Nelson, R. J., Bonman, J. M., and Leung, H. 1993. Genetic differentiation among isolates of *Pyricularia* infecting rice and weed hosts. Phytopathology 83:393-399.

Brandfass, C., and Karlovsky, P. 2008. Upscaled CTAB-based DNA extraction and real-time PCR assays for *Fusarium culmorum* and *F. graminearum* DNA in plant material with reduced sampling error. Int. J. Mol. Sci. 9: 2306-2321.

Brondani, C., Brondani, R. P. V., Garrido, L., Da, R., and Ferreira, M. E. 2000. Development of microsatellite markers for genetic analysis of *Magnaporthe grisea*. Genet. Mol. Biol. 23:753-762.

Campbell, C. L., and Madden, L. V. 1990. Introduction to Plant Disease Epidemiology. John Wiley & Sons, New York.

Chen, D., Zeigler, R. S., Leung, H., and Nelson, R. J. 1995. Population structure of *Pyricularia grisea* at two screening sites in the Philippines. Phytopathology 85:1011-1020.

Consolo, V. F., Cordo, C. A., and Salerno, G. L. 2008. DNA fingerprint and pathotype diversity of *Pyricularia oryzae* populations from Argentina. Austral. Plant Pathol. 37:357-364.

Consolo, V. F., Cordo, C. A., and Salerno, G. L. 2005. Mating-type distribution and fertility status in *Magnaporthe grisea* populations from Argentina. Mycopathologia 160:285-290.

Correll, J. C., Boza, E. J., Seyran, E., Cartwright, R. D., Jia, Y., and Lee, F. N. 2009. Examination of the rice blast pathogen population diversity in Arkansas, USA—Stable or unstable? Pages 217-228 in: Advances in Genetics, Genomics and Control of Rice Blast Disease. G.-L. Wang and B. Valent, eds. Springer, New York.

Couch, B. C., Fudal, I., Lebrun, M. H., Tharreau, D., Valent, B., van Kim, P., Nottéghem, J. L., and Kohn, L. 2005. Origins of host-specific populations of the blast pathogen *Magnaporthe oryzae* in crop domestication with subsequent expansion of pandemic clones on rice and weeds of rice. Genetics 170:613–630.

Don, L. D., Urashima, A. S., Tosa, Y., Nakayashiki, H., and Mayama, S. 1999. Population structure of the rice blast fungus in Japan examined by DNA fingerprinting. Ann. Phytopathological Soc. Jpn. 65: 15-24.

Evanno, G., Regnaut, S., and Goudet, J. 2005. Detecting the number of clusters of individuals using the software structure: A simulation study. Mol. Ecol. 14:2611-2620.

Excoffier, L., Laval, G., and Schneider, S. 2005. Arlequin 3.01: An integrated software package for population genetics data analysis. Evol. Bioinf. Online 1:47-50.

FAOSTAT. 2011. Rough rice area (000 ha), by country and geographical region, 1961-2011. Food and Agricultural Organization of the United Nations—Production Statistics. http://faostat.fao.org/site/567/desktopdefault. aspx#ancor

Fuentes, J. L., Correa-Victoria, F. J., Escobar, F., Mora, L., Duque, M. C., Deus, J. E., and Cornide, M. T. 2003. Genetic diversity analysis of the rice blast pathogen population at two locations in Cuba. Biotecnol. Apl. 20: 14-19.

Gerber, S., Mariette, S., Streiff, R., Bodénès, C., and Kremer, A. 2000. Comparison of microsatellites and amplified fragment length polymorphism markers for parentage analysis. Mol. Ecol. 9:1037-1048.

Grünwald, N. J., Goodwin, S. B., Milgroom, M. G., and Fry, W. E. 2003. Analysis of genotypic diversity data for populations of microorganisms. Phytopathology 93:738-746.

Javan-Nikkah, M., McDonald, B. A., Banke, S., and Hedjaroude, G.-A. 2004. Genetic structure of Iranian *Pyricularia grisea* populations based on rep-PCR fingerprinting. Eur. J. Plant Pathol. 110:909-919.

Jost, L. 2008. GST and its relatives do not measure differentiation. Mol. Ecol. 17:4015-4026.

Kachroo, P., Leong, S. A., and Chattoo, B. B. 1994. Pot2, an inverted repeat transposon from the rice blast fungus *Magnaporthe grisea*. Mol. Gen. Genet. 245:339-348.

Kihoro, J., Njoroge, J. B., Murage, H., Ateka, E., and Makihara, D. 2013. Investigating the impact of rice blast disease on the livelihood of the local farmers in greater Mwea region of Kenya. SpringerPlus 2:308.

Kumar, J., Nelson, R. J., and Zeigler, R. S. 1999. Population structure and dynamics of *Magnaporthe grisea* in the Indian Himalayas. Genetics 152:971-984.

Levy, M., Correa-Victoria, F. J., Zeigler, R. S., Hu, S., and Hamer, J. E. 1993. Genetic diversity of the rice blast fungus in a disease nursery in Colombia. Phytopathology 83:1427-1433.

Levy, M., Romao, J., Marchetti, M. A., and Hamer, J. E. 1991. DNA fingerprinting with dispersed repeated sequence resolves pathotype diversity in the rice blast fungus. Plant Cell 3:95-102.

Liu, J., Wang, X., Mitchell, T., Hu, Y., Liu, X., Dai, L., and Wang, G. L. 2010. Recent progress and understanding of the molecular mechanisms of the rice-*Magnaporthe oryzae* interaction. Mol. Plant Pathol. 11:419-427.

Liu, Z. J., and Cordes, J. F. 2004. DNA marker technologies and their applications in aquaculture genetics. Aquaculture 238:1-37.

Maciel, J. L., Ceresini, P. C., Castroagudin, V. L., Zala, M., Kema, G. H., and McDonald, B. A. 2014. Population structure and pathotype diversity of the wheat blast pathogen *Magnaporthe oryzae* 25 years after its emergence in Brazil. Phytopathology 104:95-107.

Miller, M. P. 1997. Tools for Population Genetic Analyses (TFPGA) v. 1.3: A Windows Program for the Analysis of Allozyme and Molecular Population Genetic Data. Department of Biological Sciences, Northern Arizona University. http://www.ccg.unam.mx/~vinuesa/tlem09/docs/TFPGADOC.PDF

Mwalyego, F. S., Kayeke, J. M., and Mghogho, R. M. 2011. ASARECA project: Livelihood improvement through integrated management practices for rainfed lowland rice. A guide for farmers. http://www.erails.net/images/tanzania/ari-uyle/ari-uyole/file/Rice%20diseases%202011.pdf

Nei, M. 1978. Estimation of average heterozygosity and genetic distance from a small number of individuals. Genetics 89:583-590.

Okori, P., Rubaihayo, P. R., Adipala, E., Fahleson, J., and Dixelius, C. 2004. Population studies of fungal pathogens: Perspectives for control with specific reference to grey leaf spot. Afr. Crop Sci. J. 12:327-342.

Park, S.-Y., Milgroom, M. G., Han, S. S., Kang, S., and Lee, Y.-H. 2003. Diversity of pathotypes and DNA fingerprint haplotypes in populations of *Magnaporthe grisea* in Korea over two decades. Phytopathology 93:1378-1385.

Peakall, R., and Smouse, P. E. 2006. GENEALEX 6: Genetic analysis in excel. Population genetic software for teaching and research. Mol. Ecol. Notes 6:288-295.

Piotti, E., Rigano, M. M., Rodino, D., Rodolfi, M., Castiglione, S., Picco, A. M., and Sala, F. 2005. Genetic structure of *Pyricularia grisea* (Cooke) Sacc. isolates from Italian paddy fields. J. Phytopathol. 153:80-86.

Pritchard, J. K., Stephens, M., and Donnelly, P. 2000. Inference of population structure using multilocus genotype data. Genetics 155:945-959.

Roumen, E., Levy, M., and Notteghem, J. L. 1997. Characterization of the European pathogen population of *Magnaporthe grisea* by DNA fingerprinting and pathotype analysis. Eur. J. Plant Pathol. 103:363-371.

Saleh, D., Milazzo, J., Adreit, H., Fournier, E., and Tharreau, D. 2014. South-East Asia is the center of origin, diversity and dispersion of the rice blast fungus, *Magnaporthe oryzae*. New Phytol. 201:1440-1456.

Sere, Y., Onasanya, A., Afolabi, A., Mignouna, H. D., and Akator, K. 2007. Genetic diversity of the blast fungus, *Magnaporthe grisea* (Hebert) Barr. in Burkina Faso. Afr. J. Biotechnol. 6:2568-2577.

Silva G. B., Prabhu, A. S., Filippi, M. C. C., Trindade M. G., Araújo, L. G., and Zambolim, L. 2009. Genetic and phenotypic diversity of *Magnaporthe oryzae* from leaves and panicles of rice in commercial fields in the State of Goiás, Brazil. Trop. Plant Pathol. 34:71-76.

Small, W. 1922. Annual report of the government mycologist for 1921. An investigation into fungi found on rice in Uganda. Uganda Prot. Dep. Agric. Annu. Rep. Pages 49-57. Rev. Appl. Mycol. 2:156-157.

Stoddart, J. A., and Taylor, J. F. 1988. Genotypic diversity: Estimation and prediction in samples. Genetics 118:705-711.

Takan, J. P., Chipili, J., Muthumeenakshi, S., Talbot, N. J., Manyasa, E. O., Bandyopadhyay, R., Sere, Y., Nutsugah, S. K., Talhinhas, P., Hossain, M., Brown, A. E., and Sreenivasaprasad, S. 2012. *Magnaporthe oryzae* populations adapted to finger millet and rice exhibit distinctive patterns of genetic diversity, sexuality and host interaction. Mol. Biotechnol. 50:145-158.

Thuan, T. N. T., Bigirimana, J., Roumen, E., Van Der Straeten, D., and Höfte, M. 2006. Molecular and pathotype analysis of the rice blast fungus in North Vietnam. Eur. J. Plant Pathol. 114:381-396.

Tredway, L. P., Stevenson, K. L., and Burpee, L. L. 2005. Genetic structure of Magnaporthe grisea population associated with St. Augustine grass and tall fescue in Georgia. Phytopathology 95:463-471.

Vos, P., Hogers, R., Bleeker, M., Reijans, M., Vanderlee, T., Hornes, M., Frijters, A., Pot, J., Peleman, J., Kuiper, M., and Zabeau, M. 1995. AFLP: New technique for DNA-fingerprinting. Nucleic Acids Res. 23:4407-4414.

Weiberg, A., and Karlovsky, P. 2009. Components of variance in transcriptomics based on electrophoretic separation of cDNA fragments (cDNA-AFLP). Electrophoresis 30:2549-2557.

Xia, J. Q., Correll, J., Lee, F. N., and Ross, W. J. 2000. Regional population diversity of *Pyricularia grisea* in Arkansas and the influence of host selection. Plant Dis. 84:877–884.

Xia, J. Q., Correll, J. C., Lee, F. N., Marchetti, M. A., and Rhoads, D. D. 1993. DNA fingerprinting to examine microgeographic variation in the *Magnaporthe grisea* population in two rice fields in Arkansas. Phytopathology 83:1029-1035.

Yeh, F. C., and Boyle, T. 1999. POPGENE version 1.3.2: Microsoft window-based freeware for population genetic analysis. Online publication. https://www.ualberta.ca/~fyeh/popgene.html

Zeigler, R. 1998. Recombination in *Magnaporthe grisea*. Annu. Rev. Phytopathol. 36:249-275.

Zhan, J., Pettway, R. E., and McDonald, B. A. 2003. The global genetic structure of the wheat pathogen *Mycosphaerella graminicola* is characterized by high nuclear diversity, low mitochondrial diversity, regular recombination and gene flow. Fungal Genet. Biol. 38:286-297.

Chapter 5: General discussion

Little is known about the mechanisms underlying rice response to *M. oryzae* under high temperature. Phenotypic and transcriptome analysis enabled us to determine whether prolonged exposure to 35^oC prior to infection has consequences on the ability of rice to resist infection. Because high temperature is known to affect the physiological functioning of plants (Hasanuzzaman et al., 2013), probably including defense responses to other stresses, it was expected that plants would universally succumb to pathogen infection after high temperature exposure due to prior metabolic expenditure. However, our data revealed that high temperature, despite reduced expression of the R gene (*Pi54*) at 35^oC compared to 28^oC, induced resistance in the rice genotypes LT and CO. This observation indicated that other genetic factors could be interacting with *Pi54* to mediate resistance. These may include resistance gene analogues (RGAs) which co-localize with *Pi54* on chromosome 11, including RPM1. Hence, the weak expression of *Pi54* at high temperature may nonetheless contribute to resistance when combined with high temperature activated RGAs. The likelihood of R gene interaction to activate several resistance pathways is, therefore, not farfetched, though at present, there is no clear experimental evidence demonstrating how two or more NB-LRR proteins augment each other, except for RPS2 and RPM1 mediated hypersensitive response (Jorgensen and Emerson, 2008). Besides this, we detected high accumulation of H_2O_2 and increased expression of ABA responsive genes in plants exposed to 35^oC. Previous reports have shown that H_2O_2 accumulates in forming papillae and can be used by peroxidases to promote cross-linking of proteins and phenolics to reinforce cell wall appositions (Thordal-Christensen et al., 1997; Brown et al., 1998; Voigt, 2014). The early induction of H_2O_2 and anti-oxidative mechanisms that protect the plant against high temperature, including POX, most likely remains active to limit both pathogen invasion and further oxidative stress, while diverting the prevailing H_2O_2 for cell wall appositions. The induction of callose by *M. oryzae* infection is apparently co-regulated by high temperature ROS induced ABA production, which is consistent with the induction of OsBBD1 in our study.

In our gene expression analysis, we also detected high expression levels of several genes representing diverse biological pathways. The most compelling was the high expression levels of OsBISAMT1, which converts SA to MeSA, across all genetic backgrounds during infection. Moreover, enhanced expression was detected in plants exposed to 35^oC compared to 28^oC. It is unknown whether conversion of SA to MeSA is a strategy to reduce or enhance H_2O_2 production, given that positive regulation of H_2O_2 by SA has been reported (Rao et al.,

1997). On the other hand, increased production of H_2O_2 has been shown to stimulate SA production (Chamnongpol et al., 1998). The regulatory networking between the two molecules is apparently rate limiting. However, if the conversion of SA to MeSA affects H_2O_2 accumulation, probably negating plant resistance, while protecting the plant from heat stress, then other mechanisms must be in place to mitigate the subsequent pathogen infection. Previous reports have shown that SAR establishment may require signals, which precede systemic accumulation of SA, such as jasmonates (Truman et al., 2007) and indole-derived metabolites (Truman et al., 2010). Furthermore, Liu et al., (2011) suggested that MeSA and a complex formed between the lipid transfer protein DIR1, glycerol lipid and lipid derivatives mediate SAR. We speculate that MeJA could be linked to SAR, reminiscent of a strong induction of jasmonate-O-methyltransferase in LT. Downstream of ROS, MeSA and MeJA there apparently exists a complex signaling network with probable complementary and inhibitory roles. How the plant processes these signals is apparently reliant on the effect of the genetic background during pathogen infection. For instance, despite carrying the same R gene (*Pi54*), LT and CO showed contrasting reaction to *M. oryzae* at 28°C, with CO displaying a more severe disease phenotype compared to LT. In addition, LT showed more intense cell wall florescence than CO. These observations were also reflected at the gene expression level, where some resistance genes, including a jacalin-like lectin (LOC_Os12g14440) that mediates broad spectrum resistance, naringenin 7-*O*-methyltransferase for sakuranetin biosynthesis and RGAs were background specific. This suggests that the genetic background plays a role in plant defense induction, and that some cultivars may have a more effective resistance against *M. oryzae* than others despite varying temperatures.

This was further intriguing in the second experiment where we examined the possible direct effects of temperature on *M. oryzae* infection in Nipponbare. As reflected by the severe disease phenotype, infection success was higher at 35°C compared to 28°C. This indicates that the resistance of Nipponbare against *M. oryzae* is negatively affected by high temperature. High temperatures can alter cell properties, including the phospholipid membrane surrounding the cytosol and internal organelles. The effect may translate into increased permeability affecting the ability of other molecules such as signaling proteins to interact with phospholipid membranes. Such changes, if they occur in the host, alter what we termed as conserved pathogen recognition patterns (CPRPs). These membrane changes and the subsequent defense responses are apparently subject to genotype specific traits which may subsequently determine infection success of the pathogen.

[134]

Predicting the impact of temperature is, however, challenging as it may also affect *M. oryzae* pathogenicity. For instance, the observed effect of high temperature on rapid disease progression and elevated expression of putative pathogenicity genes may be related to altered pathogen virulence, hyphal structural adjustments and survival strategies in a stress host environment. Our data revealed more than 100 transcripts encoding for hydrolytic enzymes including glycosyl hydrolases (pectinase, amylases, cellulases, xylanases, chitinases, glucanases), peptidases, lipases and phospholipases, all of which have been found to be involved in pathogenicity of many fungal pathogens (King et al., 2011). Thus, an increase in pathogenicity related factors likely enables *M. oryzae* to quickly adapt and overcome host defense, depending on the host genetic factors. Several genes, including *Avr* genes appear to be indispensable for *M. oryzae* infection regardless of the temperature difference, given their high expression levels in both Nip35i and Nip28i. However, the relatively higher expression in Nip35i compared to Nip28i suggests that the expression of a cognate R gene, even at reduced levels, is likely to detect the pathogen effectors and subsequently evoke ETI. This is consistent with the lower expression of *Pi54* in CO and LT at 35°C, and alternatively, a higher induction of *AvrPik/km/kp* in Nip35i. This indicates that the expression level of an *avr* gene can determine the plant capacity to detect the pathogen. Thus, R gene-mediated resistance at high temperature may depend on the *avr* gene dosage effect.

As we have not yet demonstrated the function of the genes revealed in this study, we can only speculate that the plant and pathogen specific genes induced in the rice-*M. oryzae* interaction are apparently highly interactive in conferring resistance and virulence at high temperature. Overall, our results suggest that the effects of high temperature on host resistance and pathogen infection success may be overridden by the genetic background of the host. Functional analysis of background modifier genes, including constitutively expressed NBS-LRRs, and OMTs could provide further insight into the mechanism of resistance relevant for improving rice health in a changing climate.

We also analyzed the population structure of *M. oryzae* in East Africa using amplified fragment length polymorphism (AFLP) markers, to provide a basis for future studies into the relationship between climate change and the forces that shape the population structure. Our results indicate low genetic differentiation in East African populations. Besides, pair-wise comparisons using G_{ST}, genetic identity and genetic distances also showed low genetic diversity, suggesting that *M. oryzae* populations at the studied sites were relatively homogenous and stable over the study period. It appears therefore that selection pressures

have played a weak role in altering allele frequencies on the East African populations. It is also tempting to suggest that any selection pressures that exist to influence allele frequencies are not confined to a particular geographic area. On the other hand, a strong indication of gene flow was detected among East African populations. Gene flow involves the introduction or reintroduction of genes to a population. By moving genes around, there is a potential for the spread of virulent pathotypes with highly advantageous alleles, which might contribute to drastic crop losses. Regional efforts to limit informal movement of planting materials may be necessary to prevent epidemics associated with exotic strains. The presence of two mating types in some sites further suggests that there is a possibility of the fungus to adapt to heterogenous hosts or environments quickly, and could lead to the development of novel virulences. This could be the reason for variable pathogenicities within populations analyzed in this study.

Overall, our transcriptome analysis provides a broad overview of genes and biological processes involved in rice response to high temperature and *M. oryzae*, and contain representatives of all of the major classes of defense genes. We show that different rice genetic backgrounds modify the defense response in rice. The defense response is compounded by the interaction between temperature and the genetic background, and apparently regulates the nature, timing and magnitude of ROS, hormone signaling pathways and the subsequent defense responses to *M. oryzae*. Thus, high temperature effect on cultivar response to *M. oryzae* may not be consistently similar across genotypes. Furthermore, the activation of defense response genes and infection success of the pathogen will be more dependent on the genotypes used as cultivars, and the degree of their adaptation to both high temperature and pathogen infection without tradeoffs.

On the other hand, *M. oryzae* populations from East Africa are apparently exposed to lowly variable climatic conditions, hosts and cropping systems, as indicated by relatively homogenous populations. This suggests that high temperature associated with climate change may not typically be a cause of the recent sporadic rice blast out breaks observed in East Africa, but could be related to resistance breakdown associated with old traditional cultivars; and probably genetic changes in the pathogen that could not be detected by AFLP analysis.

References

Brown, I., Trethowan, J., Kerry, M., Mansfield, J., and Bolwell, G. P. (1998) Localization of components of the oxidative cross-linking of glycoproteins and of callose synthesis in papillae formed during the interaction between non-pathogenic strains of Xanthomonas campestris and French bean mesophyll cells. Plant J. 15, 333–343.

Dat, J.F., Lopez-Delgado, H., Foyer, C.H., Scott, I.M. (1998) Parallel change in H_2O_2 and catalase during thermotolerance induced by salicylic acid or heat acclimation in mustard seedlings. Plant Physiol. 116, 1351–1357.

Hasanuzzaman, M., Nahar, K., Alam, M.d.M., Roychowdhury, Rajib., and Fujita, M. (2013) Physiological, biochemical, and molecular mechanisms of heat stress tolerance in plants. Int J Mol Sci. 14, 9643–9684.

Jorgensen, T.H., Emerson, B.C. (2008) Functional variation in a disease resistance gene in populations of Arabidopsis thaliana. Molecular Ecology 17, 4912-4923.

King, B.C., Waxman, K.D., Nenni, N.V., Walker, L.P., Bergstrom, G.C., Gibson, D.M. (2011) Arsenal of plant cell wall degrading enzymes reflects host preference among plant pathogenic fungi. Biotechnol. Biofuels 4, 4.

Liu, P.P., von Dahl, C.C., Park, S.W., Klessig, D.F. (2011) Interconnection between methyl salicylate and lipid-based long-distance signaling during the development of systemic acquired resistance in Arabidopsis and tobacco. Plant Physiol. 155, 1762–1768.

Rao, M.V., Paliyath, G., Ormrod, D., Murr, D.P., Watkins, C.B. (1997) Influence of salicylic acid on H2O2 production, oxidative stress and H2O2 metabolizing enzymes: salicylic acid-mediated oxidative damage requires H2O2. Plant Physiol 115, 137–149.

Thordal-Christensen, H., Zhang, Z., Wei, Y., and Collinge, D. B. (1997) Subcellular localization of H2O2 in plants. H2O2 accumulation in papillae and hypersensitive response during the barley–powdery mildew interaction. Plant J. 11, 1187–1194.

Truman, W., Bennett, M.H., Kubigsteltig,. I, Turnbull, C., Grant, M. (2007) Arabidopsis systemic immunity uses conserved defence signaling pathways and is mediated by jasmonates. Proc Natl Acad Sci USA, 104, 1075–1080.

Truman, W.M., Bennett, M.H., Turnbull, C.G.N., Grant, M.R. (2010) Arabidopsis auxin mutants are compromised in systemic acquired resistance and exhibit aberrant accumulation of various indolic compounds. Plant Physiol 152, 1562–1573.

Summary

It is currently hypothesized that climate change may lead to global warming, and temperatures might increase by 2-5°C at the end of the twenty-first century. However, the consequences of the expected temperature elevation on pathogen biology, epidemiology and plant host resistance have continued to provide conflicting results due to several interacting factors. The rice-*M. oryzae* pathosystem is well-studied at both the phenotypic and genomic level, and the scientific advancement in both organisms makes it suitable for understanding the mechanisms underlying plant pathogen interaction at high temperature. In the first part of this study, we analyzed the host phenotypic reactions and RNA-seq genome-wide transcript profiles of two genetic rice backgrounds, CO (*O. sativa indica*; Co39) and LT (*O. sativa japonica*; LTH), carrying the same R gene (*Pi54*), and exposed to *M. oryzae* infection, after exposure to 28°C and 35°C. Both backgrounds were more resistant at 35°C compared to 28°C. Moreover, callose deposits and cell wall fluorescence of the attacked epidermal cells were more intense at 35°C than at 28°C. However, CO had a more severe disease phenotype compared to LT at 28°C. The differential reaction of *Pi54* in the two backgrounds suggests that genetic factors other than *Pi54* determine the resistance response, and further indicates that the genetic background of *japonica* rice facilitates the function of *Pi54* more than the background of *indica* rice. Gene expression analysis further revealed substantial background transcriptional profile variation, and demonstrated that LT and CO exhibit differences in genes expressed in response to high temperature and *M. oryzae*. Hydrogen peroxide (H_2O_2) production and abscisic acid (ABA) responsive genes were more pronounced in LT compared to CO, whereas SA levels were higher in CO than LT. Both genotypes showed a high induction of OsBISAMT1, which converts SA to MeSA. Conversely, only LT showed a significant induction of jasmonate O-methyltransferase and JA induced jacalin-like lectin (LOC_Os12g14440) that mediates broad spectrum resistance. Thus, the nature, timing and magnitude of ROS and hormone signaling pathways in response to both high temperature and *M. oryzae* infection may be largely controlled by the genetic backgrounds.

In the second study, we analyzed the effect of temperature on the transcriptomes of the rice cultivar Nipponbare and its pathogen *M. oryzae* simultaneously at 35°C and 28°C using RNA-seq. Our results showed that exposure of *M. oryzae* to 35°C increased the number and expression levels of putative effectors compared to infection at 28°C. Genes involved in secondary metabolism, transport, lipid metabolism and carbohydrate metabolism also showed

increased transcription during infection at 35°C compared to 28°C. These transcription changes likely facilitated host colonization and adaptation. Indeed, we observed a more severe disease phenotype in Niponbare during *M. oryzae* infection at 35°C compared to 28°C. Moreover, *in planta* fungal biomass was significantly higher in Nip35i than Nip28i, suggesting rapid colonization of the host tissues at 35°C. The effect of high temperature on plant cell wall loosening probably facilitated rapid colonization and delivery of several proteins able to promptly manipulate the plant defense, as well as to degrade the cell wall. Several genes, including *Avr* genes appear to be indispensable for *M. oryzae* infection at high temperature, given their high expression levels at 35°C compared to 28°C. This suggests that the expression of a cognate R gene, even at reduced levels, is likely to detect the pathogen effectors and subsequently evoke ETI. This is consistent with the lower expression of *Pi54* in CO and LT at 35°C, and alternatively, a higher induction of *AvrPik/km/kp* in Nip35i. The expression level of an *avr* gene therefore determines the plant capacity to detect the pathogen under abiotic stresses that tend to reduce transcript levels of the R gene. Thus, R gene-mediated resistance at high temperature may depend on the *avr* gene dosage effect. Because the *Pik/km/kp* allele, which corresponds with a *AvrPik/km/kp* like gene in *M. oryzae* are redundant or missing in Nipponbare, it is likely that the high temperature effect on plant cell wall and membrane permeability provided a direct pass for the pathogen effectors.

Taken together, the inability of the plant to defend itself when exposed to both abiotic and biotic stresses is correlated with the absence or the degree at which abiotic stress alters both specific and general defense responses. On the other hand, temperature effect on both R gene mediated resistance and partial resistance is likely more variable than earlier envisaged, and will require intensive screening efforts to identify stable resistant gene combinations. Thus, it may be too soon to generalize the effect of the changing temperature on host resistance beyond the current study because of the significant differences in defense responses among host genotypes studied so far. The likely scenario is that some cultivars may have a more stable resistance against *M. oryzae* than others despite increasing temperatures, and research efforts to identify such stable genotypes will need to be raised.

In the third part of this study, we analyzed the genetic diversity and population structure of 88 isolates of *M. oryzae* from East Africa and representative isolates from West Africa and the Philippines using amplified fragment length polymorphism (AFLP) markers. Our results indicate low genetic differentiation in East African populations, suggesting that the

populations are relatively homogeneous. It appears that selection pressures have played a weak role in altering allele frequencies on the East African populations. It is also tempting to suggest that any selection pressures that exist to influence allele frequencies are not confined to a particular geographic area, and most likely the pathogen is exposed to lowly variable climatic conditions, hosts and cropping systems. On the other hand, a strong indication of gene flow was detected among East African populations. Although, this tends to reduce genetic differentiation among populations, if local selection and genetic drift within populations is sufficiently high it may permit emergence and spread of highly advantageous alleles. Thus, regional efforts to limit informal movement of planting materials may be necessary to prevent epidemics associated with exotic strains. The presence of two mating types in some locations indicates past signatures of evolution which may need further examination to understand. Being the first study on *M. oryzae* on rice in East Africa, the effect of the predicted climate change will need to be investigated further in subsequent studies.

Appendices

Appendix 1

Table S1: *M. oryzae* pathogenicity genes expressed in planta at 48 hours post inoculation

Gene ID	Gene name	Phenotype	Description	Nip35i Log2FC	Nip28i Log2FC
MGG_12337	MAS3	Reduced virulence	MAS3 protein	15.03	12.27
MGG_04301	PWL2	Effector (plant avirulence determinant)	conserved hypothetical protein	9.66	9.00
MGG_13863	PWL1	Effector (plant avirulence determinant)	conserved hypothetical protein	9.58	9.34
MGG_04202	GAS2/MAS3	Reduced virulence	MAS3 protein	9.50	10.63
MGG_10510	MGG_10510	Reduced virulence	ribonuclease T2	10.47	8.99
MGG_08735	MoRgs5	Unaffected pathogenicity	conserved hypothetical protein	8.47	5.77
MGG_15370	AVR-Pita	Effector (plant avirulence determinant)	Metalloproteinase	8.07	7.83
MGG_12865	MoHox7	Loss of pathogenicity	conserved hypothetical protein	6.91	6.09
MGG_13926	MoRgs8	Unaffected pathogenicity	conserved hypothetical protein	6.81	8.18
MGG_04895	ICL1	Reduced virulence	isocitrate lyase	6.58	5.75
MGG_10730	Calcium-transporting ATPase 3	Reduced virulence	calcium-transporting ATPase 3	5.96	5.26
MGG_05731	Peptidyl prolyl isomerase	Reduced virulence	peptidyl-prolyl cis-trans isomerase cyp15	4.71	4.72
MGG_09705	NMR3	Reduced virulence	nucleoside-diphosphate-sugar epimerase family protein	4.60	6.23
MGG_05531	MAC1	Reduced virulence	hypothetical protein	4.36	3.26
MGG_06148	MFP1	Reduced virulence	peroxisomal hydratase-dehydrogenase-epimerase	4.05	3.13
MGG_04685	MGG_04685	Reduced virulence	conserved hypothetical protein	3.45	2.82
MGG_01721	CrAT1	Loss of pathogenicity	carnitine O-acetyltransferase	3.35	3.02
MGG_04116	MGG_04116	Reduced virulence	SH3 domain-containing protein	3.30	2.74
MGG_06939	ABC1 protein		ABC1 protein	3.25	2.55
MGG_04628	MoCYP51A	Reduced virulence	cytochrome P450 51	3.22	2.52
MGG_00527	EMP1	Reduced virulence	hypothetical protein	3.21	2.81
MGG_01099	PTH2	Loss of pathogenicity	peptidyl-tRNA hydrolase 2	3.17	3.11
MGG_05464	endo-1,4-beta-xylanase [GH10 family]	Reduced virulence	endo-1,4-beta-xylanase	3.16	5.94
MGG_02376	HDL1	Unaffected pathogenicity	hormone-sensitive lipase	3.07	-3.92
MGG_12128	Mid1	Mixed outcome	calcium influx-promoting protein ehs1	2.98	2.05
MGG_08624	ERG2	chemistry target - phenotype unknown	C-8 sterol isomerase	2.96	-2.61
MGG_08628	MGG_08628	Reduced virulence	3'-5' exoribonuclease CSL4	2.94	2.24
MGG_09299	PAS1	Unaffected pathogenicity	peroxisome biosynthesis protein (PAS1/Peroxin-1)	2.78	2.56
MGG_02731	MGG_02731	Loss of pathogenicity	cell division control protein 42	2.77	-3.06
MGG_07667	Moatg17	Loss of pathogenicity	autophagy-related protein 17	2.75	2.46

MGG_13762	ABC3	Loss of pathogenicity	multidrug resistance protein 3	2.70	3.44
MGG_01835	PIC1	Unaffected pathogenicity	inner centromere protein	2.57	3.39
MGG_07456	MCNA	Reduced virulence	serine/threonine-protein phosphatase 2B catalytic subunit	2.53	2.35
MGG_06439	MoTea4	Loss of pathogenicity	conserved hypothetical protein	2.49	2.06
MGG_00435	MGG_00435	Loss of pathogenicity	integral membrane protein	2.48	2.79
MGG_04100		Loss of pathogenicity	cell division control protein 7	2.45	2.29
MGG_09559	MgAtg9	Loss of pathogenicity	autophagy-related protein 9	2.39	-3.56
MGG_03451	MGG_03451	Reduced virulence	conserved hypothetical protein	2.36	-3.51
MGG_09263	MGG_09263	Reduced virulence	C6 zinc finger domain-containing protein	2.25	2.55
MGG_00365	MAGA	Unaffected pathogenicity	guanine nucleotide-binding protein subunit alpha	2.20	-2.88
MGG_06368	CPKA	Loss of pathogenicity	cAMP-dependent protein kinase	2.17	2.84
MGG_02773	MoMCM1 (MADs box	Mixed outcome	MADS box protein	2.14	2.18
MGG_00803	MoSNF1	Reduced virulence	carbon catabolite-derepressing protein kinase	2.02	3.31
MGG_13137	ABC1 family protein		ABC1 family protein	-2.00	-2.24
MGG_02696	HEX1 (Woronin body major protein)	Reduced virulence	woronin body major protein	-2.02	-2.00
MGG_05332	MoPLC2	Loss of pathogenicity	1-phosphatidylinositol-4,5-bisphosphate phosphodiesterase delta 1	-2.12	-3.06
MGG_05905	Zinc-regulated transporter 2	Mixed outcome	zinc-regulated transporter 2	-2.13	-2.09
MGG_05643	Cch1	Reduced virulence	calcium-channel protein cch1	-2.21	-2.15
MGG_00124	MGG_00124	Reduced virulence	conserved hypothetical protein	-2.22	-2.10
MGG_05844	Man1	Unaffected pathogenicity	mannan endo-1,4-beta-mannosidase 1 precursor	-2.27	-2.73
MGG_08710	Vacuolar calcium ion transporter	Unaffected pathogenicity	vacuolar calcium ion transporter	-2.34	-2.60
MGG_00957	ABC1 family protein	Reduced virulence	ABC1 family protein	-2.37	-2.59
MGG_02627	ABC domain protein		ABC1 domain protein	-2.38	-4.77
MGG_02897	MoSSK1	Reduced virulence	conserved hypothetical protein	-2.46	-2.46
MGG_04708	MoSOM1	Loss of pathogenicity	conserved hypothetical protein	-2.47	-2.89
MGG_03580	Moatg4	Loss of pathogenicity	cysteine protease atg4	-2.47	-2.62
MGG_04432	MoCYP51B	Unaffected pathogenicity	cytochrome P450 51	-2.47	-2.58
MGG_07335	SUM1	Unaffected pathogenicity	cAMP-dependent protein kinase regulatory subunit	-2.50	-2.70
MGG_11174	HIK1	Unaffected pathogenicity	sensor protein gacS	-2.51	-2.92

MGG_09828	Yvc1	Mixed outcome	vacuolar conductance protein	-2.61	-3.41
MGG_06951	MGG_06951	Reduced virulence	CAAX prenyl protease 1	-2.63	2.30
MGG_12828	Moatg15	Loss of pathogenicity	conserved hypothetical protein	-2.64	-3.25
MGG_04582	MGG_04582	Reduced virulence	conserved hypothetical protein	-2.67	-2.73
MGG_02443	MGG_02443	Reduced virulence	conserved hypothetical protein	-2.69	2.18
MGG_00454	Moatg13	Reduced virulence	autophagy related protein 13p	-2.78	-3.88
MGG_05078	Calcium-transporting ATPase 3	Loss of pathogenicity	calcium-transporting ATPase 3	-2.85	-3.75
MGG_06933	CNB	Mixed outcome	calcineurin subunit B	-2.85	-2.83
MGG_10315	MPG1	Reduced virulence	Hydrophobin	-2.85	-6.01
MGG_09471	PTH9	Reduced virulence	neutral trehalase	-2.88	-3.29
MGG_14014	Moplaa	Reduced virulence	ubiquitin homeostasis protein lub1	-2.91	-2.71
MGG_05133	MoCRZ1	Reduced virulence	C2H2 type zinc finger domain-containing protein	-3.01	-2.70
MGG_05174	MGG_05174	Reduced virulence	pinin/SDK/memA domain-containing protein	-3.04	-3.00
MGG_01730	MoHox3	reduced virulence	conserved hypothetical protein	-3.05	-2.97
MGG_10633	MoAP1	Loss of pathogenicity	AP-1 complex subunit mu-1	-3.10	-3.36
MGG_00466	Cdc42	Reduced virulence	cell division control protein 42	-3.12	-3.00
MGG_12005	Spf1	Mixed outcome	cation-transporting ATPase 4	-3.13	-2.96
MGG_13239	7,8-LDS	Unaffected pathogenicity	linoleate diol synthase	-3.14	-2.62
MGG_02755	NUT1	Reduced virulence	nitrogen regulatory protein NUT1	-3.14	-3.67
MGG_02622	TGL1-1	Unaffected pathogenicity	sterol esterase TGL1	-3.19	-3.29
MGG_02370	Mir1	Unaffected pathogenicity	mitochondrial phosphate carrier protein	-3.19	-2.85
MGG_01236	SLP 1	Reduced virulence	WD repeat-containing protein slp1	-3.26	-2.76
MGG_04204	MAGC	Unaffected pathogenicity	guanine nucleotide-binding protein alpha-2 subunit	-3.28	-3.91
MGG_03146	MoRgs2	Unaffected pathogenicity	conserved hypothetical protein	-3.37	-2.88
MGG_03638	Moatg24	Unaffected pathogenicity	autophagy-related protein 24	-3.41	-4.48
MGG_02252	BUF1	Loss of pathogenicity	tetrahydroxynaphthalene reductase	-3.41	-2.61
MGG_06033	MoMSB2	Loss of pathogenicity	hypothetical protein	-3.46	-4.22
MGG_04621	MGG_04621	Reduced virulence	conserved hypothetical protein	-3.54	-3.03
MGG_02436	MGG_02436	Reduced virulence	conserved hypothetical protein	-3.55	-5.32
MGG_12175	SSM1	Reduced virulence	tyrocidine synthetase 1	-3.55	-3.71
MGG_06847	Annexin A7	Loss of pathogenicity	annexin A7	-3.60	-4.04
MGG_00447	ABC2 (Brefeldin A resistance protein)	Unaffected pathogenicity	brefeldin A resistance protein	-3.61	-2.75
MGG_08212	Moatf1	Reduced virulence	BZIP transcription factor (AtfA)	-3.62	-3.70

MGG_09125	MoSHO1	Reduced virulence	osmosensor protein	-3.67	-4.31
MGG_05201	MGB1 (guanine binding nucleitide protein)	Loss of pathogenicity	guanine nucleotide-binding protein subunit beta	-3.76	-3.28
MGG_02799	CHS5	Loss of pathogenicity	conserved hypothetical protein	-3.76	-2.89
MGG_04556	MGG_04556	Reduced virulence	alcohol dehydrogenase 1	-3.82	-3.72
MGG_01822	OSM1 (MAPK-HOG1)	Unaffected pathogenicity	mitogen-activated protein kinase HOG1	-3.84	-3.88
MGG_03726	MoRgs3	Reduced virulence	conserved hypothetical protein	-3.87	-3.57
MGG_07289	Gph1	Mixed outcome	glycogen synthase	-3.93	-4.10
MGG_04137	MGG_04137	Reduced virulence	CTLH domain-containing protein	-3.93	-3.05
MGG_00750	NOX1	Loss of pathogenicity	cytochrome b-245 heavychain subunit beta	-3.96	-4.36
MGG_03530	MGG_03530	Reduced virulence	conserved hypothetical protein	-4.03	-4.71
MGG_10017	NMR1	Reduced virulence	NmrA family protein	-4.05	-2.65
MGG_05344	MSP1	Reduced virulence	conserved hypothetical protein	-4.06	-6.27
MGG_03860	TPS1 (alpha,alpha-trehalose-phosphate synthase 1)	Loss of pathogenicity	alpha,alpha-trehalose-phosphate synthase 1	-4.13	-3.93
MGG_09551	CHS1	Reduced virulence	chitin synthase 3	-4.17	-4.22
MGG_07528	PTH3	Loss of pathogenicity	imidazoleglycerol-phosphate dehydratase	-4.21	-2.63
MGG_04428	ACE1 (zinc finger transcription factor)	Effector (plant avirulence determinant)	zinc finger transcription factor ace1	-4.26	-3.97
MGG_07460	MoHyr1	Reduced virulence	peroxiredoxin HYR1	-4.39	-4.44
MGG_02423	MGG_02423	Loss of pathogenicity	ER lumen protein retaining receptor 2	-4.39	-4.17
MGG_08600	PIC5	Reduced virulence	mannose-P-dolichol utilization defect 1 protein	-4.39	-3.10
MGG_09312	Conserved hypothetical protein	Reduced virulence	conserved hypothetical protein	-4.41	-4.58
MGG_09912	MoCMK1	Reduced virulence	calcium/calmodulin-dependent protein kinase	-4.47	-4.47
MGG_09565	PMK1	Loss of pathogenicity	mitogen-activated protein kinase	-4.66	-3.74
MGG_04629	MGG_04629	Reduced virulence	integral membrane protein	-4.75	-4.71
MGG_04853	MoHox1	reduced virulence	Homeoprotein	-4.86	-4.59
MGG_07259	MGG_07259	Reduced virulence	conserved hypothetical protein	-4.92	-3.75
MGG_04489	MNH6	Reduced virulence	nucleosome binding protein	-4.95	-3.93
MGG_05933	TGL3-1	Unaffected pathogenicity	lipase 4	-5.21	-2.14
MGG_03284	MGG_03284	Reduced virulence	DNA mismatch repair protein	-5.23	-3.68

MGG_01707	MGG_01707	Reduced virulence	conserved hypothetical protein	-5.47	-5.06
MGG_04212	OMO1	Loss of pathogenicity	L-ornithine 5-monooxygenase	-5.81	-5.53
MGG_13013	CHS6	Loss of pathogenicity	chitin synthase 8	-6.17	-5.45
MGG_05132	MoSKN7	Unaffected pathogenicity	conserved hypothetical protein	-6.62	-2.22
MGG_09098			endo-1,4-beta-xylanase	11.97	12.54
MGG_13624	ABC1 transporter CDR4		ABC transporter CDR4	4.15	-
MGG_04486	Moatg11	Unaffected pathogenicity	Taz1-interacting factor 1 (TAF1)	3.46	-
MGG_11712	MoHox6	reduced virulence	conserved hypothetical protein	3.21	-
MGG_07437	MoHox5	reduced virulence	conserved hypothetical protein	2.84	-
MGG_12958	MST12 (Transcription factor SteA)	Loss of pathogenicity	transcription factor steA	2.75	-
MGG_00345	MoRIM15	Reduced virulence	serine/threonine-protein kinase RIM15	2.69	-
MGG_09898	MGG_09898	Adenylate cyclase	adenylate cyclase	2.66	-
MGG_11454	Vacuolar calcium ion transporter	Unaffected pathogenicity	vacuolar calcium ion transporter	2.55	-
MGG_03459	PTH8	Reduced virulence	autophagy-related protein 26	2.33	-
MGG_06064	CON7	Reduced virulence	chitin synthase D	2.31	-
MGG_06971	MoSFl1	Reduced virulence	flocculation suppression protein	2.28	-
MGG_00883	MGG_00883	Loss of pathogenicity	mitogen activated protein kinase kinase kinase3	2.18	-
MGG_01215	COM1	Reduced virulence	conserved hypothetical protein	2.13	-
MGG_05664	PdeH	Mixed outcome	cAMP-specific 3',5'-cyclic phosphodiesterase 7B	2.12	-
MGG_05199	MST50p	Loss of pathogenicity	protein kinase regulator Ste50	2.06	-
MGG_01818	MAGB	Reduced virulence	guanine nucleotide-binding protein alpha-3 subunit	2.05	-
MGG_01196	Kin4	Mixed outcome	serine/threonine-protein kinase MARK2	2.03	-
MGG_07015	MGG_07015	Reduced virulence	DNA repair protein Rad7	-2.09	-
MGG_04066	Neo1	Loss of pathogenicity	phospholipid-transporting ATPase 1	-2.28	-
MGG_07297	Moatg7	Loss of pathogenicity	autophagy-related protein 7	-2.40	-
MGG_04547			endoglucanase II	-	11.18
MGG_01542	XYL2	Unaffected pathogenicity	endo-1,4-beta-xylanase	-	9.00
MGG_09618	MoRgs6	Unaffected pathogenicity	conserved hypothetical protein	-	7.38
MGG_14243	endo-1,4-beta-xylanase precursor [GH10 family]	Reduced virulence	endo-1,4-beta-xylanase precursor	-	6.11
MGG_07868	endo-1,4-beta-xylanase [GH10	Reduced virulence	endo-1,4-beta-xylanase	-	3.06

family]

MGG_05871	PTH11	Reduced virulence	integral membrane protein	-	2.86
MGG_01204	MIG1	Loss of pathogenicity	MADS-box MEF2 type transcription factor	-	2.29
MGG_11899	MGG_11899	Reduced virulence	SH3 domain-containing protein	-	2.06
MGG_01748	MGG_01748	Reduced virulence	conserved hypothetical protein	-	2.06
MGG_01381	Calcium permease	Mixed outcome	calcium permease	-	-2.03
MGG_00184	HTF1	Unaffected pathogenicity	conserved hypothetical protein	-	-2.04
MGG_06421	Tos3	Unaffected pathogenicity	calcium/calmodulin-dependent protein kinase kinase 2	-	-2.11
MGG_07971	Pmc1	Mixed outcome	calcium-transporting ATPase 1	-	-2.13
MGG_06559	NOX2	Loss of pathogenicity	cytochrome b-245 heavychain subunit beta	-	-3.50

Appendix 2

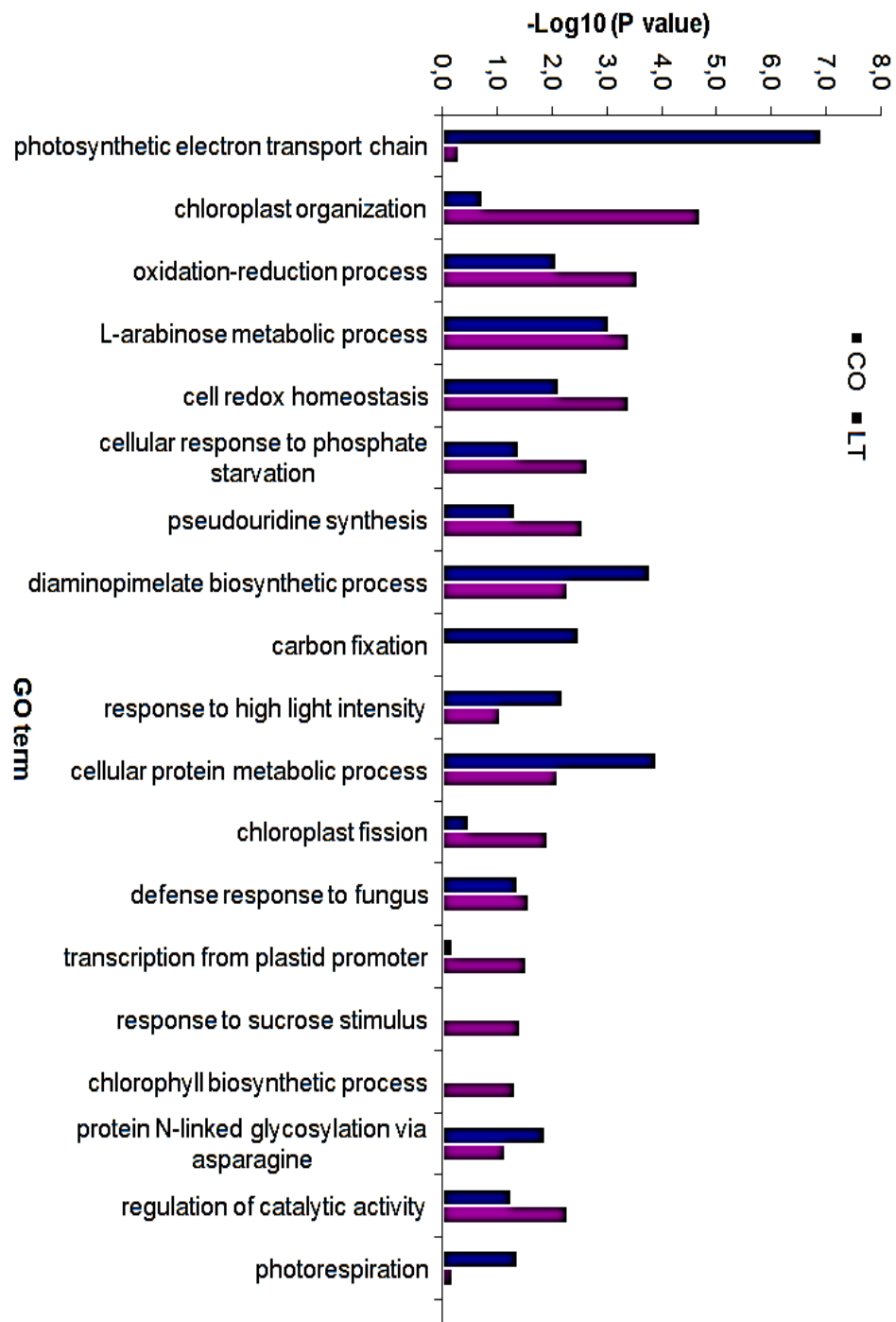Figure S1: Significant Gene Ontology (GO) enriched terms from differentially up regulated genes (fold change 4; FDR, 0.05) in plants exposed to 35°C for 7 days. Comparison of the two genetic backgrounds; Blue bars, CO+35°C; purple bars, LT+35°C.

Acknowledgements

I am indebted to many individuals who have enabled the completion of this dissertation. My deepest gratitude goes to my supervisors, Prof. Dr. Andreas von Tiedemann and Prof. Dr. Kerstin Wydra for the scientific mentorship they provided to me. Prof. von Tiedemann is a caring and patient individual whose contribution to my scientific career has been very evident. I feel privileged to have worked with him for two main reasons: first, his kind nature and willingness to assist students and second, his exceptional knowledge of plant pathology and scientific writing expertise. His interest in helping students, approachableness and outgoing nature makes association with him enjoyable. I am grateful to Prof. Wydra. Without her favor, I would not have got this PhD opportunity. She was always motivational, willing to answer my questions and provide advice about my research whenever I requested; her contribution to the success of this research is highly valued. I would like to thank Dr. Christian Möllers for accepting to be in my dissertation evaluation committee. I am grateful to Dr. Birger Koopmann. His knowledge in molecular plant pathology provided me with a clear understanding of many aspects in my research. My research would not have been possible without the assistance of technicians. My sincere thanks go to Evelin Vorbeck, Dagmar Tacke, Kerstin Höch, Marian Süß, and Daniel Kretzschmar for their technical support. I am grateful to my fellow graduate students. We worked together and supported each other in areas of need, and that was a great privilege. I am grateful to my friend, Merle Tränkner, from the Institute of Applied Plant Nutrition; she significantly contributed to my research and participated in fine tuning my dissertation. I would like to thank Prof. Dr. Ulrich Schaffrath, Dr. Hassan Ghareeb, Dr. Mark Winter and Dr. Anke Sirrenberg for their valuable comments that helped improve the quality of this dissertation. My sincere thanks also go to the Microarray and Deep-Sequencing Core Facility of the Developmental Biochemistry, University Medical Center Göttingen (UMG) for performing illumina sequencing and participation in RNA-seq data analysis. Finally, I owe deepest gratitude to my family, especially, my wife Sarah Onaga. She tolerated my absence from home for the last 4 years and prayed for my success. Above all, I would like to express my profound gratitude to the Almighty God for his love, mercy, guidance and safeguard. He has brought me this far.

This research was supported by **BMZ** funded project "Mitigating the impact of climate change on rice diseases in East Africa" which was spearheaded by AfricaRice center. The contribution of these institutions to my education and research is greatly appreciated.

Publications

Onaga, G., Wydra, K., Koopmann, B., Sere, Y., Ghareeb, H., Von Tiedemann, A. (2016) High temperature effects on *Pi54* conferred resistance to *Magnaporthe oryzae* in two genetic backgrounds of Oryza sativa (manuscript submitted)

Onaga, G., Wydra, K., Koopmann, B., Sere, Y., Von Tiedemann, A. (2016) Elevated temperature increases *inplanta* expression levels of virulence related genes in *Magnaporthe oryzae* and compromises resistance in Nipponbare (manuscript accepted with revisions)

Onaga, G., Wydra, K., Koopmann, B., Sere, Y., Von Tiedemann, A. (2014) Population Structure, Pathogenicity, and Mating Type Distribution of *Magnaporthe oryzae* Isolates from East Africa. *Phytopathology* 105(8):1137-45.

Selected conference contributions

Onaga, G., Wydra, K., Koopmann, B., Sere, Y., Von Tiedemann, A. (2013) Genomic studies on resistance of rice to blast, *Magnaporthe oryzae*, at rising temperature. Presented at the 10th International Congress of Plant Pathology, Beijing, China. See in the book of Abstracts. pg.333.

Onaga, G., Wydra, K., Koopmann, B., Sere, Y., Von Tiedemann, A. (2013) Population structure of *Magnaporthe oryzae*, the causal agent of rice blast in East Africa. 3rd Africa Rice Congress, Yaoundé, Cameroon. See the book of Abstracts. Pg.190.

Onaga, G., Wydra, K., Koopmann, B., Sere, Y., Von Tiedemann, A. (2012) Effects of High Temperature on R Gene Mediated Resistance to Rice Blast in two Genetic Backgrounds of Rice. TROPENTAG 2012.

Curriculum vitae

Personal details

Full Name   Geoffrey Onaga

Date of birth   23.02.1978

Place of Birth   Ngora, Uganda

Secondary education

1997/98   Teso College Aloet, Soroti

1993/96   Rock High School, Tororo

1985/92   St. Kizito's Primary School, Tororo

Tertiary Education

2014   PhD studies, Georg-August-University Göttingen, Germany.

2010   MSc. Crop Science, Makerere University, Kampala, Uganda.

2004   Bachelor of Science in Agriculture (Hons), Makerere University, Kampala, Uganda.

Declaration

I hereby, declare that this dissertation was undertaken independently and without any unaccredited aid.

Göttingen, 28.05.2014